The cosmological bootstrap and the analytic wavefunction

Mang Hei Gordon Lee Supervisor: Prof. Enrico Pajer Department of Applied Mathematics and Theoretical Physics, University of Cambridge.



 ${\rm May~2024}$ This thesis is submitted for the degree of Doctor of Philosophy

Declaration

This thesis is the result of my own work and includes nothing which is the outcome of work done in collaboration except as declared in the preface and specified in the text. It is not substantially the same as any work that has already been submitted, or, is being concurrently submitted, for any degree, diploma or other qualification at the University of Cambridge or any other University or similar institution except as declared in the preface and specified in the text. It does not exceed the prescribed word limit for the relevant Degree Committee

Abstract

In the past few decades there have been an overabundance of models describing inflation, a period where the universe expands exponentially quickly. This led to the rise of the cosmological bootstrap, which aims at constraining cosmological observables in a model independent way. This is achieved by directly imposing physical principles such as unitarity, locality, symmetry, and analyticity on cosmological correlators.

In this thesis we explore the consequences of two such principles: unitarity and analyticity. We show that unitarity implies a set of consistency relations among wavefunction coefficients in perturbation theory, and these relations can be generalized to fields with any mass and integer spin. Unitarity, alongside locality and scale invariance, also implies the vanishing of four-point parity odd correlators at tree level, and we show this is not true at loop level.

Analyticity in the S-matrix is linked to causality and serves as the backbone for the S-matrix bootstrap, which provides non-perturbative constraints for scattering. We show that analyticity in the wavefunction is also linked to causality. We study the analytic structure of the wavefunction in detail and demonstrate the relation between singularities in amplitudes and a subset of singularities in the wavefunction. Finally, we write down the dispersion relations of the wavefunction, which serves as a first step towards a non-perturbative bootstrap in cosmology.

Preface

This thesis is based on [1–4], which are the results of collaborative work. This is a list of the author's contribution to the publications:

- In [1], the author was responsible for generalizing the unitarity constraints to spinning fields (section 3.4, which was written jointly with Harry Goodhew) as well as checking the results for a simple example (section 4.3). The author also wrote appendix C, the WKB solution to the Klein Gordon equation for flat FLRW spacetime, which is an early version of the proof of Hermitian analyticity of the bulk-to-boundary propagator.
- In [2], the author was responsible for developing Landau analysis for the analytic wavefunction (section 2.5), as well as verifying the UV/IR sum rules for loop level (section 4.2). The author also did an early version of the soft limit of the three internal edge wavefunction presented in appendix A.4 (the final version presented in the paper is written by Scott Melville), and did some of the early calculations for the UV/IR sum rules at tree level presented in section 4.1 (the final version presented is done by Scott Melville and Santiago Agüí Salcedo).
- In [3] the author was responsible for doing the calculations of the two-vertex one-loop diagram presented in section 4, 5 and 6 (an early version of the toy model calculation in section 4 was done by Ciaran McCulloch). The author also worked with Ciaran McCulloch in computing the one-vertex one-loop wavefunction and correlators, which are presented in section 3.
- In [4] the author wrote the entire article. However the author benefited from helpful discussions with Enrico Pajer, Scott Melville, Guilherme Pimentel and Arthur Lipstein.

Acknowledgements

First of all, I would like to thank my supervisor Enrico for his unwavering support during my PhD. Thank you for encouraging me to explore different new and exciting ideas, as well as guiding me through the other aspects of academia such as scientific communication and applying for postdoc positions. I wouldn't have made it without your help.

I would like to thank all of my collaborators, including Sadra, Harry, Santi, Scott and Ciaran. I benefited greatly from many fruitful conversations with you throughout the past four years, and I look forward to working with you all in the future as well.

I would also like to express my gratitude to everyone else who are (or were) in Enrico's group, including Tanguy, Jakub, David, James, Dong Gang, Carlos, Xi, Thomas and Yaniv. You have greatly enriched my time in Cambridge, both academically and socially.

I would like to thank Aron and his group for letting me join their group meeting. I have learned a great deal, and I apologize for not having any meaningful contributions to your conversations. I have also benefited a great deal from many conversations with Ayngaran and Rifath, which I am thankful for.

I am also grateful to Croucher Foundation and Cambridge Trust for funding my PhD. Without your support finishing this PhD would not have been financially viable.

Last but not least, I would like to thank my parents as well as my brother for their support over the years. Without your support I would not possess the courage to continue down the path of theoretical physics.

Contents

1	Introduction								
2	Brie	Brief overview of the cosmological wavefunction							
	2.1	The cosmological wavefunction	17						
	2.2	Computing the wavefunction	18						
		2.2.1 Off-shell wavefunction coefficient	22						
	2.3	In-in correlators	24						
		2.3.1 Feynman rules for in-in correlators	25						
		2.3.2 In-in correlators from the wavefunction	26						
3	$Th\epsilon$	The consequences of unitarity							
	3.1	The cosmological optical theorem	28						
	3.2	Hermitian analyticity	34						
	3.3	Spinning fields	38						
	3.4	Examples	44						
		3.4.1 Contact diagram	44						
		3.4.2 Exchange diagram	45						
	3.5	Extensions beyond tree level	47						
4	App	plying the bootstrap to parity odd correlators	53						
	4.1	Review: Tree level no-go theorem for parity odd trispectrum	53						
	4.2	More about scale invariance	54						
	4.3	One site loop	56						
		4.3.1 Correlators	56						
		4.3.2 Wavefunction coefficients	60						
	4.4	Two site loop: general strategy and a toy model example	63						
		4.4.1 Momentum integrals	65						
		4.4.2 A toy model example	68						
	4.5	Trispectrum for a massless scalar	71						
		4.5.1 Conformally coupled loop	71						
		4.5.2 Massless loop	75						

5	Analyticity of the wavefunction 80								
	5.1	Analyticity and the S-matrix	80						
	5.2	Wavefunction analyticity and causality	83						
	5.3	Energy conservation condition	84						
		5.3.1 Examples: tree level	93						
		5.3.2 Examples: one loop	94						
	5.4	Landau analysis: first attempt	97						
		5.4.1 Example: massless two site loop	101						
		Example: massive two site loop	102						
		Example: three site loop	103						
		5.4.2 Thresholds for general diagrams	104						
6	Amplitude representation of the wavefunction 10								
	6.1	Amplitude representation of the wavefunction	107						
	6.2	One loop wavefunction as amplitudes	112						
		6.2.1 Total energy pole	112						
		6.2.2 Example: two site loop	114						
		6.2.3 Example: three site loop	116						
		Beyond one loop	118						
	6.3	Landau analysis: second attempt	119						
		6.3.1 General strategy	119						
		6.3.2 Example: two site loop	121						
		6.3.3 Example: three site loop	126						
	6.4	Singularities of in-in correlators	132						
7	Dispersion relation and effective field theories								
	7.1	What is an EFT for a wavefunction?	135						
	7.2	Dispersion relation and UV/IR sum rules	137						
	7.3	Example: a light scalar	139						
	7.4	Example UV completion	142						
		7.4.1 Tree level example	142						
		7.4.2 Loop level example	146						
8	Con	onclusion and outlook 149							
\mathbf{A}	Tim	ne derivatives	152						
В	WK	KB solution to the Klein Gordon equation for flat FLRW spacetime	154						
\mathbf{C}	Ten	Tensor structure							
			157						
ע	_		160						
		Classifying complexity							
		One internal edge	161 163						
	17.0	I WO HIBGING CUPE	1 (1.)						

E	Disc	continu	nity for loop diagrams	-	175
		D.4.3	Soft limit	•	172
			Reducing the complexity		
		D.4.1	Generalities		169
	D.4	Three	internal edge		169
		D.3.3	Soft limit		169
		D.3.2	Massless limit		168
		D.3.1	Generalities		163

Chapter 1

Introduction

With the advances of science in the past centuries, the quest to understand the origin and history of everything in our universe is no longer restricted to the domain of philosophy and religion. We now know that the universe is not static: in fact, it is expanding. We now know there are countless galaxies out there, and our Milky Way galaxy plays no privileged role in the universe. We now know that most of the matter content in our universe are dark energy and dark matter, which our eyes cannot directly observe.

It is understood that while the universe is mostly homogeneous and isotropic, there must be small deviations from exact homogeneity and isotropy in its primordial history, otherwise our universe will be completely homogeneous and quite boring. Currently the most widely accepted explanation of the origin of these small deviations is a period of accelerated expansion in the early universe, commonly referred to as inflation [5,6]. During this expansion period, small quantum fluctuations in the curvature of spacetime get stretched to cosmological scales and become frozen. We learn from general relativity that these curvature perturbations cause matter to collapse, and eventually this give rise to the rich structure of the universe we observe today.

Inflation is not the only theory which attempts to explain the origin of primordial perturbations. What distinguishes inflation from other theories is its success in matching experimental results. In cosmology the main arenas for testing theories are the remnant light from the hot big bang, also known as cosmic microwave background (CMB), and the distribution of galaxies, also known as large scale structure (LSS). In particular, the scalar curvature perturbation $\zeta(\mathbf{k})$ evolves linearly in the hot big bang, and so any perturbations we can measure in a cosmological survey, including temperature fluctuations in the CMB and overdensities of matter, which we collectively refer to as $\delta(\mathbf{k})$, can be related to $\zeta(\mathbf{k})$. More specifically, if we measure the correlation function of $\delta(\mathbf{k})$, then:

$$\langle \delta(\mathbf{k}_1) \dots \delta(\mathbf{k}_n) \rangle = \left[\prod_{i=1}^n T(\mathbf{k}_i) \right] \langle \zeta(\mathbf{k}_1) \dots \zeta(\mathbf{k}_n) \rangle + \mathcal{O}(\zeta^{n+1}).$$
 (1.0.1)

Here $T(\mathbf{k})$ is a transfer function which can be derived from the standard hot big bang model. In particular, the $\mathcal{O}(\zeta^{n+1})$ terms are only important due to gravitational collapse, so the correlations in the CMB should be linearly related to the statistics of $\zeta(\mathbf{k})$. If we extrapolate the CMB power spectrum (i.e. two point correlation function) to the end of inflation, we observe a mostly Gaussian spectrum which is scale invariant, and this matches the expectation of inflation very well (see figure 1.1). Most alternatives

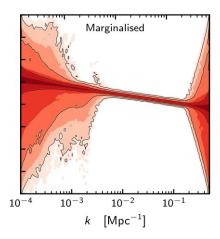


Figure 1.1: The primordial power spectrum extrapolated from the CMB. The x-axis labels the momentum k (or the angular momentum mode l), and the y-axis labels the size of the power spectrum (in log scale). Taken from [10]

to explaining the origin of structure in our universe fail at some hurdle. They fail at explaining certain features of the CMB spectrum (an example would be cosmic strings, which fail at explaining the phase coherence of the CMB power spectrum [7]¹), or they require exotic ingredients to work (for example bounce cosmology requires abandoning general relativity as the theory of gravity, or introducing ghost fields, see [9] for more details). Coupled with the fact that inflation was able to explain the flatness of our universe, as well as how CMB from different parts of the universe are correlated², inflation has been widely accepted as part of standard cosmology.

Model building in inflation Despite all its success, our understanding of inflation is far from complete. The most common model for inflation used in textbooks is the single field slow roll inflation. In this model, inflation is driven by a scalar field commonly called the inflaton. Initially the inflaton undergoes a slow roll phase, where it rolls down a potential that is almost flat and the universe expands exponentially (see figure 1.2). Eventually the inflaton exits the slow roll phase (for example, it gets trapped in a well), and inflation ends. The universe then *reheats*, i.e. standard model particles are created, then the rest of the cosmic history is matched with the standard hot big bang story.

This common textbook story has left a lot of room for interpretation. For starters, aside from the fact that the potential supports a slow roll phase, not much else was specified about the potential itself. This means in principle there could be a vast landscape of potentials which support inflation, and each of them may have their own exotic feature that distinguishes one model from another. This story can also be extended to multiple scalar fields: one could write down a multi-field potential, and have the field(s) roll down the potential in certain direction (for example see [11, 12]). This is before we even consider other fields, each with their own mass and spins, that can couple in different ways to the infalton (for

¹While cosmic strings cannot be the primary source of primordial perturbation, they can still contribute to structure formation, for example see [8].

²Naive considerations from the hot big bang would tell us different parts of the CMB are generally not in causal contact, and could have wildly different temperatures in principle. However, the observed CMB is isotropic and homogeneous up to small deviations of order $\mathcal{O}(10^{-5})$, and this is known as the horizon problem. Inflation tell us that the horizon in the early universe is shrinking, and these seemingly disconnected parts are in causal contact in the early universe, thus explaining the homogeneity and isotropy.

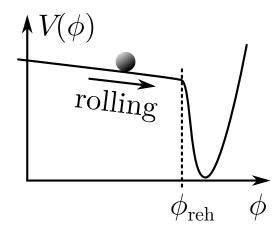


Figure 1.2: Illustration of a slow roll potential for inflation. Taken from [11]

example [13, 14]).

This seemingly infinite number of possibilities is an enticing prospect for a theorist: given enough imagination and time, it seems one could construct a model of inflation with suitable features, and use it to explain any phenomenon or embed it in another theory. And over the past few decades, theorists have indeed taken full advantage of this, and created an incredibly huge list inflationary models. For example, we have:

• Models which comes from modified gravity. Because f(R) gravity can be written as Einstein gravity coupled to a scalar field, it would be natural to understand inflation in the framework of scalar tensor theories. One of the most famous example is Starobinsky inflation [15, 16], where $f(R) = R + R^2/\mu^2$ for some mass parameter μ , and this give rise to an inflation potential of the form $V \sim \left(1 - \exp\left(-\sqrt{2/3}\phi\right)\right)^2$.

Naturally, since the Higgs field is the only elementary scalar field in the standard model, people also considered scalar tensor theories where the scalar field is the Higgs field. These models are referred to as Higgs inflation [17–21]. These models often express predictions for cosmological measurements (usually the spectral tilt n_s or the primordial tensor-to-scalar ratio r) in terms of parameters from particle physics (for instance the Higgs mass), and this usually provides constraints on these models.

- Models which comes from string theory. Inflation is considered as an EFT from some UV theory of quantum gravity, and since string theory is the leading candidate of quantum gravity, naturally people are interested in understanding how inflation works from the perspective of string theory. For example, inflation can be driven by the dynamics of branes (for example DBI inflation, see [22,23]); it can be driven by string axions (for example axion monodromy, see [24,25]); or it can arise from uplifting AdS vacuum to a metastable dS ground state (this is known as KKLT inflation, see [26]). A nice overview of inflation in string theory can be found in [27].
- Models for creating excess primordial black holes. If the size of the primordial curvature perturbation is sufficiently large, this could create a large over-density of matter after inflation ends. This over-density of matter could then collapse and form primordial black holes. The number of primordial black holes created this way depends on the tail end of the distribution of curvature perturbation. For most inflation models, which give an almost Gaussian distribution of curvature perturbation,

the number of primordial black holes created this way is very small, but one could come up with some inflation models which enhances the tail end of the distribution. One could introduce local features in the potential, for example introducing small steps and bumps (which breaks the slow roll condition briefly during inflation and increases the amplitude of primordial fluctuation for certain scales) [28–31], or create a barrier for the inflaton to tunnel through (which modify the tail end of the distribution from Gaussian to exponential) [32]. Alternatively one can modify the sound speed of the inflaton so that it oscillates, which give rise to peaks in the primordial curvature perturbation distribution [33,34].

• Models which include dissipation effects during inflation. It is commonly assumed that interactions between the inflaton and other particles are small, and we can treat it as an isolated system. However there are models where this assumption is dropped. These models are commonly referred to as warm inflation [35,36]. Since the inflaton is no longer an isolated system, naturally one needs to understand the effects of dissipation, and in general thermal noise from dissipation contributes to the primordial fluctuations on top of the usual vacuum fluctuations [37,38]. In addition, these models also leads to particle production during inflation, and can be used in place of reheating as a mechanism for producing a thermal bath of particles after inflation [39–41]. More generally dissipative effects can be understood by studying inflation as an open quantum system, see [42–44].

This is by no means an exhaustive list (a comprehensive list is presented in [45]), and each model is interesting in its own way. However, at some point we still have to pursue the answer to an important question:

How should we test for inflation itself?

At the end of the day, inflation is a scientific theory. Therefore it must have a set of predictions, commonly present in *any* inflation models, that can be directly tested. This question is particularly relevant as we probe the CMB and LSS with increasing precision. One particularly important testing grounds for the different models of inflation is the deviation from Gaussian statistics in the early universe, commonly referred to as primordial non-Gaussianities. While it has not been observed as of today, the bounds on its size has been improving over the years. Each inflation model give rise to different non-Gaussianities, and if our only way of understanding inflation is through explicit models, then verifying or falsifying inflation would require testing *all* possible models. This is an arduous (if not impossible) task. However, if we can find properties which must be present in the statistics and correlation of the primordial fluctuations from inflation, this would make testing for inflation much more reasonable.

In addition to this problem, there are two other issues with approaching inflation from a model building perspective:

• Field redefinition. Since inflation is described in the framework of quantum field theory, the common model building procedure involves writing down a Lagrangian, where the field content as well as their interactions are specified. This allow us to compute correlators, which we extrapolate and compare to correlators in the CMB and LSS. However, one could always make a field redefinition: for example, given a scalar field ϕ , we can take $\sigma = \phi + \phi^2$, and write the interactions in terms of these new σ fields. However, if we are working with physical degrees of freedoms, the observables should be independent of field redefinition (up to boundary terms). At the end of the day, we need

to link our results to measurements in the cosmological survey, say the distribution of galaxies or temperature fluctuations of the CMB, and these clearly do not share the same ambiguity in field redefinition as the inflaton. This is not manifest in the Lagrangian formalism, and it is not always manifestly clear that Lagrangian for different models are not related to each other by some clever field redefinition.

• Time evolution. The Lagrangian formalism described above is essentially describing the details of time evolution of the fields during inflation. For practical purposes this is in fact a redundancy: we cannot directly observe anything in the bulk inflationary spacetime, since the only observable we have access to are the correlators at the end of inflation. So this begs the following question: is there a way to understand features of correlators at the end of inflation if we are only given some very general features about the bulk inflationary spacetime?

All of these issues point towards the need of a model-independent way of understanding inflation. This leads us to the idea of bootstrapping.

Bootstrapping The idea of bootstrapping dates back to the early 1960s, when physicists were struggling to find a physical model to describe strong interactions. To deal with this problem, the S-matrix bootstrap was born. The idea is simple: rather than working with Lagrangians and doing perturbative calculations, one should write down the S-matrix, which is the physical observable³, and impose constraints on the S-matrix directly by physical principles such as Lorentz invariance, locality, causality and unitarity.

The original goal of the S-matrix bootstrap was ambitious: to find the S-matrix for strong interaction simply by imposing physical constraints [46,47]. This goal was not achieved, and eventually people found QCD, the physical model for describing strong interaction. However, the S-matrix bootstrap program was not a fruitless exploration. The bootstrapping idea has given us an alternative way of understanding quantum field theories, and it has yielded many interesting results. Here we list a few examples:

- Recursion relation for amplitudes. For tree level amplitudes, locality implies singularities are simple poles, and unitarity implies factorization of the corresponding residues into lower point amplitudes. By using a suitable set of momentum shifts known as BCFW momentum shifts, one could start with contact amplitudes and reconstruct every tree level amplitude for theories such as Yang-Mills theory [48–51]. In certain cases, such as N = 4 super Yang-Mills, the full amplitude can be constructed in this manner.
- Color-kinematics duality and double copy. Graviton amplitudes can be expressed roughly as the square of an amplitude in Yang-Mills theory. This can be achieved by a suitable replacement of color factors with kinematics factors [52]. This is not limited to Yang-Mills and gravity: similar relations have been found for bi-adjoint scalars and Yang-Mills, and a few other theories as well (a summary is included in [50]). Notably, these relations are much easier to read off from the amplitude itself, usually written in terms of spinor-helicity variables, rather than the usual perturbative expansions from Feynman rules.
- Analyticity of S-matrix and dispersion relations. Physical properties of the S-matrix often give rise to constraints on the analytic structure of the S-matrix. We will give an overview of this in

³More precisely this is a meta-observable: the actual observables are things that can be computed from the S-matrix, such as cross sections and decay rates.

section 5.1. Notably, this give rise to a set of dispersion relations, which relates the amplitudes to integrals their discontinuities. In the context of effective field theories (EFT), this can be used to link properties of the EFT to properties of the UV completion of the theory. This allow us to construct bounds on the EFT based on physical constraints on the UV theory, for example see [53–60]. This can also be used to explore regions between the region of validity of the EFT and a known UV completion. For instance, this can be used to understand strong interactions for energies above the regime of validity of chiral perturbation theory, but below the regime of validity of perturbative QCD [61–64].

A similarly successful idea is the conformal bootstrap, which focuses on constraining conformal field theories with symmetries and physical principles. The conformal bootstrap was able to provide a set of constraints known as the conformal bootstrap equations, which can be solved numerically using linear programming. This provides constraints on the scaling dimensions of operators in a theory, and allow us to explore critical phenomena without relying on perturbation theory. For details see [65–69].

Bootstrapping in cosmology Given the success of bootstrapping in other areas of physics, it makes sense to attempt bootstrapping in cosmology. Since inflationary spacetime is well approximated by de Sitter(dS) spacetime, early attempts at bootstrapping in cosmology generally includes full dS isometry as an input [70]. The isometry of dS generally give rise to Ward identities, a set of differential equations which the cosmological wavefunction (which we will introduce in section 2) has to satisfy, and bootstrapping involves solving those differential equations. These equations have been extended to include fields with different masses and spins [71,72], and different cosmological spacetimes as well [73]. There has also been considerable effort in understanding the connection of observables and constraints in dS in terms of AdS correlators [74–79], as well as the connection of the cosmological wavefunction to polytopes [80–85].

However, from a phenomenological perspective, inflationary theories which admits full dS isometry may not be the most interesting. This is because correlators for scalar curvature perturbations from theories which admits full dS isometry are slow roll suppressed [86]. Therefore, there has been a great deal of effort in understanding the bootless bootstrap, where invariance under special conformal transformations (or dS boosts) are not assumed [87–91], and these methods have been extended to encompass a wide range of interesting scenarios [92–96].

This thesis will be dedicated to covering some of the new and exciting developments in the cosmological bootstrap. In section 2 we will first give an overview of the cosmological wavefunction, the object that is constrained by the bootstrap. We will discuss the constraints coming from unitarity in section 3. We will study parity odd correlators in section 4 where we explore if the bootstrap constraints on tree level parity odd correlators continue to hold for one loop correlators.

The rest of the thesis will focus on exploring the analyticity of wavefunction. In section 5 we will discuss the locations of singularities of the wavefunction, which can be derived from the "energy conservation condition". We will discuss the amplitude representation of the wavefunction in section 6, where we find some of the singularities in the wavefunction can be linked to singularities of an amplitude. Section 7 will discuss EFT, dispersion relations and UV/IR sum rules for the wavefunction. Finally we will provide some conclusions and outlook in section 8.

Notations and conventions Our conventions for the Fourier transform is:

$$f(\mathbf{k}) = \int \frac{d^d k}{(2\pi)^d} e^{i\mathbf{k}\cdot\mathbf{x}} f(\mathbf{x}) . := \int_{\mathbf{k}} e^{i\mathbf{k}\cdot\mathbf{x}} f(\mathbf{x}).$$
 (1.0.2)

We label external momenta by \mathbf{k} and internal momenta by \mathbf{p} . In addition, for flat space we can define the energy as:

$$\Omega = \sqrt{|\mathbf{k}|^2 + m^2},\tag{1.0.3}$$

where m is the mass of the particle.

We use the notation $\{\mathbf{k}\}$ to denote the collection of all external momenta and similarly for other quantities, for example $\{\Omega\}$ denotes the collection of all energies.

Sometimes in our computation it is convenient to work directly with the loop integrand. For the wavefunction coefficients (which is defined in 2.1.3), we will write the following:

$$\psi_n^{\text{L-loop}}(\{\mathbf{k}\}) = \int_{\mathbf{p}_1 \dots \mathbf{p}_L} \mathcal{I}_n^{\text{L-loop}}(\{\mathbf{k}\}, \{\mathbf{p}\}). \tag{1.0.4}$$

In addition, in loop calculations momentum entering the vertex is **p**.

Generally we write a wavefunction in terms of its (off-shell) external energies ω and its external momenta (we will elaborate on what we mean by on-shell and off-shell in section 2). For a general n-point wavefunction coefficient or correlator, we write:

$$\omega_T = \sum_{a=1}^n \omega_a \,. \tag{1.0.5}$$

In addition, we commonly write our results in terms of symmetric polynomials of external energies. For instance, for three point correlators or wavefunction coefficients, we have:

$$e_2 = \omega_1 \omega_2 + \omega_1 \omega_3 + \omega_2 \omega_3, \qquad e_3 = \omega_1 \omega_2 \omega_3. \tag{1.0.6}$$

For four point correlators or wavefunction coefficients we will also make use of the following notation:

$$\omega_L = \omega_1 + \omega_2,$$
 $\omega_R = \omega_3 + \omega_4,$ $\mathbf{s} = \mathbf{k}_1 + \mathbf{k}_2 = -(\mathbf{k}_3 + \mathbf{k}_4),$ (1.0.7)

$$e_4 = \omega_1 \omega_2 \omega_3 \omega_4$$
, $p_{\pm} = p_1 \pm p_2$. (1.0.8)

This is not to be confused with the notation E_L and E_R (which is $k_1 + k_2 + |\mathbf{s}|$ and $k_3 + k_4 + |\mathbf{s}|$) that is commonly used in the literature (where $k_i = |\mathbf{k}_i|$ and $p_i = |\mathbf{p}_i|$, and $k_i = \omega_i$ when the particles are on-shell). In particular, the wavefunction coefficients and correlators take a particularly compact form when written using the following differential operators (see e.g. [70, 97, 98])

$$O_k^{(i)} = 1 - k\partial_{\omega_i} \,, \tag{1.0.9}$$

where i = L, R an $\omega_{L,R}$ were defined in (1.0.7).

Chapter 2

Brief overview of the cosmological wavefunction

Before going into the details of the bootstrap, we need to specify the object we are bootstrapping. For the cosmological bootstrap, we commonly work with the cosmological wavefunction. We will first define this object and explain how to compute it. We will then explain what we mean by the off-shell wavefunction coefficients, and elaborate on the need to define such an object. We will also explore how the cosmological wavefunction can be related to the in-in correlators, which can be extrapolated to correlators in the cosmic microwave background.

2.1 The cosmological wavefunction

Given a quantum field theory (and some cosmological background), the field-theoretic wavefunction, or just the wavefunction in short, is a state in the field theory projected onto the field basis at a given time. For a theory with a single field, it can be written as follow:

$$\Psi[\phi_0, \eta_0] = \langle \phi_0, \eta_0 | \psi \rangle. \tag{2.1.1}$$

We will be looking exclusively at the Bunch-Davies vacuum state, i.e. the vacuum where the mode functions (solutions to the free equation of motion, see (2.2.2)) are conformally related to plane waves, so from here on Ψ labels the Bunch-Davies vacuum state. Also notice the wavefunction has an explicit time dependence. For cases where we study the wavefunction in flat space, we will take the surface $t = 0^1$. For dS, since we are generally interested in the end of inflation, we will take $\eta_0 = 0$, i.e. the future conformal boundary of dS.

Readers familiar with canonical quantum gravity may wonder if this wavefunction is related to the wavefunction of the universe, and it is possible that one can obtain the field-theoretic wavefunction by some appropriate WKB expansion (for example, looking at the large volume limit of the wavefunction²). We will not explore this connection further in the rest of the thesis, and instead will focus on looking at

¹This choice is taken for convenience, since Minkowski spacetime is time translation invariant.

²Interested readers may look at [99], where the Hartle-Hawking wavefunction for single field inflation is studied in the large volume limit.

quantum field theories with a fixed cosmological background.

One can show that the wavefunction can be obtained from a path integral. For example, for a theory with a single scalar, the wavefunction is simply:

$$\Psi[\phi_0, \eta_0] = \int_{BD}^{\phi(\eta_0) = \phi_0} D\phi \, e^{iS[\phi]}. \tag{2.1.2}$$

This is reminiscent to the way in-out correlators in flat space can be computed by a path integral. The proof can be found in [100].

The wavefunction is usually expanded in terms of a set of wavefunction coefficients:

$$\Psi[\phi_0, \eta_0] = \exp\left(\sum_{n=2}^{\infty} \frac{1}{n!} \int_{\mathbf{k}_1 \dots \mathbf{k}_n} \delta^{(3)}(\sum_i \mathbf{k}_i) \psi_n(\{\mathbf{k}\}) \prod_i^n \phi(\mathbf{k}_i)\right). \tag{2.1.3}$$

The generalization to multi-fields and spinning particles are straightforward: just add the relevant indicies and labels on the fields and the wavefunction coefficients, and sum over all the indicies in (2.1.3).

2.2 Computing the wavefunction

In this section we will explain how to compute the wavefunction coefficients in perturbation theory. Ideally we would like to follow the standard procedures in QFT textbooks, and write down a generating functional Z[J] for the theory (here J is some source). From this, we can determine our object of interest (in our case, wavefunction coefficients) by taking derivatives of J. However, in defining the wavefunction we have introduced a constant time surface, and the field on this surface is fixed to have some value ϕ_0 . This is a different boundary condition from the usual path integral, and we need to implement this carefully.

Mode function and propagators Let us change the integration variable for the path integral (2.1.2) in the following way:

$$\phi(\mathbf{k}, \eta) = \tilde{\phi}(\mathbf{k}, \eta) + \varphi(\mathbf{k}, \eta). \tag{2.2.1}$$

The integration variable is now φ , and ϕ satisfies the free equation of motion in Fourier space:

$$\mathcal{E}\tilde{\phi}(\mathbf{k},\eta) = 0. \tag{2.2.2}$$

For example, in flat space, we have:

$$\mathcal{E} = \partial_t^2 + k^2 + m^2. \tag{2.2.3}$$

In addition, $\tilde{\phi}$ satisfies the boundary condition:

$$\tilde{\phi}(\eta_0) = \phi_0, \qquad \lim_{\eta \to -\infty(1 - i\epsilon)} \tilde{\phi}(\eta) = 0.$$
(2.2.4)

We may now write the path integral (2.1.2) as³:

$$\Psi[\phi_0, \eta_0] = \int_{BD}^{\varphi(\eta_0)=0} D\varphi \, \exp\left(iS_{\text{bdy}}[\phi_0] + i \int_{-\infty(1-i\epsilon)}^{\eta_0} d\eta \int_{\mathbf{k}} \frac{1}{2} \varphi(\mathbf{k}, \eta) \mathcal{E}\varphi(\mathbf{k}, \eta) + \mathcal{L}_{int}[\tilde{\phi} + \varphi]\right). \quad (2.2.5)$$

³Here I omitted dependence on the time derivatives of $\tilde{\phi}$ and φ . For a careful treatment see [101]

The boundary term comes from integrating the bulk Lagrangian by parts. For our case it does not have to vanish for an arbitrary time surface at time η_0 , therefore we have to keep track of it.

Now one can follow the standard derivations in QFT textbooks (for example, see [102]) to obtain the following expression [101]:

$$\Psi[\phi_0, \eta_0] = \mathcal{N} \exp\left(iS_{\text{bdy}}[\phi_0]\right) \exp\left(i\int_{-\infty(1-i\epsilon)}^{\eta_0} d\eta \int_{\mathbf{k}} \mathcal{L}_{int} \left[\tilde{\phi} - i\frac{\delta}{\delta J(\mathbf{k})}\right]\right) \times \exp\left(-i\int_{-\infty(1-i\epsilon)}^{\eta_0} d\eta \int_{\mathbf{k}} J(\mathbf{k})\mathcal{E}^{-1}(\mathbf{k}, \eta)J(-\mathbf{k})\right). \quad (2.2.6)$$

Here \mathcal{N} is just some normalization. Crucially, \mathcal{L}_{int} is written in terms of $\tilde{\phi} - i \frac{\delta}{\delta J(\mathbf{k})}$, rather than $-i \frac{\delta}{\delta J(\mathbf{k})}$ alone. This means we need to keep track of time evolution from $\tilde{\phi}$, and this introduces an additional propagator into our perturbative calculation.

Fortunately all propagators in our calculation can be written in terms of the mode functions, which are solutions to the free equation of motion (2.2.2). Generally \mathcal{E} are second order differential operators, and hence there are two linearly independent solutions. Since we are interested in the Bunch-Davies vacuum, we pick one of the solution (which we label as ϕ^+) as the solution which conformally looks like a plane wave, i.e.

$$\lim_{\eta \to -\infty} \phi^+(k, \eta) \sim \frac{1}{a(\eta)} e^{ik\eta}.$$
 (2.2.7)

We can pick the other solution, which we label as ϕ^- , to be the solution which is linearly independent of ϕ^+ . Usually this is the complex conjugate of ϕ^+ , however there may be some subtleties with branch cuts. We will see this in section 3.2

We can now write down the two type of propagators in our calculation. The first one is the bulk-to-boundary propagator $K(k,\eta)$, which keeps track of the time evolution of $\tilde{\phi}$. It is defined in the following way:

$$\tilde{\phi}(\mathbf{k}, \eta) = K(k, \eta)\phi_0(\mathbf{k}). \tag{2.2.8}$$

The bulk-to-boundary propagator satisfies the following:

$$\mathcal{E}K(k,\eta) = 0, \qquad \lim_{\eta \to 0} K(k,\eta) = 1, \qquad \lim_{\eta \to -\infty(1-i\epsilon)} K(k,\eta) = 0. \tag{2.2.9}$$

The second one is the bulk-to-bulk propagator $G(k; \eta, \eta')$, which comes from doing the functional derivatives with respect to the source $J(\mathbf{k})$. The bulk-to-bulk propagator satisfies the following:

$$\mathcal{E}G(k;\eta,\eta') = \delta(\eta - \eta'), \qquad \lim_{\eta \to 0} G(k;\eta,\eta') = 0, \qquad \lim_{\eta \to -\infty(1-i\epsilon)} G(k;\eta,\eta') = 0. \tag{2.2.10}$$

Given the mode function ϕ^+ , the bulk-to-boundary propagator is given by:

$$K(k,\eta) = \frac{\phi^{+}(k,\eta)}{\phi^{+}(k,\eta_{0})}.$$
(2.2.11)

The bulk-to-bulk propagator is given by:

$$G_{p}(\eta, \eta') = i \left[\theta(\eta - \eta') \left(\phi_{p}^{+}(\eta') \phi_{p}^{-}(\eta) - \frac{\phi_{p}^{-}(\eta_{0})}{\phi_{p}^{+}(\eta_{0})} \phi_{p}^{+}(\eta) \phi_{p}^{+}(\eta') \right) + (\eta \leftrightarrow \eta') \right].$$
 (2.2.12)

Here $\theta(\eta_1 - \eta_2)$ is the Heaviside step function. For real k we can also express the bulk-to-bulk propagator in terms of the bulk-to-boundary propagator as:

$$G(k; \eta_1, \eta_2) = iP_k \left(K^*(k, \eta_1) K(k, \eta_2) \theta(\eta_1 - \eta_2) + (\eta_1 \leftrightarrow \eta_2) - K(k, \eta_1) K(k, \eta_2) \right), \tag{2.2.13}$$

where the power spectrum P_k is given by:

$$P_k = |\phi^+(k, \eta_0)|^2. \tag{2.2.14}$$

Notice that the bulk-to-bulk propagator is simply a Feynman propagator with an additional homogeneous term, which ensures the boundary conditions (2.2.10) are satisfied.

Feynman rules for the wavefunction We are now in a position to state the Feynman rules. Given a Feynman diagram,

- Label every vertex by a time η_i . For every vertex, write down $\int_{-\infty}^{\eta_0} \frac{d\eta_i}{a(\eta_i)^{d+1}} F(\eta_i, \{\mathbf{k}\})$, where $F(\eta_i, \{\mathbf{k}\})$ corresponds to the vertex factors from the interactions.
- For each loop in the diagram, write down $\int \frac{d^d p_l}{(2\pi)^d}$, where \mathbf{p}_l is the loop momentum.
- For every internal line, write down $G(p, \eta_l, \eta_r)$, where η_l, η_r are the time labels of the verticies the propagator is attached to and p refers to the momentum of the internal line.
- For every external line, write down $K(k, \eta_i)$, η_i refers to the time label of the vertex the propagator is attached to and k refers to the momentum of the external line.
- Multiply by an overall factor of i^{L-1} where L is the number of loops, then carry out the time integration as well as the loop momentum integration.

Let us compute the wavefunction coefficients in two simple cases.

Contact diagram Let us compute the following three point contact diagram for a single massless scalar in dS, which is given by the interaction $g\phi^3$:

The mode function for a massless scalar field in dS satisfies:

$$\left(\partial_{\eta}^{2} - \frac{2}{\eta}\partial_{\eta} + k^{2}\right)\phi^{+} = 0. \tag{2.2.16}$$

The solution is simply:

$$\phi^{+}(k,\eta) = \frac{1}{\sqrt{2k^3}} (1 - ik\eta)e^{ik\eta}.$$
 (2.2.17)

Here I set H = 1 for convenience, and set the spacetime to have (3 + 1) dimensions. Since the contact diagram only contains external lines, we only need to know the bulk-to-boundary propagators, which we can easily write down with the mode function. The wavefunction is:

$$\psi_3(k_1, k_2, k_3) = ig \int_{-\infty(1-i\epsilon)}^{\eta_0} \frac{d\eta}{\eta^4} \prod_{i=1}^3 \frac{(1-ik_i\eta)}{(1-ik_i\eta_0)} e^{ik_T(\eta-\eta_0)}.$$
 (2.2.18)

Here we defined $k_T = k_1 + k_2 + k_3$. Notice here we also added an $i\epsilon$ prescription to ensure the convergence of the integral as $\eta \to -\infty$.

To compute this integral, expand the product and carry out integration by parts. In the limit $\eta_0 \to 0$, this gives:

$$\psi_3(k_1, k_2, k_3) = 6g \left[\frac{i}{3\eta_0^3} + \frac{ik_T^2}{3\eta_0} - \frac{ie_2}{3\eta_0} + \left(e_3 - k_T e_2 + \frac{k_T^3}{3} \right) \left(\log(-ik_T \eta_0) + \gamma_E + \dots \right) \right]. \tag{2.2.19}$$

where e_2 and e_3 are defined in (1.0.6) (with ω replaced by k). In the computation we evaluated a time integral (which is an exponential integral) in the limit $\eta_0 \to 0$:

$$\int_{-\infty(1-i\epsilon)}^{\eta_0} \frac{d\eta}{\eta} e^{ik_T \eta} = \gamma_E + \log(-ik_T \eta_0) + \dots$$
 (2.2.20)

Notice all the terms in (2.2.19) are divergent as $\eta_0 \to 0$, so let's discuss them. The first three terms are all imaginary, and we need to add counterterms to remove them. Since $\Psi \sim \int \mathcal{D}\phi \, e^{iS}$, to remove them we need to modify the action with real counterterms, which is what we usually do in QFT. Also notice these terms can be expressed in terms of fields and their derivatives in position space.

There is also a term that diverges logarithmically in (2.2.19). This is an example of a secular IR divergence that is common in field theories in dS. This divergence arises because the interaction term $\mathcal{L}_{int} = \frac{g}{\eta^4}\phi^3$ diverges as $\eta \to 0$. This type of divergence is often absent when we consider interactions with derivatives. For instance, if we compute the same diagram with $\mathcal{L}_{int} = g\dot{\phi}^3$ (where the dot denotes $\frac{d}{dt} = \eta \frac{d}{d\eta}$), we obtain the following instead:

$$\psi_{3}(k_{1}, k_{2}, k_{3}) = ig \int_{-\infty}^{\eta_{0}} \frac{d\eta}{\eta^{4}} \prod_{a=1}^{3} \left(\eta \partial_{\eta} K(k_{a}, \eta) \right)$$

$$= ig \int_{-\infty}^{\eta_{0}} d\eta \, k_{1}^{2} k_{2}^{2} k_{3}^{2} \eta^{2} e^{ik_{T}(\eta - \eta_{0})}$$

$$= 6g \frac{k_{1}^{2} k_{2}^{2} k_{3}^{2}}{k_{T}^{3}}.$$
(2.2.21)

Exchange diagram As a second example let us compute the following four point exchange diagram for a single massive scalar in flat space.



Following the Feynman rules, we obtain the following expression:

$$\psi_4 = g^2 \int_{-\infty}^0 dt_1 \int_{-\infty}^0 dt_2 K(\Omega_1, \eta_1) K(\Omega_2, \eta_1) G(\Omega_s, \eta_1, \eta_2) K(\Omega_3, \eta_2) K(\Omega_4, \eta_2). \tag{2.2.22}$$

Since we are looking at flat space, the mode function is simply a plane wave, so here $K(\Omega_i, t) = e^{i\Omega_i t}$. We also have $\Omega_s = \sqrt{(\mathbf{k}_1 + \mathbf{k}_2)^2 + m^2}$. A straightforward calculation yields:

$$\psi_4 = \frac{g^2}{2\Omega_s \Omega_T E_L} + \frac{g^2}{2\Omega_s \Omega_T E_R} - \frac{g^2}{2\Omega_s E_L E_R} = \frac{g^2}{\Omega_T E_L E_R},$$
(2.2.23)

where we introduced the shorthand notation $E_L = \Omega_1 + \Omega_2 + \Omega_s$, $E_R = \Omega_3 + \Omega_4 + \Omega_s$ and $\Omega_T = \Omega_1 + \Omega_2 + \Omega_3 + \Omega_4$.

An interesting feature of this calculation is that there are cancellations of the Ω_s poles. Moreover, we can express the wavefunction coefficient for a four point exchange diagram in flat space as:

$$\Omega_T \psi_4 = \frac{g^2}{E_L E_R} = \psi_3^{\text{contact}}(\Omega_1, \Omega_2, \Omega_s) \psi_3^{\text{contact}}(\Omega_3, \Omega_4, \Omega_s). \tag{2.2.24}$$

In words, the exchange wavefunction coefficient is related to the product of two contact wavefunction coefficients. This is an example of a recursion relation for the flat space wavefunction, and we will explore this in detail in section 5.3.

2.2.1 Off-shell wavefunction coefficient

In the examples of the previous section we find that the wavefunction coefficients are expressed as functions of energies of internal and external lines. In general a scalar wavefunction coefficient can be written as follow:

$$\psi_n(\{\Omega_k\}, \{\mathbf{k}\}). \tag{2.2.25}$$

For flat space the energies are fixed to be $\Omega_k = \sqrt{|\mathbf{k}|^2 + m^2}$, while for dS (or general cosmological spacetime) the "energies" are fixed to be $\Omega_k = |\mathbf{k}|^4$. For theories with derivative interactions the wavefunction coefficients depend explicitly on the momentum \mathbf{k} , as they appear in the vertex factors⁵.

For the purpose of bootstrapping the wavefunction coefficients, fixing the energies in terms of momentum is often too restrictive. In particular we are often interested in the analytic continuation of the wavefunction coefficients in terms of its kinematics: even though such procedures often bring us to unphysical kinematics, they often give us new insight into physical observables. If we choose to analytically continue in \mathbf{k} , then it is easy to see that the analytic continuation of the wavefunction coefficients would have highly undesirable properties. For every energy variable, we introduce a new branch cut due as the energy is related to the square root of the momentum. Now we need to keep track of these branch cuts on top of additional branch cuts from the functional form of the wavefunction, for instance logarithmic branch cuts from UV divergences in loops or secular divergences due to time dependence of interactions.

⁴Technically this is an abuse of notation: there is no time translation symmetry for dS or general cosmological backgrounds. While the wavefunction are expressed as function of these "energies", we should not interpret this as some sort of conserved quantity.

 $^{^5}$ For integer spinning fields their wavefunction coefficients also depend on polarization tensors. Naturally they are contracted with other polarization tensors or ${\bf k}$

For this reason, we will study the off-shell wavefunction coefficients, which are defined as:

$$\psi_n(\{\omega\}, \{\mathbf{k}\}). \tag{2.2.26}$$

The essential difference is that the energy variables ω are no longer fixed in terms of the momentum \mathbf{k} . To recover the usual *on-shell* wavefunction coefficients, where the energies are fixed in terms of the momentum, simply substitute $\omega = \Omega_k$.

Every bootstrap rule can be written in terms of the off-shell wavefunction coefficients, and usually doing so results in less ambiguity in the bootstrap rules. For instance, the following expression:

$$\frac{\partial}{\partial k_1} \psi_3(k_1, k_2, k_3, \mathbf{k}_1, \mathbf{k}_2, \mathbf{k}_3) \tag{2.2.27}$$

is ambiguous: k_1 is the norm of \mathbf{k}_1 , therefore we need to properly state the action of the derivative on \mathbf{k}_1^6 . However, the following is unambiguous:

$$\frac{\partial}{\partial \omega_1} \psi_3(\omega_1, \omega_2, \omega_3, \mathbf{k}_1, \mathbf{k}_2, \mathbf{k}_3). \tag{2.2.28}$$

We will encounter many instances where we take derivatives with respect to the energies and/or analytically continue them. In the rest of this thesis we will implicitly assume the wavefunction coefficients are all off-shell to avoid any ambiguities.

LSZ definition for the off-shell wavefunction coefficients There is a way to define the off-shell wavefunction coefficients in terms of in-out correlators. The idea is to modify the LSZ reduction formula used for S-matricies.

Recall that perturbatively, by considering the Feynman rules, we can write an amplitude as:

$$S_n(\{\omega\}, \{\mathbf{k}\}) = \left[\prod_{v=1}^V \int_{-\infty}^{+\infty} dt_v e^{i\omega_v t_v}\right] \left[\prod_{\ell=1}^L \int \frac{d^3 \mathbf{p}_\ell}{(2\pi)^d}\right] \prod_{i=1}^I G_i^F(\{\mathbf{k}\}, \{\mathbf{p}\}), \tag{2.2.29}$$

One can show that this expression can be written as:

$$\left[\prod_{j=1}^{n} \int_{-\infty}^{+\infty} dt_{j} e^{i\omega_{j}t_{j}} \mathcal{E}_{j}\right] \langle \Omega_{\text{out}} | T \hat{\Phi}_{\mathbf{k}}(t_{1}) ... \hat{\Phi}_{\mathbf{k}_{n}}(t_{n}) | \Omega_{\text{in}} \rangle_{c} = \mathcal{S}_{n} \left(\{\omega\}, \{\mathbf{k}\}\right) \delta_{D}^{(3)} \left(\mathbf{k}_{1} + ... + \mathbf{k}_{n}\right) . \quad (2.2.30)$$

T represents the time ordering of operators, and the subscript c reminds us to only consider the connected components. The details of the derivation are provided in most QFT textbooks, for example see [103]. (2.2.30) can be interpreted as follow: the operators \mathcal{E} amputates the in-out time ordered correlator, and by putting the energies on-shell this recovers the amplitude.

Notice how (2.2.29) looks similar to the expression for the off-shell wavefunction coefficient. It seems reasonable that we can define an LSZ procedure in flat space. Let us consider the case in flat space, where

⁶This is because we can write $\mathbf{k}_1 = k_1 \hat{\mathbf{k}}_1$. Differentiating $\hat{\mathbf{k}}_1$ gives zero if $\hat{\mathbf{k}}_1$ is independent of k_1 . But now we have to worry about how to define $\hat{\mathbf{k}}_1$, and whether we can define it independently of k_1 . By going off-shell we avoid this ambiguity altogether.

in perturbation theory the wavefunction coefficients can be written as:

$$\psi(\{\omega\}, \{\mathbf{k}\}) = \left[\prod_{v=1}^{V} \int_{-\infty}^{0} dt_{v} e^{i\omega_{v} t_{v}}\right] \left[\prod_{\ell=1}^{L} \int \frac{d^{3} \mathbf{p}_{\ell}}{(2\pi)^{d}}\right] \prod_{i=1}^{I} G_{i}(\{\mathbf{k}\}, \{\mathbf{p}\}).$$
 (2.2.31)

There are two key differences between amplitudes and wavefuntion coefficients:

- The out-state is not in the asymptotic future, but rather a state at t=0. Therefore the time integration domain is $-\infty < t < 0$.
- Bulk-to-boundary propagators are used rather than Feynman propagators. While this does not affect the amputation procedure (as the difference between the Feynman and bulk-to-bulk propagator is a term which vanishes after the action of \mathcal{E}), the difference is reflected in the out-state we choose. In particular, since we chose $G \to 0$ as $t \to 0$, we should choose a state with zero field fluctuation.

Based on this, we can show that the wavefunction coefficient as:

$$\left[\prod_{j=1}^{n} \int_{-\infty}^{0} dt_{j} \, e^{i\omega_{j}t_{j}} \mathcal{E}_{j} \right] \langle \phi(0) = 0 | T \, \hat{\Phi}_{\mathbf{k}_{1}}(t_{1}) ... \hat{\Phi}_{\mathbf{k}_{n}}(t_{n}) \, | \Omega_{\mathrm{in}} \rangle_{c} = \psi_{n} \left(\{\omega\}, \{\mathbf{k}\} \right) \, \tilde{\delta}_{D}^{(3)} \left(\sum_{a}^{n} \mathbf{k}_{a} \right) \,, \quad (2.2.32)$$

where $|\phi(0) = 0\rangle$ is the field eigenstate annihilated by $\hat{\Phi}_{\mathbf{k}}(t)$ at t = 0.

We can also write down the dS wavefunction in a similar manner: just use \mathcal{E} for the equation of motion in dS, and replace $e^{i\omega_j t_j}$ with the bulk-to-boundary propagators $K_{\omega_j}(\eta)$.

2.3 In-in correlators

We do not measure the wavefunction directly from cosmological observations. This priviledge belongs to *in-in correlators*. They are defined as follow:

$$_{\text{in}}\langle 0|O_1(\mathbf{k}_1,\eta_1)\dots O_n(\mathbf{k}_n,\eta_n)|0\rangle_{\text{in}}.$$
 (2.3.1)

Here $O(\mathbf{x}, \eta)$ are field operators and $|0\rangle_{\text{in}}$ is the vacuum state in the far past (and we usually take the Bunch-Davies vacuum). In cosmology we are interested in the case $O(\mathbf{k}, \eta) = \zeta(\mathbf{k})$, since these are the correlation functions which are eventually extrapolated to the correlations of the CMB and LSS.

Notice that the correlator is sandwiched by two in vacuum state, rather than one in vacuum and one out vacuum state (which is the object computed in everyone's first QFT course), hence the name in-in correlator. These objects have an incredibly rich history in condensed matter physics, where it is used to study out-of-equilibrium systems [104]. The formalism for computing these in-in correlators is commonly referred to as in-in formalism, or Schwinger-Keldysh formalism, and they are necessary under the following context⁷.

• The system has dissipation and hence time evolution is not unitary. If we consider inflation as an EFT, where there are higher energy degrees of freedoms, in principle energy can flow from the inflaton to these extra degrees of freedom. However we will not explore this in depth here.

⁷In cases where interactions can be turned off in the far past and future, and in cases where there is thermal equilibrium, one can simply obtain the in-in correlator from an in-out correlator, see [105].

• Interactions cannot be turned off in the far future. This is always true in our case even if we consider a single field scalar in dS, as the effects from the expanding background cannot be ignored. For example, a ϕ^3 theory in dS has $\mathcal{L}_{int} = \frac{g}{\eta^4}\phi^3$, which diverges as we move towards the boundary $\eta \to 0$.

2.3.1 Feynman rules for in-in correlators

In-in correlators has its own Feynman rules, which we will state here [106].

- Draw vertices corresponding to the interaction terms in the action.
- Label each vertex as time ordered or anti-time ordered. Time-ordered vertices are drawn as shaded circles, and anti-time ordered vertices as open circles. Also assign to each vertex a conformal time η_a with a = 1, ..., I labelling the I internal lines. Diagrams with opposite labelling are related by complex conjugation as in (4.4.4).
- In addition to factors of i arising from spatial derivatives, each time-ordered vertex carries another factor of -i and each anti-time ordered vertex a factor of i. Since all possible time orderings are summed over, if a diagram contains an even number of spatial derivatives in total, only its real part appears in the final correlator. Similarly, with an odd number of spatial derivatives, only the imaginary part appears.
- Draw internal lines connecting the vertices pairwise. Assign each internal line a 3-momentum \mathbf{p} . For each $\phi(\mathbf{k}_i)$ in the correlator, draw one external line, connecting a vertex to a horizontal line representing the asymptotic future. Label each external line with its associated 3-momentum \mathbf{k}_i . Write down a 3-momentum conserving δ distribution for each vertex. The total number of lines meeting at each vertex is fixed as usual by the fields appearing in the relevant interaction.
- With $f_k(\eta)$ the mode function for a given field, for each line, write down a propagator as follows:

(2.3.7)

 $=G_{-}(\mathbf{k},\eta)=f_{k}(\eta)f_{k}^{*}(\eta_{f})$

- Integrate over all momenta of internal lines and over the conformal times η_i of the vertices, with a factor of $a^{1+d}(\eta_i)$, where a is the scale factor and d the number of spatial dimensions, for each conformal time η_i .
- Multiply by a combinatorial factor depending on the number of ways of contracting fields in the vertices to produce the same diagram.

Notice the number of Feynman diagrams increases as 2^V , where V is the number of vertices. For example, a tree level exchange process requires four Feynman diagrams. This is one of the main advantages of working with wavefunction coefficients: the number of diagrams do not increase exponentially with V.

2.3.2 In-in correlators from the wavefunction

Since in-in correlators are the physical observables, we would like to relate the wavefunction coefficients, which are the objects we bootstrap. This is given by the Born rule, which is simply:

$$\langle \phi(\mathbf{k}_1, \eta_0) \dots \phi(\mathbf{k}_n, \eta_0) \rangle = \int D\phi_0 |\Psi[\phi_0, \eta_0]|^2 \phi_0(\mathbf{k}_1, \eta_0) \dots \phi_0(\mathbf{k}_n, \eta_0)$$
(2.3.8)

By expanding $|\Psi|^2$, we can express in-in correlators in terms of wavefunction coefficients. Concretely, let us define:

$$\rho_n(\{\omega\}, \{\mathbf{k}\}) = \psi_n(\{\omega\}, \{\mathbf{k}\}) + \psi_n^*(\{\omega\}, -\{\mathbf{k}\})$$
(2.3.9)

Since we are expanding the modulus of Ψ , the in-in correlators are written in terms of ρ_n . For a parity even theory ρ_n is simply 2 Re ψ_n . At tree level an *n*-point in-in correlator is given by ρ_n and lower point wavefunction coefficients. For example, let us consider the two point function (i.e. the power spectrum):

$$\langle \phi(\mathbf{k}_1)\phi(\mathbf{k}_2)\rangle = (2\pi)^d \delta^{(d)}(\mathbf{k}_1 + \mathbf{k}_2) P_k. \tag{2.3.10}$$

Then we have the following:

$$P_{\omega} = \frac{1}{\rho_2(\omega)}.\tag{2.3.11}$$

There are similar relations for higher point functions. Let us define:

$$\langle \phi(\mathbf{k}_1) \dots \phi(\mathbf{k}_n) \rangle = (2\pi)^d \delta^{(d)} \left(\sum_{a=1}^n \mathbf{k}_a \right) B_n(\{\mathbf{k}\}, \{\omega\}).$$
 (2.3.12)

Then, for three point and four point correlators at tree level are given by:

$$B_3(\omega_1, \omega_2, \omega_3) = -\frac{\rho_3(\omega_1, \omega_2, \omega_3)}{\prod_{a=1}^3 \rho_2(\omega_a)}$$
(2.3.13)

$$B_4(\omega_1, \omega_2, \omega_3, \omega_4) = -\frac{1}{\prod_{a=1}^4 \rho_2(\omega_a)} \left[\rho_4 - \frac{\rho_3 \rho_3}{\rho_2} \right]$$
 (2.3.14)

At loop level this is more complicated. We can obtain new loop contributions from integrating tree level wavefunction coefficients. Diagrammatically this can be interpreted as taking tree level wavefunction coefficients and gluing external legs together to form loops. For example, at one loop order,

$$B_4(\omega_1, \omega_2, \omega_3, \omega_4) = \rho_4^{1L}(\omega_1, \omega_2, \omega_3, \omega_4) + \int_{\mathbf{p}} P_p \rho_6^{\text{tree}}(\omega_1, \omega_2, \omega_3, \omega_4, \omega_p, \omega_p)$$
 (2.3.15)

Notice there is a contribution from ρ_6^{tree} , i.e. the tree level wavefunction coefficient ψ_6 . Another example would be the one loop power spectrum, which schematically can be written as:

$$P_{\omega}^{1L} = (P_{\omega}^{\text{tree}})^{2} \rho_{2}^{1L}(\omega) + \frac{1}{4!} \int_{\mathbf{p}} P_{p} \rho_{4}^{\text{tree}}(\omega, \omega_{p}, \omega_{p}, \omega) + \frac{1}{2} \frac{1}{(3!)^{2}} \int_{\mathbf{p}} P_{p_{1}} P_{p_{2}} \rho_{3}^{\text{tree}}(\omega, \omega_{p_{1}}, \omega_{p_{2}}) \rho_{3}^{\text{tree}}(\omega, \omega_{p_{1}}, \omega_{p_{2}}),$$

$$(2.3.16)$$

where $\mathbf{p}_1 = \mathbf{p}$ and $\mathbf{p}_2 = \mathbf{k} - \mathbf{p}$. Similarly at two loops one would expect the in-in correlator to get contributions from the one loop and tree level wavefunction coefficients as well.

Chapter 3

The consequences of unitarity

One of the most essential features of quantum mechanics is the ability to interpret the overlap between states as probability of a measurement. For this to be true, we require two features:

- Norm of states are positive. This is obvious as negative probabilities do not make sense.
- Norm of states are preserved. Probability of all possible measurements need to add up to one, and
 for this reason we commonly normalize the initial states to have unit norm. However, if the norm
 of a state changes over time, we cannot interpret overlap of states as probabilities as they no longer
 add up to one.

These features are collectively known as unitarity. In this section we will explore the consequences of unitary time evolution in perturbation theory: namely, the wavaefunction coefficients must obey a set of consistent relations known as the cosmological optical theorem. Graphically, they are represented as a set of cutting rules which relate larger and more complicated Feynman diagrams to smaller and simpler diagrams. We will explain how to prove the cosmological optical theorem for fields with any mass, integer spin and in any FLRW spacetime (which admits a Bunch-Davies vacuum), and provide some simple examples. In the end we will briefly discuss extensions of the cutting rules to loop level as well as beyond perturbation.

3.1 The cosmological optical theorem

In quantum mechanics, time evolution is governed by a time evolution operator $\hat{U}(t,t_0)$, i.e. we have $|\psi(t)\rangle = \hat{U}(t,t_0)|\psi(t_0)\rangle$. In order for the norm of the state to be preserved under time evolution, these time evolution operators must satisfy the following relation:

$$\hat{U}^{\dagger}\hat{U} = 1. \tag{3.1.1}$$

As long as the norm of states at some time t_0 are all positive, they will continue to have positive norm at any given time t. We are interested in exploring the consequences of this constraint in perturbation theory, and to do this let us move to the interaction picture. Here the time evolution operator for the

states is given by:

$$\hat{U}(t, t_0) = \mathcal{T} \exp\left(-i \int_{t_0}^t dt' \, \hat{H}_{\text{int}}(t')\right), \tag{3.1.2}$$

where \mathcal{T} denotes time ordering of operators. Since we are in perturbation theory, we can expand the exponential and obtain a series in terms of \hat{H}_{int} . Schematically, we can write the following:

$$\hat{U} = 1 + \delta \hat{U}. \tag{3.1.3}$$

Therefore, (3.1.1) implies the following:

$$\delta \hat{U} + \delta \hat{U}^{\dagger} = -\delta \hat{U}^{\dagger} \delta \hat{U}. \tag{3.1.4}$$

(3.1.4) is a non-linear equation which links different orders of perturbation theory together. This is telling us that different orders in perturbation theory are not completely independent under unitary time evolution. Now we need to understand how to convert this formal expression into a relation between wavefunction coefficients in perturbation theory.

Review: optical theorem for amplitudes To get a hint on how to proceed, let us review perturbative unitarity for amplitudes. In this case we can write (3.1.4) as:

$$\langle \mathbf{k}_{1} \dots \mathbf{k}_{n} | \delta \hat{U} | \mathbf{k}_{1'} \dots \mathbf{k}_{m'} \rangle + \langle \mathbf{k}_{1} \dots \mathbf{k}_{n} | \delta \hat{U}^{\dagger} | \mathbf{k}_{1'} \dots \mathbf{k}_{m'} \rangle = -\langle \mathbf{k}_{1} \dots \mathbf{k}_{n} | \delta \hat{U}^{\dagger} \delta \hat{U} | \mathbf{k}_{1'} \dots \mathbf{k}_{m'} \rangle. \tag{3.1.5}$$

Here $|\mathbf{k}_1 \dots \mathbf{k}_n\rangle$ is an *n*-particle state. Here we recognize the term on the left hand side is in fact a *n* to *m* amplitude plus its conjugate:

$$A_{m\to n} = -i\langle \mathbf{k}_1 \dots \mathbf{k}_n | \delta \hat{U} | \mathbf{k}_{1'} \dots \mathbf{k}_{m'} \rangle, \quad A_{n\to m}^* = i\langle \mathbf{k}_1 \dots \mathbf{k}_n | \delta \hat{U}^{\dagger} | \mathbf{k}_{1'} \dots \mathbf{k}_{m'} \rangle. \tag{3.1.6}$$

By inserting the identity operator $\not \pm_X |X\rangle\langle X|$ (here $\not \pm_X$ simply denotes summing over all intermediate states), the right hand side can also be expressed in terms of a product of amplitudes as well. More concretely,

$$2\text{Im } A_{m \to n} = \sum_{X} A_{n \to X}^* A_{m \to X}. \tag{3.1.7}$$

This is known as the *optical theorem*. This result can be used to relate decay rate to scattering amplitudes given by exchange processes, relate forward scattering amplitude to the total cross section, etc (for more details see any QFT textbook, for example [103]). The goal for the rest of this section is to derive a similar relation for wavefunction coefficients.

Cosmological Optical Theorem: first derivation This discussion follows the derivation presented in [100]. Let us consider the simple case of $H_{\text{int}} = \lambda \phi^3$ in dS. To proceed, let us follow the derivation of the optical theorem for amplitudes, but replace the ket state with $|0\rangle$:

$$\langle \mathbf{k}_1 \dots \mathbf{k}_3 | \delta \hat{U} | 0 \rangle + \langle \mathbf{k}_1 \dots \mathbf{k}_3 | \delta \hat{U}^{\dagger} | 0 \rangle = -\langle \mathbf{k}_1 \dots \mathbf{k}_3 | \delta \hat{U}^{\dagger} \delta \hat{U} | 0 \rangle. \tag{3.1.8}$$

Now we write the left hand side as wavefunction coefficients. We have:

$$\langle \mathbf{k}_1 \dots \mathbf{k}_3 | \delta \hat{U} | 0 \rangle = \psi_3(\omega_1, \omega_2, \omega_3, \mathbf{k}_1, \mathbf{k}_2, \mathbf{k}_3). \tag{3.1.9}$$

However,

$$\langle \mathbf{k}_1 \dots \mathbf{k}_3 | \delta \hat{U}^{\dagger} | 0 \rangle \neq \psi_3^*(\omega_1, \omega_2, \omega_3, \mathbf{k}_1, \mathbf{k}_2, \mathbf{k}_3).$$
 (3.1.10)

Let us consider the leading order $\mathcal{O}(\lambda)$ and see what $\langle \mathbf{k}_1 \dots \mathbf{k}_3 | \delta \hat{U}^{\dagger} | 0 \rangle$ is. In terms of Feynman diagrams this correspond to a contact diagram, i.e. a diagram with no internal lines. We have:

$$\langle \mathbf{k}_1 \dots \mathbf{k}_3 | \delta \hat{U}^{\dagger} | 0 \rangle = \lambda^* \int_{-\infty}^{\eta_0} \frac{d\eta}{\eta^4} \prod_{i=1}^3 K(\omega_i, \eta).$$
 (3.1.11)

Now we exploit a crucial property of the bulk-to-boundary propagators for fields satisfying Bunch-Davies initial condition:

$$K(\omega, \eta) = K^*(-\omega^*, \eta). \tag{3.1.12}$$

We refer to this property as Hermitian analyticity, and we refer to $K^*(-\omega^*, \eta)$ as the Hermitian analytic image of $K(\omega, \eta)$. We will explore this property in detail in section 3.2. For now, to convince ourselves that this is indeed true, let us look at two simple examples. For massless scalars we have:

$$K(-\omega^*, \eta) = \left[(1 + i\omega^* \eta) e^{-i\omega^* \eta} \right]^* = (1 - i\omega \eta) e^{i\omega \eta} = K(\omega, \eta). \tag{3.1.13}$$

Similarly, for conformally coupled scalars we also have:

$$K(-\omega^*, \eta) = \left[\frac{\eta}{\eta_0} e^{-i\omega^* \eta}\right]^* = \frac{\eta}{\eta_0} e^{i\omega \eta} = K(\omega, \eta). \tag{3.1.14}$$

If the bulk-to-boundary propagator is Hermitian analytic, we can write:

$$\langle \mathbf{k}_1 \dots \mathbf{k}_3 | \delta \hat{U}^{\dagger} | 0 \rangle = \lambda^* \int_{-\infty}^{\eta_0} \frac{d\eta}{\eta^4} \prod_{i=1}^3 K^*(-\omega_i^*, \eta) = \psi_3^*(-\omega_1^*, -\omega_2^*, -\omega_3^*).$$
 (3.1.15)

Let us look at the right hand side of (3.1.8). After inserting the identity operator, it becomes:

$$- \sum_{X} \langle \mathbf{k}_{1} \dots \mathbf{k}_{3} | \delta \hat{U}^{\dagger} | X \rangle \langle X | \delta \hat{U} | 0 \rangle.$$
 (3.1.16)

Conveniently, at $\mathcal{O}(\lambda)$ this is zero. Therefore we have the following result:

The cosmological optical theorem (for contact diagram)

$$\psi_3(\omega_1, \omega_2, \omega_3) + \psi_3^*(-\omega_1^*, -\omega_2^*, -\omega_3^*) = 0. \tag{3.1.17}$$

Generalizing this result for more complicated diagrams proved to be a challenge. This is because if we look at (3.1.16), we notice that $\langle \mathbf{k}_1 \dots \mathbf{k}_3 | \delta \hat{U}^{\dagger} | X \rangle$ is not simply a wavefunction coefficient or its complex conjugate. It is entirely possible to work in canonical quantization and express this object in terms of a

combination of wavefunction coefficients (and this is how the cosmological optical theorem was derived for an exchange diagram in [100]¹), but as the Feynman diagram grows more complicated, the derivation becomes more cumbersome. Let us explore a different path forward.

The Disc operator Let us define the *Disc* operator as follow:

$$\operatorname{Disc}_{\omega_{1}...\omega_{i}} f(\omega_{1}...\omega_{i}, \omega_{i+1}...\omega_{n}, \{\mathbf{k}\}) = f(\omega_{1}...\omega_{i}, \omega_{i+1}...\omega_{n}, \{\mathbf{k}\}) - f^{*}(\omega_{1}...\omega_{i}, -\omega_{i+1}^{*}...-\omega_{n}^{*}, -\{\mathbf{k}\}).$$

$$(3.1.18)$$

There are a few things to note about this Disc operator:

- The argument in f^* is changed, and so this cannot be interpreted as the usual discontinuity (which is $\lim_{\epsilon \to 0^+} f(x + i\epsilon) f(x i\epsilon)$).² We are only calling it "Disc" because its role in the cosmological optical theorem is reminiscent of a discontinuity.
- If an energy argument appears below the Disc operator, it remains unchanged. Otherwise the energy is analytically continued to $-\omega^*$. Note that this implies that we are allowed to analytically continue the function from ω to $-\omega^*$. We will see in section 5.2 that we can always analytically continue $\psi_n(\omega)$ in this way for external energies ω , as wavefunction coefficients are always analytic in the lower half complex plane. However, for internal energies this is less clear. For tree level diagrams we expect this to be true (at least for flat space and dS), since the bulk-to-bulk propagators are expressed in terms of Hankel functions (which only has a branch cut in the negative real axis). We leave a detailed study of analyticity in internal off-shell energy to the future.
- The momentum in f^* is always flipped: in particular we always have to flip the momentum even if it corresponds to the momentum of an internal line (regardless of whether its corresponding energy is flipped or not). This is enforced by momentum conservation.

Based on our experience with the contact diagram, the expectation is that we can express the left hand side of (3.1.4) as the Disc of some wavefunction coefficients. Therefore, instead of trying to work everything out directly from (3.1.4), let us ask the following question directly: given a Feynman diagram corresponding to a wavefunction coefficient ψ_n , what is $Disc \psi_n$?

In the remainder of the section we will proof the following for a wavefunction coefficient ψ_{n+m} from a general tree level diagram:

The cosmological optical theorem (for any tree level diagram)

$$\operatorname{Disc}_{\omega_{s}} i\psi_{n+m}(\{\omega\}; \omega_{p_{1}}, \dots, \omega_{s}, \dots, \omega_{p_{I}}; \{\mathbf{k}\}) = -iP_{\omega_{s}} \operatorname{Disc}_{\omega_{s}} i\psi_{n+1}(\omega_{1}, \dots, \omega_{n}, \omega_{s}; \{\omega_{p}\}; \{\mathbf{k}\}) \times \operatorname{Disc}_{\omega_{s}} i\psi_{m+1}(\omega_{n+1}, \dots, \omega_{m+n}, \omega_{s}; \{\omega_{p}\}; \{\mathbf{k}\}).$$

$$(3.1.19)$$

Here ω_p and ω_s are energies for internal lines (which we have taken off-shell and analytically continued). It is much easier to understand this expression in terms of Feynman diagrams, where it manifests itself as a set of *cutting rules*, see figure 3.1.

¹An alternative derivation from the perspective of Schrödinger equation is also presented in [107]

²Nonetheless, this can be treated as the usual discontinuity in the variables $\omega_{i+1}^2 \dots \omega_n^2$. To see this, take $\omega = |\omega| - i\epsilon$ (so

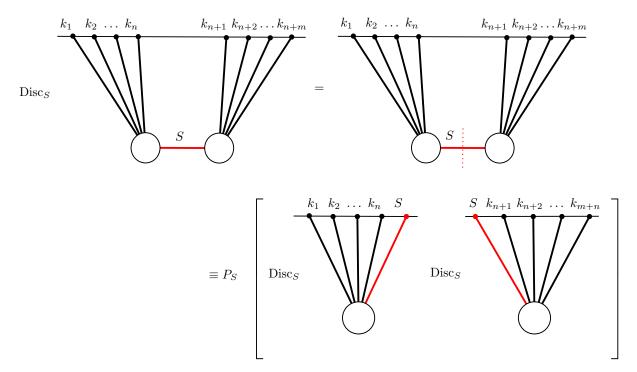


Figure 3.1: Diagrammatic representation of the single-cut rules defined in (3.1.19) demonstrating the interpretation of the right-hand side as the cutting of an internal line in the diagram on the left-hand side. A cut line is pushed to the bounday, i.e. it is substituted by two external lines and a factor of the power spectrum. The discontinuity should be taken of each of the two resulting diagrams. The circles represent an arbitrary tree-level diagram with any number of internal lines.

Proof of the cosmological optical theorem For simplicity we will consider theories with scalar fields. We will generalize to spinning fields in section 3.3.

Consider a general tree-level diagram representing a perturbative contribution to ψ_n . Applying the Feynman rules for a wavefunction coefficient, the diagram translates into the following expression:

$$\psi_n(\{\omega\}; \{\omega_p\}, \omega_s; \{\mathbf{k}\}) = -i \int \left(\prod_A^V d\eta_A F_A(\mathbf{k}, \mathbf{p}) \right) \left(\prod_a^n K_{\omega_a} \right) \left(\prod_i^{I-1} G_{\omega_{p_i}} \right) G_{\omega_s} , \qquad (3.1.20)$$

where we have written the momentum for internal lines as **p**. We would like to compute $\underset{\omega_s}{\text{Disc}} \psi_n(\{\omega\}; \{\mathbf{k}\})$, where ω_s is an (off-shell) internal energy. To do this we would need to know the Hermitian analytic image of $\psi_n(\{\omega\}; \{\omega_p\}; \{\mathbf{k}\})$. We have:

$$\psi_{n}^{*}(\{-\omega^{*}\};\{-\omega_{p}^{*}\},\omega_{s};\{-\mathbf{k}\}) = i \int \left(\prod_{A}^{V} d\eta_{A} F_{A}^{*}(-\mathbf{k},-\mathbf{p})\right) \times \left(\prod_{a}^{n} K_{-\omega_{a}^{*}}^{*}\right) \left(\prod_{i}^{I-1} G_{-\omega_{p_{i}}^{*}}^{*}\right) G_{\omega_{s}}^{*},$$
(3.1.21)

Now we use the following:

we have
$$\omega^2 = |\omega|^2 - i\epsilon$$
, then $(-\omega^*)^2 = |\omega|^2 + i\epsilon$, so $\operatorname{Disc} f(\omega) = -\operatorname{disc}_{\omega^2} f(\omega^2) = \lim_{\epsilon \to 0^+} f(\omega^2 - i\epsilon) - f^*(\omega^2 + i\epsilon)$

• Unitarity Since $U = \exp(-i \int d\eta H_{\text{int}}(\eta))$, unitarity implies H_{int} is Hermitian. In terms of Feynman rules this translates to the following:

$$F_A(\mathbf{k}, \mathbf{p}) = F_A^*(-\mathbf{k}, -\mathbf{p}). \tag{3.1.22}$$

This is simply the multivariable version of the statement that if we have a real function f(x), its Fourier transform f(k) necessarily obeys $f(k) = f^*(-k)$.

• Bunch-Davies vacuum Bulk-to-boundary propagators for fields satisfying Bunch-Davies initial condition are Hermitian analytic, i.e. $K(\omega, \eta) = K^*(-\omega^*, \eta)$. In addition, this also implies the following for the bulk-to-bulk propagator:

$$G_{\omega_p}(\eta, \eta') = G^*_{-\omega_x^*}(\eta, \eta').$$
 (3.1.23)

Once again we will postpone the discussion of this condition to section 3.2.

• Factorization of bulk-to-bulk propagator We will also need the following:

$$\operatorname{Im} G_{\omega_s}(\eta, \eta') = 2P_{\omega_s} \operatorname{Im} K(\omega_s, \eta) \operatorname{Im} K(\omega_s, \eta'). \tag{3.1.24}$$

The imaginary part of the bulk-to-bulk propagator factorizes. This is the crucial property which allow us to "cut" internal propagators, and can easily be proven from (2.2.13).

From the properties above, it is very easy to see the following:

$$\psi_n^*(\{-\omega^*\}; \{-\omega_p^*\}, \omega_s; \{-\mathbf{k}\}) = i \int \left(\prod_A^V d\eta_A F_A(\mathbf{k}, \mathbf{p}) \right) \times \left(\prod_a^n K_{\omega_a} \right) \left(\prod_i^{I-1} G_{\omega_{p_i}} \right) G_{\omega_s}^*.$$
(3.1.25)

Therefore, the Disc of the wavefunction is:

$$\operatorname{Disc}_{\omega_{s}} i\psi_{n+m}^{*}(\{\omega\}; \{\omega_{p}\}, \omega_{s}; \{-\mathbf{k}\}) = -\int \left(\prod_{A}^{V} d\eta_{A} F_{A}(\mathbf{k}, \mathbf{p})\right) \left(\prod_{a}^{n} K_{\omega_{a}}\right) \left(\prod_{m}^{I-1} G_{\omega_{p_{m}}}\right) 2\operatorname{Im} G_{\omega_{s}}$$

$$= -\int \left(\prod_{A}^{V_{L}} d\eta_{A} F_{A}(\mathbf{k}, \mathbf{p})\right) \left(\prod_{B}^{V_{R}} d\eta_{B} F_{B}(\mathbf{k}, \mathbf{p})\right) \left(\prod_{a}^{n} K_{\omega_{a}}\right) \left(\prod_{b}^{m} K_{\omega_{b}}\right)$$

$$\times \left(\prod_{i}^{I_{L}} G_{\omega_{p_{i}}}\right) \left(\prod_{j}^{I_{R}} G_{\omega_{p_{j}}}\right) 4P_{\omega_{s}} \operatorname{Im} K(\omega_{s}, \eta_{l}) \operatorname{Im} K(\omega_{s}, \eta_{r}), \qquad (3.1.26)$$

where we have used $V_L(V_R)$ to denote the collection of verticies on the left (right) side of the cut line (and similarly for $I_L(I_R)$). It is straightforward to see that the right hand side is simply $P_{\omega_s} \underset{\omega_s}{\text{Disc}} \psi_{n+1} \underset{\omega_s}{\text{Disc}} \psi_{m+1}$, which completes the proof of (3.1.19).

³Another simple way to see this is that when we take derivative of fields we get $\partial_i \to ik_i$, so the minus sign of **k** cancels with the minus sign from complex conjugate.

The cosmological optical theorem continues to hold true even if the interaction involves time derivatives (in which case we have to take derivative of the propagators) [1]. For details see appendix A.

3.2 Hermitian analyticity

Our derivation relies heavily on the fact that bulk-to-boundary propagators for fields satisfying the Bunch-Davies initial condition obeys Hermitian analyticity, i.e. $K(\omega, \eta) = K^*(-\omega^*, \eta)$. We will now demonstrate that this is true for a massive field in a fairly generic FLRW background spacetime, assuming the equation of motion for the free field is also Hermitian analytic.

Bulk-to-boundary propagator We will consider here scalar fields with a quadratic action of the form

$$S = \int d\eta \, d^3 \mathbf{x} \, a^2(\eta) \, \left(\frac{1}{2} \phi'^2 - \frac{c_s^2(\eta)}{2} (\partial_i \phi)^2 - \frac{1}{2} a^2(\eta) m^2(\eta) \phi^2 \right) \,. \tag{3.2.1}$$

This is the most general quadratic action of a real scalar field to leading (quadratic) order in derivatives. The mode functions $\phi(k, \eta)$ satisfy a second order differential equation of the form⁴

$$\phi_k''(\eta) + p(k, \eta)\phi_k'(\eta) + q(k, \eta)\phi_k(\eta) = 0, \qquad (3.2.2)$$

where

$$p(k,\eta) = \frac{2a'}{a}, \qquad q(k,\eta) = c_s^2(\eta)k^2 + a^2(\eta)m^2(\eta),$$
 (3.2.3)

and the prime denotes time derivative. We will assume that c_s , a, $\frac{a'}{a}$ and m are real and analytic functions. Generically this equation has two independent solutions, and following the procedure described in 2.2 we take the solution which satisfies

$$\lim_{\eta \to -\infty} \phi_k^+(\eta) \propto a^{-1}(\eta) e^{ic_s k\eta} \tag{3.2.4}$$

and construct the bulk-to-boundary propagator $K(k,\eta) = \phi_k^+(\eta)/\phi_k^+(\eta_0)$. Proving Hermitian analyticity amounts to proving the following:

$$\phi_k^+(\eta) = A(k, \eta_0) [\phi_{-k^*}^+(\eta)]^*. \tag{3.2.5}$$

In other words, $\phi_k^+(\eta)$ and $[\phi_{-k^*}^+(\eta)]^*$ are linearly dependent. It is well known [108] that two solutions of the same differential equation are linearly dependent if their Wronskian, namely

$$W(k,\eta) \equiv W\left(\phi^{+}(k,\eta), \left[\phi^{+}_{-k^{*}}(\eta)\right]^{*}\right) = \phi_{k}^{+}(\eta) \,\,\partial_{\eta} \left[\phi^{+}_{-k^{*}}(\eta)\right]^{*} - \left[\phi^{+}_{-k^{*}}(\eta)\right]^{*} \,\partial_{\eta}\phi_{k}^{+}(\eta), \tag{3.2.6}$$

vanishes everywhere. Furthermore, if two functions both satisfy the same differential equation of the form in (3.2.2) and their Wronskian is zero at some point η_i then, because the Wronskian is given by

$$W(k,\eta) = W(k,\eta_i)e^{-\int_{\eta_i}^{\eta} p(k,\eta')d\eta'},$$
(3.2.7)

⁴Here we will express the energies as k, i.e. on-shell energy, but it is natural to extend the derivation to off-shell quantities.

it must vanish everywhere (see e.g. [109]) by virtue of the assumption that p and q are analytic on this domain.

First let us show that $\left[\phi_{-k^*}^+(\eta)\right]^*$ is indeed a solution to the same equation of motion under the assumption that p and q are Hermitian analytic. We take the complex conjugate of (3.2.2) and replace $k \to -k^*$ everywhere to give

$$\partial_{\eta}^{2} \left[\phi_{-k^{*}}^{+}(\eta) \right]^{*} + p^{*}(-k^{*}, \eta) \partial_{\eta} \left[\phi_{-k^{*}}^{+}(\eta) \right]^{*} + q^{*}(-k^{*}, \eta) \left[\phi_{-k^{*}}^{+}(\eta) \right]^{*} = 0.$$
 (3.2.8)

This equation of motion coincides with (3.2.2) if p and q are Hermitian analytic.

Since c_s and a are real, it is very straightforward to see that:

$$\lim_{n \to -\infty} W(k, \eta) = 0. \tag{3.2.9}$$

With this we have shown that the bulk-to-boundary propagators are Hermitian analytic if the equation of motion is also Hermitian analytic.

We would like to understand when it is valid to impose Bunch-Davies initial condition. A careful analysis reveals the following:

• $c_s k \eta$ diverges in the infinite past, otherwise the mode function does not behave like a plane wave. In other words,

$$\lim_{n \to -\infty} c_s k \neq 0. \tag{3.2.10}$$

• (3.2.4) has no dependence on m or a (except through the prefactor of a^{-1}). By rewriting (3.2.2) as

$$(a(\eta)\phi_k(\eta))'' + \left(c_s^2(\eta)k^2 + a^2(\eta)m^2(\eta) - \frac{a''(\eta)}{a(\eta)}\right)a(\eta)\phi_k(\eta) = 0,$$
(3.2.11)

we see that the last two terms multiplying $a\phi_k$ must be negligible compared to $c_s^2k^2$ in this limit,

$$\lim_{n \to -\infty} am \ll c_s k \,, \tag{3.2.12}$$

$$\lim_{n \to -\infty} \frac{a''}{a} \ll c_s^2 k^2. \tag{3.2.13}$$

 \bullet For the solution to behave like a plane wave c_s needs to be approximately constant. To quantify this we insert this asymptotic solution into the differential equation which gives

$$\lim_{\eta \to -\infty} c_s^2 k^2 \left(-2 \frac{c_s'}{c_s} \eta - \left(\frac{c_s'}{c_s} \eta \right)^2 + 2i \frac{c_s'}{c_s} \frac{1}{c_s k} + i \frac{c_s''}{c_s} \frac{\eta}{c_s k} \right) e^{ic_s k \eta} = 0. \tag{3.2.14}$$

For this to be an asymptotic solution, we generically require that each of the terms in the bracket

vanishes individually and so

$$\lim_{\eta \to -\infty} \frac{d \log(c_s)}{d \log(\eta)} \ll 1, \tag{3.2.15}$$

$$\lim_{\eta \to -\infty} \frac{d^2 \log(c_s)}{d \log(\eta)^2} \ll c_s k \eta. \tag{3.2.16}$$

One can also show this by making a WKB approximation (see e.g. [109]) of the mode function in a general flat FLRW spacetime, where we can see generically that $\phi_{\pm} = e^{ik\sigma_{\pm}(k,\eta)}/a$, where σ is Hermitian analytic. The details are included in Appendix B.

Bulk-to-bulk propagators In order to extend our results to diagrams with more than one internal line we also need to prove that for a generic background

$$G_{-p^*}^*(\eta, \eta') = G_p(\eta, \eta').$$
 (3.2.17)

In general the mode function $\phi_k^+(\eta)$ may have branch cuts in terms of k which may create complications when we try to prove the Hermitian analyticity of $G_p(\eta, \eta')$: namely, we may have $A^*(k, \eta_0) \left[\phi_{-k^*}^-(\eta)\right]^* \neq \phi_k^-(\eta)$. To proceed, we can bypass these issues by writing $\phi_k^-(\eta)$ purely in terms of $\phi_k^+(\eta)$. To do this we need to know the Hermitian analytic properties of $\phi_k^-(\eta)$ (i.e. the complex conjugate of $\phi_k^+(\eta)$) in addition to those of $\phi_k^+(\eta)$, which we have already established. To determine these, consider that $\phi_k^\pm(\eta)$ are defined to have a Wronskian

$$W_k(\eta) \equiv a^2(\eta) \left(\phi_k^+(\eta) \partial_\eta \phi_k^-(\eta) - \phi_k^-(\eta) \partial_\eta \phi_k^+(\eta) \right) = -i. \tag{3.2.18}$$

We can treat this as a differential equation in $\phi_k^-(\eta)$,

$$\partial_{\eta}\phi_k^-(\eta) - \frac{\partial_{\eta}\phi_k^+(\eta)}{\phi_k^+(\eta)}\phi_k^-(\eta) = -\frac{i}{a^2(\eta)\phi_k^+(\eta)},\tag{3.2.19}$$

which can be formally solved:

$$\phi_k^-(\eta) = -\phi_k^+(\eta) \int_{\eta_0}^{\eta} \frac{i}{a^2(\eta')\phi_k^+(\eta')^2} d\eta' + \frac{\phi_k^+(\eta)}{\phi_k^+(\eta_0)} \phi_k^-(\eta_0).$$
(3.2.20)

If the above assumptions are valid we can then exploit the Hermitian analytic properties of $\phi_k^+(\eta)$ to give

$$\left[\phi_{-k^*}^-(\eta)\right]^* = A(k,\eta_0)\phi_k^+(\eta) \int_{\eta_0}^{\eta} \frac{i}{a^2(\eta')\phi_k^+(\eta')^2} d\eta' + \frac{\phi_k^+(\eta)}{\phi_k^+(\eta_0)} \left[\phi_{-k^*}^-(\eta_0)\right]^*$$
(3.2.21)

$$= A(k, \eta_0) \frac{\phi_k^+(\eta)}{\phi_k^+(\eta_0)} \phi_k^-(\eta_0) - A(k, \eta_0) \phi_k^-(\eta) + \frac{\phi_k^+(\eta)}{\phi_k^+(\eta_0)} \left[\phi_{-k^*}^-(\eta_0)\right]^*, \tag{3.2.22}$$

where A was defined in (3.2.5). The bulk-to-bulk propagator (2.2.13) can be expressed in terms of the mode functions as:

$$G_p(\eta, \eta') = i\theta(\eta - \eta') \left(\phi_p^+(\eta') \phi_p^-(\eta) - \frac{\phi_p^-(\eta_0)}{\phi_p^+(\eta_0)} \phi_p^+(\eta) \phi^+(\eta') \right) + (\eta \leftrightarrow \eta'), \tag{3.2.23}$$

and its Hermitian analytic image is

$$G_{-p^*}^*(\eta, \eta') = -i\theta(\eta - \eta') \left[\phi_{-p^*}^+(\eta')\right]^* \left(\left[\phi_{-p^*}^-(\eta)\right]^* - \frac{\left[\phi_{-p^*}^-(\eta_0)\right]^*}{\left[\phi_{-p^*}^+(\eta_0)\right]^*} \left[\phi_{-p^*}^+(\eta)\right]^* \right) + \eta \leftrightarrow \eta'.$$
 (3.2.24)

Using the relationships in (3.2.5) and (3.2.22) we find this is equal to $G_p(\eta, \eta')$ and so the bulk-to-bulk propagator has to be Hermitian analytic whenever the bulk-to-boundary propagator is.

As a concrete example let us consider a massive scalar field in dS. The mode functions are:

$$\phi_k^+(\eta) = +ie^{-i\frac{\pi}{2}\left(\nu + \frac{1}{2}\right)}\sqrt{\pi}\frac{H}{2}(-\eta)^{\frac{3}{2}}H_{\nu}^{(2)}(-k\eta), \qquad (3.2.25)$$

$$\phi_k^-(\eta) = -ie^{+i\frac{\pi}{2}\left(\nu + \frac{1}{2}\right)}\sqrt{\pi}\frac{H}{2}(-\eta)^{\frac{3}{2}}H_{\nu}^{(1)}(-k\eta). \tag{3.2.26}$$

Here $\nu = \sqrt{\frac{9}{4} - \frac{m^2}{H^2}}$. Hankel functions $H_{\nu}^{(2)}(z)$ have a branch cut $-\infty < z \le 0$, so we have to be careful when we take $k \to -k^*$. We take k to have a small imaginary part, and send $-k\eta \to e^{i\pi}(-k\eta)$:

$$[\phi_{-k^*}^+(\eta)]^* = -ie^{+i\frac{\pi}{2}\left(\nu^* + \frac{1}{2}\right)}\sqrt{\pi}\frac{H}{2}(-\eta)^{\frac{3}{2}}H_{\nu^*}^{(2)}(e^{i\pi}(-k\eta)), \qquad (3.2.27)$$

$$[\phi_{-k^*}^-(\eta)]^* = +ie^{-i\frac{\pi}{2}\left(\nu^* + \frac{1}{2}\right)}\sqrt{\pi}\frac{H}{2}(-\eta)^{\frac{3}{2}}H_{\nu^*}^{(1)}(e^{i\pi}(-k\eta)). \tag{3.2.28}$$

When ν is real we will recover the original Hankel functions but when ν is purely imaginary we pick up a minus sign, this cancels with the sign change in the exponential factor as

$$H_{-\nu}^{(1)}(z) = e^{\pm i\pi\nu} H_{\nu}^{(1)}(z), \qquad (3.2.29)$$

$$H_{-\nu}^{(2)}(z) = e^{-i\pi\nu} H_{\nu}^{(2)}(z), \qquad (3.2.30)$$

With this we can drop the complex conjugation on ν . We would like to change the argument in the Hankel function back to $-k\eta$, and we have to be careful about the branch cut of the Hankel function when we do so. Concretely, in our case we have (see Section 10.11 of [110]):

$$H_{\nu}^{(1)}(e^{i\pi}z) = -e^{-i\pi\nu}H_{\nu}^{(2)}(z), \tag{3.2.31}$$

$$H_{\nu}^{(2)}(e^{i\pi}z) = e^{i\pi\nu}H_{\nu}^{(1)}(z) + 2\cos(\pi\nu)H_{\nu}^{(2)}(z), \tag{3.2.32}$$

which gives the following:

$$\left[\phi_{-k^*}^+(\eta)\right]^* = i\phi_k^+(\eta),\tag{3.2.33}$$

$$\left[\phi_{-k^*}^-(\eta)\right]^* = i\phi_k^-(\eta) + 2\cos(\pi\nu)\phi_k^+(\eta). \tag{3.2.34}$$

Notice that we have $A^*(k,\eta_0) \left[\phi_{-k^*}^-(\eta)\right]^* \neq \phi_k^-(\eta)$, contrary to naive expectations. Instead it is a combination of $\phi_k^-(\eta)$ and $\phi_k^+(\eta)$. When we substitute this into the Hermitian analytic image of (3.2.24), we

obtain:

$$G_{-p^*}^*(\eta, \eta') = -i\theta(\eta - \eta') \left[\phi_{-p^*}^+(\eta')\right]^* \left[\phi_{-p^*}^+(\eta)\right]^* \left(\frac{\phi_{-p^*}^-(\eta)}{\phi_{-p^*}^+(\eta)} - \frac{\phi_{-p^*}^-(\eta_0)}{\phi_{-p^*}^+(\eta_0)}\right)^* + (\eta \leftrightarrow \eta')$$

$$= i\theta(\eta - \eta')\phi_p^+(\eta')\phi_p^+(\eta) \left(\frac{\phi_p^-(\eta)}{\phi_p^+(\eta)} - 2i\cos(\pi\nu) - \frac{\phi_p^-(\eta_0)}{\phi_p^+(\eta_0)} + 2i\cos(\pi\nu)\right) + (\eta \leftrightarrow \eta')$$

$$= G_p(\eta, \eta'). \tag{3.2.35}$$

Therefore the bulk-to-bulk propagator is still Hermitian analytic.

3.3 Spinning fields

In this section we discuss the generalization of the cosmological optical theorem to integer spin fields. The ingredients we will need to proof the cosmological optical theorem for spinning fields are the same as the scalar case: Hermitian analyticity of the bulk-to-boundary propagator as well as reality of the vertex factors. For concreteness we focus on the very general class of free theories for such fields that was developed in [111]⁵

$$S = \int d^3x dt \, a^3 \, \frac{1}{2s!} \left[(\dot{\Phi}^{i_1 \dots i_s})^2 - \frac{c_s^2}{a^2} (\partial_j \Phi^{i_1 \dots i_s})^2 - \frac{\delta c_s^2}{a^2} (\partial_j \Phi^{ji_2 \dots i_s})^2 - m^2 (\Phi^{i_1 \dots i_s})^2 \right] \,, \tag{3.3.1}$$

where $\Phi^{i_1...i_s}$ is a totally-symmetric, traceless tensor with only spatial indices, $i_1 = 1, 2, 3$. This theory arises in generic models of inflation where the background of the inflaton selects a preferred time foliation of spacetime into spatial hypersurfaces. The above expression can be written in a covariant way by using the Goldstone boson π of time translations to upgrade the spatial tensor $\Phi^{i_1...i_s}$ to a covariant spacetime tensor. The coupling of $\Phi^{i_1...i_s}$ to π is also dictated by this constructions but we will not need this here. Notice that $\Phi^{i_1...i_s}$ has (2s+1) components, which each create states ("particles") with helicities $0, \pm 1, \ldots, \pm s$, respectively.

Hermitian analyticity of the propagators The equation of motion for the field $\Phi_{i_1...i_s}$ is given by:

$$\Phi_{i_1...i_s}'' + 2\frac{a'}{a}\Phi_{i_1...i_s}' - c_s^2\partial^2\Phi_{i_1...i_s} - \delta c_s^2\partial_{i_1}\partial_j\Phi_{j...i_s} + m^2a^2\Phi_{i_1...i_s} = 0.$$
 (3.3.2)

The field can be separated into two parts:

$$\Phi_{i_1...i_s} = \Phi_{i_1...i_s}^T + \Phi_{i_1...i_s}^R, \tag{3.3.3}$$

where $\Phi^T_{i_1...i_s}$ is the transverse part of the field, obeying

$$\partial_j \Phi_{j...i_s}^T = 0, \tag{3.3.4}$$

and $\Phi^R_{i_1...i_s}$ is the remainder. It is straightforward to see that Φ^T has 2 degrees of freedom and represents the components with helicity $\pm s$, while Φ^R has 2s-1 components with lower helicities.

⁵For theories which cannot be described by this particular action, one can simply repeat the procedures described in this section to check if the propagators are Hermitian analytic.

For Φ^T , the penultimate term in (3.3.2) vanishes, and the equation of motion becomes:

$$\Phi_{i_1...i_s}^{T''} + 2\frac{a'}{a}\Phi_{i_1...i_s}^{T'} - c_s^2\partial^2\Phi_{i_1...i_s}^T + m^2a^2\Phi_{i_1...i_s}^T = 0.$$
(3.3.5)

This equation is in the same form as (3.2.2), therefore we can directly apply the analysis in Section 3.2 to show that the propagators of Φ^T are Hermitian analytic. For Φ^R we can take the divergence of (3.3.2), which gives us:

$$(\partial_j \Phi_{j...i_s}^R)'' + 2\frac{a'}{a}(\partial_j \Phi_{j...i_s}^R)' - (c_s^2 + \delta c_s^2)\partial^2(\partial_j \Phi_{j...i_s}^R) + m^2 a^2(\partial_j \Phi_{j...i_s}^R) = 0.$$
 (3.3.6)

Once again the equation is in the same form as (3.2.2), but with c_s^2 replaced with $c_s^2 + \delta c_s^2$. We can again directly apply the analysis in Section 3.2. Working in Fourier space, this tells us that $ik_j\Phi_{j...i_s}^R$ is Hermitian analytic. Since $i\mathbf{k}$ is Hermitian analytic, and $ik_j\Phi_{j...i_s}^R$ has exactly 2s-1 degrees of freedom, we deduce that the propagators of Φ^R are also Hermitian analytic. We conclude that the propagator of the full field Φ must be Hermitian analytic, which establishes the crucial property of our derivation of single-cut rules for free fields of any integer spin (in the spontaneously boost-breaking theories of [111]).

Helicity basis and the diagonalization of propagators For practical calculations, we would like to work in a basis where the propagators have a simple form. This can be achieved by looking at the helicity basis of the fields. These are irreps of ISO(3), the isometry group of a flat FLRW spacetime. As we show below, fields of different helicities decouple from each other and the corresponding propagators in this basis become diagonal.

The only non-diagonal term in the action is

$$k_j \Phi_{ji_2...i_s}(\mathbf{k}) k_l \Phi_{li_2...i_s}(-\mathbf{k}) = \Phi_{i_1...i_s} k_{i_1} k_{j_1} \delta_{i_1 j_1} \dots \delta_{i_s j_s} \Phi_{j_1...j_s}$$
(3.3.7)

$$\equiv \Phi_{i_1...i_s}(\mathbf{k}) M_{i_1...i_s j_1...j_s}(\mathbf{k}) \Phi_{j_1...j_s}(-\mathbf{k}). \tag{3.3.8}$$

We are guaranteed to be able to diagonalise this term because it is real and symmetric in i's and j's. To understand this diagonalisation procedure, let's start by looking at the vector case, s = 1, for which the tensor equation can be understood as a matrix multiplication, and so is diagonalised by finding the eigenvalues, λ^h , and eigenvectors, ϵ^h , of M,

$$M_{ij}(\mathbf{k})\epsilon_i^h(\mathbf{k}) = \lambda^h(\mathbf{k})\epsilon_i^h(\mathbf{k}),$$
 (no sum on h). (3.3.9)

The eigenvalues of M are

$$\lambda^{\pm} = 0, \qquad \qquad \lambda^0 = k^2. \tag{3.3.10}$$

We define the eigenvectors so that they satisfy the inversion relationship $\epsilon^h(-\mathbf{k}) = \epsilon^h(\mathbf{k})^*$,

$$\epsilon_i^{\pm} = (\mathbf{k} \times (\mathbf{k} \times \hat{n}) \pm i | \mathbf{k} | \mathbf{k} \times \hat{n})_i , \qquad (3.3.11)$$

$$\epsilon_i^0 = ik_i \tag{3.3.12}$$

for some normal vector \hat{n} that is perpendicular to \mathbf{k} .

Here we will make the following prescription: when we take the wavefunction off-shell, we do not analytically continue $|\mathbf{k}| \to \omega$ in the polarization tensor. This ensures these eigenvectors are not functions of off-shell energies. This prescription will be helpful in showing the Hermitian analyticity of the interaction vertex in the helicity basis.

These eigenvectors are orthogonal to each other,

$$\left[\epsilon_i^h(\mathbf{k})\right]^* \epsilon_i^{h'}(\mathbf{k}) = C^h(k^2)\delta^{hh'}, \qquad \text{(no sum on h)}, \qquad (3.3.13)$$

where $C^h(k^2)$ is a polynomial in k^2 (so is guaranteed to be Hermitian analytic) that comes from the normalisation of the eigenvectors. We can therefore express M and the identity in terms of these eigenvectors as

$$M_{ij} = k_i k_j = \epsilon_i^h(\mathbf{k}) \frac{1}{C^h(k^2)} \lambda^h(\mathbf{k}) \left[\epsilon_j^h(\mathbf{k}) \right]^*$$
(3.3.14)

$$\delta_{ij} = \epsilon_i^h(\mathbf{k}) \frac{1}{C^h(k^2)} \left[\epsilon_j^h(\mathbf{k}) \right]^* \tag{3.3.15}$$

We can then see that in the so called "helicity basis",

$$\Phi^h(\mathbf{k}) \equiv \Phi_i(\mathbf{k})\epsilon_i^h(\mathbf{k}),\tag{3.3.16}$$

the action diagonalises,

$$S_2 = \frac{1}{2} \int \frac{d^3k}{(2\pi)^3} d\eta a^2 \sum_{h=\pm 0} \left\{ (\Phi^h(\mathbf{k}))' \partial_\tau - \Phi^h(\mathbf{k}) \left[c_s^2 k^2 - m^2 + \delta c_s^2 \lambda^h \right] \right\} \frac{1}{C^h(k^2)} \Phi^h(-\mathbf{k}). \tag{3.3.17}$$

This also makes it clear why we imposed that $\epsilon^h(-\mathbf{k}) = \epsilon^h(\mathbf{k})^*$ as it ensures that

$$\Phi^{h}(-\mathbf{k}) = \Phi_{i}(-\mathbf{k}) \left[\epsilon_{i}^{h}(\mathbf{k}) \right]^{*}. \tag{3.3.18}$$

Now that we have our eigenvectors for the spin-1 case this procedure can be generalised to arbitrary spin. To keep the symmetries of our field manifest we define a symmetric, traceless basis containing 2s+1 tensors which are constructed from the symmetrised direct product of s copies of the vector ϵ^h ,

$$\epsilon_{i_1\dots i_s}^s = \epsilon_{i_1}^+ \dots \epsilon_{i_s}^+, \tag{3.3.19}$$

$$\epsilon_{i_1\dots i_s}^{s-1} = \epsilon_{(i_1}^+ \dots \epsilon_{i_{s-1}}^+ \epsilon_{i_s}^0,$$
(3.3.20)

$$\epsilon_{i_1...i_s}^{s-2} = \epsilon_{(i_1}^+ \dots \epsilon_{i_{s-2}}^+ \epsilon_{i_{s-1}}^0 \epsilon_{i_s)}^0 + \frac{1}{3} \epsilon_{(i_1}^+ \dots \epsilon_{i_{s-2}}^+ \delta_{i_{s-1}i_s)}^+, \tag{3.3.21}$$

:

$$\epsilon_{i_1...i_s}^0 = \epsilon_{i_1}^0 \dots \epsilon_{i_s}^0 + \frac{s!}{6} \epsilon_{(i_1}^0 \dots \epsilon_{i_{s-2}}^0 \delta_{i_{s-1}i_s})$$
(3.3.22)

:

$$\epsilon_{i_1\dots i_s}^{-s} = \epsilon_{i_1}^{-} \dots \epsilon_{i_s}^{-}. \tag{3.3.23}$$

The tracelessness of these terms relies on the relationship $\epsilon^+ = \epsilon^{-*}$ which ensures that any contractions

like $\epsilon_i^{\pm}\epsilon_i^{\pm}$ vanish by orthogonality. It can be shown that these tensors inherit the orthogonality of the vectors so

$$M_{i_1...i_s j_1...j_s} = \epsilon_{i_1...i_s}^h(\mathbf{k}) \frac{1}{C^h(k^2)} \lambda^h(\mathbf{k}) \left[\epsilon_{j_1...j_s}^h(\mathbf{k}) \right]^*, \tag{3.3.24}$$

$$\delta_{i_1 j_1} \dots \delta_{i_s j_s} = \epsilon_{i_1 \dots i_s}^h(\mathbf{k}) \frac{1}{C^h(k^2)} \left[\epsilon_{j_1 \dots j_s}^h(\mathbf{k}) \right]^*.$$
 (3.3.25)

where C^h is given, as for the vector case, by

$$\left[\epsilon_{i_1...i_s}^h(\mathbf{k})\right]^* \epsilon_{i_1...i_s}^{h'}(\mathbf{k}) = C^h \delta^{hh'},$$
 (no sum on h). (3.3.26)

The action is therefore exactly that given in (3.3.17) but with h running from -s to s. As this is diagonal, it gives a separate differential equation for each helicity mode⁶,

$$(a^2 \Phi^{h'}(\mathbf{k}))' - a^2 \Phi^{h} \left[c_s^2 k^2 - m^2 + \delta c_s^2 \lambda^h \right] = 0, \tag{3.3.27}$$

which ensures that the propagators are diagonal in this basis,

$$K_k^{hh'}(\eta) = \delta^{hh'} K_k^h(\eta) \qquad \text{(no sum on } h), \tag{3.3.28}$$

$$G_p^{hh'}(\eta) = \delta^{hh'} C^h(k^2) G_p^h(\eta)$$
 (no sum on h). (3.3.29)

Here, K_k^h and G_p^h are constructed from the positive energy modefunctions that satisfy (3.3.27) subject to the Bunch-Davies initial condition (3.2.4) with the substitution

$$c_s \to \sqrt{c_s^2 + \frac{\lambda^h}{k^2} \delta c_s^2}. \tag{3.3.30}$$

This is k independent because $\lambda^h \propto k^2$ for all h. The proof that these propagators are Hermitian analytic therefore follows similarly to the scalar case.

Interaction verticies The helicity basis is particularly useful in showing the reality of the vertex factors. In the helicity basis, a generic interaction vertex has the following form when we take the energies off-shell:

$$S_n = g_n \sum_{\{h_a\}} \int d\eta a^4(\eta) \int \prod_{a=1}^n \left[\frac{d^3 k_a}{(2\pi)^3} \right] \left(\prod_{a=1}^n \Phi_{\omega_a}^{h_a}(\eta) \right) F^{\{h_a\}}(\{\mathbf{k}_a\}).$$
(3.3.31)

The interaction vertex is constructed by taking various contractions of $\epsilon_{i_1...i_s}^{h_a}(\mathbf{k}_a)$ and $i\mathbf{k}_a$ (the latter comes from a spatial derivative). Clearly $i\mathbf{k}$ is Hermitian analytic since $(i(-\mathbf{k}))^* = i\mathbf{k}$. Next, we look at the Hermitian analytic image $\left[\epsilon_{i_1...i_s}^h(-\mathbf{k})\right]^*$. Under our prescription, when we take the energies offshell, the polarization tensors do not depend on the off-shell energies ω , hence it is easy to see that $F_A(\mathbf{k}, \mathbf{p}) = F_A^*(-\mathbf{k}, -\mathbf{p})^7$.

⁶The contribution from $C^h(k^2)$ factorises out.

⁷In [1] a slightly different prescription is used: all polarization tensors $\epsilon^h_{i_1...i_s}$ should be factorized outside all the Disc's. This is because in the paper the Disc is taken with respect to k (which is on-shell), and hence the Disc operator also acts on the polarization tensors. In our prescription we take the polarization tensors to only depend on on-shell quantities and we take the Disc of off-shell energies, and so this issue is bypassed.

With the reality of the interaction vertex and the Hermitian analyticity of the propagators, we can simply replicate the proof of the cosmological optical theorem for the scalar case and extend it to integer spinning fields. Due to the form of the propagator, polarization tensors associated with bulk-to-bulk propagators must also come with a sum over helicities. Therefore, we have the following single-cut rules:

$$\operatorname{Disc}_{\omega_{s}} i \psi_{n+m}^{\{h_{a}\}\{h_{b}\}}(\{\omega\}; \omega_{p_{1}} \dots, \omega_{s}, \dots, \omega_{p_{I}}; \{\mathbf{k}\}) = \sum_{h} -i P_{\Phi}^{h}(\omega_{s}) \operatorname{Disc}_{\omega_{s}} i \psi_{n+1}^{\{h_{a}\}, h}(\{\omega_{a}\}, \omega_{s}; \{\omega_{p}\}; \{\mathbf{k}_{a}\}) \times \operatorname{Disc}_{\omega_{s}} i \psi_{m+1}^{\{h_{b}\}, h}(\{\omega_{b}\}, \omega_{s}; \{\omega_{p}\}; \{\mathbf{k}_{b}\}).$$
(3.3.32)

Here P_{Φ}^{h} is the power spectrum of the exchanged field,

$$P_{\Phi}^{h}(\omega_s) = C^h |\Phi^{h}(\omega_s)|^2, \tag{3.3.33}$$

where C^h is defined in (3.3.26) and we take the positive energy mode functions for the fields.

Spin-1 example For spin-1, the action (3.3.1) reads:

$$S = \int d^3x dt \, a^3 \frac{1}{2} \left[(\dot{\sigma}^i)^2 - \frac{c_s^2}{a^2} (\partial_j \sigma^i)^2 - \frac{\delta c_s^2}{a^2} (\partial_i \sigma^i)^2 - m^2 (\sigma^i)^2 \right]. \tag{3.3.34}$$

This action encompasses a large class of spin-1 fields. For instance, consider the dS invariant action a massive spin-1 field in dS:

$$S = \int d^4x \sqrt{-g} \left[-\frac{1}{4} F_{\mu\nu} F^{\mu\nu} - \frac{1}{2} (m^2 + 3H^2) A_{\mu} A^{\mu} \right]. \tag{3.3.35}$$

Spinning fields in dS are irreducible representations of the full dS isometry group SO(1,4). Each representation is labelled by a scaling dimension Δ (or the mass of the field), which labels the SO(1,1) subgroup, as well as l, which labels the SO(3) subgroup [112]. Naturally by considering the SO(3) subgroup we can write down a helicity basis for the fields, and so we expect the propagators for spinning fields in dS to be Hermitian analytic.

In the context of effective field theory of inflation (see [113]), (3.3.35) is indeed a special case of (3.3.34). Generally speaking we would like to construct an effective field theory using building blocks which are invariant under rotation, and so we should be looking at three vectors (rather than four vectors) as our fundamental building block. In unitary gauge this is particularly easy to achieve, as the Goldstone modes for time diffeomorphism obeys $\pi = 0$ (this is the gauge where constant time slices corresponds to slices of constant inflaton) and we have⁸:

$$A_0 = \phi, \qquad A_i = -\frac{1}{a}\sigma_i. \tag{3.3.36}$$

⁸For general cases we need to write A_{μ} in terms of both σ_i, ϕ, π to preserve diffeomorphism invariance. See section 3 of [111] for more details.

If we expand the action (3.3.35) in terms of these fields, we obtain:

$$S = \int d^3x dt a^3 \frac{1}{2} \left(\left[(\dot{\sigma}^i)^2 - \frac{1}{a^2} (\partial_j \sigma^i)^2 - m^2 (\sigma^i)^2 \right] + \left[-\frac{1}{a^2} (\partial_i \phi)^2 + \frac{2}{a^2} (\dot{\sigma}^i - H \sigma^i) \partial_i \phi - (m^2 + 3H^2) \phi^2) \right] \right).$$
(3.3.37)

The terms in the first line corresponds to the terms in (3.3.34), with $c_s^2 = 1$ and $\delta c_s^2 = 0$. It is also easy to see that ϕ is in fact an auxiliary field as it does not have a kinetic term. We could integrate it out and this give rise to non-local interaction terms in σ_i .

Let us return to (3.3.34) and study its mode functions. They are given by [111]:

$$\sigma_{\omega}^{h}(\eta) = H \frac{\sqrt{\pi}}{2} e^{\frac{i\pi}{2}(\nu + \frac{1}{2})} (-\eta)^{3/2} H_{\nu}^{(2)}(-c_{h}\omega\eta). \tag{3.3.38}$$

Here $c_1^2 = c_s^2$ and $c_0^2 = c_s^2 + \delta c_s^2$. Based on our discussion for massive scalar fields, it is straightforward to see that these mode function are Hermitian analytic⁹.

Spin-2 examples For spin-2, let us look at explicit examples involving massive gravity and general relativity.

The simplest case is that of general relativity. In this theory, the (massless) graviton has the same (positive energy) mode functions as massless scalar field in dS, so when we take the energies off-shell we have:

$$\gamma_{ij}(\omega, \mathbf{k}) = \sum_{h} \epsilon_{ij}^{h}(\mathbf{k}) \frac{H}{M_{\rm P} \omega^{3/2}} (1 - i\omega\eta) e^{i\omega\eta} , \qquad (3.3.39)$$

where now $h = \pm 2$ since the lower-helicty modes are removed by diff invariance. As we have seen for the scalar field, the propagators corresponding to this mode function must be Hermitian analytic.

As an example of an interaction, consider the cubic graviton interaction induced by the spatial Ricci scalar $R^{(3)}$ [114]:

$$F^{\lambda_1 \lambda_2 \lambda_3}(\mathbf{k}_1, \mathbf{k}_2, \mathbf{k}_3) = i^2 \left(k_{2i} k_{2j} \epsilon_{ij}^{\lambda_1}(\mathbf{k}_1) \right) \epsilon_{lm}^{\lambda_2}(\mathbf{k}_2) \epsilon_{lm}^{\lambda_3}(\mathbf{k}_3)$$

$$- 2i^2 \left(\epsilon_{ij}^{\lambda_1}(\mathbf{k}_1) k_{3l} \right) \epsilon_{li}^{\lambda_2}(\mathbf{k}_2) \left(k_{2m} \epsilon_{jm}^{\lambda_3}(\mathbf{k}_3) \right) + (\text{cyclic}). \quad (3.3.40)$$

The two spatial derivatives are Hermitian analytic thanks to factor of i^2 in front, and the polarization tensors can be taken to obey Hermitian analyticity because of our prescription.

As a more interesting example, we also look at the propagators in a theory of massive gravity (see [115]

⁹In the case of dS invariant spin-1 fields, we could also study the equation of motion $(\nabla^2 - m^2 - 3H^2)A_{\mu} = 0$ directly without referring to the action (3.3.35). The solution can be diagonalised in helicity modes, and the equation of motion for each helicity mode is Hermitian analytic. This also applies for integer spin-l representations of dS. See appendix A of [14].

for more details):

$$S = \frac{1}{4} \int d^4x \left[-\nabla_{\rho} h_{\mu\nu} \nabla^{\rho} h^{\mu\nu} - (m^2 + 2H^2) h_{\mu\nu} h^{\mu\nu} + \nabla^{\rho} h_{\rho\mu} \nabla_{\nu} h^{\nu\mu} - \nabla_{\mu} h \nabla_{\nu} h^{\mu\nu} + \frac{1}{2} \nabla_{\mu} h \nabla^{\mu} h + \frac{1}{2} (m^2 - H^2(d - 2)) h^2 \right], \quad (3.3.41)$$

As shown in the paper, the mode function for the helicity mode +2 and +1 are found to be:

$$\gamma_{\omega}^{+2}(\eta) = (-\omega \eta)^{3/2} H_{i\mu}^{(2)}(-\omega \eta), \tag{3.3.42}$$

$$\gamma_{\omega}^{+1}(\eta) = \eta(-\omega\eta)^{1/2} \left(2\omega\eta H_{i\mu-1}^{(2)}(-\omega\eta) - (3+2i\mu)H_{i\mu}^{(2)}(-\omega\eta) \right). \tag{3.3.43}$$

We immediately notice that the +2 helicity has a Hermitian analytic propagator. For the +1 helicity mode, we use the recurrence relation of Hankel function to rearrange the mode function as:

$$\gamma_{\omega}^{+1}(\eta) = \eta(-\omega\eta)^{1/2} \left(-3 + 2\eta \frac{d}{d\eta}\right) H_{i\mu}^{(2)}(-\omega\eta), \tag{3.3.44}$$

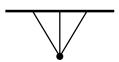
from which we see that this mode function will give rise to a Hermitian analytic propagator.

3.4 Examples

Let us verify the cosmological optical theorem with a few simple examples.

3.4.1 Contact diagram

Let us first consider three point contact diagrams:



Since there are no internal lines, the expectation is that $\psi_3(\omega) + \psi_3^*(-\omega^*) = 0$. We will look at two examples:

Single massless scalar in dS We have computed ψ_3 for a single massless scalar for the three point contact diagram, and the expression is given by (2.2.19). We go off-shell (i.e. replacing k_a with ω_a) and compute $\psi_3^*(-\omega^*)$:

$$\psi_3^*(-\omega_1^*, -\omega_2^*, -\omega_3^*) = 6g \left[-\frac{i}{3\eta_0^3} - \frac{i\omega_T^2}{3\eta_0} + \frac{ie_2}{3\eta_0} - \left(e_3 - \omega_T e_2 + \frac{\omega_T^3}{3} \right) \left(\log(-i\omega_T \eta_0) + \gamma_E + \dots \right) \right]. \quad (3.4.1)$$

Here we made use of the following fact: by placing the branch cut of the logarithm on the negative real axis, for $r = |r|e^{i\theta}$, we have:

$$(\log(-r^*))^* = (\log|r| - i(\pi + \theta))^* = \log r + i\pi. \tag{3.4.2}$$

Since $\log(-i\omega_T\eta_0) = \log(-\omega_T\eta_0) + i\frac{\pi}{2}$, we have:

$$\log\left(-i(-\omega_T^*)\eta_0\right)^* = \log(-i\omega_T\eta_0). \tag{3.4.3}$$

By comparing with (3.4.1), we find that:

$$\psi_3^*(-\omega_1^*, -\omega_2^*, -\omega_3^*) = -\psi_3(\omega_1, \omega_2, \omega_3), \tag{3.4.4}$$

so the optical theorem holds.

Massless scalars with a vector field in dS Let us consider the same contact diagram, but with the following interaction:

$$\mathcal{L}_{int} = g\phi_1 \partial_i \phi_2 A^i, \tag{3.4.5}$$

 ϕ_1 and ϕ_2 are massless fields in dS and A_i is a massless vector. To compute this diagram, first let us write down the bulk-to-boundary propagator for a massless vector, which is:

$$K_{\omega}^{\lambda\lambda'}(\eta) = e^{i\omega(\eta - \eta_0)} \delta_{\lambda\lambda'}. \tag{3.4.6}$$

The wavefunction coefficient is given by:

$$\psi_3^{\lambda}(\omega_1, \omega_2, \omega_3, \mathbf{k}_1, \mathbf{k}_2, \mathbf{k}_3) = ig \int_{-\infty}^{\eta_0} \frac{d\eta}{\eta^4} \eta^2(\mathbf{k}_2 \cdot \epsilon^{\lambda}(\mathbf{k}_3)) \frac{(1 - i\omega_1\eta)(1 - i\omega_2\eta)}{(1 - i\omega_1\eta_0)(1 - i\omega_2\eta_0)} e^{i\omega_T(\eta - \eta_0)}$$

$$= g(\mathbf{k}_2 \cdot \epsilon^{\lambda}(\mathbf{k}_3)) \left[-\frac{1}{\eta_0} - i(\omega_1 + \omega_2) + i\frac{\omega_1\omega_2}{\omega_T} + i\omega_3 \log(-i\omega_T\eta_0) \right]. \tag{3.4.7}$$

Let us see if the optical theorem holds. We have $(\epsilon^{\lambda}(-\mathbf{k}))^* = \epsilon^{\lambda}(\mathbf{k})$, and from the discussion of the massless scalar calculation the logarithm term is Hermitian analytic. All of the terms inside the bracket remains unchanged, while the momentum \mathbf{k}_2 outside gains a minus sign. Therefore it is straightforward to see that:

$$\psi_3^{\lambda}(\omega_1, \omega_2, \omega_3, \mathbf{k}_1, \mathbf{k}_2, \mathbf{k}_3) = -(\psi_3^{\lambda}(-\omega_1^*, -\omega_2^*, -\omega_3^*, -\mathbf{k}_1, -\mathbf{k}_2, -\mathbf{k}_3))^*. \tag{3.4.8}$$

3.4.2 Exchange diagram

Let us now consider wavefunction coefficients for an exchange diagram:

$$\bigvee$$

We would like to verify (3.1.19). Let us consider the following:

Scalar in flat space We have computed ψ_4 for this diagram, and it is given by (2.2.23). We have:

$$\operatorname{Disc}_{\omega_s} i\psi_4 = \frac{g^2}{\omega_T(\omega_L + \omega_s)(\omega_R + \omega_s)} - \frac{g^2}{\omega_T(\omega_L - \omega_s)(\omega_R - \omega_s)} = \frac{2g^2\omega_s}{(\omega_L^2 - \omega_s^2)(\omega_R^2 - \omega_s^2)}.$$
 (3.4.9)

Here $\omega_L = \omega_1 + \omega_2$ and $\omega_R = \omega_3 + \omega_4$. Since we have:

$$\operatorname{Disc}_{\omega_s} i\psi_3(\omega_1, \omega_2, \omega_s) = \frac{g}{\omega_L + \omega_s} - \frac{g}{\omega_L - \omega_s} = \frac{2\omega_s g}{\omega_L^2 - \omega_s^2},\tag{3.4.10}$$

and $P_s = \frac{1}{2\omega_s}$, we can easily see that

$$-P_s \underset{\omega_s}{\text{Disc}} i\psi_3(\omega_1, \omega_2, \omega_s) \underset{\omega_s}{\text{Disc}} i\psi_3(\omega_3, \omega_4, \omega_s) = \frac{2g^2 \omega_s}{(\omega_L^2 - \omega_s^2)(\omega_R^2 - \omega_s^2)}, \tag{3.4.11}$$

so (3.1.19) is clearly true.

Massless graviton in dS In the effective field theory of inflation one can construct operators from extrinsic curvature and compute graviton correlators. Let us pick a simple one from [116] and compute the four graviton exchange trispectrum. For simplicity we pick the following term in the action:

$$S_I = \frac{1}{3!} \int d^3x dt \, a^3 \dot{\gamma}_{ij} \dot{\gamma}_{jk} \dot{\gamma}_{ki} \tag{3.4.12}$$

$$= -\frac{1}{3!} \sum_{\lambda_1, \lambda_2, \lambda_3} \int d\eta d^3k \, \epsilon_{ij}^{\lambda_1}(\mathbf{k}_1) \epsilon_{jl}^{\lambda_2}(\mathbf{k}_2) \epsilon_{li}^{\lambda_3}(\mathbf{k}_3) \frac{1}{H\eta} \partial_\eta \gamma_{k_1}^{\lambda_1} \partial_\eta \gamma_{k_2}^{\lambda_2} \partial_\eta \gamma_{k_3}^{\lambda_3}. \tag{3.4.13}$$

where we have set the coupling constant to unity to simplify our notation. Let us set $M_P = 1$ for simplicity. The mode function and bulk-to-boundary propagator of the graviton are

$$\gamma_{\omega}^{\lambda}(\eta) = \frac{H}{\sqrt{\omega^3}} (1 - i\omega\eta) e^{i\omega\eta} \tag{3.4.14}$$

$$K_{\omega}^{\lambda\lambda'}(\eta) = \delta^{\lambda\lambda'} K_{\omega}(\eta) = \delta^{\lambda\lambda'} (1 - i\omega\eta) e^{i\omega\eta}. \tag{3.4.15}$$

With this, we can easily obtain the wavefunction coefficient $\psi_3^{\lambda_1\lambda_2\lambda_3}$ as

$$\psi_3^{\lambda_1 \lambda_2 \lambda_3} = 2\epsilon_{ij}^{\lambda_1}(\mathbf{k}_1)\epsilon_{jl}^{\lambda_2}(\mathbf{k}_2)\epsilon_{li}^{\lambda_3}(\mathbf{k}_3)\frac{\omega_1^2 \omega_2^2 \omega_3^2}{H\omega_T^3}.$$
 (3.4.16)

It is straightforward to obtain the bulk-to-bulk propagator

$$G_{p}^{\lambda\lambda'}(\eta,\eta') = 2\delta^{\lambda\lambda'}G_{p}(\eta,\eta')$$

$$= 2i\delta^{\lambda\lambda'}\left(\theta(\eta-\eta')\frac{H^{2}(1+ip\eta)(1-ip\eta')}{p^{3}}e^{-ip(\eta-\eta')} + \theta(\eta'-\eta)\frac{H^{2}(1+ip\eta')(1-ip\eta)}{p^{3}}e^{ip(\eta-\eta')} - \frac{H^{2}(1-ip\eta)(1-ip\eta')}{p^{3}}e^{ip(\eta+\eta')}\right).$$
(3.4.17)

Then we find

$$\psi_{4}^{\lambda_{1}\lambda_{2}\lambda_{3}\lambda_{4}} = -i\sum_{\lambda} \int_{-\infty}^{0} d\eta \int_{-\infty}^{0} d\eta' \frac{\eta\eta'}{H^{2}} 2i\epsilon_{ij}^{\lambda_{1}}(\mathbf{k}_{1})\epsilon_{jl}^{\lambda_{2}}(\mathbf{k}_{2})\epsilon_{li}^{*\lambda_{1}}(\mathbf{p}_{s})\epsilon_{mn}^{\lambda_{3}}(\mathbf{k}_{3})\epsilon_{np}^{\lambda_{4}}(\mathbf{k}_{4})\epsilon_{pm}^{\lambda}(\mathbf{p}_{s})$$

$$e^{i\omega_{L}\eta}e^{i\omega_{R}\eta'}\omega_{1}^{2}\omega_{2}^{2}\omega_{3}^{2}\omega_{4}^{2}\partial_{\eta}\partial_{\eta'}\left[\left(\theta(\eta-\eta')\frac{H^{2}(1+i\omega_{s}\eta)(1-i\omega_{s}\eta')}{\omega_{s}^{3}}e^{-i\omega_{s}(\eta-\eta')}\right)\right]$$

$$+\left(\theta(\eta'-\eta)\frac{H^{2}(1-i\omega_{s}\eta)(1+i\omega_{s}\eta')}{\omega_{s}^{3}}e^{i\omega_{s}(\eta-\eta')}\right) - \left(\frac{H^{2}(1-i\omega_{s}\eta)(1-i\omega_{s}\eta')}{\omega_{s}^{3}}e^{i\omega_{s}(\eta+\eta')}\right)\right]. \quad (3.4.19)$$

Evaluating the integral gives us the following:

$$\psi_4^{\lambda_1 \lambda_2 \lambda_3 \lambda_4} = \sum_{\lambda} \frac{2\omega_1^2 \omega_2^2 \omega_3^2 \omega_4^2 \omega_s}{\omega_T^5} \epsilon_{ij}^{\lambda_1}(\mathbf{k}_1) \epsilon_{jl}^{\lambda_2}(\mathbf{k}_2) \epsilon_{li}^{*\lambda}(\mathbf{p}_s) \epsilon_{mn}^{\lambda_3}(\mathbf{k}_3) \epsilon_{np}^{\lambda_4}(\mathbf{k}_4) \epsilon_{pm}^{\lambda}(\mathbf{p}_s)$$

$$\times \left[\left(\frac{24}{E_R} + \frac{12\omega_T}{E_R^2} + \frac{4\omega_T^2}{E_R^3} - \frac{24}{\omega_s} \right) + \left(\frac{24}{E_L} + \frac{12\omega_T}{E_L^2} + \frac{4\omega_T^2}{E_L^3} - \frac{24}{\omega_s} \right) + \left(\frac{4\omega_T^5}{E_R^3 E_L^3} \right) \right]. \tag{3.4.20}$$

Here $E_L = \omega_L + \omega_s$, $E_R = \omega_R + \omega_s$. Adding the Hermitian analytic image reads:

$$\operatorname{Disc}_{\omega_{s}} i \psi_{4}^{\lambda_{1} \lambda_{2} \lambda_{3} \lambda_{4}} = \sum_{\lambda} \frac{2i \omega_{1}^{2} \omega_{2}^{2} \omega_{3}^{2} \omega_{4}^{2} \omega_{s}}{\omega_{T}^{5}} \epsilon_{ij}^{\lambda_{1}}(\mathbf{k}_{1}) \epsilon_{jl}^{\lambda_{2}}(\mathbf{k}_{2}) \epsilon_{li}^{*\lambda_{1}}(\mathbf{p}_{s}) \epsilon_{min}^{\lambda_{3}}(\mathbf{k}_{3}) \epsilon_{np}^{\lambda_{4}}(\mathbf{k}_{4}) \epsilon_{pm}^{\lambda}(\mathbf{p}_{s})$$

$$\times \left[\left(\frac{24}{E_{R}} + \frac{12\omega_{T}}{E_{R}^{2}} + \frac{4\omega_{T}^{2}}{E_{R}^{3}} + \frac{24}{E_{L} - 2\omega_{s}} + \frac{12\omega_{T}}{(E_{L} - 2\omega_{s})^{2}} + \frac{4\omega_{T}^{2}}{(E_{L} - 2\omega_{s})^{3}} \right) + \left(\frac{24}{E_{L}} + \frac{12\omega_{T}}{E_{L}^{2}} + \frac{4\omega_{T}^{2}}{E_{L}^{3}} + \frac{24}{E_{R} - 2\omega_{s}} + \frac{12\omega_{T}}{(E_{R} - 2\omega_{s})^{2}} + \frac{4\omega_{T}^{2}}{(E_{R} - 2\omega_{s})^{3}} \right) + \left(\frac{4\omega_{T}^{5}}{E_{R}^{3} E_{L}^{3}} \right) + \left(\frac{4\omega_{T}^{5}}{(E_{R} - 2\omega_{s})^{3}(E_{L} - 2\omega_{s})^{3}} \right) \right].$$

$$(3.4.21)$$

The power spectrum is given by:

$$P_{\omega_s}^{\gamma} = 2\langle \gamma^{\lambda}(\mathbf{p}_s) \gamma^{\lambda}(-\mathbf{p}_s) \rangle' = \frac{2H^2}{\omega_s^3}.$$
 (3.4.22)

Therefore, we have:

$$\sum_{\lambda} -iP_{\omega_{s}}^{\gamma} \operatorname{Disc}_{\omega_{s}} i\psi_{3}^{\lambda_{1}\lambda_{2}\lambda}(k_{1}, k_{2}, p_{s}, \mathbf{k}_{1}, \mathbf{k}_{2}) \operatorname{Disc}_{\omega_{s}} i\psi_{3}^{\lambda\lambda_{3}\lambda_{4}}(k_{3}, k_{4}, p_{s}, \mathbf{k}_{3}, \mathbf{k}_{4})$$

$$= \sum_{\lambda} 8i\omega_{1}^{2}\omega_{2}^{2}\omega_{3}^{2}\omega_{4}^{2}\omega_{s}\epsilon_{ij}^{\lambda_{1}}(\mathbf{k}_{1})\epsilon_{jl}^{\lambda_{2}}(\mathbf{k}_{2})\epsilon_{li}^{*\lambda}(\mathbf{p}_{s})\epsilon_{mn}^{\lambda_{3}}(\mathbf{k}_{3})\epsilon_{np}^{\lambda_{4}}(\mathbf{k}_{4})\epsilon_{pm}^{\lambda}(\mathbf{p}_{s}) \left[\left(\frac{1}{(E_{L} - 2\omega_{s})^{3}} \frac{1}{E_{R}^{3}}\right) + \left(\frac{1}{E_{L}^{3}} \frac{1}{(E_{R} - 2\omega_{s})^{3}}\right) + \left(\frac{1}{(E_{L} - 2\omega_{s})^{3}} \frac{1}{(E_{R} - 2\omega_{s})^{3}}\right)\right].$$
(3.4.23)

With this, it is straightforward to verify the single-cut rule for this interaction.

3.5 Extensions beyond tree level

The cosmological optical theorem described so far is quite limited in scope: it only works for tree level in perturbation theory. Ideally we would like to extend this to work for loops, and eventually to beyond

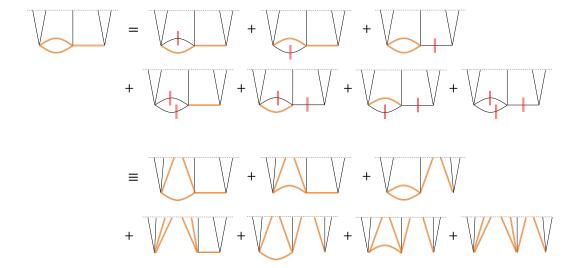


Figure 3.2: Taking the Disc relates the wavefunction to all possible ways of cutting the diagram. This diagram is taken from [117].

perturbation theory. Here we will explore extensions of the optical theorem beyond tree level.

Loop level This has been achieved in [117]. Their result relates the Disc of the wavefunction to the Disc of all possible cuts of the Feynman diagram. As an example see figure 3.2.

More precisely, the result is:

$$i \underset{\text{lines}}{\text{Disc}} \left[i \, \psi^{(D)} \right] = \sum_{\text{cuts}} \left[\prod_{\substack{\text{cut} \\ \text{momenta}}} \int P \right] \prod_{\text{subdiagrams}} (-i) \underset{\text{cut lines}}{\text{Disc}} \left[i \, \psi^{\text{(subdiagram)}} \right], \quad (3.5.1)$$

The proof of this result relies on understanding how the Disc operator acts on a product of bulk-to-bulk propagators. Notice that they do not analytically continue the energy for any bulk-to-bulk propagator. This is because in a loop diagram, the energies p depend on the loop momentum which is integrated over, and naively analytically continuing the energies (or trying to bring them off shell) would create ambiguity. Because of this, the Disc operator acts on every bulk-to-bulk propagator in the perturbative expansion, which causes the proliferation of diagrams.

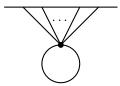
If we want to avoid this issue, we need to come up with an analytic continuation procedure which leaves the propagator unchanged under the Disc operation. Here we will describe an incomplete attempt at creating such a procedure.

Analytic continuation of internal energies for loops The idea is to use analytically continue in a way which allows the following:

$$\operatorname{Disc} i\psi_n(\{\omega\}, \{\mathbf{k}\}) = 0 \tag{3.5.2}$$

for any diagram in perturbation theory. In doing so, we can replicate the proof of the single cut rule: the Disc operator will commute through the propagators and the vertex factor, hitting only the subset of propagators which we want to cut, and this will work even if the rest of the diagram contains loops.

Let us first look at the simplest case, the one site loop:



Let us write down the integral for the wavefunction coefficient, which is:

$$\psi_n(\{\omega\}, \Lambda) = \frac{1}{2\pi^2} \int_0^{\Lambda} dp \, p^2 \prod_{i=1}^n K(\omega_i) G(p, \eta, \eta), \tag{3.5.3}$$

where I have introduced a cutoff Λ to regulate any potential UV divergences. Now observe the following:

$$\psi_n^*(\{-\omega^*\}, -\Lambda) = \frac{1}{2\pi^2} \int_0^{-\Lambda} dp \, p^2 \prod_{i=1}^n K^*(-\omega_i^*) G^*(p, \eta, \eta)$$

$$= -\frac{1}{2\pi^2} \int_0^{\Lambda} dp \, (-p)^2 \prod_{i=1}^n K^*(-\omega_i^*) G^*(-p, \eta, \eta)$$

$$= -\psi_n(\{\omega\}, \Lambda). \tag{3.5.4}$$

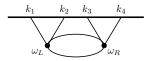
We redefined $p \to -p$ when going from the first line to the second line, and Hermitian analyticity is used when going from the second to the third line¹⁰. For example, in flat space we can compute this diagram to obtain (see appendix D.2 for details):

$$\psi_n = \frac{1}{16\pi^2 \omega_T} \left[2\Lambda(\Lambda - \omega_T) + \omega_T^2 \log\left(\frac{2\Lambda}{\omega_T}\right) \right]. \tag{3.5.5}$$

It is easy to see that $\psi_n(\omega, \Lambda) + \psi_n^*(-\omega, -\Lambda) = 0$.

It shouldn't be surprising that there exist a procedure for this loop diagram: these diagrams usually shift the mass or the coupling constant, and clearly the Disc operator should commute with a coupling constant or mass in a unitary theory.

More surprisingly, we can still do something similar for the two site loop:



Let us illustrate this once again by using a hard cutoff. The integrand can be written as (we leave the

¹⁰There are potentially subtleties with $i\epsilon$ prescriptions when I go from p to -p if there are branch cuts in the bulk-to-bulk propagators. We leave a careful study of this to the future

details in appendix D.3):

$$\psi_{4}(\omega_{1}, \dots, \omega_{4}, \omega_{s}, \Lambda) = \frac{g^{2}}{2\pi^{2}} \int d\eta_{1} d\eta_{2} a^{4}(\eta_{1}) a^{4}(\eta_{2}) \prod_{i=1}^{4} K(\omega_{i})$$

$$\times \int_{\omega_{s}}^{\Lambda} dp_{+} \int_{-\omega_{s}}^{\omega_{s}} dp_{-} \frac{p_{+}^{2} - p_{-}^{2}}{\omega_{s}} G(p_{1}, \eta_{1}, \eta_{2}) G(p_{2}, \eta_{1}, \eta_{2}) \quad (3.5.6)$$

In writing down the expression, we have taken $s = |\mathbf{k}_1 + \mathbf{k}_2|$ off-shell. There is no ambiguity in doing so: s is not being integrated over.

By manipulating the integrand, one can show the following:

$$\psi_4(\omega_1, \dots, \omega_4, \omega_s, \Lambda) + \psi_4^*(-\omega_1^*, \dots, -\omega_4^*, -\omega_s, -\Lambda) = 0.$$
(3.5.7)

One can verify with explicit examples, for instance (5.3.51). There is a good reason why analytically continuing s to ω_s should give us the right answer. ψ_4 can always be written as:

$$\psi_4(\omega_1 \dots \omega_4, s, t, u, \{\Lambda\}). \tag{3.5.8}$$

Here $t = |\mathbf{k}_1 + \mathbf{k}_3|$ and $u = |\mathbf{k}_1 + \mathbf{k}_4|$. This is purely from kinematics, and holds non-perturbatively. Therefore it is reasonable that our procedure should involve analytically continuing off-shell versions of s, t, u.

More generally, given ψ_n , we write down all intermediate energies, for example $s_{12} = |\mathbf{k}_1 + \mathbf{k}_2|$, $s_{123} = |\mathbf{k}_1 + \mathbf{k}_2 + \mathbf{k}_3|$ and so on. We then define off-shell energies for these variables. We hypothesize the wavefunction coefficients should satisfy:

The contact COT hypothesis (for all orders in perturbation theory)

$$\operatorname{Disc} i\psi_n(\{\omega_e\}, \{\omega_i\}, \{\mathbf{k}\}, \{\Lambda\}) = 0 \tag{3.5.9}$$

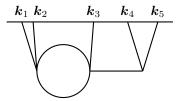
Here ω_e are off-shell external energies, ω_i are off-shell intermediate energies.

To prove this hypothesis we need to understand the integral measure for an arbitrary diagram. In general the measure is given by (the square root of) the Cayley-Menger determinant (see D.4 as well as [118, 119]), and to prove the hypothesis we need to how to properly analytically continue and flip the external energies within the measure¹¹. In addition it would be nice to properly understand how this procedure works for dimensional regularization and potential issues with branch cuts and $i\epsilon$ prescriptions.

If we are able to prove this hypothesis, then we could extend the single cut rules to loop diagrams. For

¹¹After the submission of the original version of the thesis in May, [120] was published, where the authors showed how to properly analytically continue the integration measure. See section 7 of the paper for details.

instance, consider the following diagram:



Let $s_l = |\mathbf{k}_1 + \mathbf{k}_2|$ and $s_r = |\mathbf{k}_4 + \mathbf{k}_5|$. Since the diagram can be written as:

$$\psi_{5}(\{\omega\}, \omega_{s_{l}}, \omega_{s_{r}}, \Lambda) = \int d\eta_{1} d\eta_{2} d\eta_{3} a^{4}(\eta_{1}) a^{4}(\eta_{2}) a^{4}(\eta_{3}) \prod_{i=1}^{5} K(\omega_{i})$$

$$\times \int_{\omega_{s_{l}}}^{\Lambda} dp_{+} \int_{-\omega_{s_{l}}}^{\omega_{s_{l}}} dp_{-} \frac{p_{+}^{2} - p_{-}^{2}}{\omega_{s_{l}}} G(p_{1}, \eta_{1}, \eta_{2}) G(p_{2}, \eta_{1}, \eta_{2}) G(\omega_{s_{r}}, \eta_{2}, \eta_{3}), \quad (3.5.10)$$

it is easy to see that $\underset{\omega_{s_r}}{\operatorname{Disc}} \psi_5$ corresponds to only cutting the right internal propagator. It would be nice to understand how this works for more complicated diagrams.

Beyond perturbation theory One of the ideas for generalizing the cosmological optical theorem, at least in dS, is to use holography. It is known that wavefunction coefficients in dS can be written as CFT correlators which lives on the future conformal boundary of dS [121]. The hope is to use ideas from the conformal bootstrap to provide non-perturbative constraints to the wavefunction coefficients.

Naively one may try to impose reflection positivity on the wavefunction coefficients. Reflection positivity is a constraint coming from the positivity of norms of states. Roughly speaking, in Euclidean signature a CFT correlator is reflection positive if it obeys:

$$\langle O(-\mathbf{x}_1, -\tau_1) \dots O(-\mathbf{x}_n, -\tau_n) O(\mathbf{x}_n, \tau_n) \dots O(\mathbf{x}_1, \tau_1) \rangle > 0.$$
(3.5.11)

A reflection positive correlator in Euclidean signature gives states with positive norm once we Wick rotate back to Lorentzian signature. This is also where we see why this idea doesn't work for wavefunction coefficients: the future conformal boundary of dS is Euclidean. There is no reason to Wick rotate to Lorentzian signature, therefore naturally this idea does not apply.

Another idea is to understand bulk unitarity of dS in terms of properties of the operator product expansion of the boundary CFT. For example, the equation (3.1.19) looks reminiscent to the relation between conformal blocks for four point CFT correlators $g_{\Delta,l}(u,v)$ and coefficients for three point CFT correlators $f_{\phi\phi O}$ [66]. However, this is only true for tree level, and this is not clear by looking at (3.5.1) that this idea works in general.

The main problem in using holography as a guide to generalize the COT is that many properties of the boundary field theory are poorly understood. For instance, it is unclear if the state operator correspondence exists [122], and it is unclear if an operator product expansion converges [123]. There are also very few concrete examples to experiment with (one of the few being [124]). As a result progress on generalizing the COT using holography has been slow.

There has been development in understanding unitarity non-perturbatively using in-in correlators [122,

123]. The main idea is to write down a spectral representation of an in-in correlator, then demand the spectral density to be positive (which translates to the positivity of the norm). While the wavefunction coefficients has been helpful in understanding perturbative unitarity, it may be possible that we need to look to the in-in correlators to properly understand non-perturbative unitarity ¹².

¹²Alternatively, one may use some procedure as in [105] to define an in-out object from in-in correlators, then study the consequence of unitarity by looking at this new in-out object.

Chapter 4

Applying the bootstrap to parity odd correlators

One of the more interesting consequences of the cosmological bootstrap is its constraints on parity odd correlators. By geometric considerations, parity odd signals are absent from the power spectrum and the bispectrum, hence the leading signal would come from the trispectrum. In particular parity odd trispectrum has attracted attention due to hints of detection from galaxy surveys [125, 126]. On the theoretical side it is beneficial to understand parity odd signals from the primordial universe, as they may hint towards exotic physics [127–131].

It has been noted previously that parity odd trispectrum for massless scalars is always zero in tree level in-in calculations [132], however more recently it is discovered that the vanishing of in-in correlators is in fact a consequence of the cosmological bootstrap [133]. In this section we will briefly review how unitarity, locality and scale invariance force the parity odd tree level trispectrum to be zero for a massless scalar, with interactions mediated by scalars and massless spinning particles. We will then explore the validity of this claim beyond tree level. By computing explicit examples of one loop diagrams, we will see that the one loop parity odd trispectrum is non-zero in general, even if the interaction involves only scalars.

4.1 Review: Tree level no-go theorem for parity odd trispectrum

Let us first quickly review the no-go theorem for tree level parity odd trispectrum of massless scalars in dS. The argument is taken from [133], and relies on the the following properties:

- Unitarity. We covered this extensively in section 3.
- Manifest locality. This is the requirement that interactions are built out of fields and their derivatives in the same spacetime point [134]. It can be shown that for massless scalars, this gives the following constraint known as the manifestly local test (MLT):

$$\frac{\partial}{\partial \omega_e} \psi_n(\{\omega\})|_{\omega_e = 0} = 0, \tag{4.1.1}$$

where ω_e is the energy of an external leg.

 Scale invariance. This means that for three spatial dimensions, the wavefunction of a massless scalar obeys:

$$\psi_n(\{\lambda\omega\}, \{\lambda\mathbf{k}\}) = \lambda^3 \psi_n(\{\omega\}, \{\mathbf{k}\}). \tag{4.1.2}$$

Then the proof can be summarized as follow:

- For parity odd interaction $\rho_4^{PO}(\mathbf{k}) = \frac{1}{2} (\rho_4(\mathbf{k}) \rho_4(-\mathbf{k}))$. Using the definition (2.3.9) this means the parity odd part of ρ_4 must be pure imaginary. As a consequence ψ_4 must have an imaginary part for the parity odd part of ρ_4 (and subsequently the trispectrum) to be non-zero.
- Let us consider ψ_4 from a contact diagram. The contact COT is given by:

$$\psi_4(\{\omega\}, \{\mathbf{k}\}) + \psi_4^*(\{-\omega\}, \{-\mathbf{k}\}) = 0. \tag{4.1.3}$$

Combined with (4.1.2) (where we set $\lambda = -1$), this implies ψ_4 for a contact diagram is purely real, and cannot contribute to the parity odd part of ρ_4 . Using the same argument, ψ_n for a contact diagram is real for any n.

• The single cut COT allow us to express the partial energy poles of an exchange ψ_4 in terms of ρ_3 computed from a contact ψ_3 , and by imposing the MLT, one can fully fix the exchange ψ_4 in terms of contact ψ_3 (see [134]). Notice that the constraint equations (4.1.1) are real. Combined with the fact that the contact ψ_3 (and hence ρ_3) is always real or purely imaginary if the interaction is mediated by scalars or massless spinning fields¹, this implies the exchange ψ_4 is also real, and cannot contribute to parity odd part of ρ_4 .

Hence, we arrive at the conclusion:

Tree level parity odd trispectrum for a massless scalar is zero for a local, unitary theory with (IR-finite) interactions mediated by scalars or massless spinning fields.

4.2 More about scale invariance

The above derivation heavily relies on the assumption of scale invariance. Suppose we we modify the scaling behaviour of the wavefunction coefficient to be in the following way²:

$$\psi_n(\{\lambda\omega\}, \{\lambda\mathbf{k}\}) = \lambda^{3+\delta}\psi_n(\{\omega\}, \{\mathbf{k}\}). \tag{4.2.1}$$

¹In the case of scalars ψ_3 is always zero due to momentum conservation. For massless spinning fields the scaling has integer dimension, and so ψ_3 is always either real or purely imaginary. In addition, since this result comes from considering the overall scaling, ψ_3 cannot go from real to purely imaginary by changing the interactions involved, assuming the fields involved are the same. For massive spinning fields this is no longer true, so one can break parity by coupling to massive spinning fields.

²The author would like to thank Ayngaran Thavanesan for many fruitful discussions regarding this point.

Let us see what this means for the contact ψ_n . Combining our new scale invariance condition with the COT, this implies:

$$\psi_n(\{\omega\}, \{\mathbf{k}\}) - \psi_n^*(\{\omega\}, \{\mathbf{k}\}) = [e^{i\pi\delta} - 1]\psi_n^*(\{\omega\}, \{\mathbf{k}\}). \tag{4.2.2}$$

There is a non-zero imaginary component for the contact wavefunction coefficient if δ is non-zero. Because the exchange ψ_4 is fixed in terms of the contact ψ_3 this also implies the exchange ψ_4 will get an imaginary part.

This result is significant in the following way:

- Cosmological measurements tell us the power spectrum scales approximately as k^3 , however there are corrections to the scaling dimensions. These corrections (commonly written as $n_s 1$) are proportional to the slow roll parameters. The argument above tell us that the parity odd trispectrum is slow roll suppressed, on top of any additional suppression coming from the interaction vertices.
- When we have IR secular divergences, this will generally generate additional logarithmic terms. This breaks scale invariance, and so the no-go theorem no longer holds. See [133] for more details.
- Last but not least, when we regulate UV divergences, this will result in violation of (4.1.2). This is particularly easy to see in the case of dimensional regularization, where we compute the trispectrum in $d = 3 + \delta$ instead. Therefore in general we expect an imaginary part in the wavefunction coefficient in dimensional regularization, and it is multiplied by powers of the regulator δ . This is not a harmless term that vanishes as $\delta \to 0$: since there is a UV divergence, we expect terms which goes as $1/\delta$, and so we will obtain a finite imaginary contribution to the wavefunction coefficient in the end.

The last statement is why the no-go theorem generally fails beyond tree level. In the remainder of the section we will make this argument precise. However, before we do this, we need to learn more about dimensional regularization in de Sitter.

Prescription for dimensional regularization In de Sitter spacetime, dimensional regularization is not as straightforward as in flat space (see [135–137] for pioneering work on loop contributions in de Sitter). Naively, we would only analytically continue the number of spatial dimensions in the momentum integral from 3 to $d=3+\delta$. However, doing so breaks scale invariance, and this is manifest in the appearance of logarithmic terms of the form $\log(k/\mu)$ in loop diagrams, even in the absence of IR divergences. To ensure manifest scale invariance, the authors of [138] suggested to analytically continue the mode functions as well. In Minkowski this would be inconsequential because the mode functions are always $e^{i\Omega t}$ with $\Omega = \sqrt{\mathbf{k}^2 + m^2}$ in any number of dimensions. Conversely, in de Sitter the number of spatial dimensions appears in the index of the Hankel function, which must be carefully tracked.

Working with Hankel functions H_{ν} with a general complex index $\nu(d)$ is possible but leads to complicated algebraic manipulations. To avoid this while maintaining manifest scale invariance, we will employ a trick used in [117]: we analytically continue both the number of spatial dimensions and the mass of the field in such a way that the index of the Hankel function is always $\nu = 3/2$. For scalar fields, this results

in the following mode functions

$$f_k(\eta) = (-H\eta)^{\delta/2} \frac{H\eta}{\sqrt{2k}} e^{ik\eta}$$
 (conformally coupled scalar), (4.2.3)

$$f_k(\eta) = (-H\eta)^{\delta/2} \frac{H}{\sqrt{2k^3}} (1 - ik\eta) e^{ik\eta}$$
 (massless scalar), (4.2.4)

where δ should be taken to zero at the end of the calculation. For later convenience, notice that we can write the mode functions also as

$$f_k(\eta) = -\frac{1}{\sqrt{2k}} (iH\partial_k)^{1+\delta/2} e^{ik\eta}$$
 (conformally coupled scalar) (4.2.5)

$$f_k(\eta) = \frac{H^2}{\sqrt{2k^3}} (iH\partial_k)^{\delta/2} (1 - k\partial_k) e^{ik\eta}$$
 (massless scalar). (4.2.6)

This will be useful to simplify some of the calculations.

4.3 One site loop

We will first look at the simplest loop diagram: the diagram where the loop has a single interaction vertex and hence a single bulk-bulk propagator. Interestingly, for both parity even and parity odd interactions, the contribution of these diagrams to correlators vanishes in dimensional regularization (dim reg) in Minkowski and in de Sitter spacetime, if the fields in the loop are massless. This is somewhat analogous to what happens for amplitudes. Conversely, one-loop one-vertex diagrams with massless fields generate non-vanishing contributions to wavefunction coefficients in general. A detailed cancellations among different terms in the wavefunction when computing correlators then ensures that these two results are compatible. As we will discuss, the physical reason is that for correlators there is no energy-momentum flow inside the loop, while for wavefunction coefficients the total energy of the diagrams flows from the boundary into the loop.

Moreover, we generalize our analysis to massive fields running in the loop and present several explicit results. Our finding are summarised in Table 4.1.

As a last remark, we notice that one-loop one-vertex diagrams cam be made to vanish by fiat by applying normal ordering to all interactions. While this is a possible way to bypass the calculations in this section, we find it nevertheless interesting to discuss what happens for non normal ordered interactions for at least two reasons: first this gives us a simple toy model of an exact cancellation of a term in the wavefunction when computing correlators, which could be an instance of a more general phenomenon, and because normal ordering would not remove similar contributions at higher loop order.

4.3.1 Correlators

Let's start computing a simple one-loop, one-vertex contribution to a correlator. For concreteness we focus on a four-point function, but the same discussion applies for any n-point function. For simplicity of exposition, we consider a single scalar field.

Minkowski spacetime We start in Minkowski, and then discuss de Sitter spacetime. To use the Feynmann rules to compute correlators we need the bulk-boundary and bulk-bulk propagators, which in

	de Sitter			Minkowski	
	m = 0	$m = \sqrt{2}H$	$m \neq 0, \sqrt{2}H$	m = 0	$m \neq 0$
$\psi_4^{(1L)}$	IR divergences?	$\log k$	complicated	$\log k$	$\log m$
$B_4^{(1L)}$	0	0	analytic	0	analytic

Table 4.1: Summary of the results of the one-loop one-vertex diagrams. Here $\log k$ denotes schematically the logarithm of some combination of external kinematics; correlators marked 'analytic' are analytic in the external kinematics; where logarithms appear during regularisation of loop integrals, they can be removed entirely by a judicious choice of the renormalisation scale. The non-analytic terms in ψ_4 cancel out with other non-analytic terms related to tree-level wavefunction coefficients when computing correlators.

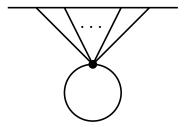


Figure 4.1: one site loop diagram for a n-point correlator.

Minkowski are simply

$$G_{+}(t,k) = \frac{e^{i\Omega t}}{2\Omega}, \qquad G_{+-}(t_1,t_2,p) = G_{-+}^{*}(t_1,t_2,p) = \frac{e^{i\Omega(t_1-t_2)}}{2\Omega},$$
 (4.3.1)

$$G_{++}(t_1, t_2, p) = \frac{e^{i\Omega(t_2 - t_1)}}{2\Omega} \theta(t_1 - t_2) + (t_1 \leftrightarrow t_2) . \tag{4.3.2}$$

where $\Omega = \sqrt{k^2 + m^2}$ is the on-shell energy and the labels \pm refer to interactions in the time ordered time evolution of the ket or anti-time ordered time evolution of the bra in the in-in correlator. Since our results will not depend on the number of spatial or time derivatives, we consider a simple polynomial interaction,

$$\mathcal{L}_{\text{int}} = \int_{\mathbf{r}} \frac{\lambda}{6!} \phi^6. \tag{4.3.3}$$

For the diagram in Figure 4.1 we have

$$B_4 = 2 \operatorname{Re} \left[\frac{i\lambda}{2} \int_{\mathbf{p}} \int_{\infty}^{0} dt \, G_{++}(t, t, p) \prod_{a}^{4} G_{+}(t, k_a) \right]. \tag{4.3.4}$$

The crucial point is that, since the bulk-bulk propagator is evaluated at coincident times, the oscillating exponentials cancel each other and the dependence on loop momentum is only given by the overall normalization factor

$$G_{++}(t,t,p) = \frac{e^{i\Omega(t-t)}}{2\Omega} = \frac{1}{2\sqrt{p^2 + M^2}} \xrightarrow{M \to 0} \frac{1}{2p}.$$
 (4.3.5)

For a massless scalar this reduces to a power law dependence, $G_{++} \propto 1/p$. Notice that the dependence would still be a power law in the presence of time and space derivatives from local interactions. Now we

regulate the loop integral in \mathbf{p} using dim reg. Since the integral is a power of p, it vanishes in dim reg³

$$\int dp^d p^\alpha = 0 \quad \text{(dim reg)}. \tag{4.3.6}$$

This is intuitive because there is no scale in the integrand with which to write a dimensionally correct result. We conclude that a loop of a massless particle with a single vertex does not contribute to Minkowski correlators. This would remain true if we computed the correlator at unequal times.

If the field running in the loop is massive the momentum integral no longer vanishes in dim reg. Instead we have the following:

$$B_4 = \frac{1}{8\Omega_1 \Omega_2 \Omega_3 \Omega_4} \int_{\mathbf{p}} \frac{\lambda}{4\Omega_n \Omega_T^{(4)}},\tag{4.3.7}$$

where $\Omega_p = \sqrt{p^2 + m^2}$ and $\Omega_T^{(4)} = \Omega_1 + \Omega_2 + \Omega_3 + \Omega_4$ is the total energy entering the diagram. This integral can be evaluated to give:

$$B_4 = \frac{1}{8\Omega_1 \Omega_2 \Omega_3 \Omega_4} \frac{\lambda m^2}{16\pi^2 k \Omega_T^{(4)}} \left(\frac{1}{\delta} + \log \frac{m}{\mu} + (\text{analytic}) \right), \tag{4.3.8}$$

where μ is a renormalization scale. Notice that the result is analytic in the external kinematics.

Massless scalars on de Sitter spacetime Something very similar happens for massless fields in de Sitter spacetime. The in-in correlator is given by:

$$B_4 = 2 \operatorname{Re} \left[\frac{i\lambda}{2} \int_{\mathbf{p}} \int_{-\infty}^{0} \frac{d\eta}{\eta^{d+1}} G_{++}(\eta, \eta, p) \prod_{a}^{4} G_{+}(\eta, k_a) \right]. \tag{4.3.9}$$

At coincident times, the bulk-to-bulk propagator reads:

$$G_{++}(\eta, \eta, p) = \frac{H^2}{2p^3} (1 - ip\eta)(1 + ip\eta)e^{ip(\eta - \eta)} = \frac{H^2}{2p^3} (1 + p^2\eta^2). \tag{4.3.10}$$

The propagator is simply a polynomial in p, so in dim reg this vanishes just like the Minkowski correlator. A similar cancellation also occurs for conformally coupled scalars in de Sitter as well. The vanishing of this contribution is familiar from scattering amplitudes and is usually described by saying that there is no flow of energy or momentum through the loop from the external kinematics. In the absence of both a mass and external kinematics, the loop has no way to satisfy dimensional analysis and must hence vanish.

Massive scalars on de Sitter spacetime Similarly to the case of massive scalars on Minkowski spacetime, the one-loop one-vertex diagram on de Sitter is not expected to vanish for massive fields. The mode function for a massive scalar on de Sitter in the dim reg procedure described in Section 4.2 is

$$f_k(\eta) = \frac{i\sqrt{\pi}H^{1+\frac{\delta}{2}}}{2}(-\eta)^{\frac{3+\delta}{2}}H_{\nu}^{(1)}(-k\eta), \tag{4.3.11}$$

³Had we used a cutoff regularization we would have found power law divergences, to be removed by renormalization, but no left over logarithmic running

with $\nu = \sqrt{\frac{9}{4} - \frac{m^2}{H^2}}$ and $H^{(1)}$ the Hankel function of the first kind. The one-loop trispectrum for a massive scalar with a $\lambda \phi^6/6!$ interaction at conformal time η_f is then given by the following integral:

$$B_{4} = \operatorname{Re}\left(i\lambda \frac{\pi^{4} H^{8+4\delta}}{256} (-\eta_{f})^{2(3+\delta)} H_{\nu}^{(1)*}(-k_{1}\eta_{f}) \dots H_{\nu}^{(1)*}(-k_{4}\eta_{f})\right)$$

$$\int_{\mathbf{R}} \int_{-\infty}^{\eta_{f}} d\eta a^{4+\delta}(\eta) (-\eta)^{2(3+\delta)} H_{\nu}^{(1)}(-k_{1}\eta) \dots H_{\nu}^{(1)}(-k_{4}\eta) \frac{\pi H^{2+\delta}}{4} (-\eta)^{3+\delta} \left| H_{\nu}^{(1)}(-p\eta) \right|^{2} .$$

$$(4.3.12)$$

As $H_{\nu}^{(1)}(x) \sim x^{-\nu}$ as $x \to 0$, we must rescale the correlator in order to find a finite value as $\eta_f \to 0$. The resulting correlator is

$$B_{4}' = \operatorname{Re}\left(i\lambda \frac{\pi^{4}H^{8+4\delta}}{256} \left(\frac{2^{\nu}\Gamma(\nu)}{\pi}\right)^{4} \right)$$

$$\int_{\mathbf{p}} \int_{-\infty}^{0} d\eta a^{4+\delta}(\eta)(-\eta)^{2(3+\delta)} H_{\nu}^{(1)}(-k_{1}\eta) \dots H_{\nu}^{(1)}(-k_{4}\eta) \frac{\pi H^{2+\delta}}{4}(-\eta)^{3+\delta} \left|H_{\nu}^{(1)}(-p\eta)\right|^{2}. \quad (4.3.13)$$

Since the momentum integral vanishes in dim reg for massless and conformally-coupled scalars, and because it contains fewer Hankel functions, it is reasonable to attempt that integral first:

$$\mathcal{I}_{p} = \int \frac{\mathrm{d}^{3+\delta}p}{(2\pi)^{3}} \Big| H_{\nu}^{(1)}(-p\eta) \Big|^{2}. \tag{4.3.14}$$

For $\nu = \frac{3}{2}$ (massless) and $\nu = \frac{1}{2}$ (conformally-coupled), the integrand is a sum of power laws in p and vanishes in dim reg. Strictly, however, \mathcal{I}_p converges only for $\text{Re}(\delta) < -2$ and $-3 - \delta < \text{Re}(2\nu) < 3 + \delta$ (due to the behavior of the Hankel function as $p \to \infty$ and $p \to 0$ respectively). Then,

$$\mathcal{I}_{p} = \frac{2^{2+\delta} \csc(\pi \nu) \sec\left(\frac{\pi \delta}{2}\right)}{\left(2\pi\right)^{3+\delta} \left(-\eta\right)^{3+\delta} \Gamma\left(-\frac{1}{2} - \frac{\delta}{2}\right)} \left[-\Gamma\left(\frac{3+\delta}{2} - \nu\right) \frac{{}_{2}F_{1}\left(\frac{3+\delta}{2}, \frac{3+\delta}{2} - \nu, 1 - \nu; 1\right)}{\Gamma(1-\nu)} \sin\left(\frac{\pi \delta}{2} - \pi\nu\right) + \Gamma\left(\frac{3+\delta}{2} + \nu\right) \frac{{}_{2}F_{1}\left(\frac{3+\delta}{2}, \frac{3+\delta}{2} + \nu, 1 + \nu; 1\right)}{\Gamma(1+\nu)} \sin\left(\frac{\pi \delta}{2} + \pi\nu\right) \right]. \quad (4.3.15)$$

When $Re(\delta) < -2$ this expression can be simplified as:

$$\mathcal{I}_{p} = \frac{2^{2+\delta}\pi \csc(\pi\nu)\sec\left(\frac{\pi\delta}{2}\right)\Gamma(-2-\delta)}{(2\pi)^{3+\delta}\left(-\eta\right)^{3+\delta}\Gamma(-\frac{1}{2}-\frac{\delta}{2})\Gamma(-\frac{1}{2}-\frac{\delta}{2}-\nu)\Gamma(-\frac{1}{2}-\frac{\delta}{2}+\nu)} \left[\frac{\sin\left(\frac{\pi\delta}{2}-\pi\nu\right)}{\cos\left(\frac{\pi\delta}{2}-\pi\nu\right)} - \frac{\sin\left(\frac{\pi\delta}{2}+\pi\nu\right)}{\cos\left(\frac{\pi\delta}{2}+\pi\nu\right)}\right].$$
(4.3.16)

We analytically continue this expression in δ and study its behavior as $\delta \to 0$. One can check that this expression indeed gives zero for a massless or a conformally-coupled scalar, as expected. More generally, the $\Gamma(-2-\delta)$ term in the integral will contribute a δ^{-1} divergence in dim reg.

From the factors of H^{δ} in the time integral and the δ^{-1} divergence in the momentum integral, terms like $\log \frac{H}{\mu}$ will appear in the final correlator. However, as long as the time integral is IR-convergent, i.e. $\operatorname{Re} \nu < \frac{\delta+3}{4}$, scale invariance is unbroken, which fixes the form of the correlator and precludes any $\log \frac{k}{\mu}$ terms, where k stands for some combination of the external momenta. As on Minkowski spacetime, the resulting trispectrum must then be analytic in the external kinematics.

4.3.2 Wavefunction coefficients

Now let's try and perform the same calculation using the wavefunction formalism.

Massless scalar in Minkowski spacetime Let's start with massless scalars. In flat spacetime the wavefunction propagators are

$$K_{\mathbf{k}}(t) = e^{ikt}, \qquad G_{\mathbf{k}}(t_1, t_2) = \frac{1}{2ik} \left(e^{ik(t_2 + t_1)} - e^{ik(t_2 - t_1)} \right) \theta(t_1 - t_2) + (t_1 \leftrightarrow t_2).$$
 (4.3.17)

With an interaction $\lambda \phi^6/6!$, the relevant wavefunction coefficients are⁴

$$\psi_6^{\text{tree}}(\mathbf{k}_1, \dots, \mathbf{k}_6) = i \int_{-\infty(1-i\varepsilon)}^0 dt \, e^{ik_T^{(6)}t} \lambda \tag{4.3.18}$$

$$=\frac{\lambda}{k_T^{(6)}}, \quad \text{and} \tag{4.3.19}$$

$$\psi_4^{(1L)}(\mathbf{k}_1, \dots, \mathbf{k}_4) = \int_0^0 dt \, \frac{\lambda}{2} e^{ik_T^{(4)}t} \int_{\mathbf{R}} \frac{1}{2ip} \left[e^{2ipt} - 1 \right]. \quad \text{Performing the time integral first,}$$
 (4.3.20)

$$= \int_{\mathbf{p}} \frac{\lambda}{-4p} \left[\frac{1}{k_T^{(4)} + 2p} - \frac{1}{k_T^{(4)}} \right]. \tag{4.3.21}$$

This last integral is UV divergent and needs to be regularized. In dimensional regularisation, the second term in brackets in $\psi_4^{(1L)}(\mathbf{k}_1,\ldots,\mathbf{k}_4)$ vanishes; while the first term in \overline{MS} , gives

$$\psi_4^{(1L)}(\mathbf{k}_1 \dots \mathbf{k}_4) = -\frac{6\lambda}{32\pi^2} k_T^{(4)} \ln \frac{k_T^{(4)}}{\mu}.$$
 (4.3.22)

This non-vanishing result is intriguing because we had just found that a similar 1-loop 1-vertex contribution vanishes for correlators. We will show shortly show that the two results are compatible and that indeed the term in (4.3.22) cancels exactly with another term when computing B_4 . Here we would like to make some general remarks. Notice that in the wavefunction calculation there is a flow of energy from the external kinematics though the loop. This is visible in the denominator $k_T^{(4)} + 2p$ in (4.3.21) arising after performing the time integrals. This is naively surprising because we are computing a diagram that is identical to that for the correlator where we stated that there is no energy-momentum flow through the loop. The resolution is that the wavefunction, in contrast to a correlator, provides the answer to a boundary value problem where ϕ has been specified at some time, which we take to be t=0 here. This explicit boundary condition breaks time translation invariance and energy can flow from this boundary. Indeed, it is precisely the total energy that flows into the loop, because the boundary is attached to all external legs. Also, since the boundary does not break spatial translations, there is no flow of spatial momentum through the loop, only energy. At the mathematical level, the origin of the energy flow through the loop is the boundary term in the wavefunction's bulk-bulk propagator G, which is absent in the correlator's bulk-bulk propagator G_{++} . A more colorful way to say this is that the bulk-bulk propagator in the loop represents the quantum fluctuation of a virtual particle. In the correlator, such fluctuations are unconstrained, but

⁴Notice that given our definition of the bulk-bulk propagator in (4.3.17), which includes a factor of i, the correct Feynman rule is to introduce a factor of i^{1-L} , where L is the number of loops, and no factor of i on the vertices, which simply result in a factor of λ .

in the wavefunction they must obey the boundary condition that ϕ takes some fixed value at t = 0. This requires the quantum fluctuation to turn off as the interaction vertex is pushed toward t = 0, which in turn requires knowledge of this fix boundary and hence a breaking of time translations. This mechanism is actually closerly related to how the recursion relations for the Minkowski wavefunction were derived in [80].

Now use the wavefunction coefficients to find the trispectrum. Performing the average over ϕ in the Born rule we find

$$B_4 = \frac{1}{\prod_a^4 2 \operatorname{Re} \psi_2(k_a)} \left[\rho^{(1L)}(\{\mathbf{k}\}) + \int_{\mathbf{p}} \frac{\rho^{\operatorname{tree}}(\{\mathbf{k}\}, \mathbf{p}, -\mathbf{p})}{2 \operatorname{Re} \psi_2(p)} \right]$$
(4.3.23)

where $\{\mathbf{k}\} = \{\mathbf{k}_1, \dots, \mathbf{k}_4\}$ and ρ denotes the coefficient of the diagonal part of the density matrix $|\Psi|^2$,

$$\rho^{(1L)}(\{\mathbf{k}\}) = \psi_4^{(1L)}(\mathbf{k}_1, \dots, \mathbf{k}_4) + \psi_4^{(1L)}(-\mathbf{k}_1, \dots, -\mathbf{k}_4)^*$$
(4.3.24)

$$\rho^{\text{tree}}(\{\mathbf{k}\}, \mathbf{p}, -\mathbf{p}) = \psi_6^{\text{tree}}(\mathbf{k}_1, \dots, \mathbf{k}_4, \mathbf{p}, -\mathbf{p}) + \psi_6^{\text{tree}}(-\mathbf{k}_1, \dots, -\mathbf{k}_4, -\mathbf{p}, \mathbf{p})^*. \tag{4.3.25}$$

The free power spectrum in Minkowski is 1/2k and so Re $\psi_2 = -k$. For the parity even contribution in (4.3.3) we can simply drop the minus sign on the momenta. Then, the first contribution to B_4 in (4.3.23) is

$$-\frac{1}{\prod_{a}^{4} 2 \operatorname{Re} \psi_{2}(k_{a})} \rho^{(1L)}(\{\mathbf{k}\}) = \frac{1}{16e_{4}} 2 \operatorname{Re} \psi_{4}^{(1L)}(\mathbf{k}_{1}, \dots, \mathbf{k}_{4})$$
(4.3.26)

$$= \frac{1}{8e_4} \cdot \frac{-6\lambda}{32\pi^2} k_T^{(4)} \ln \frac{k_T^{(4)}}{\mu}.$$
 (4.3.27)

The second is

$$-\frac{1}{\prod_{a}^{4} 2\operatorname{Re}\psi_{2}(k_{a})} \int_{\mathbf{p}} \frac{\rho^{\operatorname{tree}}(\{\mathbf{k}\}, \mathbf{p}, -\mathbf{p})}{2\operatorname{Re}\psi_{2}(p)} = \frac{1}{16e_{4}} \frac{1}{2} \int_{\mathbf{p}} \frac{1}{2p} 2\operatorname{Re}\psi_{6}^{\operatorname{tree}}(\mathbf{k}_{1}, \dots, \mathbf{k}_{4}, \mathbf{p}, \mathbf{p})$$
(4.3.28)

$$= \frac{1}{8e_4} \frac{1}{2} \int_{\mathbf{p}} \frac{1}{2p} \frac{\lambda}{k_T^{(4)} + 2p}.$$
 (4.3.29)

The momentum integral is just -1 times that of $\psi_4^{(1L)}(\mathbf{k}_1 \dots \mathbf{k}_4)$, so the two contributions to the trispectrum cancel.

The cancellation of the logarithmic term in the one site loop diagram is an example of a more general result. Namely, the total energy branch point from the wavefunction always cancels when computing the in-in correlator. We will discuss this further in section 6.4.

Massive scalar in Minkowski spacetime For massive scalars we no longer expect the contribution from $\rho^{(1L)}$ and ρ^{tree} to cancel. Let us calculate $\psi_{\mathbf{k}_1...\mathbf{k}_4}^{(1L)}$ explicitly. We have:

$$\psi_{\mathbf{k}_{1}...\mathbf{k}_{4}}^{(1L)} = \int^{0} dt \frac{\lambda}{2} e^{i\Omega_{T}^{(4)}t} \int_{\mathbf{p}} \frac{1}{2i\Omega_{p}} [e^{2i\Omega_{p}t} - 1]$$

$$= \frac{\lambda}{2\Omega_{T}^{(4)}} \int_{\mathbf{p}} \frac{1}{\Omega_{T}^{(4)} + 2\sqrt{p^{2} + m^{2}}}.$$
(4.3.30)

In the regime $m > \Omega_T^{(4)}$ this integral can evaluated easily, since we can write the integral as:

$$\psi_{\mathbf{k}_{1}...\mathbf{k}_{4}}^{(1L)} = \frac{\lambda}{8\pi^{2}\Omega_{T}^{(4)}} \int_{0}^{\infty} dp \frac{p^{2+\delta}}{\sqrt{p^{2}+m^{2}}} \sum_{n=0}^{\infty} \left(\frac{-\Omega_{T}^{(4)}}{2\sqrt{p^{2}+m^{2}}}\right)^{n}.$$
 (4.3.31)

Evaluating this integral gives

$$\psi_{\mathbf{k}_{1}...\mathbf{k}_{4}}^{(1L)} = \sum_{n=0}^{\infty} \frac{\lambda}{16\pi^{2}\Omega_{T}^{(4)}} \left(\frac{-\Omega_{T}^{(4)}}{2}\right)^{n} m^{2-n-\delta} \frac{\Gamma(\frac{3}{2})\Gamma(\frac{n}{2}+\delta-1)}{\Gamma(\frac{n+1}{2})}$$

$$= \frac{\lambda}{16\pi^{2}\Omega_{T}^{(4)}} \left(m^{2} - \frac{(\Omega_{T}^{(4)})^{2}}{2}\right) \left(\frac{1}{\delta} + \log\frac{m}{\mu} + (\text{analytic})\right). \tag{4.3.32}$$

Compared to B_4 we have an extra contribution of the form $\Omega_T^{(4)} \log m$, and we expect this to be cancelled by the term from ρ^{tree} . Indeed, we find that for $m > \Omega_T^{(4)}$:

$$\begin{split} \frac{1}{\prod_{a}^{4} 2 \operatorname{Re} \psi_{2}(k_{a})} \int_{\mathbf{p}} \frac{\rho^{\operatorname{tree}}(\{\mathbf{k}\}, \mathbf{p}, -\mathbf{p})}{2 \operatorname{Re} \psi_{2}(p)} &= \frac{1}{16e_{4}} \frac{1}{2} \int_{\mathbf{p}} \frac{1}{2\Omega_{p}} 2 \operatorname{Re} \psi_{6\mathbf{k}_{1}...\mathbf{k}_{4}\mathbf{p}\mathbf{p}} \\ &= \frac{1}{8e_{4}} \frac{\lambda}{2} \int_{\mathbf{p}} \frac{1}{2\sqrt{p^{2} + m^{2}}} \frac{1}{\Omega_{T}^{(4)} + 2\sqrt{p^{2} + m^{2}}} \\ &= \frac{1}{8e_{4}} \sum_{n=0}^{\infty} \frac{\lambda}{32\pi^{2}} \left(\frac{-\Omega_{T}^{(4)}}{2} \right)^{n} m^{1-n+\delta} \frac{\Gamma(\frac{3}{2})\Gamma(\frac{n-1}{2} - \delta)}{\Gamma(\frac{n}{2} + 1)} \\ &= \frac{1}{8e_{4}} \frac{\lambda}{16\pi^{2}} \frac{\Omega_{T}^{(4)}}{2} \left(\frac{1}{\delta} + \log \frac{m}{\mu} + (\operatorname{analytic}) \right). \end{split} \tag{4.3.33}$$

Therefore, using (4.3.23), the contributions of the form $\Omega_T^{(4)} \log m$ cancels in B_4 , and we obtain the expression in (4.3.8).

De Sitter spacetime We can consider a similar $\lambda \sigma^6/6!$ interaction of a conformally-coupled scalar on de Sitter. Since such a field is massive, as $\eta_0 \to 0$ it decays. Formally, to avoid this issue, we consider the wavefunction of the re-scaled field σ/η_0 in this limit; this amounts to factoring out all factors of η_0 in the propagators. With this prescription, and using the scale-invariant dim reg procedure discussed in Section 4.2, the wavefunction propagators are

$$K_{\mathbf{k}}(\eta) = (-\eta)^{\delta} \eta e^{ik\eta} \tag{4.3.34}$$

$$G_{\mathbf{k}}(\eta_1, \eta_2) = i \frac{\left(H^2 \eta_1 \eta_2\right)^{1 + \frac{\delta}{2}}}{2k} \left[e^{-ik(\eta_2 - \eta_1)} \theta(\eta_1 - \eta_2) + (\eta_1 \leftrightarrow \eta_2) - e^{ik(\eta_1 + \eta_2)} \right]. \tag{4.3.35}$$

The relevant wavefunction coefficients are

$$\psi_6^{\text{tree}}(\mathbf{k}_1, \dots, \mathbf{k}_6) = i\lambda \int_{-\infty(1-i\varepsilon)}^0 d\eta \frac{1}{(-H\eta)^{4+\delta}} (-\eta)^{6+3\delta} e^{ik_T^{(6)}\eta}$$
(4.3.36)

$$= -\frac{\lambda e^{2\pi i\delta}\Gamma(3+2\delta)}{H^{4+\delta} \left(k_T^{(6)}\right)^{3+2\delta}} \tag{4.3.37}$$

and

$$\psi_4^{(1L)}(\mathbf{k}_1 \dots \mathbf{k}_4) = \frac{\lambda}{2} \int_{-\infty(1-i\varepsilon)}^0 d\eta \frac{1}{(-H\eta)^{4+\delta}} (-\eta)^{4+2\delta} e^{ik_T^{(4)}\eta} \int \frac{d^{3+\delta}p}{(2\pi)^{3+\delta}} \frac{i(H^2\eta^2)^{1+\frac{\delta}{2}}}{2p} \left[1 - e^{2ip\eta}\right]. \quad (4.3.38)$$

The first term in the brackets yields a power law in p after the time integral is performed, and vanishes in dim reg. The time integral in the second term is essentially the same as in ψ_6^{tree} :

$$\psi_4^{(1L)}(\mathbf{k}_1 \dots \mathbf{k}_4) = \frac{\lambda}{2} \int \frac{\mathrm{d}^{3+\delta} p}{(2\pi)^{3+\delta}} \frac{H^{2(1+\frac{d}{2})}}{2p} \frac{\Gamma(3+2\delta)e^{2\pi i\delta}}{H^{4+\delta} \left(k_T^{(4)} + 2p\right)^{3+2\delta}}.$$
 (4.3.39)

This momentum integral is finite:

$$\psi_4^{(1L)}(\mathbf{k}_1 \dots \mathbf{k}_4) = \frac{i\lambda e^{2\pi i\delta}}{2^{8+3\delta} \pi^{\frac{3+\delta}{2}} H^2 \left(ik_T^{(4)}\right)^{1+\delta}} \frac{\Gamma(2+\delta)\Gamma(1+\delta)}{\Gamma(\frac{3+\delta}{2})}; \tag{4.3.40}$$

since it is analytic in the momenta as $\delta \to 0$, it could be removed by local counter-terms. Local counter-terms would then also have to be added to remove the contribution of $\psi_6^{\rm tree}$ to the trispectrum.

More generally, consider either conformally coupled scalars or massless scalar with IR finite interactions, i.e. the resulting correlators do not diverge as $\eta_0 \to 0$. The integrals encountered when considering the one site loop diagram for these fields can be grouped into two types: the first type is

$$\mathcal{I}_{m}^{1} = \int_{-\infty}^{0} d\eta \,\, \eta^{n+m+2\delta} e^{ik_{T}^{(4)}\eta} \int_{0}^{\infty} dp \frac{p^{2+m+\delta}}{2p^{3}},\tag{4.3.41}$$

which vanishes in dim reg. The second type is:

$$\mathcal{I}_{m}^{2} = \int_{-\infty}^{0} d\eta \, \eta^{n+m+2\delta} e^{ik_{T}^{(4)}\eta} \int_{0}^{\infty} dp \frac{p^{2+m+\delta}}{2p^{3}} e^{2ip\eta}
= \int_{0}^{\infty} dp \frac{(-i)^{n+m+\delta} \Gamma(n+m+1+2\delta)p^{-1+m+\delta}}{(k_{T}^{(4)}+2p)^{n+m+1+2\delta}},$$
(4.3.42)

where m=0,1,2. By power counting this momentum integral is always convergent for $n \geq 0$, which is always true for IR finite interactions. Hence terms coming from these integrals are always finite and analytic in $k_T^{(4)}$.

When we consider more general massive scalars, the integrals involved are much harder to solve. Namely, we have to integrate over products of Hankel functions, and we expect the result not to be analytic in $k_T^{(4)}$ in general.

4.4 Two site loop: general strategy and a toy model example

For the rest of the section we will be focusing on the parity-odd trispectrum generated by the two site loop diagram in Figure 4.2. We will first discuss it in general and then present a series of explicit calculation in increasing order of complexity, culminating with the case of single-clock inflation.

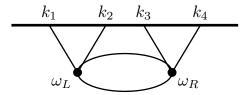


Figure 4.2: Two site loop diagram for the trispectrum.

To begin, let's derive an integral expression for the diagram in Figure 4.2. To this end, consider a general interaction Hamiltonian of the form

$$H_{\text{int}}(\{\mathbf{k}\}, \eta) = \int_{-\infty}^{0} d\eta \left[F_{\text{PO}}(\{\mathbf{k}\}, \eta) + F_{\text{PE}}(\{\mathbf{k}\}, \eta) \right] \phi(k_a) \phi(k_b) \phi(k_c) \phi(k_d), \tag{4.4.1}$$

where $F_{\text{PO,PE}}$ denote the vertices corresponding to a local interaction with an odd or even number of spatial derivatives, respectively, of which examples will be given later on. We can use the Feynman rules outlined in section 2.3.1 to write the trispectrum as:

$$B_4(k_1, k_2, k_3, k_4) = \sum_{a,b=\pm} \int_{-\infty}^{\eta_0} d\eta_1 \int_{-\infty}^{\eta_0} d\eta_2 \int_{\mathbf{p}} \delta^{(3)}(\mathbf{p}_1 + \mathbf{p}_2 + \mathbf{s}) G_a(k_1, \eta_1) G_a(k_2, \eta_1)$$

$$\times F_{PO}(\mathbf{k}_1, \mathbf{k}_2, \eta_1) G_{ab}(p_1, \eta_1, \eta_2) G_{ab}(p_2, \eta_1, \eta_2) F_{PE}(\mathbf{k}_3, \mathbf{k}_4, \eta_2) G_b(k_3, \eta_2) G_b(k_4, \eta_2) , \quad (4.4.2)$$

where we used

$$\mathbf{s} = \mathbf{k}_1 + \mathbf{k}_2 = -\mathbf{k}_3 - \mathbf{k}_4. \tag{4.4.3}$$

In-in diagrams are related pairwise. If D represents a diagram with a particular choice of vertices on the + or - contours (from the time evolution of the bra and the ket), and \bar{D} represents a diagram when each vertex sit on the opposite contour, $+ \leftrightarrow -$, then

$$D = \bar{D}(-1)^n \,, \tag{4.4.4}$$

with n the number of spatial derivatives. This ensures that in Fourier space parity-even correlators are real and parity-odd correlators are purely imaginary, as it should be for Hermitian operators in position space. Since we are considering a contribution with an overall odd number of spatial derivatives, we only need the imaginary part of the integral in (4.4.2). We can then write

$$B_4 = B_{4A} + B_{4B}, (4.4.5)$$

where, for future convenience, we separate the trispectrum into two contributions,

$$B_{4A} = 2 \text{Im} \int_{-\infty}^{\eta_0} d\eta_1 \int_{-\infty}^{\eta_0} d\eta_2 \int_{\mathbf{p}} \delta^{(3)}(\mathbf{p}_1 + \mathbf{p}_2 + \mathbf{s}) G_+(k_1, \eta_1) G_+(k_2, \eta_1)$$

$$\times F_{PO}(\mathbf{k}_1, \mathbf{k}_2, \eta_1) G_{++}(p_1, \eta_1, \eta_2) G_{++}(p_2, \eta_1, \eta_2) F_{PE}(\mathbf{k}_3, \mathbf{k}_4, \eta_2) G_+(k_3, \eta_2) G_+(k_4, \eta_2) , \quad (4.4.6)$$

$$B_{4B} = 2\operatorname{Im} \int_{-\infty}^{\eta_0} d\eta_1 \int_{-\infty}^{\eta_0} d\eta_2 \int_{\mathbf{p}} \delta^{(3)}(\mathbf{p}_1 + \mathbf{p}_2 + \mathbf{s}) G_+(k_1, \eta_1) G_+(k_2, \eta_1)$$

$$\times F_{PO}(\mathbf{k}_1, \mathbf{k}_2, \eta_1) G_{+-}(p_1, \eta_1, \eta_2) G_{+-}(p_2, \eta_1, \eta_2) F_{PE}(\mathbf{k}_3, \mathbf{k}_4, \eta_2) G_-(k_3, \eta_2) G_-(k_4, \eta_2). \tag{4.4.7}$$

There is one last general result that will be very useful in the following explicit calculations. We will often encounter integrals of the following form:

$$\int_{-\infty}^{\eta_0} d\eta \, (-H\eta)^{n+\delta} e^{ik\eta} = (iH\partial_k)^{n+\delta} \int_{-\infty}^{\eta_0} d\eta \, e^{ik\eta},\tag{4.4.8}$$

where n is an integer. This tells us that the trispectrum can often be written in terms of derivative operators acting on a simpler integral. In dimensional regularization, this leads to the following simplification. Suppose we want to evaluate

$$2\operatorname{Im}(\partial_k)^n(iH\partial_k)^{\delta}I(k),$$

and I(k) is the result of a UV-divergent integral, which can be written as:

$$I(k) = \frac{I_0(k)}{\delta} + I_1(k) + \mathcal{O}(\delta).$$

For the cases we will interested in, where IR divergences are absent, I(k), $I_0(k)$ and $I_1(k)$ are all real as consequence of unitarity [133]. Then we can expand the derivative operator in the following way:

$$(iH\partial_k)^{\delta} = 1 + \delta \log(iH\partial_k) + \dots = 1 + \delta \left(\log(H\partial_k) + \frac{i\pi}{2}\right) + \dots$$

Here the logarithm is understood as a power series in ∂_k . The terms from $\log(H\partial_k)$ acting on I(k) are all real, so if we want to isolate the imaginary part, we find that:

$$2\operatorname{Im}(\partial_k)^n (iH\partial_k)^{\delta} I(k) = \pi(\partial_k)^n I_0(k). \tag{4.4.9}$$

In other words, only the coefficient of the $1/\delta$ part of the simpler integral I(k) contributes to the final result. Since we only want the imaginary part when we compute the parity-odd trispectrum, we will only need to compute the this leading divergence and then multiply by $i\pi\delta$. This is a great simplification because it dispenses us from computing the finite term $I_1(k)$ of the UV-divergent integral, which is in general much more complicated. Moreover, these manipulations already tell us that the parity-odd trispectrum is actually UV-finite! This is important because for the class of theories we consider here the tree-level contribution vanishes in general [132, 133] and so it would have been impossible to re-absorb the UV divergence into a counterterm.

4.4.1 Momentum integrals

The mode function of massless scalars and conformally coupled scalars can be written as derivative operators acting on a plane wave as in (4.2.5). Hence, in general, we can recast B_{4A} into the following form:

$$B_{4A} = 2\text{Im} \int_{\mathbf{p}} \delta^{(3)}(\mathbf{p}_1 + \mathbf{p}_2 + \mathbf{s}) \tilde{F}(\{\mathbf{k}\}, \mathbf{p}_1, \mathbf{p}_2) I_{\text{flat}}, \tag{4.4.10}$$

where \tilde{F} is a differential operator which depends on the form of the interactions F_{PE} and F_{PO} , and

$$I_{\text{flat}} = \int_{-\infty}^{\eta_0} d\eta_1 \int_{-\infty}^{\eta_0} d\eta_2 e^{i\omega_L \eta_1} e^{i\omega_R \eta_2} \left(e^{ip_1(\eta_2 - \eta_1)} \theta(\eta_1 - \eta_2) + e^{ip_1(\eta_1 - \eta_2)} \theta(\eta_2 - \eta_1) \right) \times \left(e^{ip_2(\eta_2 - \eta_1)} \theta(\eta_1 - \eta_2) + e^{ip_2(\eta_1 - \eta_2)} \theta(\eta_2 - \eta_1) \right), \quad (4.4.11)$$

is a simpler integral involving only plane waves (hence the label "flat"). To simplify our notation we will define

$$\omega_L = k_1 + k_2,$$
 $\omega_R = k_3 + k_4$ $k_T = \sum_{a}^{4} k_a = \omega_L + \omega_R.$ (4.4.12)

The time integral I_{flat} gives:

$$I_{\text{flat}} = \frac{1}{k_T} \left(\frac{1}{p_1 + p_2 + \omega_L} + \frac{1}{p_1 + p_2 + \omega_R} \right). \tag{4.4.13}$$

It will be convenient to change the integration measure of the momentum integral in the following way:

$$\int \frac{d^{3+\delta}p}{(2\pi)^3} \delta^{(3)}(\mathbf{p}_1 + \mathbf{p}_2 + \mathbf{s}) f(\mathbf{p}) = \frac{1}{8\pi^2} \int_s^\infty dp_+ \int_{-s}^s dp_- \frac{p_1 p_2}{s} f(\mathbf{p}). \tag{4.4.14}$$

where $p_{+} = p_{1} + p_{2}$ and $p_{-} = p_{1} - p_{2}$. After performing the p_{-} integral, the remaining integral takes two possible forms. The first is

$$A_n = \int_s^\infty dp_+(p_+)^{\delta+n} I_{\text{flat}}.$$
 (4.4.15)

As discussed above, we are only interested in the UV-divergent part of the integral. To find it, first note that:

$$A_n = \int_0^\infty dp_+(p_+)^{\delta+n} I_{\text{flat}} - \int_0^s dp_+(p_+)^{\delta+n} I_{\text{flat}}$$
 (4.4.16)

For $\omega_L > 0$ and $\omega_R > 0$, the second integral is finite. The first integral can be written in terms of gamma functions, and can be simplified to give:

$$A_n = \frac{(-1)^n}{\delta} \frac{\omega_L^n + \omega_R^n}{k_T} + \text{(finite)}.$$
 (4.4.17)

The second possible form of the p_+ integral is

$$Z_n = \int_s^\infty dp_+(p_+)^{\delta+n} \log\left(\frac{p_+ + s}{p_+ - s}\right) I_{\text{flat}}.$$
 (4.4.18)

At first glance, this integral looks like it has both UV and IR divergence. However when we evaluate the integral there is no IR divergence. This is because after we evaluate the integral, we get either $\log(p_+ - s)$ multiplied by some power of $(p_+ - s)$ (which is convergent) or dilogarithms which are not divergent. As

an example, consider the case where n=2. We obtain:

$$Z_{2} = \frac{1}{2} \left(-(p_{+} - s)(p_{+} + s - 2\omega_{L}) \log(p_{+} - s) + (p_{+} + s)(p_{+} - s - 2\omega_{L}) \log(p_{+} + s) \right) |_{p_{+} = s}$$

$$+ s(s + \omega_{L}) + \omega_{L}^{2} \left(\operatorname{Li}_{2} \left(\frac{s - \omega_{L}}{s + \omega_{L}} \right) - \frac{\pi^{2}}{6} \right) + (\omega_{L} \to \omega_{R}) + (\operatorname{UV divergent terms}). \quad (4.4.19)$$

This is not divergent after substituting $p_{+} = s$. A similar story applies to any integer n.

To find the UV-divergent part of Z_n , we consider this integral instead:

$$\frac{dZ_n}{ds} = \int_s^\infty dp_+ p_+^{n+\delta} \left(\frac{1}{p_+ + s} + \frac{1}{p_+ - s} \right) I_{\text{flat}}.$$
 (4.4.20)

This integral can be simplified by using partial fraction. Since this integral is not IR-divergent, we evaluate it in the same way as we did for A_n :

$$\frac{dZ_n}{ds} = \frac{1}{k_T \delta} \left[\frac{(-\omega_L)^n - (-s)^n}{-\omega_L + s} + \frac{(-\omega_L)^n - s^n}{-\omega_L - s} + \frac{(-\omega_R)^n - (-s)^n}{-\omega_R + s} + \frac{(-\omega_R)^n - s^n}{-\omega_R - s} \right]. \tag{4.4.21}$$

This can be simplified into:

$$\frac{dZ_n}{ds} = \frac{(-1)^{n-1}}{k_T \delta} \sum_{r=0}^{n-1} (\omega_L^{n-r-1} + \omega_R^{n-r-1})(s^r + (-s)^r). \tag{4.4.22}$$

Therefore we obtain:

$$Z_n = \frac{(-1)^{n-1}}{k_T \delta} \sum_{r=0}^{n-1} \frac{1}{r+1} (\omega_L^{n-r-1} + \omega_R^{n-r-1}) (s^{r+1} - (-s)^{r+1}). \tag{4.4.23}$$

We can compute the out-of-time-ordered part of the trispectrum in a similar way:

$$B_{4B} = 2\text{Im} \int_{\mathbf{p}} \delta^{(3)}(\mathbf{p}_1 + \mathbf{p}_2 + \mathbf{s}) \tilde{F}(\{\mathbf{k}\}, \mathbf{p}_1, \mathbf{p}_2) J_{\text{flat}},$$
(4.4.24)

where

$$J_{\text{flat}} = \int_{-\infty}^{\eta_0} d\eta_1 \int_{-\infty}^{\eta_0} d\eta_2 e^{i\omega_L \eta_1} e^{-i\omega_R \eta_2} e^{i(p_1 + p_2)(\eta_1 - \eta_2)}.$$
 (4.4.25)

Evaluating the time integral gives us:

$$J_{\text{flat}} = \frac{-1}{(p_1 + p_2 + \omega_L)(p_1 + p_2 + \omega_R)}.$$
 (4.4.26)

For the integral over the loop momentum we will encounter integrals again two different forms. The first is

$$\tilde{A}_n = \int_s^\infty dp_+(p_+)^{\delta+n} J_{\text{flat}}.$$
(4.4.27)

Applying the same argument as we did for A_n , we obtain:

$$\tilde{A}_n = \frac{(-1)^n}{\delta} \frac{\omega_L^n - \omega_R^n}{\omega_L - \omega_R} + (\text{finite}) = \frac{(-1)^n}{\delta} \sum_{m=0}^{n-1} \omega_L^m \omega_R^{n-m-1} + (\text{finite}). \tag{4.4.28}$$

The second possible form is

$$\tilde{Z}_n = \int_s^\infty dp_+ p_+^{n+\delta} \log \left(\frac{p_+ + s}{p_+ - s} \right) J_{\text{flat}}. \tag{4.4.29}$$

Applying the same argument as we did for Z_n , we obtain:

$$\tilde{Z}_{n} = \frac{(-1)^{n-1}}{\delta(\omega_{L} - \omega_{R})} \sum_{r=0}^{n-1} \frac{1}{r+1} (\omega_{L}^{n-r-1} - \omega_{R}^{n-r-1}) (s^{r+1} - (-s)^{r+1})
= \frac{(-1)^{n-1}}{\delta} \sum_{r=0}^{n-1} \frac{1}{r+1} \left(\sum_{m=0}^{n-r-2} \omega_{L}^{m} \omega_{R}^{n-r-2-m} \right) (s^{r+1} - (-s)^{r+1}).$$
(4.4.30)

By looking at (4.4.28) and (4.4.30), we notice that if we take enough derivatives with respect to ω_L and ω_R we will get zero. For example, if we consider:

$$(\partial_{\omega_L})^{n_L}(\partial_{\omega_R})^{n_R}\tilde{A}_n, \tag{4.4.31}$$

the result is zero for $n_L + n_R \ge n$. Similarly for \tilde{Z}_n , we will get zero if $n_L + n_R \ge n - 1$. Since we need to take derivatives of these master integrals when computing the trispectrum, we will find that B_{4B} vanishes.

Our general strategy for computing the trispectrum will be the following: write down the trispectrum as a differential operator acting on an integral, recasting the integral in terms of the master integrals A_n and Z_n , then use our result from (4.4.17) and (4.4.23) to compute the divergent part and hence the final trispectrum.

4.4.2 A toy model example

As a warm up example, let us consider a parity-odd trispectrum from the following interactions:

$$\mathcal{L}_{PO} = \epsilon^{ijk} \partial_i \sigma_1 \partial_j \sigma_2 \partial_k \sigma_a \sigma_b, \qquad \mathcal{L}_{PE} = (\partial_i \sigma_3) \sigma_4 (\partial^i \sigma_a) \sigma_b, \qquad (4.4.32)$$

where all of the fields are conformally coupled scalars. Let's begin to consider the time-ordered part of the trispectrum B_{4A} . We have the integral:

$$B_{4A} = 2i \operatorname{Im} \int \frac{d^{3+\delta}p}{(2\pi)^3} \int \frac{d\eta_1}{(-H\eta_1)^{4+\delta}} \int \frac{d\eta_2}{(-H\eta_2)^{4+\delta}} (i^3(-H\eta_1)^3) (\mathbf{k}_1 \times \mathbf{k}_2 \cdot \mathbf{p}_1)$$

$$\times (i^2(-H\eta_2)^2(\mathbf{k}_3 \cdot \mathbf{p}_1)) G_+(k_1, \eta_1) G_+(k_2, \eta_1) G_{++}(p_1, \eta_1, \eta_2)$$

$$\times G_{++}(p_2, \eta_1, \eta_2) G_+(k_3, \eta_2) G_+(k_4, \eta_2). \quad (4.4.33)$$

First, we recast this integral in terms of an operator acting on a simpler integral. By counting powers of η_1 and η_2 , we get:

$$B_{4A} = 2i \operatorname{Im} \frac{(-H\eta_0)^4 H^5}{64k_1 k_2 k_3 k_4} (i\partial_{\omega_L})^{3+\delta} (i\partial_{\omega_R})^{2+\delta} \int \frac{d^{3+\delta}p}{(2\pi)^3} \frac{i^3 (\mathbf{k}_1 \times \mathbf{k}_2 \cdot \mathbf{p}_1) i^2 (\mathbf{k}_3 \cdot \mathbf{p}_1)}{p_1 p_2} I_{\text{flat}}. \tag{4.4.34}$$

As argued in the previous section, we only need to compute:

$$B_{4A} = i \frac{2\pi\delta(H\eta_0)^4 H^5}{64k_1 k_2 k_3 k_4} (\mathbf{k}_1 \times \mathbf{k}_2)^i (\mathbf{k}_3)^j (\partial_{\omega_L})^3 (\partial_{\omega_R})^2 \int \frac{d^{3+\delta}p}{(2\pi)^3} (\mathbf{p}_1)_i (\mathbf{p}_1)_j \frac{1}{p_1 p_2} I_{\text{flat}}. \tag{4.4.35}$$

Here we encounter the following tensorial integral

$$I_{ij}^{(2)} = \int \frac{d^{3+\delta}p}{(2\pi)^3} (\mathbf{p}_1)_i (\mathbf{p}_1)_j \frac{1}{p_1 p_2} I_{\text{flat}}, \tag{4.4.36}$$

which we can re-write as

$$I_{ij}^{(2)} = I_0^{(2)} \delta_{ij} + \frac{s_i s_j}{s^2} I_2^{(2)}. \tag{4.4.37}$$

Since this integral is contracted with $\mathbf{k}_1 \times \mathbf{k}_2$, the term $I_2^{(2)}$ does not contribute. Therefore we only need $I_0^{(2)}$, which is given by:

$$I_0^{(2)} = \frac{1}{2} (\delta_{ij} I_{ij}^{(2)} + \frac{s_i s_j}{s^2} I_{ij}^{(2)}). \tag{4.4.38}$$

More explicitly, the integral is:

$$I_0^{(2)} = \int \frac{d^{3+\delta}p}{(2\pi)^3} \frac{p_1^2 - \frac{(\mathbf{p_1 \cdot s})^2}{s^2}}{2p_1p_2} I_{\text{flat}}.$$
 (4.4.39)

This integral can be recast into the form:

$$I_0^{(2)} = \frac{1}{8\pi^2} \frac{A_2 - s^2 A_0}{6}. (4.4.40)$$

Putting this back into B_{4A} , we have:

$$B_{4A} = i \frac{2\pi (H\eta_0)^4 H^5}{64k_1 k_2 k_3 k_4} (\mathbf{k}_1 \times \mathbf{k}_2) \cdot (\mathbf{k}_3) (\partial_{\omega_L})^3 (\partial_{\omega_R})^2 \left(\frac{1}{8\pi^2} \frac{A_2 - s^2 A_0}{6} \right)$$

$$= -i \frac{(\mathbf{k}_1 \times \mathbf{k}_2 \cdot \mathbf{k}_3) H^9 \eta_0^4}{64\pi k_1 k_2 k_3 k_4 k_T^6} (\omega_L^2 - 6\omega_L \omega_R + 3\omega_R^2 - 10s^2). \tag{4.4.41}$$

The procedure for computing B_{4B} is similar, except we replace $I_{\rm flat}$ with $J_{\rm flat}$. This gives us:

$$B_{4B} = i \frac{2\pi (H\eta_0)^4 H^5}{64k_1 k_2 k_3 k_4} (\mathbf{k}_1 \times \mathbf{k}_2) \cdot (\mathbf{k}_3) (\partial_{\omega_L})^3 (\partial_{\omega_R})^2 \left(\frac{1}{8\pi^2} \frac{\tilde{A}_2 - s^2 \tilde{A}_0}{6} \right). \tag{4.4.42}$$

Here we are taking $n_L=3$ derivatives with respect to ω_L and $n_R=2$ derivatives with respect to ω_R . Since $n_L+n_R=5$ while the index of \tilde{A} is 2 and 0, we expect B_{4B} to vanish. This is confirmed by (4.4.28), which tells us that $\tilde{A}_0=0$ and $\tilde{A}_2=\frac{k_T}{\delta}$. Since $B_{4B}=0$, the only contribution to the trispectrum is B_{4A} . In summary, the one-loop two-vertex parity-odd trispectrum is

$$B_4^{\text{PO}} = B_{4A} = -i \frac{(\mathbf{k}_1 \times \mathbf{k}_2 \cdot \mathbf{k}_3) H^9 \eta_0^4}{64\pi k_1 k_2 k_3 k_4 k_0^2} (\omega_L^2 - 6\omega_L \omega_R + 3\omega_R^2 - 10s^2). \tag{4.4.43}$$

A few comments are in order:

- The result is UV finite, as anticipated around (4.4.9). This is important because there is no tree-level counterterm to absorb this divergence.
- The result has the expected scaling $B_4 \sim \eta_0^4/k^5$ for the trispectrum of a conformally coupled scalar, and is indeed parity odd because of the combination $\mathbf{k}_1 \times \mathbf{k}_2 \cdot \mathbf{k}_3$.
- The result is surprising simple: it is just a rational function in the momenta with the usual normalization $1/(k_1k_2k_3k_4)$ and only a total-energy pole at $k_T = 0$. This is the same structure as

a tree-level contact diagram. The crucial difference is that B_4 cannot come from a contact wavefunction coefficient ψ_4 that obeys the cosmological optical theorem [100]. To see this, notice that at tree-level contact order, B_4 would need to come from a purely imaginary $\psi_4 \sim ik^3$, but then $\psi_4(k, \mathbf{k}) + \psi_4^*(-k, -\mathbf{k}) = 2\psi_4(k, \mathbf{k}) \neq 0$. This check could be used to detect whether a given rational function arises or not as a contact diagram in a *unitary* EFT.

• Intriguingly B_4^{PO} in (4.4.43) could be attributed to a contact diagram in a non-unitary EFT. Indeed the expression in (4.4.43) contains the kinematic structures of a local EFT, which were identified recently in [139]. Non-unitary EFTs are expected to arise generically in open quantum systems. We will pursue this elsewhere.

Loop computation with cutoff regularization One may worry if our result is simply an artifact from dim reg. To show that the result is independent of regularization scheme, let us compute the integral (4.4.33) with cutoff regularization. The integral in cutoff regularization reads:

$$B_{4A} = 2i \operatorname{Im} \int \frac{d\eta_1}{(-H\eta_1)^4} \int \frac{d\eta_2}{(-H\eta_2)^4} \int^{\Lambda a(\eta_1)} \frac{d^3p}{(2\pi)^3} (i^3(-H\eta_2)^3) (\mathbf{k}_1 \times \mathbf{k}_2 \cdot \mathbf{p}_1)$$

$$\times (i^2(-H\eta_2)^2(\mathbf{k}_3 \cdot \mathbf{p}_1)) G_+(k_1, \eta_1) G_+(k_2, \eta_1) G_{++}(p_1, \eta_1, \eta_2)$$

$$\times G_{++}(p_2, \eta_1, \eta_2) G_+(k_3, \eta_2) G_+(k_4, \eta_2). \quad (4.4.44)$$

Before proceeding, let us note the following:

- The cutoff is $\Lambda a(\eta_2)$ instead of just Λ . This is because we would like to impose a cutoff on the physical momentum [140], which is the relevant physical quantity, rather than the comoving momentum.
- When computing the nested time integrals, the domain for the time integrals also needs to be modified as:

$$\int_{-\infty}^{0} d\eta_1 \int_{-\infty}^{\eta_1(1+\frac{H}{\Lambda})} d\eta_2. \tag{4.4.45}$$

This is because if we allow η_2 to be arbitrarily close to η_1 , we are probing regions that have energy above the cutoff.

With this in mind, let us compute the integrals. Doing the angular part of the loop momentum integral give us:

$$B_{4A} = 2i \operatorname{Im} \frac{(H\eta_0)^4 H^5}{64k_1 k_2 k_3 k_4} (\mathbf{k}_1 \times \mathbf{k}_2) \cdot \mathbf{k}_3 (\partial_{\omega_L})^3 (\partial_{\omega_R})^2 \times \frac{1}{8\pi^2} \frac{1}{6} \int_{-\infty}^0 d\eta_1 \int_{-\infty}^{\eta_1(1+\frac{H}{\Lambda})} d\eta_2 \int_s^{\frac{\Lambda}{H\eta_2}} dp_+ (p_+^2 - s^2) e^{i\omega_L \eta_1} e^{i\omega_R \eta_2} e^{ip_+(\eta_2 - \eta_1)} + (\omega_L \leftrightarrow \omega_R). \quad (4.4.46)$$

Let us define the following:

$$B_{4A} := 2i \operatorname{Im} \frac{(H\eta_0)^4 H^5}{64k_1 k_2 k_3 k_4} (\mathbf{k}_1 \times \mathbf{k}_2) \cdot \mathbf{k}_3 (\partial_{\omega_L})^3 (\partial_{\omega_R})^2 \frac{1}{8\pi^2} \frac{1}{6} A_2^{\Lambda}(\omega_L, \omega_R). \tag{4.4.47}$$

Now we compute A_2^{Λ} . First we do the momentum integral and obtain:

$$A_{2}^{\Lambda} = \int_{-\infty}^{0} d\eta_{1} \int_{-\infty}^{\eta_{1}(1+\frac{H}{\Lambda})} d\eta_{2} \frac{1}{(\eta_{1}-\eta_{2})^{3}} e^{i\omega_{L}\eta_{1}} e^{i\omega_{R}\eta_{2}}$$

$$\left[\frac{i}{H^{2}\eta_{2}^{2}} e^{i\frac{\Lambda(\eta_{2}-\eta_{1})}{H\eta_{2}}} (-\Lambda^{2}(\eta_{1}\eta_{2})^{2} + 2iH\eta_{2}\Lambda(\eta_{1}-\eta_{2}) + H^{2}\eta_{2}^{2}(2+s^{2}(\eta_{1}-\eta_{2})^{2}) + e^{is(\eta_{2}-\eta_{1})}(2i+2s(\eta_{2}-\eta_{1})) \right] + (\omega_{L} \leftrightarrow \omega_{R}). \quad (4.4.48)$$

The second line is a rapidly oscillating integral as $\Lambda \to \infty$, and so it averages to zero. Therefore we just need to integrate the third line. Doing the η_2 integral gives:

$$A_2^{\Lambda} = \int_{-\infty}^0 d\eta_1 e^{i\omega_T \eta_1} \left[\frac{-i\Lambda^2}{H^2 \eta_1^2} + \frac{\Lambda(s - \omega_R)}{H \eta_1} - i(\omega_R^2 - s^2) \operatorname{Ei} \left(\frac{iH\eta_1}{\Lambda} (s + \omega_R) \right) \right] + (\omega_L \leftrightarrow \omega_R). \tag{4.4.49}$$

We only want the imaginary part of this integral. The first two terms can easily be seen to be real by performing a Wick rotation in η_1 . Notice that the $(\partial_{\omega_L})^3$ operator in (4.4.47) bring down factors of η_1 , which ensures convergence of the integral. In addition, we know that the exponential integral has an expansion:

$$Ei(z) = \gamma + \log(z) + \sum_{k=1}^{\infty} \frac{z^k}{k \, k!},$$
 (4.4.50)

where γ is the Euler-Mascheroni constant. The exponential integral Ei(z) is the sum of a logarithm and an entire function, so we can integrate the series expansion term by term. In particular, we find that since $z = \frac{iH\eta_1}{\Lambda}(s+\omega_R)$ here, the terms in the series are seen to be purely real upon performing a Wick rotation. Keeping the imaginary part leaves us with:

$$\operatorname{Im} A_2^{\Lambda} = \int_{-\infty}^0 d\eta_1 e^{i\omega_T \eta_1} \pi(s^2 - \omega_R^2) + (\omega_L \leftrightarrow \omega_R) = \frac{\pi}{\omega_T} (\omega_R^2 - s^2 + \omega_L^2 - s^2). \tag{4.4.51}$$

Note again that $(\partial_{\omega_L})^3$ ensures convergence of the log η term, which hence does not contribute to the imaginary part. Notice that the final result is independent of the cutoff Λ . Substituting (4.4.51) into (4.4.47) and doing the ∂_{ω_L} and ∂_{ω_R} derivatives returns (4.4.43), which is the result from dim reg.

We now move on to cases in which the external legs are massless scalars, which are more directly relevant for inflationary phenomenology.

4.5 Trispectrum for a massless scalar

4.5.1 Conformally coupled loop

We now compute the contribution from the one-loop diagram in Figure 4.2, where the four external legs correspond to a single massless scalar denoted by ϕ . First, we show the result in the case in which the fields in the loop are two conformally coupled scalars σ_a and σ_b . This represents a phenomenologically viable model of inflation with spectator massive fields. Second, we perform the calculation in single-clock inflation where all lines represent the same massless scalar ϕ .

Conformally coupled spectator scalars: $: \phi \phi \to \sigma_a \sigma_b \to \phi \phi$ Since we would like to consider a phenomenologically viable model, where the scalar field ϕ can be identified with the Goldstone boson π of time-translations in the effective field theory of inflation [113,141], we consider interactions where ϕ has at least one time derivative, which would arise from δg^{00} , or two spatial derivative, which would arise from perturbations to the extrinsic curvature K_{ij} . For concreteness, we will consider the trispectrum from the following two interactions:

$$\mathcal{L}_{PO} = \epsilon_{ijk} \,\partial_{il}\phi \,\dot{\phi}\partial_{il}\sigma_a\partial_k\sigma_b, \tag{4.5.1}$$

$$\mathcal{L}_{PE} = \partial_{ij}\phi \,\partial_i \sigma_a \partial_j \dot{\phi} \sigma_b. \tag{4.5.2}$$

where $\sigma_{a,b}$ are conformally coupled and ϕ is massless. As in the previous section, we want to write down the corresponding integral as some differential operators acting on a simpler integral. The differential operator corresponding to the left vertex, which we choose to be the one with an odd number of spatial derivatives, is given by⁵

$$\hat{L} = i^5 \left[\mathbf{k}_1 \cdot (\mathbf{p}_1 \times \mathbf{p}_2)(\mathbf{k}_1 \cdot \mathbf{p}_1) k_2^2 O_{k_1}^{(L)} + \mathbf{k}_2 \cdot (\mathbf{p}_1 \times \mathbf{p}_2)(\mathbf{k}_2 \cdot \mathbf{p}_1) k_1^2 O_{k_2}^{(L)} \right] (-i\partial_{\omega_L}) (-iH\partial_{\omega_L})^{6+2-4} , \quad (4.5.3)$$

where we defined $O_k^{(i)} = 1 - k\partial_{\omega_i}$. Notice that for both the conformally couple fields and for $\dot{\phi}$ we don't need a dedicated differential operator because the mode functions are already proportional to a plane wave and the overall factor of η is captured by the ∂_{ω_L} operator. This can be simplified into:

$$\hat{L} = H^4(\mathbf{k}_1 \times \mathbf{k}_2)^i \left(k_2^2 O_{k_1}^{(L)} \mathbf{k}_1^j - k_1^2 O_{k_2}^{(L)} \mathbf{k}_2^j \right) (\partial_{\omega_L})^5(\mathbf{p}_1)_i(\mathbf{p}_1)_j$$
(4.5.4)

Similarly for the right vertex, we have:

$$\hat{R} = (\mathbf{k}_3 \cdot \mathbf{k}_4) \left(k_4^2 O_{k_3}^{(R)} \mathbf{k}_3^i + k_3^2 O_{k_4}^{(R)} \mathbf{k}_4^i \right) (-iH\partial_{\omega_R})^{5+2-4} (-i\partial_{\omega_R}) (\mathbf{p}_1)_i$$
(4.5.5)

The trispectrum is:

$$B_{4A} = (2\pi i\delta) \frac{H^{19}}{16k_1^3 k_2^3 k_3^3 k_4^3} (\mathbf{k}_1 \times \mathbf{k}_2)^i \left(k_2^2 O_{k_1}^{(L)} \mathbf{k}_1^j - k_1^2 O_{k_2}^{(L)} \mathbf{k}_2^j \right) \times (\mathbf{k}_3 \cdot \mathbf{k}_4) \left(k_4^2 O_{k_3}^{(R)} \mathbf{k}_3^l + k_3^2 O_{k_4}^{(R)} \mathbf{k}_4^l \right) (\partial_{\omega_L})^5 (\partial_{\omega_R})^4 I_{ijl}^{(3)}, \quad (4.5.6)$$

where $I_{ijl}^{(3)}$ is given by:

$$I_{ijl}^{(3)} = \int \frac{d^3p}{(2\pi)^3} \frac{(\mathbf{p}_1)_i(\mathbf{p}_1)_j(\mathbf{p}_1)_l}{4p_1p_2} I_{\text{flat}}.$$
 (4.5.7)

where I_{flat} was given in (4.4.13). Once again we can separate the tensorial integral into scalar integrals (this can be done more systematically as discussed in Appendix C):

$$I_{ijl}^{(3)} = \left(\frac{I_1^{(3)}}{s}(s_i\delta_{jk} + s_j\delta_{ik} + s_k\delta_{ij}) + \frac{I_3^{(3)}}{s^3}s_is_js_k\right). \tag{4.5.8}$$

⁵Here we separated $-i\partial_{\omega_L}$, which accounts for the factor of η in $\dot{\phi}$ from all other factors of $a^{-1} = -H\eta$ from $\sqrt{-g}$, derivatives and the conformally coupled mode functions, which are accounted for by $(-i\partial_{\omega_L})^4$.

Notice that this expression assumes $s = |\mathbf{s}| \neq 0$, but it otherwise does not depend on s. For our purposes, we only need I_1 because the other terms vanish once contracted with the epsilon tensor. This is given by

$$I_1^{(3)} = \frac{1}{2} \left(\frac{1}{s} s_i \delta_{jl} I_{ijl}^{(3)} - \frac{1}{s^3} s_i s_j s_l I_{ijl}^{(3)} \right). \tag{4.5.9}$$

More explicitly, we have:

$$I_1^{(3)} = \int_{\mathbf{p}} \frac{s^2 p_1^2(\mathbf{p}_1 \cdot \mathbf{s}) - (\mathbf{p}_1 \cdot \mathbf{s})^3}{s^3 p_1 p_2} I_{\text{flat}}.$$
 (4.5.10)

Computing this integral gives us:

$$B_{4A} = (2\pi i\delta) \frac{H^{19}}{16k_1^3 k_2^3 k_3^3 k_4^3} \left(k_2^2 O_{k_1}^{(L)}(\mathbf{k}_1 \cdot \mathbf{s}) - k_1^2 O_{k_2}^{(L)}(\mathbf{k}_2 \cdot \mathbf{s}) \right) (\mathbf{k}_3 \cdot \mathbf{k}_4)$$

$$\times \left(k_4^2 O_{k_3}^{(R)} \mathbf{k}_3 \cdot (\mathbf{k}_1 \times \mathbf{k}_2) + k_3^2 O_{k_4}^{(R)} \mathbf{k}_4 \cdot (\mathbf{k}_1 \times \mathbf{k}_2) \right) (\partial_{\omega_L})^5 (\partial_{\omega_R})^4 \frac{1}{32\pi^2} \frac{A_2 - s^2 A_0}{12}. \quad (4.5.11)$$

Using our general results for the A integrals, this can be further simplified into:

$$B_{4A} = i \frac{H^{19}}{16k_1^3k_2^3k_3^3k_4^3} \left[k_2^2 O_{k_1}^{(L)}(\mathbf{k}_1 \cdot \mathbf{s}) - k_1^2 O_{k_2}^{(L)}(\mathbf{k}_2 \cdot \mathbf{s}) \right] (\mathbf{k}_3 \cdot \mathbf{k}_4)$$

$$\times \left[k_4^2 O_{k_3}^{(R)} \mathbf{k}_3 \cdot (\mathbf{k}_1 \times \mathbf{k}_2) + k_3^2 O_{k_4}^{(R)} \mathbf{k}_4 \cdot (\mathbf{k}_1 \times \mathbf{k}_2) \right] \left[\frac{1}{16\pi} \frac{3360(18s^2 - 3\omega_L^2 + 10\omega_L\omega_R - 5\omega_R^2)}{k_T^{10}} \right]. \quad (4.5.12)$$

Since $O_k^{(L)}$ and $O_k^{(R)}$ each provides an extra derivative, B_{4A} has a k_T pole of order 12. This matches with the standard expectation that the order p of the k_T pole is [87]

$$p = 1 + \sum_{i} (\Delta_i - 4) = 1 + (10 - 4) + (9 - 4) = 12.$$
 (4.5.13)

Similarly, we can compute B_{4B} :

$$B_{4B} = (2\pi i\delta) \frac{H^{19}}{16k_1^3 k_2^3 k_3^3 k_4^3} \left(k_2^2 O_{k_1}^{(L)}(\mathbf{k}_1 \cdot \mathbf{s}) - k_1^2 O_{k_2}^{(L)}(\mathbf{k}_2 \cdot \mathbf{s}) \right) (\mathbf{k}_3 \cdot \mathbf{k}_4)$$

$$\times \left(k_4^2 O_{k_3}^{(R)} \mathbf{k}_3 \cdot (\mathbf{k}_1 \times \mathbf{k}_2) + k_3^2 O_{k_4}^{(R)} \mathbf{k}_4 \cdot (\mathbf{k}_1 \times \mathbf{k}_2) \right) (\partial_{\omega_L})^5 (\partial_{\omega_R})^4 \frac{1}{32\pi^2} \frac{\tilde{A}_2 - s^2 \tilde{A}_0}{12}. \quad (4.5.14)$$

Since $n_L = 5$, $n_R = 4$ and $n \ge 2$, we have $n_L + n_R > n$, so when we take derivatives we find $B_{4B} = 0$, as anticipated. In summary the final result is $B_4^{PO} = B_{4A}$ as given in (4.5.12). The same remark as at the end of the previous section apply to this surprisingly simple result as well.

Same internal fields Next we want to consider the case in which there is a single spectator scalar, with a conformally coupled mass. If we simply replace $\sigma_1 = \sigma_2 = \sigma$ in the above example, the spatial derivatives for the internal fields in the parity even vertex can all be removed by integration by parts. As a result the trispectrum vanishes. Instead, by direct investigation we found that the following interactions

provide a non-vanishing result that is minimal in terms of number of derivatives:

$$\mathcal{L}_{PO} = \epsilon_{ijk} \,\partial_{il}\phi \,\dot{\phi}\partial_{jl}\sigma\partial_{k}\sigma,\tag{4.5.15}$$

$$\mathcal{L}_{PE} = \partial_{ij}\phi \,\partial_{ij}\sigma\dot{\phi}\sigma. \tag{4.5.16}$$

Consider the left vertex first. We need the differential operator

$$\hat{L} = iH^{4}(\mathbf{k}_{1} \times \mathbf{k}_{2}) \cdot \mathbf{p}_{1} \left(k_{2}^{2} O_{k_{1}}^{(L)} \mathbf{k}_{1} \cdot \mathbf{p}_{1} - k_{1}^{2} O_{k_{2}}^{(L)} \mathbf{k}_{2} \cdot \mathbf{p}_{1} \right) (\partial_{\omega_{L}})^{5}
+ iH^{4}(\mathbf{k}_{1} \times \mathbf{k}_{2}) \cdot \mathbf{p}_{2} \left(k_{2}^{2} O_{k_{1}}^{(L)} \mathbf{k}_{1} \cdot \mathbf{p}_{2} - k_{1}^{2} O_{k_{2}}^{(L)} \mathbf{k}_{2} \cdot \mathbf{p}_{2} \right) (\partial_{\omega_{L}})^{5}$$
(4.5.17)

Since $(\mathbf{k}_1 \times \mathbf{k}_2) \cdot \mathbf{p}_1 = (\mathbf{k}_1 \times \mathbf{k}_2) \cdot (-\mathbf{s} - \mathbf{p}_1) = -(\mathbf{k}_1 \times \mathbf{k}_2) \cdot \mathbf{p}_2$, this simplifies to

$$\hat{L} = iH^4(\mathbf{k}_1 \times \mathbf{k}_2)^i \left(k_2^2 O_{k_1}^{(L)} \mathbf{k}_1^j - k_1^2 O_{k_2}^{(L)} \mathbf{k}_2^j \right) (\partial_{\omega_L})^5(\mathbf{p}_1)_i [(\mathbf{p}_1)_j - (\mathbf{p}_2)_j]. \tag{4.5.18}$$

The right vertex gives:

$$\hat{R} = H^3 \left((\mathbf{k}_3 \cdot \mathbf{p}_1)^2 O_{k_3}^{(R)} k_4^2 + (\mathbf{k}_4 \cdot \mathbf{p}_1)^2 O_{k_4}^{(R)} k_3^2 \right) (\partial_{\omega_R})^4 + (\mathbf{p}_1 \to \mathbf{p}_2). \tag{4.5.19}$$

So the trispectrum is found to be

$$B_{4A} = (2\pi i\delta) \frac{H^{19}}{16k_1^3 k_2^3 k_3^3 k_4^3} (\mathbf{k}_1 \times \mathbf{k}_2)^i \left(k_2^2 O_{k_1}^{(L)} \mathbf{k}_1^j - k_1^2 O_{k_2}^{(L)} \mathbf{k}_2^j \right) \times \left(k_4^2 O_{k_3}^{(2)} \mathbf{k}_3^l \mathbf{k}_3^m + k_3^2 O_{k_4}^{(2)} \mathbf{k}_4^l \mathbf{k}_4^m \right) (\partial_{\omega_L})^5 (\partial_{\omega_R})^4 I_{ijlm}, \quad (4.5.20)$$

where

$$I_{ijlm} = \int_{\mathbf{p}} \frac{1}{4p_1 p_2} \left((\mathbf{p}_1)_i (\mathbf{p}_1)_j (\mathbf{p}_1)_l (\mathbf{p}_1)_m + (\mathbf{p}_1)_i (\mathbf{p}_1)_j (\mathbf{p}_2)_l (\mathbf{p}_2)_m \right)$$

$$- (\mathbf{p}_1)_i (\mathbf{p}_2)_j (\mathbf{p}_1)_l (\mathbf{p}_1)_m - (\mathbf{p}_1)_i (\mathbf{p}_2)_j (\mathbf{p}_2)_l (\mathbf{p}_2)_m \right) I_{\text{flat}}. \quad (4.5.21)$$

Since we can always exchange $(\mathbf{p}_1)_i$ for $-(\mathbf{p}_2)_i$ (as it is contracted with $\mathbf{k}_1 \times \mathbf{k}_2$), and we can also exchange \mathbf{p}_1 for \mathbf{p}_2 by changing the integration variable from \mathbf{p}_1 to $-\mathbf{p}_1 - \mathbf{s}$, the integral simplifies into:

$$I_{ijlm} = \int_{\mathbf{p}} \frac{4(\mathbf{p}_1)_i(\mathbf{p}_1)_j(\mathbf{p}_1)_l(\mathbf{p}_1)_m + 2(\mathbf{p}_1)_i(\mathbf{s})_j(\mathbf{p}_1)_l(\mathbf{p}_1)_m}{4p_1p_2}.$$
 (4.5.22)

With this, we can use the tensor structure results in Appendix C to compute the tensorial integral in terms of scalar integrals. This yields:

$$I_{ijlm} = \frac{1}{16\pi^2} \frac{1}{30} \left[\left(\delta_{il} \delta_{jm} + \delta_{im} \delta_{jl} \right) \left(A_4 - 2s^2 A_2 + s^4 A_0 \right) + \left(\delta_{il} s_j s_m + \delta_{im} s_j s_l \right) \left(A_2 - s^2 A_0 \right) \right]. \tag{4.5.23}$$

Putting this back in the trispectrum, we obtain:

$$B_{4A} = i \frac{H^{19}}{16k_1^3k_2^3k_3^3k_4^3} \left[\left(k_2^2 O_{k_1}^{(L)} \mathbf{k}_1 - k_1^2 O_{k_2}^{(L)} \mathbf{k}_2 \right) \cdot \left(k_4^2 O_{k_3}^{(2)} (\mathbf{k}_1 \times \mathbf{k}_2 \cdot \mathbf{k}_3) \mathbf{k}_3 + k_3^2 O_{k_4}^{(2)} (\mathbf{k}_1 \times \mathbf{k}_2 \cdot \mathbf{k}_4) \mathbf{k}_4 \right) \right.$$

$$\times \frac{-1}{8\pi} \frac{192(126s^4 + \omega_L^4 - 20\omega_L^3 \omega_R + 60\omega_L^2 \omega_R^2 - 40\omega_L \omega_R^3 + 5\omega_R^4 - 14s^2 (3\omega_L^2 - 10\omega_L \omega_R + 5\omega_R^2))}{k_T^{10}}$$

$$+ \left(k_2^2 O_{k_1}^{(L)} (\mathbf{k}_1 \cdot \mathbf{s}) - k_1^2 O_{k_2}^{(L)} (\mathbf{k}_2 \cdot \mathbf{s}) \right) \left(k_4^2 O_{k_3}^{(2)} (\mathbf{k}_1 \times \mathbf{k}_2 \cdot \mathbf{k}_3) (\mathbf{k}_3 \cdot \mathbf{s}) + k_3^2 O_{k_4}^{(2)} (\mathbf{k}_1 \times \mathbf{k}_2 \cdot \mathbf{k}_4) (\mathbf{k}_4 \cdot \mathbf{s}) \right)$$

$$\times \frac{1}{8\pi} \frac{1344(18s^2 - 3\omega_L^2 + 10\omega_L \omega_R - 4\omega_R^2)}{k_T^{10}} \right]. \tag{4.5.24}$$

To compute B_{4B} , we just need to replace A_n in (4.5.23) with \tilde{A}_n . But once again $n_L = 5$, $n_R = 4$ and $n \ge 4$, so $n_L + n_R > n$ and we have $B_{4B} = 0$.

Permutations One also need to sum over permutations when calculating the correlator. For instance, it is necessary to also consider the correlator when the left and right vertices are swapped. Notice that the polynomials and the operators in the final result above are not symmetric under the exchange of ω_L and ω_R , hence the correlator does not vanish upon summing over permutations.

Similarly one may worry whether summing over the (s, t, u) channels may result in some cancellation. However, when considering these permutations, one also needs to redefine ω_L and ω_R : for the t-channel, $\omega_L = k_1 + k_3$ while for the u-channel, $\omega_L = k_1 + k_4$. In general, summing over different channels does not result in cancellation of the correlator as well.

4.5.2 Massless loop

We now consider the case of single-clock inflation, where all lines represent a massless scalar ϕ , to be identified with the Goldstone boson π of time translations in the EFT of inflation. Conceptually the calculation is just the same as in previous examples. However the main new difficulty is to find interactions that give a non-vanishing result when symmetrised. The idea is that we have to include a sufficient number of derivatives such that all ϕ 's appearing in the parity-odd interaction are distinct from each other. Furthermore, we also need a sufficient number of derivatives in the parity-even interactions to ensure that, after the loop integral has been computed, a term of the form $\mathbf{k}_1 \times \mathbf{k}_2 \cdot \mathbf{k}_3$ can be generated. This results in a large number of derivatives and hence an algebraically more complex result, but no new conceptual issue emerges.

A minimal choice of interactions that gives a non-vanishing result is

$$\mathcal{L}_{PO} = \lambda_{PO} \epsilon_{ijk} \partial_m \partial_n \phi \, \partial_n \partial_i \phi \, \partial_m \partial_l \partial_j \phi \, \partial_l \partial_k \phi, \tag{4.5.25}$$

$$\mathcal{L}_{PE} = \lambda_{PE} \dot{\phi}^2 (\partial_i \partial_j \phi)^2 \tag{4.5.26}$$

Let's follow a by now familiar script and start building the relevant differential operators. For the parityodd interaction, the tensor structure of the vertex looks like:

$$F_{PO}(p_1, p_2, k_1, k_2) = \frac{i^9}{a^9} \mathbf{k}_2 \cdot (\mathbf{p}_1 \times \mathbf{p}_2)(\mathbf{k}_1 \cdot \mathbf{p}_1)(\mathbf{k}_1 \cdot \mathbf{k}_2)(\mathbf{p}_1 \cdot \mathbf{p}_2) + \text{permutations}$$
(4.5.27)

Notice that since $\mathbf{p}_1 + \mathbf{p}_2 + \mathbf{k}_1 + \mathbf{k}_2 = 0$, we can always rearrange the cross product to take the form

 $\pm \mathbf{k}_2 \cdot (\mathbf{p}_1 \times \mathbf{p}_2)$. Carefully considering all the permutations, we obtain:

$$(-ia)^{9}F_{PO} = -2(\mathbf{k}_{1} \times \mathbf{k}_{2}) \cdot \mathbf{p}_{1} \left\{ (\mathbf{k}_{1} \cdot \mathbf{k}_{2})(\mathbf{p}_{1} \cdot \mathbf{p}_{2})(\mathbf{k}_{1} - \mathbf{k}_{2}) \cdot (\mathbf{p}_{1} - \mathbf{p}_{2}) + (\mathbf{p}_{2} \cdot \mathbf{k}_{1})(\mathbf{p}_{2} \cdot \mathbf{k}_{2})\mathbf{p}_{1} \cdot (\mathbf{k}_{1} - \mathbf{k}_{2}) - (\mathbf{p}_{1} \cdot \mathbf{k}_{1})(\mathbf{p}_{1} \cdot \mathbf{k}_{2})\mathbf{p}_{2} \cdot (\mathbf{k}_{1} - \mathbf{k}_{2}) + [(\mathbf{k}_{1} \cdot \mathbf{p}_{2})(\mathbf{k}_{2} \cdot \mathbf{p}_{1}) - (\mathbf{p}_{1} \cdot \mathbf{k}_{1})(\mathbf{k}_{2} \cdot \mathbf{p}_{2})(\mathbf{p}_{1} \cdot \mathbf{p}_{2} + \mathbf{k}_{1} \cdot \mathbf{k}_{2})] \right\}$$

$$(4.5.28)$$

Note that \mathbf{p}_1 and \mathbf{p}_2 can be exchanged by changing the integration variable. Since we also sum over permutations on the parity-even vertex as well, we have:

$$(-ia)^{9}V_{PO} = -2(\mathbf{k}_{1} \times \mathbf{k}_{2}) \cdot \mathbf{p}_{1} \left[2(\mathbf{k}_{1} \cdot \mathbf{k}_{2})(\mathbf{p}_{1} \cdot \mathbf{p}_{2})(\mathbf{p}_{1} \cdot \mathbf{r}) - 2(\mathbf{k}_{1} \cdot \mathbf{p}_{1})(\mathbf{k}_{2} \cdot \mathbf{p}_{1})(\mathbf{p}_{2} \cdot \mathbf{r}) \right.$$
$$\left. - ((\mathbf{k}_{1} \cdot \mathbf{s})(\mathbf{p}_{1} \cdot \mathbf{k}_{2}) - (\mathbf{k}_{2} \cdot \mathbf{s})(\mathbf{p}_{1} \cdot \mathbf{k}_{1}))(\mathbf{p}_{1} \cdot \mathbf{p}_{2} + \mathbf{k}_{1} \cdot \mathbf{k}_{2}) \right]. \tag{4.5.29}$$

Here I defined $\mathbf{r} = \mathbf{k}_1 - \mathbf{k}_2$. Now we can use $\mathbf{p}_1 \cdot \mathbf{p}_2 = \frac{1}{2}(s^2 - p_1^2 - p_2^2)$ to simplify this further.

The tensor structure for the parity-even vertex is straightforward to obtain. Note that only one internal line can have a spatial derivative, otherwise it can be shown that the integral gives us zero. The trispectrum can now be written as:

$$B_{4A} = (2\pi i\delta) \frac{\lambda_{PO}\lambda_{PE}H^8}{8k_1^3k_2^3k_3^3k_4^3} \int_{\mathbf{p}} \hat{L}\hat{R} \frac{H^4}{4p_1^3p_2^3} I_{\text{flat}}.$$
 (4.5.30)

The left operator is given by:

$$\hat{L} = (L^{(2a)} + L^{(2b)} + L^{(4)})(-iH\partial_{\omega_L})^5 O_{k_1}^{(L)} O_{k_2}^{(L)} O_{p_1}^{(L)} O_{p_2}^{(L)}, \tag{4.5.31}$$

$$L^{(2a)} = -2(\mathbf{k}_1 \times \mathbf{k}_2)^i \left[\frac{3}{2} (\mathbf{k}_1 \cdot \mathbf{k}_2) \mathbf{r}^j - \frac{1}{2} (k_1^2 \mathbf{k}_2^j - k_2^2 \mathbf{k}_1^j) \right] (s^2 - p_1^2 - p_2^2) (\mathbf{p}_1)_i (\mathbf{p}_1)_j, \tag{4.5.32}$$

$$L^{(2b)} = -2(\mathbf{k}_1 \times \mathbf{k}_2)^i \left[(\mathbf{k}_1 \cdot \mathbf{k}_2)^2 \mathbf{r}^j - (\mathbf{k}_1 \cdot \mathbf{k}_2)(k_1^2 \mathbf{k}_2^j - k_2^2 \mathbf{k}_1^j) \right] (\mathbf{p}_1)_i (\mathbf{p}_1)_j, \tag{4.5.33}$$

$$L^{(4)} = 4(\mathbf{k}_1 \times \mathbf{k}_2)^i (\mathbf{k}_1)^j (\mathbf{k}_2)^l (\mathbf{r})^m (\mathbf{p}_1)_i (\mathbf{p}_1)_i (\mathbf{p}_1)_l (\mathbf{p}_2)_m.$$
(4.5.34)

The right vertex becomes:

$$\hat{R} = 2\left((\mathbf{k}_3)^i (\mathbf{k}_3)^j k_4^2 O_{k_3}^{(R)} O_{p_1}^{(R)} + (\mathbf{k}_4)^i (\mathbf{k}_4)^j k_3^2 O_{k_4}^{(R)} O_{p_1}^{(R)} \right) p_2^2 (\mathbf{p}_1)_i (\mathbf{p}_1)_j (-iH\partial_{\omega_R})^2 (-i\partial_{\omega_R})^2$$

$$(4.5.35)$$

Let us separate the trispectrum into three terms, where each term corresponds to one of the operators above:

$$B_{4A} = B_{4A}^{2a} + B_{4A}^{2b} + B_{4A}^{4}. (4.5.36)$$

The first term is

$$\begin{split} B_{4A}^{2a} &= (2\pi i) \frac{\lambda_{PO} \lambda_{PE} H^{14}}{8k_1^3 k_2^3 k_3^3 k_4^3} (-2) (\mathbf{k}_1 \times \mathbf{k}_2)^i \left[\frac{3}{2} (\mathbf{k}_1 \cdot \mathbf{k}_2) \mathbf{r}^j - \frac{1}{2} (k_1^2 \mathbf{k}_2^j - k_2^2 \mathbf{k}_1^j) \right] \\ &\times 2 \left((\mathbf{k}_3)^l (\mathbf{k}_3)^m k_4^2 O_{k_3}^{(R)} + (\mathbf{k}_4)^l (\mathbf{k}_4)^m k_3^2 O_{k_4}^{(R)} \right) (-iH\partial_{\omega_L})^5 (-i\partial_{\omega_R})^4 O_{k_1}^{(L)} O_{k_2}^{(L)} I_{ijlm}^{2a}, \end{split} \tag{4.5.37}$$

where

$$I_{ijlm}^{2a} := \frac{1}{8} (\delta_{il}\delta_{jm} + \delta_{im}\delta_{jl})I_0^{2a} + \frac{1}{8s^2} (\delta_{il}s_js_m + \delta_{im}s_js_l)I_2^{2a}. \tag{4.5.38}$$

Similarly, the second term is

$$B_{4A}^{2b} = (2\pi i) \frac{\lambda_{PO} \lambda_{PE} H^{14}}{8k_1^3 k_2^3 k_3^3 k_4^3} (-2) (\mathbf{k}_1 \times \mathbf{k}_2)^i \left[(\mathbf{k}_1 \cdot \mathbf{k}_2) \mathbf{r}^j - (k_1^2 \mathbf{k}_2^j - k_2^2 \mathbf{k}_1^j) \right] (\mathbf{k}_1 \cdot \mathbf{k}_2)$$

$$\times 2 \left((\mathbf{k}_3)^l (\mathbf{k}_3)^m k_4^2 O_{k_3}^{(R)} + (\mathbf{k}_4)^l (\mathbf{k}_4)^m k_3^2 O_{k_4}^{(R)} \right) (-iH\partial_{\omega_L})^5 (-i\partial_{\omega_R})^4 O_{k_1}^{(L)} O_{k_2}^{(L)} I_{ijlm}^{2b}, \quad (4.5.39)$$

where

$$I_{ijlm}^{2b} := \frac{1}{8} (\delta_{il}\delta_{jm} + \delta_{im}\delta_{jl})I_0^{2b} + \frac{1}{8s^2} (\delta_{il}s_js_m + \delta_{im}s_js_l)I_2^{2b}$$

$$(4.5.40)$$

The B_{4A}^4 integral can be written similarly:

$$B_{4A}^{4} = (2\pi i) \frac{\lambda_{PO}\lambda_{PE}H^{14}}{8k_{1}^{3}k_{2}^{3}k_{3}^{3}k_{4}^{3}} 4(\mathbf{k}_{1} \times \mathbf{k}_{2})^{i}(\mathbf{k}_{1})^{j}(\mathbf{k}_{2})^{k}(\mathbf{r})^{l}$$

$$\times 2\left((\mathbf{k}_{3})^{m}(\mathbf{k}_{3})^{n}k_{4}^{2}O_{k_{3}}^{(R)} + (\mathbf{k}_{4})^{m}(\mathbf{k}_{4})^{n}k_{3}^{2}O_{k_{4}}^{(R)}\right)(-iH\partial_{\omega_{L}})^{5}(-i\partial_{\omega_{R}})^{4}O_{k_{1}}^{(L)}O_{k_{2}}^{(L)}I_{ijklmn}^{4}, \quad (4.5.41)$$

where

$$I_{ijklmn}^{4} = \frac{1}{57} \left(\delta_{im} (\delta_{jk} \delta_{ln} + \text{perm}) + \delta_{in} (\delta_{jk} \delta_{lm} + \text{perm}) \right) I_{0}^{4a}$$

$$+ \frac{1}{456} \left(\frac{\delta_{im}}{s^{2}} (s_{j} s_{k} \delta_{ln} + \text{perm}) + \frac{\delta_{in}}{s^{2}} (s_{j} s_{k} \delta_{lm} + \text{perm}) \right) I_{2}^{4a}$$

$$+ \frac{1}{76} \left(\frac{\delta_{im}}{s^{4}} s_{j} s_{k} s_{l} s_{n} + \frac{\delta_{in}}{s^{4}} s_{j} s_{k} s_{l} s_{m} \right) I_{4}^{4a}$$

$$+ \frac{1}{8} \left(\frac{\delta_{im}}{s^{2}} (\delta_{jk} s_{l} s_{n} + \text{perm}) + \frac{\delta_{in}}{s^{2}} (\delta_{jk} s_{l} s_{m} + \text{perm}) \right) I_{1}^{4b}$$

$$+ \frac{1}{8} \left(\frac{\delta_{im}}{s^{4}} (s_{j} s_{k} s_{l} s_{n}) + \frac{\delta_{in}}{s^{2}} (s_{j} s_{k} s_{l} s_{m}) \right) I_{3}^{4b}.$$

$$(4.5.42)$$

Each of these terms can be obtained by using the tensor structure formula derived in Appendix C. Then, we using our general strategy of rewriting integrals in terms of the A_n and Z_n master integrals. Eventually, it can be shown that:

$$I_{0}^{2a} = \frac{1}{27720(\omega_{L} + \omega_{R})^{3}} \left[3404s^{6} - 44s^{4} \left(142\omega_{L}^{2} + 106\omega_{L}\omega_{R} + 221\omega_{R}^{2} \right) + 33s^{2} \left(201\omega_{L}^{4} + 623\omega_{L}^{3}\omega_{R} + 855\omega_{L}^{2}\omega_{R}^{2} + 229\omega_{L}\omega_{R}^{3} + 104\omega_{R}^{4} \right) - 231 \left(20\omega_{L}^{6} + 60\omega_{L}^{5}\omega_{R} + 51\omega_{L}^{4}\omega_{R}^{2} + 3\omega_{L}^{2}\omega_{R}^{3} + 11\omega_{L}^{2}\omega_{R}^{4} + 13\omega_{L}\omega_{R}^{5} + 6\omega_{R}^{6} \right) \right]$$

$$I_{2}^{2a} = \frac{-7784s^{6} + 88s^{4} \left(83\omega_{L}^{2} + 38\omega_{L}\omega_{R} + 121\omega_{R}^{2} \right) - 33s^{2} \left(51\omega_{L}^{4} + 203\omega_{L}^{3}\omega_{R} + 391\omega_{L}^{2}\omega_{R}^{2} + 121\omega_{L}\omega_{R}^{3} + 50\omega_{R}^{4} \right)}{13860(\omega_{L} + \omega_{R})^{3}}$$

$$I_{2}^{2b} = \frac{172s^{4} - 24s^{2} \left(11\omega_{L}^{2} + 9\omega_{L}\omega_{R} + 17\omega_{R}^{2} \right) + 21 \left(9\omega_{L}^{4} + 27\omega_{L}^{3}\omega_{R} + 35\omega_{L}^{2}\omega_{R}^{2} + 9\omega_{L}\omega_{R}^{3} + 4\omega_{R}^{4} \right)}{1260(\omega_{L} + \omega_{R})^{3}}$$

$$I_{2}^{2b} = \frac{2s^{2} \left(-97s^{2} + 60\omega_{L}^{2} + 30\omega_{L}\omega_{R} + 87\omega_{R}^{2} \right)}{315(\omega_{L} + \omega_{R})^{3}}$$

$$(4.5.45)$$

$$I_{0}^{4a} = \frac{1}{360360(\omega_{L} + \omega_{R})^{3}} \left[-10212s^{6} + 156s^{4} \left(142\omega_{L}^{2} + 106\omega_{L}\omega_{R} + 221\omega_{R}^{2} \right) \right. \\
\left. - 143s^{2} \left(201\omega_{L}^{4} + 623\omega_{L}^{3}\omega_{R} + 855\omega_{L}^{2}\omega_{R}^{2} + 229\omega_{L}\omega_{R}^{3} + 104\omega_{R}^{4} \right) \\
\left. + 1287 \left(20\omega_{L}^{6} + 60\omega_{L}^{5}\omega_{R} + 51\omega_{L}^{4}\omega_{R}^{2} + 3\omega_{L}^{3}\omega_{R}^{3} + 11\omega_{L}^{2}\omega_{R}^{4} + 13\omega_{L}\omega_{R}^{5} + 6\omega_{R}^{6} \right) \right]$$

$$(4.5.46)$$

$$I_{2}^{4a} = \frac{1}{720720(\omega_{L} + \omega_{R})^{3}} \left[1168476s^{6} - 156s^{4} \left(8830\omega_{L}^{2} + 4366\omega_{L}\omega_{R} + 12983\omega_{R}^{2} \right) \right. \\
\left. + 143s^{2} \left(2865\omega_{L}^{4} + 11075\omega_{L}^{3}\omega_{R} + 20691\omega_{L}^{2}\omega_{R}^{2} + 6337\omega_{L}\omega_{R}^{3} + 2636\omega_{R}^{4} \right) \right. \\
\left. + 11583 \left(20\omega_{L}^{6} + 60\omega_{L}^{5}\omega_{R} + 51\omega_{L}^{4}\omega_{R}^{2} + 3\omega_{L}^{3}\omega_{R}^{3} + 11\omega_{L}^{2}\omega_{R}^{4} + 13\omega_{L}\omega_{R}^{5} + 6\omega_{R}^{6} \right) \right]$$

$$I_{4}^{4a} = \frac{1}{480480(\omega_{L} + \omega_{R})^{3}} \left[-1122380s^{6} + 52s^{4} \left(10638\omega_{L}^{2} + 2666\omega_{L}\omega_{R} + 14013\omega_{R}^{2} \right) \right. \\
\left. + 715s^{2} \left(201\omega_{L}^{4} + 623\omega_{L}^{3}\omega_{R} + 855\omega_{L}^{2}\omega_{R}^{2} + 229\omega_{L}\omega_{R}^{3} + 104\omega_{R}^{4} \right) \right. \\
\left. - 6435 \left(20\omega_{L}^{6} + 60\omega_{L}^{5}\omega_{R} + 51\omega_{L}^{4}\omega_{R}^{2} + 3\omega_{L}^{3}\omega_{R}^{3} + 11\omega_{L}^{2}\omega_{R}^{4} + 13\omega_{L}\omega_{R}^{5} + 6\omega_{R}^{6} \right) \right]$$

$$I_{1}^{4b} = \frac{-818s^{6} + 44s^{4} \left(25\omega_{L}^{2} + 16\omega_{L}\omega_{R} + 38\omega_{R}^{2} \right) - 33s^{2} \left(18\omega_{L}^{4} + 59\omega_{L}^{3}\omega_{R} + 89\omega_{L}^{2}\omega_{R}^{2} + 25\omega_{L}\omega_{R}^{3} + 11\omega_{R}^{4} \right)}{13860(\omega_{L} + \omega_{R})^{3}}$$

$$\left. - 2s^{4} \left(-04s^{2} + 55s^{2} + 25s^{2} + 23s^{2} + 32s^{2} + 32s^{2} \right) \right.$$

$$\left. - 2s^{4} \left(-04s^{2} + 55s^{2} + 55s^{2} + 23s^{2} + 32s^{2} + 32s^{2} \right) \right.$$

$$\left. - 3s^{2} \left(-3s^{2} + 55s^{2} + 25\omega_{L}\omega_{R}^{3} + 11\omega_{R}^{4} \right) \right.$$

$$\left. - 3s^{2} \left(-3s^{2} + 55s^{2} + 25s^{2} + 23s^{2} + 32s^{2} + 32s^{2} \right) \right.$$

$$\left. - 3s^{2} \left(-3s^{2} + 55s^{2} + 25s^{2} + 23s^{2} + 32s^{2} + 32s^{2} \right) \right.$$

$$\left. - 3s^{2} \left(-3s^{2} + 55s^{2} + 25s^{2} + 23s^{2} + 32s^{2} \right) \right.$$

$$\left. - 3s^{2} \left(-3s^{2} + 55s^{2} + 25s^{2} + 23s^{2} + 32s^{2} \right) \right.$$

$$\left. - 3s^{2} \left(-3s^{2} + 55s^{2} + 25s^{2} + 25s^{2} + 32s^{2} +$$

 $I_3^{4b} = -\frac{2s^4 \left(-94s^2 + 55\omega_L^2 + 22\omega_L\omega_R + 77\omega_R^2\right)}{495(\omega_L + \omega_R)^3}$ (4.5.50)

To obtain B_{4B} , we simply replace A_n with \tilde{A}_n and Z_n with \tilde{Z}_n . However, in the calculation, we find that $n \geq 6$, while $n_L \geq 5$ and $n_R \geq 4$. Hence when we take derivatives, we find $B_{4B} = 0$ and so only B_{4A} contributes to the two-vertex one-loop trispectrum.

Signal-to-noise estimates In this section we have computed the parity odd trispectrum for a massless scalar at loop level, and showed that they are generally non-zero. This is an interesting scenario as usually loop corrections are smaller than a corresponding tree level contribution when perturbations are under control. In this case, due to the no-go theorems [132,133], the leading B_4^{PO} signal arises at one loop order, and in principle can be as large as allowed by the data. With this in mind, it is worth estimating the signal-to-noise ratio of the parity odd trispectrum. In particular, we want to know the relative signal-to-noise ratio compared to the parity even tree level trispectrum, as this tell us whether we can detect parity odd signals before we detect parity even signals.

The signal-to-noise ratio S/N is an estimate of when a signal becomes observable, which happens when S/N > 1. To be as general as possible we don't commit to a specific observable. Instead we assume we can measure the profile of $\phi(\mathbf{k})$ in some volume $V \sim k_{\min}^{-3}$ with a resolution $k_{\max} > k_{\min}$. For an *n*-point function the signal-to-noise ratio is

$$\left(\frac{S}{N}\right)^2 = V^n \int_{\mathbf{k}_1...\mathbf{k}_n} \frac{\langle \prod_a^n \phi(\mathbf{k}_a) \rangle \langle \prod_a^n \phi(\mathbf{k}_a) \rangle}{\langle \prod_a^n \phi(\mathbf{k}_a)^2 \rangle}.$$
(4.5.51)

For simplicity we consider a model with two interactions:

$$H_{\rm int} = \frac{1}{\Lambda_{\rm PO}^9} \partial_i^9 \phi^4 + \frac{1}{\Lambda_{\rm PE}^6} \partial_{\mu}^6 \phi^4 \,, \tag{4.5.52}$$

where ∂_i^9 denotes some unspecified contraction of nine spatial derivatives and ∂_μ^6 that of six temporal or

spatial derivatives. Here $\Lambda_{\text{PE,PO}}$ are the scales suppressing the respective higher-dimensional interactions. By scale invariance, $B_4 \sim k^{-9}$. Therefore we estimate the parity odd trispectrum to be:

$$B_4^{\rm PO} \sim \left(\frac{H}{\Lambda_{\rm PO}}\right)^9 \left(\frac{H}{\Lambda_{\rm PE}}\right)^6 \frac{H^4}{k^9} \frac{1}{16\pi^2} \,.$$
 (4.5.53)

Here the factor of $1/(4\pi)^2$ appears because the leading signal is a one loop diagram. In this model there is an associated parity even trispectrum at tree level. A rough estimate gives:

$$\mathcal{B}_4^{\text{PE}} \sim \left(\frac{H}{\Lambda_{PE}}\right)^6 \frac{H^4}{k^9} \,. \tag{4.5.54}$$

Provided the instrumental noise for in the parity even and parity odd measurements is comparable, and both measurements are based on the same dataset, we obtain the following:

$$\frac{(S/N)_{PO}}{(S/N)_{PE}} = \left(\frac{H}{\Lambda_{PO}}\right)^9 \frac{1}{16\pi^2} \ll 1.$$
 (4.5.55)

This implies the parity odd signal can only be seen after the parity even signal. However, if the systematics and the instrument noise are not expected to break parity (or to do so by a small amount), the noises for the parity odd and parity even measurements can be different. In those cases it can make sense to search for parity odd trispectrum in the data despite the fact that we have not detected any parity even trispectrum in the sky yet.

Chapter 5

Analyticity of the wavefunction

Moving beyond perturbation theory has proved to be a great challenge for the cosmological bootstrap. Ideas such as the cosmological optical theorem, manifest locality have no obvious extensions beyond perturbation theory. It is therefore natural to look to other bootstrap programs for ideas. One such example is the S-matrix bootstrap. In the S-matrix bootstrap, analyticity is the key component for everything. It has links to physical principles such as causality and crossing, and it also allow us to construct useful bounds such as the Froissart bound and positivity bounds.

If we are to follow in the footsteps of the S-matrix bootstrap, we will need the analytic structure of the wavefunction. In the rest of the thesis we will turn our attention to the analytic wavefunction, a program dedicated to understanding wavefunction analyticity in a similar way to the S-matrix. In this section we will first briefly review the consequences of analyticity in the S-matrix. We will then briefly argue why analyticity in the wavefunction is linked to causality. Then, we will study the analytic structure of the wavefunction in full detail by using a heuristic argument known as the energy conservation condition. We will then explain why the energy conservation condition is true by using Landau analysis, which is also employed for amplitudes.

5.1 Analyticity and the S-matrix

Here we give a lightning review on the analytic structure of the S-matrix. The analytic S-matrix (and S-matrix bootstrap) has been studied extensively since the 1960s, and a complete overview of the subject would require too much time. Therefore, we will focus on some key results (some of which we have found analogous results for the wavefunction). Readers interested in learning more about the S-matrix bootstrap can refer to [50, 142–147].

The most extensively studied object in the S-matrix bootstrap is the 2-to-2 scattering amplitude. The 2-to-2 scattering amplitude depends on the Mandelstam variables s, t, u, which obeys $s + t + u = 4m^2$ (for external particles with the same mass). If we analytically continue s and study the analytic structure of the S-matrix in this variable, we obtain figure 5.1.

The key features of figure 5.1 can be summarized as follow:

• Causality Causality implies the S-matrix must be analytic in the upper half plane (or lower half plane, depending on the convention used) up to some *anomalous thresholds* which are contained in

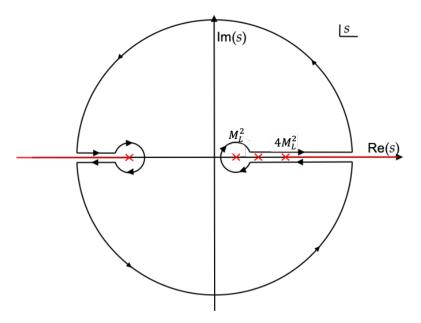


Figure 5.1: The analytic structure of the 2-to-2 scattering amplitude in the complex s plane.

some region $|s| < R(t)^1$. This is proved by Bros, Epstein and Glaser [148], and one of the assumptions used is microcausality, i.e. $[\phi(x), \phi(y)] = 0$ for spatially separated points x and y.

The link between analyticity and causality is not unique to relativistic theories. This is shown by Kramers and Kroinig [149, 150], who derived relations between the real and imaginary part of the refractive indicies. Here causality simply means the response at time t cannot depend on anything at a later time t' > t. This type of causality has been studied extensively for in the context of scattering (for both classical and non-relativistic quantum systems), for more details the readers can refer to [151]. We will see this causality condition has implications on the analyticity of the wavefunction as well.

• Unitarity The location of the singularities also encodes the spectrum of intermediate states of the scattering process. This is a consequence of unitarity. In particular, the optical theorem reads²:

$$\operatorname{disc}_{s}T(s,t) = \frac{1}{2i}\left(T(s+i\epsilon,t) - T(s-i\epsilon,t)\right) = \sum_{X} T_{2\to X} T_{2\to X}^{\dagger}.$$
 (5.1.1)

where X goes over all intermediate states. This interpretation is made even more clear in perturbation theory, where the intermediate states are multi-particle states. One can draw a Feynman diagram for each process, and the discontinuity operator can be represented as a plane which cuts the internal lines. For a theory with a single scalar one finds a set of singularities known as normal thresholds, which corresponds to exchanging n-intermediate particles. The location of the singularities are given by $s = (nm)^2$. Generally tree level diagrams give rise to poles, and loop level diagrams give rise to branch points. We will see something very similar for the wavefunction.

¹Here we assume t < 0

²This discontinuity operator is not the Disc operator used in the cosmological optical theorem.

• Crossing symmetry Roughly speaking this is telling us scattering processes in different channels are in fact described by the same analytic function, and they are connected by analytic continuation. For instance, electron-positron annihilation and Compton scattering are linked together by crossing. The pole and branch cuts on the negative real axis in figure 5.1 corresponds to singularities in the *u*-channel, and by going in an arc in the upper half plane (for sufficiently large *s*) one can show the *s*-channel amplitude can be analytically continued to the (complex conjugate of) *u*-channel amplitude. Unfortunately, we do not have much to say about crossing for the wavefunction.

The S-matrix bootstrap has been used to derive non-perturbative bounds for scattering processes. These bounds are often derived by studying properties of some general non-perturbative expressions of the S-matrix, which comes from physical principles and symmetry. These include:

• Partial wave expansion For 2-to-2 scattering, we can always boost ourselves to the center of mass frame by Lorentz invariance. There we can use representation theory to show that the S-matrix can be written as [146]:

$$T(s,t) = \sum_{J} a_{J}(s) P_{J}^{(d)} \left(1 + \frac{2t}{s - 4m^{2}} \right).$$
 (5.1.2)

 $P_J^{(d)}$ is given by some Gegenbauer polynomial (up to some normalization factors). In d=3 this reduces to a Legendre polynomial. This representation has been used to derive non-perturbative unitarity bounds as well as the famous Froissart bound [152], which states that the total cross section must obey $\sigma_{\text{tot}} \leq s(\log s)^2$ as $s \to \infty$.

Writing down the partial wave expansion for the wavefunction in flat space proved to be a challenge. This is because in our definition of the wavefunction we are looking at the vacuum state at a particular time t, and this implicitly chooses a foliation of time, which spontaneously breaks Lorentz boost. Since boost is broken, one cannot freely go to the COM frame, and this generally means the partial wave expansion are not diagonal in l, the orbital angular momentum. (for example see [153]).

In dS, we do not have Lorentz invariance to begin with. However one could interpret the dS isometry group in d+1 dimension as the Lorentz group in d+2 dimension, and it may be possible to find some partial wave expansion reminiscent to (5.1.2).

• **Dispersion relation** With the analytic structure of the S-matrix, a straightforward application of Cauchy's theorem gives us the dispersion relation:

$$T(0,t) = \int_{M_L^2}^{\infty} \frac{ds}{2\pi i} \frac{\operatorname{disc}_s T(s,t)}{s} + \int_{M_L^2}^{\infty} \frac{du}{2\pi i} \frac{\operatorname{disc}_u T(s,t)}{s} + \mathcal{C}^{\infty} [T],$$
 (5.1.3)

where $C^{\infty}[T]$ represents the contour integral for asymptotically large s, and M_L represents the mass of the lightest particle which couples to the external fields. This representation is particularly helpful for deriving *positivity bounds*, a series of bounds on the Wilson coefficients of an EFT. Write the amplitude in the following expansion:

$$T(s,t) = \sum_{n=0}^{\infty} s^n c_n(t),$$
 (5.1.4)

where the EFT coefficients c_n can be straightforwardly related to the couplings which appear in the

EFT action. Then it is straightforward to see that:

$$c_n(t) = \int_{M_L^2}^{\infty} \frac{ds}{2\pi i} \frac{\operatorname{disc}_s T(s, t)}{s^{n+1}} + \int_{M_L^2}^{\infty} \frac{du}{2\pi i} \frac{\operatorname{disc}_u T(s, t)}{s^{n+1}} + \mathcal{C}_n^{\infty} [T],$$
 (5.1.5)

where, once again, $C_n^{\infty}[T]$ represents the contour integral for asymptotically large s. Due to the Froissart bound, $C_n^{\infty}[T]$ usually vanishes. By using unitarity and causality, one can constrain the right hand side of (5.1.5), and this give us a set of inequalities for the Wilson coefficients [53–60] (also see [154] where these ideas are applied to the EFT of inflation).

We will see in section 7 that we can also write down dispersion relations for the wavefunction.

5.2 Wavefunction analyticity and causality

In the rest of this chapter we will explore the analytic structure of the wavefunction. Let us address an important question first:

Which variable's analyticity are we interested in We need to pick a suitable variable, analytically continue said variable, then study its analyticity. Naturally there are many choices we can make. While we would love to pick some sort of Mandelstam variable just like in amplitudes, as mentioned previously the wavefunction either breaks the Lorentz group spontaneously (in flat space), or does not admit Lorentz group as a symmetry (in dS), and so we have yet to find the analogue of the Mandelstam variable for the wavefunction. In addition, in the case of dS we are often interested in cases where dS boosts (i.e. special conformal transformations) are broken, and those wavefunctions coefficients would likely not obey the full dS isometry.

The choice we make is the following: given a wavefunction coefficient $\psi_n(\{\omega\}, \{\mathbf{k}\})$, we analytically continue in the off-shell energies, and study the analyticity of one of its off-shell energies (say ω_1).

This choice is natural for two reasons. The first reason is that most of our bootstrap rules are expressed in terms of analytically continuing off-shell energies. For instance, the cosmological optical theorem is defined through the Disc operator, where we analytically continue in ω . The manifest locality test is defined through taking derivatives with respect to ω . Given most of our operations so far are expressed in terms of ω , it makes sense to study analyticity in ω , as we may have a chance of understanding the constraints of these rules in the complex ω plane.

The second reason is that analyticity in ω is linked to causality. We will explore this now.

Analyticity in ω is linked to causality To understand the link between analyticity and causality, let us study the LSZ expression for the off-shell flat space wavefunction coefficients, given in (2.2.32). First notice that the time integration domain is from $-\infty < t < 0$, i.e. the wavefunction is expressed in terms of responses to sources from the past.

$$\int_{-\infty}^{0} dt \, e^{i\omega t} \, \mathcal{E}\hat{\Phi}_{\mathbf{k}}(t) = \int_{-\infty}^{\infty} dt \, \Theta(-t) \, e^{i\omega t} \, \mathcal{E}\hat{\Phi}_{\mathbf{k}}(t) . \tag{5.2.1}$$

These type of response function are necessarily analytic in the lower half complex plane of ω : this is close in spirit to the Kramers-Kroinig dispersion relations. We can also see it in a different way: if Im $\omega \geq 0$, the

integral would not converge properly as $t \to -\infty$. From this we obtain our first result for the analyticity of the wavefunction:

The wavefunction coefficients $\psi_n(\{\omega\}, \{k\})$ must be analytic in the lower half complex plane of all of its external energies ω .

It is easy to see how this result generalizes to some simple cases in dS: since we replace $e^{i\omega\eta}$ by the bulk-to-boundary propagators, we simply need to know their behavior. For massless scalars and spin-2 fields the bulk-to-boundary propagators are $(1-i\omega\eta)e^{i\omega\eta}$, so it is easy to see that it is true. For conformally coupled scalars and massless spin-1 fields their bulk-to-boundary propagators are proportional to plane waves, so obviously the result also holds. For massive fields the bulk-to-boundary propagators are given by Hankel functions, which goes as $e^{i\omega\eta}/\eta$ as $\eta \to -\infty$. So it is very likely that this result also holds for fields with any mass.

Note that the causality we use is not microcausality, i.e. $[\phi(x), \phi(y)] = 0$ for spacelike separated points x, y. It would be nice to see how to implement microcausality into the picture.

5.3 Energy conservation condition

In the rest of the section we will focus on the flat space wavefunction. Since we are ultimately interested in applying our results to cosmology, naturally we should address the following question:

How does studying the flat space wavefunction help us? Since inflation is well approximated by dS, it seems like studying flat space is not helpful for us. However, in simple cases, we can directly relate the wavefunction in dS to the flat space wavefunction.

Consider ψ_3 in dS with the interaction $\mathcal{L} = g\dot{\phi}^3$. The wavefunction is:

$$\psi_3^{\text{dS}} = 6g \frac{\omega_1^2 \omega_2^2 \omega_3^2}{\omega_T^3} = \omega_1^2 \omega_2^2 \omega_3^2 \partial_{\omega_T}^2 \left(\frac{g}{\omega_T}\right). \tag{5.3.1}$$

Notice that $\frac{g}{\omega_T}$ is just the flat space wavefunction for ϕ^3 interaction.

In general, under the following assumption, it is possible to write the dS wavefunction in terms of derivatives of the flat space wavefunction [98]:

- No IR divergence in interactions.
- The theory contains only massless or conformally coupled scalars.

This result is due to the form of the mode function for the massless and conformally coupled scalars, which can be related to a plane wave by taking derivatives. These assumptions are satisfied for theories with shift symmetry (for example by the EFToI [113]). It should also be possible to extend this result to loop integrands (in fact we have utilized this idea extensively in section 4.4).

This is important as these derivative operators give us a controlled way of relating the analytic structure of the dS wavefunction to the analytic structure of the flat space wavefunction. In particular, taking derivatives do not change the location of the singularities, it only changes its order (for example it can change a logarithmic branch point to a pole). As a result, by studying the analytic structure of the flat

space wavefunction, we can also get the analytic structure for simple theories in dS which satisfy the assumptions stated above.

It is worth noting that by considering the integral representation of Hankel function, it may be possible to relate the flat space wavaefunction to the dS wavefunction for fields with arbitrary mass. For instance, we can use the following [155]:

$$H_{\nu}^{(1)}(z) = \frac{\Gamma(\frac{1}{2} - \nu)(\frac{1}{2}z)^{\nu}}{i\pi\Gamma(\frac{1}{2})} \int_{1+i\infty}^{(1+)} dt \, e^{izt} (t^2 - 1)^{\nu - \frac{1}{2}}, \tag{5.3.2}$$

or similar integral representations to relate the mode function of a massive scalar to a plane wave. However, this give us some integral operators in general, and depending on the contour this may introduce some new singularities. We will leave a careful study of this procedure to the future.

Working in flat space also has another advantage: for polynomial interactions, there is a purely algebraic set of recursion relations which simplifies the calculation of the wavefunction significantly. We will review this now.

Recursion representation of the wavefunction It has been shown in [82] that the wavefunction coefficients in flat space admit an elegant representation in terms of canonical forms of polytopes. The relations work diagram by diagram. More in detail, take a diagram contributing to a given wavefunction coefficient ψ_n , and remove all external lines. This give a "skeleton" diagram with V vertices and I internal lines. Associate to each vertex a total vertex energy x_A , with $A = 1, \ldots, V$. Also, to each internal line associate an energy y_m , with $m = 1, \ldots, I$. For tree diagrams all y_m 's are fixed in terms of external spatial momenta by momentum conservation at each vertex, but at loop level this is not the case. The dependence of wavefunction coefficients on vertex energies x and internal-line energies y can now be written as

$$\psi_n = \psi_n(x_1, x_2, \dots, x_V; y_1, y_2, \dots, y_I). \tag{5.3.3}$$

This dependence can be determined by the following recursion relation

$$\left(\sum_{A}^{V} x_{A}\right) \psi_{n}(\{x_{A}\}) = \sum_{m}^{I} \operatorname{Cut}_{m} \psi_{n}(\dots, x_{B} + y_{m}, \dots, x_{B'} + y_{m}, \dots),$$
 (5.3.4)

where the operation Cut_m means that one should remove the m-th internal line and add its energy y_m to each of the vertex energies that that line connected. If after the line is cut the diagram becomes disconnected one should interpret $\operatorname{Cut}_m \psi_n$ as the product of the wavefunction coefficients shifted by y_m of the disconnected parts, $\psi_{n'} \times \psi_{n-n'}$ with n' < n. Notice that in the recursion relation all coupling constants are omitted, but can be easily re-inserted if desired. The recursion relation can be represented graphically as

$$\left(\sum_{A} x_{A}\right) \left(\psi_{n}\right) = \sum_{m} \left(\psi_{n'}\right)_{\stackrel{-}{+y_{m}} \stackrel{-}{-+y_{m}}} \left(\psi_{n-n'}\right) + \left(\psi_{n}\right)_{\stackrel{+}{+y_{m}}} \left(\psi_{$$

Using this relation over and over again, one can reduce any diagram to a diagram with one vertex and no internal lines, for which the initial condition of the recursion is

$$\psi_1^{\text{tree}}(x) = \bullet_x = \frac{1}{x}. \tag{5.3.6}$$

Note that (5.3.5) is the perturbative version of the Hamilton-Jacobi equation which determines the time evolution of the wavefunction, and (5.3.6) corresponds to a Bunch-Davies initial condition (see [107] for a recent review of this Schrödinger picture³).

Sometimes an example is worth a thousand words. Tree-level examples of the two- and three-site chains are

$$\psi_{2}^{\text{tree}}(x_{1}, x_{2}; y) = \frac{\psi_{1}^{\text{tree}}(x_{1} + y)\psi_{1}^{\text{tree}}(x_{2} + y)}{x_{T}} = \frac{1}{(x_{1} + x_{2})(x_{1} + y)(x_{2} + y)}, \qquad (5.3.7)$$

$$\psi_{3}^{\text{tree}}(x_{1}, x_{2}, x_{3}; y_{1}, y_{2}) = \frac{\psi_{2}^{\text{tree}}(x_{1}, x_{2} + y_{2})\psi_{1}^{\text{tree}}(x_{3} + y_{2}) + \psi_{1}^{\text{tree}}(x_{1} + y_{1})\psi_{2}^{\text{tree}}(x_{2} + y_{1}, x_{3})}{\sum_{A}^{3} x_{A}}$$

$$= \frac{\left(\frac{1}{x_{1} + x_{2} + y_{2}} + \frac{1}{x_{2} + x_{3} + y_{1}}\right)}{(x_{1} + x_{2} + x_{3})(x_{1} + y_{1})(x_{2} + y_{1} + y_{2})(x_{3} + y_{2})}. \qquad (5.3.8)$$

For loop diagrams, the recursion relation produce the loop *integrand*, as opposed to the integral. To make the distinction clear, we introduce the following notation

$$\psi_n^{L\text{-loop}}(\{\mathbf{k}\}) = \int_{\mathbf{p}_1, \dots, \mathbf{p}_L} \mathcal{I}_n^{L\text{-loop}}(\{\mathbf{k}\}, \{\mathbf{p}\}), \qquad (5.3.9)$$

where the set of external momenta $\{\mathbf{k}\}$ and internal momenta $\{\mathbf{p}\}$ will be connected to the recursion relations shortly. Examples of a one-loop diagram with one or two vertices are

$$\mathcal{I}_{1}^{1-\text{loop}}(x;y) = \frac{1}{x}\psi_{1}^{\text{tree}}(x+2y) = \frac{1}{x(x+2y)},$$
(5.3.10)

$$\mathcal{I}_{2}^{1-\text{loop}}(x_{1}, x_{2}; y_{1}, y_{2}) = \frac{1}{x_{1} + x_{2}} \left[\psi_{2}^{\text{tree}}(x_{1} + y_{1}, x_{2} + y_{1}) + \psi_{2}^{\text{tree}}(x_{1} + y_{2}, x_{2} + y_{2}) \right]$$

$$= \frac{1}{(x_{1} + x_{2})(x_{1} + y_{1} + y_{2})(x_{2} + y_{1} + y_{2})} \left[\frac{1}{(x_{1} + x_{2} + 2y_{2})} + \frac{1}{(x_{1} + x_{2} + 2y_{1})} \right].$$
(5.3.11)

Notice that, loosely speaking, the recursion relation is giving us the result of the integrand expanded in partial fractions.

From the recursion representation of the wavefunction, we can derive the following result:

The off-shell wavefunction coefficient $\psi_n(\omega_a, \mathbf{k}_a)$ at any order in perturbation theory is analytic in the complex ω_1 -plane at fixed real, positive values of $(\omega_{a\neq 1}, \mathbf{k}_a)$, except for singularities along the negative real axis, $\omega_1 \leq 0$. The location of singularities corresponds to the vanishing of the partial energy of a connected sub-diagram (the energy-conservation condition).

³In particular, compare (5.3.5) with Figure 2 of [107].

The physical picture. In perturbation theory, $\psi_n(\omega_a, \mathbf{k}_a)$ can be represented as a sum over Feynman-Witten diagrams in which each interaction vertex represent an integral of the schematic form

$$\int_{-\infty}^{0} dt \ f_{\omega_1}^*(t) \dots f_{\omega_n}^*(t) = \int_{-\infty}^{0} dt \ e^{+i\omega_T t} \,, \tag{5.3.12}$$

where $\omega_T = \sum_{j=1}^n \omega_j$ is the total energy flowing into the vertex from its n legs. Evaluating these integrals requires a prescription to handle the limit $t \to -\infty$. This comes from imposing that the infinite past the system is in the Minkowski ground state. This ensures that the effect of interactions become small in the far past and the integral converges. This is the precise analog of the choice of the Bunch-Davies initial state in accelerating FLRW spacetimes. In practice, this physical picture is achieved by deforming the integration contour in the far past to $t \to -\infty(1-i\epsilon)$, such that $e^{i\omega_T t}$ provides an exponential suppression for each interaction vertex in the infinite past. However, as already recognized in [80], if there is an energy-conserving vertex at which $\omega_T = 0$, then this exponential suppression is removed and such an infinitely long-lived interactions can produce singularities in the Bunch-Davies wavefunction.

This is precisely analogous to a long-lived (on-shell) internal state producing divergences in a scattering amplitude. In the amplitude context, the tree-level exchange of a single on-shell line produces a simple pole and the loop-level exchange of multiple on-shell lines produces a branch cut. For the wavefunction, the integral representation introduced above makes it clear that tree-level wavefunction coefficients also possess simple poles, while branch cuts are produced only at loop level. The conceptual difference is that, rather than being determined by where intermediate lines go on-shell, the non-analyticities in the wavefunction are determined by where interaction vertices become energy-conserving and hence the factors in the denominators of (5.3.7)-(5.3.8) or (5.3.10)-(5.3.11) vanish.

This heuristic argument is illustrated in Fig. 5.2, where we summarise our conjectured analytic structure for the off-shell ψ_1, ψ_2 and ψ_3 by considering the values of ω_1 for which there exists a diagram with an energy-conserving vertex. Before attempting to prove that this simple rule indeed captures all of the non-analyticities in the perturbative wavefunction coefficients, we will show how it can be used to systematically generate a list of singular points for any off-shell ψ_n .

Tree-level poles. The simplest way to enumerate all possible poles in the perturbative wavefunction is to proceed inductively, beginning with the off-shell $\psi_{n=1}$ with a single external leg and then adding further external legs one at a time. This is useful because an off-shell diagram with n external legs entering the same bulk vertex with energies $(\omega_1, ..., \omega_n)$ and momenta $(\mathbf{k}_1, ..., \mathbf{k}_n)$ is identical to the same off-shell diagram with a single external leg entering that vertex with energy $\sum_{a=1}^{n} \omega_a$ and momenta $\sum_{a=1}^{n} \mathbf{k}_a$, and therefore will give poles that are analogous to those of a lower-point diagram. Because of this we find it convenient to also include quadratic vertices in our analysis, corresponding to perturbative correction from the linear mixing of fields. So for the first three wavefunction coefficients,

 ψ_1 : The only tree-level diagram for a single (off-shell) external line carrying energy ω_1 is:

$$\stackrel{\boldsymbol{\omega}_1}{\bullet} \tag{5.3.13}$$

For an interaction with no derivatives, the corresponding wavefunction coefficient is simply $\psi_1 \propto 1/\omega_1$ and contains a simple pole at $\omega_1 = 0$. Adding derivatives only produces positive powers of ω_1 or \mathbf{k}_1 ,

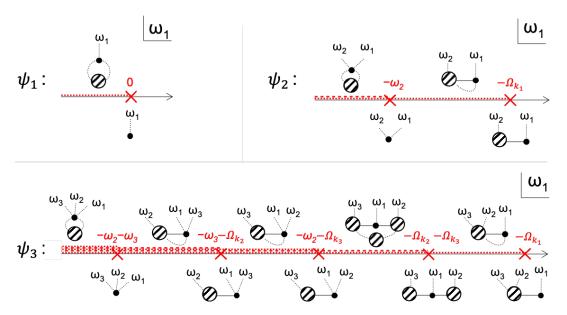


Figure 5.2: The analytic structure in the complex ω_1 -plane for the off-shell wavefunction coefficients, (ψ_1, ψ_2, ψ_3) , in a theory with massless particles. In all cases we analytically continue ω_1 with the other ω_j and k_j held fixed at real positive values, and to provide a concrete order for the singularities we assume that $\omega_j \geq k_j$ and $\omega_j > \omega_{j'}$ if j > j'. Red crosses/lines indicate poles/branch cuts, and for each the diagram responsible is shown. Solid/dashed lines denote on/off-shell legs.

and so cannot lead to any additional singularities.

 ψ_2 : When two lines carry energies (ω_1, ω_2) and momenta $(\mathbf{k}_1, \mathbf{k}_2 = -\mathbf{k}_1)$ into the bulk, there are now two possibilities. Either (a) the two lines both terminate on the same interaction vertex,

$$\begin{array}{c} \omega_2 & \omega_1 \\ \bullet \end{array}$$
 (5.3.14)

in which case we find the same result as for ψ_1 (with $\omega_1 \to \omega_1 + \omega_2$), or (b) the two lines end on different vertices,

where we have used a solid internal line to denote that this is on-shell (i.e. carries an energy $\Omega_{\mathbf{k}_1} = \sqrt{k_1^2 + m^2}$, where m is the mass of the field being exchanged). The black vertex carries zero energy when $\omega_1 = -\Omega_{k_1}$, and this is a qualitatively new threshold that develops when there is more than one external line. We have used hatched blob to indicate that the details of the ω_2 coupling are unimportant for this threshold—of course one could relabel the external arguments and similarly conclude that there is a pole at $\omega_2 = -\Omega_{k_2}$ independently of the coupling to the ω_1 external line. So up to this permutation, there are 2 simple poles which can appear in ψ_2 , at

$$\omega_1 + \omega_2 = 0 ,$$
 $\omega_1 + \Omega_{k_1} = 0 .$
(5.3.16)

 ψ_3 : With three lines carrying energy and momentum into the bulk, there are now three options. The first possibility is that all of the external lines terminate on the same vertex,

$$\omega_3 \omega_2 \omega_1$$
 (5.3.17)

which produces a simple pole at $\omega_1 + \omega_2 + \omega_3 = 0$ just like in ψ_1 above (with $\omega_1 \to \omega_1 + \omega_2 + \omega_3$). The second possibility is that just two of the external lines terminate on the same vertex: this can happen *either* as,

$$\overset{\omega_3}{\smile}\overset{\omega_2}{\smile}\overset{\omega_1}{\smile} \tag{5.3.18}$$

which produces a simple pole at $\omega_1 = -\Omega_{k_1}$ just like in ψ_2 above, or as,

$$\omega_3 \qquad \omega_1 \qquad \omega_2$$

$$(5.3.19)$$

which produces a simple pole at $\omega_1 + \omega_2 = -\Omega_{k_3}$, again like in ψ_2 above (with $\omega_1 \to \omega_1 + \omega_2$ and $\mathbf{k}_1 \to \mathbf{k}_1 + \mathbf{k}_2$) and up to permutations of the external legs. Finally, there is a qualitatively new threshold which corresponds to the three external legs terminating on different vertices,

$$\overset{\omega_3}{ } \overset{\omega_1}{ } \overset{\omega_2}{ }$$
 (5.3.20)

which produces a simple pole at $\omega_1 = -\Omega_{k_2} - \Omega_{k_3}$. Again, permuting the labels of the external energies implies analogous poles also in ω_2 and ω_3 . Overall, up to this permutation of the external leg labels, ψ_3 can therefore have simple poles at 4 locations:

$$\omega_{1} + \omega_{2} + \omega_{3} = 0 ,$$

$$\omega_{1} + \omega_{2} + \Omega_{k_{3}} = 0 ,$$

$$\omega_{1} + \Omega_{k_{2}} + \Omega_{k_{3}} = 0 ,$$

$$\omega_{1} + \Omega_{k_{1}} = 0 .$$
(5.3.21)

Based on this recursive pattern, we see that each time n is increased a qualitatively new kind of threshold appears (in addition to the thresholds which exist for all lower-point coefficients). A simple algorithm for explicitly listing all of these poles in a given ψ_n at tree level is the following,

Energy-conservation condition (at tree-level):

For each partition of the n external legs into q subsets, each with a total energy ω_a and total momentum \mathbf{k}_a (for a=1,...,q), there can be a pole in ψ_n whenever,

$$\omega_1 + \sum_{a=2}^{q} \sqrt{|\mathbf{k}_a|^2 + m_a^2} = 0 \tag{5.3.23}$$

where m_a is the mass of any field that can couple to the external legs in subset a.

As an illustration, consider the off-shell four-point coefficient, ψ_4 . Up to permutations of the particle labels, this algorithm produces a list of 7 possible poles for every set of masses m_j which the exchanged fields may have:

Partition	Pole conditions	
$\{1, 2, 3, 4\}$	$\omega_1 + \omega_2 + \omega_3 + \omega_4 = 0$	
$\{1,2,3\},\{4\}$	$\omega_1 + \omega_2 + \omega_3 + \Omega_{k_4} = 0$	
$\{1,2\},\{3,4\}$	$\omega_1 + \omega_2 + \Omega_{ \mathbf{k}_3 + \mathbf{k}_4 } = 0$	(5.3.24)
$\{1\}, \{2, 3, 4\}$	$\omega_1 + \Omega_{ \mathbf{k}_2 + \mathbf{k}_3 + \mathbf{k}_4 } = 0$	(0.0.24)
$\{1,2\},\{3\},\{4\}$	$\omega_1 + \omega_2 + \Omega_{k_3} + \Omega_{k_4} = 0$	
$\{1\}, \{2\}, \{3,4\}$	$\omega_1 + \Omega_{k_2} + \Omega_{ \mathbf{k}_3 + \mathbf{k}_4 } = 0$	
$\{1\}, \{2\}, \{3\}, \{4\}$	$\omega_1 + \Omega_{k_2} + \Omega_{k_3} + \Omega_{k_4} = 0$	

where $\Omega_{k_a} = \sqrt{k_a^2 + m_a^2}$ is the energy associated with any of the massive fields that can be exchanged in that channel. This list is indeed exhaustive of all of the poles we will find in explicit examples below.

Loop-level branch cuts. Beyond tree level, the wavefunction is no longer a rational function and can develop branch cuts in the complex ω -planes. These cuts can be viewed as a continuum of poles which arise from integrating a rational integrand (determined by the recursion relations reviewed in Sec. 5.3) over continuous loop momenta. To systematically enumerate all possible branch points that can be generated by loops, it is again useful to proceed inductively starting from $\psi_{n=1}$,

 ψ_1 : When a single line carries energy ω_1 and momentum $\mathbf{k}_1 = 0$ into the bulk, it must terminate on an interaction vertex. At loop level, this vertex may also be connect to internal lines, each of which carries a momentum \mathbf{q}_a which is related to the momenta flowing in the loop (and hence integrated over). For instance, in the diagram,

$$\stackrel{\omega_1}{\diamondsuit}$$
 (5.3.25)

the black vertex conserves energy when,

$$\omega_1 = -\Omega_{q_1} - \Omega_{q_2},\tag{5.3.26}$$

where $\Omega_{q_a} = \sqrt{q_a^2 + m_a^2}$ is the energy of the internal lines (which have masses m_a). Note that momentum-conservation requires $\mathbf{q}_1 + \mathbf{q}_2 = 0$. Integrating over all values of \mathbf{q}_1 therefore creates a

continuum of poles on the negative ω_1 axis, which begins at the value,

$$-\min_{\substack{\mathbf{q}_1\\(\mathbf{q}_1+\mathbf{q}_2=0)}} (\Omega_{q_1} + \Omega_{q_2}) = -m_1 - m_2. \tag{5.3.27}$$

In general, allowing for an arbitrary number I of internal lines to be connected to the black interaction vertex, there will be a continuum of poles on the negative real axis beginning at,

$$\omega_1 = -\min_{\substack{\mathbf{q}_a \\ (\sum_{a=1}^I \mathbf{q}_a = 0)}} \left(\sum_{a=1}^I \Omega_{q_a} \right) = -\sum_{a=1}^I m_a, \tag{5.3.28}$$

where the m_a are the masses of the internal lines. Note that when the theory includes massless particles this branch cut threshold coincides with the tree-level pole, but for gapped theories these non-analyticities are separated.

 ψ_2 : With two external lines, there are again two possibilities. The first is that the two lines both terminate on the same interaction vertex, e.g.

$$\begin{array}{ccc}
\omega_2 & \omega_1 \\
\bullet & & \\
\end{array}$$

$$(5.3.29)$$

in which case we have a branch cut (i.e. a continuum of poles) on the negative real axis which begins at $\omega_1 + \omega_2 = -\sum_{a=1}^{I} m_a$, just as for ψ_1 (with $\omega_1 \to \omega_1 + \omega_2$). The qualitatively new threshold is when the two lines end on different vertices,

$$\overset{\omega_2}{\bigcirc}\overset{\omega_1}{\longrightarrow}$$
 (5.3.30)

in which case the internal momenta are now constrained as $\sum_{a=1}^{I} \mathbf{q}_a = \mathbf{k}_1$ by momentum conservation. Consequently, the branch cuts from diagrams of this kind begin at

$$\omega_1 = -\min_{\substack{\mathbf{q}_a \\ (\sum_{a=1}^I \mathbf{q}_a = \mathbf{k}_1)}} \left(\sum_{a=1}^I \Omega_{q_a} \right) = -\sqrt{k_1^2 + \left(\sum_{a=1}^I m_a\right)^2}.$$
 (5.3.31)

Note that when all of the internal lines carry the same mass, the minimum is achieved at $\mathbf{q}_a = \mathbf{k}_1/I$ for every a and this threshold is simply $\omega_1 = -\sqrt{k_1^2 + (Im)^2}$, and again would coincide with the tree-level pole in any theory which contains massless exchange. This threshold is analogous to the I-particle threshold for scattering amplitudes, which comes about because with relativistic energy $\omega_1^2 - |\mathbf{k}_1|^2 = (Im)^2$ the off-shell particle 1 can decay into I on-shell particles of mass m. As usual, the freedom to relabel the external leg arguments implies an analogous branch cut in ω_2 .

 ψ_3 : With three external legs, there are again three possibilities. They could all terminate on the same

vertex,

$$\omega_3 \omega_2 \omega_1$$
(5.3.32)

which reproduces the same $\omega_1 + \omega_2 + \omega_3 = -\sum_{a=1}^{I} m_a$ branch cuts as in ψ_1 above (with $\omega_1 \to \omega_1 + \omega_2 + \omega_3$). Two could terminate on the same vertex, either as

$$\omega_3 \qquad \omega_2 \qquad \omega_1 \qquad (5.3.33)$$

which reproduces the same $\omega_1 = -\sqrt{k_1^2 + (Im)^2}$ type branch cuts as in ψ_2 above, or as,

which produces a branch cut with threshold $\omega_1 + \omega_2 = -\sqrt{k_3^2 + (Im)^2}$ following the same ψ_2 argument (with $\omega_1 \to \omega_1 + \omega_2$ and $\mathbf{k}_1 \to \mathbf{k}_1 + \mathbf{k}_2 = -\mathbf{k}_3$). The third possibility is that all three legs terminate on different vertices,

$$\begin{array}{ccc}
\omega_3 & \omega_1 & \omega_2 \\
\bullet & \bullet & \bullet \\
\bullet & \bullet & \bullet
\end{array}$$
(5.3.35)

This produces a qualitatively new threshold due to the different momentum conservation conditions for the \mathbf{q}_a . For instance, for I=2 internal lines connected to the black vertex and considering a single loop momentum \mathbf{p} , this threshold occurs at

$$\omega_1 = -\min_{\mathbf{p}} \left(\Omega_{|\mathbf{k}_3 + \mathbf{p}|} + \Omega_{|\mathbf{k}_2 - \mathbf{p}|} \right) . \tag{5.3.36}$$

The precise value of this minimum depends on the relative size of \mathbf{k}_3 and \mathbf{k}_2 , but again we note that in the limit of massless internal lines the branch cut extends all the way to the tree-level pole (which corresponds to $\mathbf{p} = 0$).

We see that for every tree-level diagram leading to a simple pole there is a corresponding series of loop-level diagrams (labelled by I) that create a branch cut at related thresholds. When the exchanged fields are massless all thresholds approach the location of a corresponding tree-level pole. The general conclusion is therefore:

Energy-conservation condition (at loop level):

When loops of massless fields are included, every pole in ψ_n becomes a branch point. In massive theories, for each pole there is an infinite series of branch points at successively lower negative values of ω_1 (with a separation determined by the mass gap).

This closely parallels the analytic structure of scattering amplitudes, for which each tree-level channel produces a corresponding pole at the single-particle threshold (e.g. $s=m^2$), and then loops in each of these channels produce branch cuts at the multi-particle thresholds (e.g. $s=4m^2, 9m^2, ...$).

Altogether, we have shown how a simple heuristic argument that links singularities in the wavefunction to long-lived interactions in the bulk (i.e. those that have vanishing total energy) can be used to generate a systematic list of where we expect to find poles and branch cuts in the complex ω -planes. Next, we will confirm that these lists are indeed an exhaustive classification of the singularities in some concrete wavefunction coefficients computed in perturbation theory.

5.3.1Examples: tree level

Since the Minkowski wavefunction coefficients are particularly simple at tree-level (they are given directly by the recursion relation of Sec. 5.3), for the following examples we allow for arbitrary interaction vertices.

One vertex. Let's start by considering tree-level diagrams with a single vertex. These are all related to the starting solution of the recursion relation $\psi_1^{\text{tree}}(x) = 1/x$. For one, two and three external legs respectively these are given by

$$\psi_1(\omega_1) = \stackrel{\omega_1}{\bullet} = \frac{F_1(\omega_1)}{\omega_1}, \qquad (5.3.37)$$

$$\psi_2(\omega_1, \omega_2; \mathbf{k}_1) = \underbrace{\overset{\omega_2}{\smile}}_{\omega_1} = \frac{F_2(\omega_1, \omega_2, \mathbf{k}_1)}{\omega_1 + \omega_2}, \qquad (5.3.38)$$

$$\psi_{2}(\omega_{1}, \omega_{2}; \mathbf{k}_{1}) = \psi_{2} \qquad = \frac{F_{2}(\omega_{1}, \omega_{2}, \mathbf{k}_{1})}{\omega_{1} + \omega_{2}}, \qquad (5.3.38)$$

$$\psi_{3}(\omega_{1}, \omega_{2}, \omega_{3}; \mathbf{k}_{1}, \mathbf{k}_{2}) = \psi_{3} \qquad = \frac{F_{3}(\omega_{1}, \omega_{2}, \omega_{3}; \mathbf{k}_{1}, \mathbf{k}_{2})}{\omega_{1} + \omega_{2} + \omega_{3}}, \qquad (5.3.39)$$

where F_1 , F_2 and F_3 are vertex factors. We find poles at $\omega_1 = 0$, $\omega_1 = -\omega_2$ and $\omega_1 = -\omega_2 - \omega_3$, in agreement with the energy-conservation condition of the previous section.

Two vertices. Diagrams with two vertices are a bit more interesting. They are all related to the second term in the recursion relation, $\psi_2(x_1, x_2; y)$ in (5.3.7), and they only appear for two or more external legs. For ψ_2 with 2 vertices, we find

$$\psi_2(\omega_1, \omega_2; \mathbf{k}) = \frac{V}{\omega_1 \omega_2} = \frac{F_L(\omega_1; \mathbf{k}) F_R(\omega_2; \mathbf{k})}{(\omega_1 + \Omega_k)(\omega_2 + \Omega_k)(\omega_1 + \omega_2)}.$$
 (5.3.40)

There are poles at $\omega_1 = -\omega_2$, as well as $\omega_1 = -\Omega_k$, which are predicted by the energy-conservation condition. For ψ_3 with 2 vertices, there are two possibilities. We can have ω_1 alone on one of the vertices, which gives:

$$\psi_3 = (\omega_1 \omega_3 \omega_1) = \frac{\tilde{F}_L(\omega_2, \omega_3; \mathbf{k}_1) \tilde{F}_R(\omega_1; \mathbf{k}_1)}{(\omega_1 + \Omega_{k_1})(\omega_2 + \omega_3 + \Omega_{k_1})(\omega_1 + \omega_2 + \omega_3)},$$
(5.3.41)

and so we find poles at $\omega_1 = -\omega_2 - \omega_3$ and $\omega_1 = -\Omega_{k_1}$. We can also have ω_1 and another external leg on the same vertex, which gives:

$$\psi_{3} = V + (2 \leftrightarrow 3)$$

$$= \frac{\tilde{F}_{L}(\omega_{1}, \omega_{2}; \mathbf{k}_{3})\tilde{F}_{R}(\omega_{3}; \mathbf{k}_{3})}{(\omega_{3} + \Omega_{k_{3}})(\omega_{1} + \omega_{2} + \Omega_{k_{3}})(\omega_{1} + \omega_{2} + \omega_{3})} + (2 \leftrightarrow 3).$$
(5.3.42)

In addition to $\omega_1 = -\omega_2 - \omega_3$ we also find $\omega_1 = -\omega_2 - \Omega_{k_3}$ and $\omega_1 = -\Omega_{k_2} - \omega_3$.

Three vertices. For ψ_3 with three vertices there are 3 different permutations for the location of external leg. If ω_1 is attached to the vertex on the side we have:

$$\psi_{3} = \downarrow \downarrow \downarrow \downarrow \downarrow + (2 \leftrightarrow 3)$$

$$= \frac{F_{A}(\omega_{1}; \mathbf{k}_{1}) F_{B}(\omega_{2}; \mathbf{k}_{1}, \mathbf{k}_{2}) F_{C}(\omega_{3}; \mathbf{k}_{3}) \left(\frac{1}{\omega_{1} + \omega_{2} + \Omega_{k_{3}}} + \frac{1}{\omega_{2} + \omega_{3} + \Omega_{k_{1}}}\right)}{(\omega_{1} + \omega_{2} + \omega_{3})(\omega_{1} + \Omega_{k_{1}})(\omega_{2} + \Omega_{k_{1}} + \Omega_{k_{3}})(\omega_{3} + \Omega_{k_{3}})} + (2 \leftrightarrow 3).$$

$$(5.3.43)$$

Poles are located at $\omega_1 = -\omega_2 - \omega_3$, $\omega_1 = -\Omega_{k_1}$, $\omega_1 = -\omega_2 - \Omega_{k_3}$ and $\omega_1 = -\Omega_{k_2} - \omega_3$.

If ω_1 is attached to the middle vertex we have:

$$\psi_{3} = \begin{array}{c} \stackrel{\omega_{2} \quad \omega_{1} \quad \omega_{3}}{\longleftarrow} \\ = \frac{F_{A}(\omega_{2}; \mathbf{k}_{2}) F_{B}(\omega_{1}; \mathbf{k}_{1}, \mathbf{k}_{2}) F_{C}(\omega_{3}; \mathbf{k}_{3}) \left(\frac{1}{\omega_{1} + \omega_{3} + \Omega_{k_{2}}} + \frac{1}{\omega_{1} + \omega_{2} + \Omega_{k_{3}}}\right)}{(\omega_{1} + \omega_{2} + \omega_{3})(\omega_{3} + \Omega_{k_{3}})(\omega_{1} + \Omega_{k_{2}} + \Omega_{k_{3}})(\omega_{3} + \Omega_{k_{3}})}.$$

$$(5.3.44)$$

Here we find a pole at $\omega_1 = -\Omega_{k_2} - \Omega_{k_3}$ as well as $\omega_1 = -\omega_2 - \omega_3$, $\omega_1 = -\omega_2 - \Omega_{k_3}$ and $\omega_1 = -\Omega_{k_2} - \omega_3$. All these poles correspond precisely to the list of tree-level singularities predicted by the energy-conservation condition for ψ_n with n = 1, 2 and 3. Now we move on to consider loop diagrams.

5.3.2 Examples: one loop

At one-loop, the computation of wavefunction coefficients becomes more involved due to the integration over the loop momentum. To streamline our presentation, we will therefore now focus on polynomial interactions. We also give only the final results here in the main text, and describe the technical details of the computations in appendix D.

One vertex. Consider the following diagram:



in which all external legs are to be attached to the single vertex. Define ω_1 to be the total energy entering the vertex. Since there is only one vertex, the energy-conservation condition predicts a branch point at

the threshold,

$$\omega_1 = -\min_{\mathbf{p}} \left(2\Omega_p \right) = -2M,\tag{5.3.45}$$

where M is the mass of the internal line forming the loop. This diagram corresponds to the integral,

$$\omega_1 \psi_1^{\text{1-loop}} = \int_{\mathbf{p}} \frac{1}{\omega_1 + 2\Omega_p} ,$$
 (5.3.46)

and is evaluated explicitly in App. D.2. The result is,

$$\omega_1 \psi_1^{\text{1-loop}} = \frac{2\omega_1}{16\pi^2} \sqrt{4M^2 - \omega_1^2} \arcsin\left(\sqrt{\frac{2M - \omega_1}{4M}}\right) + \text{analytic} , \qquad (5.3.47)$$

see (D.2.5). Note that the UV divergence is analytic in ω_1 (and can therefore be absorbed into local counter-terms). There is a branch point at $\omega_1 = -2M$ due to the argument of the arcsin exceeding unity, but otherwise $\omega_1 \psi_1^{\text{1-loop}}$ is analytic in the complex ω_1 plane.

If the internal field is massless, the branch point is located at $\omega_1 = 0$, so the branch cut starts at the location of the tree-level pole. Indeed, taking the massless limit of (5.3.47) gives,

$$\psi_1^{\text{1-loop}} = -\frac{\omega_1}{16\pi^2} \log(\omega_1) + \text{analytic} ,$$
 (5.3.48)

which has a logarithmic branch point at $\omega_1 = 0$ (with the conventional branch cut running along the negative real axis, $\omega_1 < 0$). So this simple example agrees with our energy-conservation condition.

Two vertices. Now consider the following two-vertex one-loop diagram:

$$u_1$$
 u_2
 u_1
 u_2
 u_3
 u_4
 u_4
 u_5
 u_4
 u_5
 u_5

which contributes to $\psi_2^{\text{1-loop}}$. Define **k** to be the momentum entering the left vertex and exiting the right vertex, and ω_1 , ω_2 to be the energies entering each vertex. The energy-conservation condition predicts the following singularities in the complex ω_1 plane:

(i)
$$\omega_1 = -\sqrt{k^2 + (M_1 + M_2)^2}$$
,

(ii)
$$\omega_1 = -\omega_2 - 2M_1$$
.

(iii)
$$\omega_1 = -\omega_2 - 2M_2$$
.

The diagram in (5.3.49) corresponds to the integral:

$$\omega_{12}\psi_2^{\text{1-loop}}(\omega_1, \omega_2; k) = \int_{\mathbf{p}} \frac{1}{(\omega_1 + \Omega_{q_1} + \Omega_{q_2})(\omega_2 + \Omega_{q_2})} \left[\frac{1}{\omega_{12} + 2\Omega_{q_1}} + \frac{1}{\omega_{12} + 2\Omega_{q_2}} \right] . \tag{5.3.50}$$

where $q_1 = |\mathbf{p}|$ and $q_2 = |\mathbf{k} - \mathbf{p}|$ are the momenta of the internal lines and $\omega_{12} = \omega_1 + \omega_2$ is the total energy. This integral is evaluated in detail in App. D.3, and given in (D.3.22) in terms of incomplete

elliptic integrals. For finite values of M and k, it has a branch point at $\omega_1 = -\sqrt{k^2 + 4M^2}$ in the complex ω_1 plane, as predicted by the energy-conservation condition.

The second singularity predicted by the energy-conservation condition appears when either M or k vanish, as shown in (D.3.35) and (D.3.36). For the case of massless internal edges, the incomplete elliptic integrals simplify to dilogarithms, and (5.3.50) can be written as,

$$\omega_{12}\psi_{2}^{\text{1-loop}} = \frac{1}{8\pi^{2}} \left[\frac{\omega_{2} \log (\omega_{1} + k) - \omega_{1} \log (\omega_{2} + k)}{\omega_{1} - \omega_{2}} - \frac{\omega_{12}}{2k} \left(\frac{1}{2} \log^{2} \left(\frac{\omega_{1} + k}{\omega_{2} + k} \right) + \text{Li}_{2} \left(\frac{k - \omega_{2}}{k + \omega_{1}} \right) + \text{Li}_{2} \left(\frac{k - \omega_{1}}{k + \omega_{2}} \right) \right) + \text{analytic} \right]. \quad (5.3.51)$$

The singularities in the complex ω_1 plane are⁴

- (i) $\omega_1 = -k$, from both $\log(\omega_1 + k)$ and $\operatorname{Li}_2\left(\frac{k \omega_2}{k + \omega_1}\right)$.
- (ii) $\omega_1 = -\omega_2$, from both $\text{Li}_2\left(\frac{k-\omega_1}{k+\omega_2}\right)$ and $\text{Li}_2\left(\frac{k-\omega_2}{k+\omega_1}\right)$ (while the dilogarithm is finite at that point, it is not smooth).

This list of singularities matches exactly the predictions of the energy-conservation condition. It is also worth mentioning that the first line of (D.3.35) is not singular at $\omega_1 = \omega_2$ (at fixed $k \neq -\omega_2$), since this apparent pole has zero residue.

Three vertices. Let's move on to the most complicated one-loop diagram we will consider, involving three vertices:

$$q_{31}$$
 ω_3
 q_{23}
 ω_2

$$(5.3.52)$$

Momentum conservation at each vertex fixes all but one of the internal momenta (which we denote by \mathbf{p}), and also sets $\mathbf{k}_1 + \mathbf{k}_2 + \mathbf{k}_3 = 0$. This diagram then corresponds to the integral,

$$\omega_{123}\psi_3^{\text{1-loop}} = \int_{\mathbf{p}} \frac{1}{(\omega_1 + \Omega_{q_{12}} + \Omega_{q_{31}})(\omega_2 + \Omega_{q_{12}} + \Omega_{q_{23}})(\omega_3 + \Omega_{q_{23}} + \Omega_{q_{31}})} \sum_{\text{perm.}}^{6} \frac{1}{(\omega_{123} + 2\Omega_{q_{12}})(\omega_{23} + \Omega_{q_{12}} + \Omega_{q_{31}})} .$$

$$(5.3.53)$$

which is discussed in App. D.4. The singularities expected from the energy-conservation condition are:

- (i) $\omega_1 = -\min_{\mathbf{p}}(\Omega_{q_{31}} + \Omega_{q_{12}})$. This gives $\omega_1 = -|\mathbf{k}_1|$ for massless internal lines.
- (ii) $\omega_1 = -\omega_2 \min_{\mathbf{p}}(\Omega_{q_{23}} + \Omega_{q_{31}})$. This gives $\omega_1 = -\omega_2 |\mathbf{k}_3|$ for massless internal lines.
- (iii) $\omega_1 = -\omega_3 \min_{\mathbf{p}}(\Omega_{q_{12}} + \Omega_{q_{23}})$. This gives $\omega_1 = -\omega_3 |\mathbf{k}_2|$ for massless internal lines.
- (iv) $\omega_1 = -\omega_2 \omega_3 \sum_{a=1}^2 M_a$. This gives $\omega_1 = -\omega_2 \omega_3$ for massless internal lines.

⁴Recall that the dilogarithm $\text{Li}_2(z)$ has a branch point at z=1 and the conventional branch cut goes from z=1 to $z=\infty$ along the real axis.

Evaluating the integral (5.3.53) in full generality is a difficult task in d=3 dimensions: the main complication is that the boundary of the integration region for the $\{\Omega_{q_{12}}, \Omega_{q_{23}}, \Omega_{q_{31}}\}$ internal energies is a non-trivial surface (defined by a hyperelliptic curve).

For simplicity, let us consider here the case where all internal fields are massless and let us further suppose that one of the external fields carries zero spatial momentum, say $\mathbf{k}_3 = 0$ (though note that we are not fixing ω_3). In this limit $\mathbf{k}_1 = -\mathbf{k}_2$ (and so we denote their common magnitude as k), and the integration region degenerates to the same region encountered in the two-vertex diagram above. Consequently $\psi_3^{\text{1-loop}}$ can be written in a closed form in terms of dilogarithms. The full expression is left in App. D.4 (equation (D.4.19)), however we notice that it is analytic in the complex ω_1 plane (at fixed $\{\omega_2, \omega_3, k\}$) modulo branch points at:

(i)
$$\omega_1 = -k$$
, where $\psi_3^{\text{1-loop}} \sim \log(\omega_1 + k)$,

(ii)
$$\omega_1 = -\omega_2$$
, where $\psi_3^{\text{1-loop}} \sim \text{Li}_2\left(-\frac{\omega_2 - k}{\omega_1 + k}\right)$ and $\text{Li}_2\left(-\frac{\omega_1 - k}{\omega_2 + k}\right)$,

(iii)
$$\omega_1 = -\omega_3 - k$$
, where $\psi_3^{1-\text{loop}} \sim \log(\omega_{13} + k)$,

(iv)
$$\omega_1 = -\omega_{23}$$
, where $\psi_3^{\text{1-loop}} \sim \text{Li}_2\left(-\frac{\omega_{23}-k}{\omega_1+k}\right)$ and $\text{Li}_2\left(-\frac{\omega_{13}-k}{\omega_2+k}\right)$.

This precisely saturates the list of singularities expected from the energy-conservation condition.

Having established the validity of the energy-conservation condition in a number of examples, we now turn to a robust "proof" that wavefunction integrals generically possess singularities in these locations.

5.4 Landau analysis: first attempt

In this section, we develop the analogue of the Landau analysis commonly used in amplitude literature. This provides a list of necessary conditions for a point in kinematic space to be singular. We will see that the list of singularities from the energy conservation condition is contained within the list of singularities from the Landau analysis.

From the recursion relations we know that ψ_n can always be written in the following form:

$$\psi_n(\{\omega\}, \{\mathbf{k}\}) = \int_{\mathbf{p}_1, \dots, \mathbf{p}_L} \frac{F(\{\omega\}, \{\mathbf{k}\}, \{\mathbf{p}\})}{\prod_{j=1}^{2V+L-2} S_j(\{\omega\}, \{\mathbf{k}\}, \{\mathbf{p}\})}.$$
 (5.4.1)

Here S_j are linear functions of the internal and external energies, and $F(\{\omega\}, \{\mathbf{k}\}, \{\mathbf{p}\})$ can always be expressed in terms of a sum of products of S_j times analytic functions of \mathbf{k} from derivative interactions.

We would like to find all singular points of ψ_n without explicitly computing the integral. Similar technology has been developed in the amplitude literature, leading to a set of conditions for singularity known as the Landau equations (for a review on Landau conditions for amplitudes, see [142], [156], [146]). We will review some key ideas used to derive the Landau equations, and show how they can be used to find singularities for wavefunction coefficients as well.

Singularities: one integral variable. Consider the following expression:

$$f(z_1, \dots, z_n) = \int_C dw \, g(z_1, \dots, z_n, w).$$
 (5.4.2)

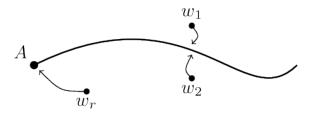


Figure 5.3: Usual picture for singularities in the case with one integration variable. Here w_r gives an endpoint singularity, while w_1 and w_2 gives a pinch singularity.

Here C denotes a contour in the complex w plane. $g(z_1, \ldots, z_n, w)$ contains singularities, and their positions in the complex w plane are determined by an algebraic equation $S(z_1, \ldots, z_n, w) = 0$. Changing z_1, \ldots, z_n corresponds to changing the position of poles in the complex w plane.

Singular points in $g(z_1, ..., z_n, w)$ can be avoided by deforming the contour C, and this prevents singularities from developing in $f(z_1, ..., z_n)$. However, contour deformation cannot avoid the following singularities:

- When a singularity approaches the endpoint of the contour C, which is fixed by the boundary conditions of the integral. This is known as an endpoint singularity.
- When two different singularities approach the contour from opposite sides and pinch the contour in between. This is known as a pinch singularity.

Singularities: multiple integral variables. In order to illustrate how singularities can develop in cases with multiple integral variables, let us consider the case of two complex integral variables:

$$f(z_1, \dots, z_n) = \int_C dw_1 dw_2 g(w_1, w_2, z_1, \dots, z_n).$$
 (5.4.3)

The hypercontour C is a two (real) dimensional surface in a four (real) dimensional space. In general the hypercontour would have a set of boundaries, and each of them would be described by an equation:

$$\tilde{S}_i = 0. (5.4.4)$$

For instance, suppose the integration region is given by:

$$f(z_1, \dots, z_n) = \int_1^\infty dw_1 \int_{-1}^1 dw_2 g(w_1, w_2, z_1, \dots, z_n).$$
 (5.4.5)

Then the boundaries of the hypercontour would be given by:

$$\tilde{S}_1 = w_1 - 1 = 0, (5.4.6)$$

$$\tilde{S}_{2+} = w_2 + 1 = 0, (5.4.7)$$

$$\tilde{S}_{2-} = w_2 - 1 = 0. (5.4.8)$$

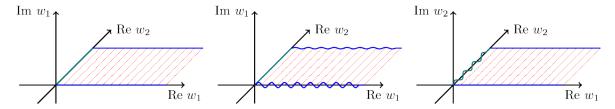


Figure 5.4: The hypercontour for the integral (5.4.5), sketched in three of the four (real) directions. The left figure shows the undistorted integration contour. The boundary \tilde{S}_{2+} and \tilde{S}_{2-} is indicated by blue lines, while the boundary \tilde{S}_1 is indicated by a teal line. Since the equation for \tilde{S}_{2+} and \tilde{S}_{2-} only fixes w_2 , they are allowed to deform in the imaginary w_1 direction, as shown in the middle figure. The right figure shows the allowed deformation for the boundary \tilde{S}_1 , which is in the imaginary w_2 direction.

Notice that each of the equation $\tilde{S}_i = 0$ describe a two (real) dimensional surface in a four (real) dimensional space. This is less constraining than the single integral variable case: since the hypercontour C is two dimensional, its boundary should be one dimensional. This implies that the boundary of the contour is not rigidly fixed: we are allowed to deform the boundary as long as it remains on the surface described by the equation \tilde{S} . See Fig. 5.4.

Since the allowed deformations are all constrained on a surface $\tilde{S}_i = 0$, the boundary of the contour cannot be deformed in the normal direction of the surface, which is described by the vector with components:

$$\frac{\partial \tilde{S}_i}{\partial \boldsymbol{w}} = \left(\frac{\partial \tilde{S}_i}{\partial w_1}, \frac{\partial \tilde{S}_i}{\partial w_2}\right). \tag{5.4.9}$$

Similarly, the singularities for the function $g(w_1, w_2, z_1, \dots, z_n)$ are described by algebraic equations of the form:

$$S_i(w_1, w_2, z_1, \dots, z_n) = 0.$$
 (5.4.10)

Once again these are two dimensional surfaces, and their normal vectors are $\frac{\partial S_i}{\partial w}$. The singular surface in general may not be planar, since the equation $S_i = 0$ may not be linear.

Given a set of singular surfaces and boundary constraint surfaces, there are three ways where singularities can emerge from the integral $I(z_1, \ldots, z_n)$:

- A singular surface approaches the boundary of the hypercontour in the normal direction of a constraint surface, such that no deformation can be carried out to avoid the singular surface. This is analogous to the endpoint singularities in the one dimensional case.
- Two surfaces approaches each other from opposite sides of the hypercontour, and they pinch the hypercontour in between. This is analogous to the pinch singularities in the one dimensional case.
- A single surface may become locally cone-like and pinch the contour in the vertex of the cone, see Fig. 5.6. It is also a pinch singularity, but unlike the single integral variable case, only one singularity surface is involved. In this case, the normal vector near the vertex satisfies the following:

$$\frac{\partial S_i}{\partial \boldsymbol{w}} = 0. \tag{5.4.11}$$

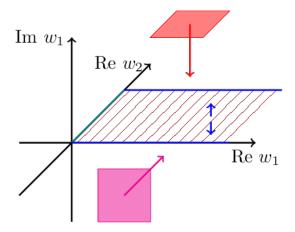


Figure 5.5: As the boundary \tilde{S}_{2+} and \tilde{S}_{2-} can be deformed in the imaginary w_1 direction (indicated by the blue arrows in the figure), the contour can be deformed downwards to avoid the red surface approaching from above (along Im w_1). However, the boundary is fixed along Re w_2 , so the contour cannot be deformed to avoid the magenta surface approaching from that direction, which results in an endpoint singularity.

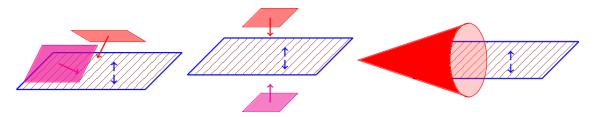


Figure 5.6: Consider a contour that can be deformed in the vertical direction (indicated by the blue arrows). In the left panel, the contour can deform downwards to avoid colliding with the red and magenta surfaces. However, if the surfaces approach from the opposite side as in the middle panel, a contour deformation cannot avoid the pinch. Finally, a cone like surfaces, such as that in the right panel, can pinch a contour on its own.

It is also possible to have multiple surfaces pinching the hypercontour, or multiple surfaces approaching the boundary of the hypercontour. In general, given a function of the form (5.4.5), a singularity can form if:

ullet For a subset I of the singularity surfaces and a subset \tilde{I} of boundary constraints, the following is satisfied:

$$S_i = \tilde{S}_j = 0 \ (i \in I, j \in \tilde{I}).$$
 (5.4.12)

For amplitudes the analogous condition gives $p_i^2 = m_i^2$. Here I cannot be an empty set, but \tilde{I} can be empty.

• For some real and non-zero choice of a_i and \tilde{a}_j , the normal vectors of the singularity surfaces in subset I and boundary constraints in \tilde{I} must satisfy:

$$\sum_{i \in I} a_i \frac{\partial S_i}{\partial \boldsymbol{w}} + \sum_{j \in \tilde{I}} \tilde{a}_j \frac{\partial \tilde{S}_j}{\partial \boldsymbol{w}} = 0.$$
 (5.4.13)

In other words, the normal vectors are linearly dependent. For amplitudes, this gives $\sum_i \alpha_i p_i = 0$.

These are the necessary conditions for the formation of singularities. However, these conditions are not sufficient: one needs to check whether the singularities actually appear. This is similar to the pseudo thresholds in amplitudes: the Landau analysis may predict singular points that are not present for physical configurations. We will see that something similar also occurs for wavefunction coefficients.

Feynman parameters. The constants a_i in the normal vector condition looks suspiciously like Feynman parameters in the usual Landau analysis. Indeed, if we consider the following integral:

$$\psi_n(\omega_1, \dots, \omega_n) = \int_{\mathbf{p}_1, \dots, \mathbf{p}_L} \left[\prod_{n=1}^{2V+L-2} \int_0^1 d\alpha_n \right] \frac{\delta(1 - \sum \alpha_n) F}{(\sum_{i=1}^{2V+L-2} \alpha_i S_i)^{2V+L-2}},$$
 (5.4.14)

we find the condition (5.4.13) again, but with a_i replaced by the Feynman parameters α_i . Just like for amplitudes, this does not introduce new singularities [142]. In contrast to a_i , which is just restricted to be non-zero, we have $\alpha_i \in [0, 1]$. This provides a stricter criterion for singularities to arise in ψ_n .

5.4.1 Example: massless two site loop

As a first example let's consider the massless two-vertex integral, which can be written in the following form (see D.3):

$$\psi_2^{\text{1-loop}}(\omega_1, \omega_2) = \frac{1}{8\pi^2(\omega_1 + \omega_2)k} \int_k^{\infty} dp_+ \int_{-k}^k dp_- \frac{(p_+ + p_-)(p_+ - p_-)}{(\omega_1 + \omega_2 + p_+ + p_-)(\omega_1 + p_+)(\omega_2 + p_+)}.$$
 (5.4.15)

The singular surfaces are:

$$S_1 = \omega_1 + p_+ = 0, (5.4.16)$$

$$S_2 = \omega_2 + p_+ = 0, (5.4.17)$$

$$S_3 = \omega_1 + \omega_2 + p_+ + p_- = 0. \tag{5.4.18}$$

In addition, the boundary is described by the following equations:

$$\tilde{S}_1 = p_+ - k = 0, \tag{5.4.19}$$

$$\tilde{S}_{2+} = p_- + k = 0, \tag{5.4.20}$$

$$\tilde{S}_{2-} = p_- - k = 0. (5.4.21)$$

As an example, consider:

$$S_3 = \tilde{S}_{2+} = \tilde{S}_1 = 0. (5.4.22)$$

Solving this gives $\omega_1 + \omega_2 = 0$. Now we check the normal-vector condition:

$$a_3 \frac{\partial S_3}{\partial p_+} + \tilde{a}_1 \frac{\partial \tilde{S}_1}{\partial p_+} + \tilde{a}_{2+} \frac{\partial \tilde{S}_{2+}}{\partial p_+} = a_3 + \tilde{a}_1 = 0, \tag{5.4.23}$$

$$a_3 \frac{\partial S_3}{\partial p_-} + \tilde{a}_1 \frac{\partial \tilde{S}_1}{\partial p_-} + \tilde{a}_{2+} \frac{\partial \tilde{S}_{2+}}{\partial p_-} = a_3 + \tilde{a}_{2+} = 0. \tag{5.4.24}$$

Clearly this can be satisfied if $a_3 = -\tilde{a}_1 = -\tilde{a}_{2+}$. Going through the procedure for all combinations of the

surfaces, we eventually find the following list of potential singularities:

$$S_1 = \tilde{S}_1 = 0 \Rightarrow \omega_1 = -k, \tag{5.4.25}$$

$$S_2 = \tilde{S}_1 = 0 \Rightarrow \omega_2 = -k, \tag{5.4.26}$$

$$S_3 = \tilde{S}_{2+} = \tilde{S}_1 = 0 \Rightarrow \omega_1 + \omega_2 = 0,$$
 (5.4.27)

$$S_3 = \tilde{S}_{2-} = \tilde{S}_1 = 0 \Rightarrow \omega_1 + \omega_2 = -2k,$$
 (5.4.28)

$$S_1 = S_2 = 0 \Rightarrow \omega_1 = \omega_2 \text{ (if } \omega_2 < -k).$$
 (5.4.29)

Notice this list is larger than the list of physical singularities. Let's examine these extra singularities:

- The $\omega_1 + \omega_2 = -2k$ singularity is not found in the full expression (5.3.51). This suggests that the residue of the pole is vanishing.
- For $S_2 = 0$, we must have $\omega_2 < -k$. Since we restrict ourselves to positive ω_2 , the pinch singularity from (5.4.29) is not visible in the complex ω_1 plane. This is linked to the fact that the integral has a finite value at $\omega_1 = \omega_2$ when $\omega_2 > -k$.

Example: massive two site loop

The boundary of integration changes when the internal lines become massive. Consider the case where both internal lines have the same mass. The integral becomes:

$$\psi_2^{\text{1-loop}}(\omega_1, \omega_2) = \frac{1}{8\pi^2(\omega_1 + \omega_2)k} \int_{\sqrt{k^2 + 4m^2}}^{\infty} d\Omega_+ \int_{-k\delta}^{k\delta} d\Omega_- \frac{\Omega_+^2 - \Omega_-^2}{(\omega_1 + \omega_2 + \Omega_+ + \Omega_-)(\omega_1 + \Omega_+)(\omega_2 + \Omega_+)}.$$
(5.4.30)

Here we have:

$$\delta = \frac{\sqrt{\Omega_+^2 - k^2 - 4m^2}}{\sqrt{\Omega_+^2 - k^2}}. (5.4.31)$$

The details on how to obtain and evaluate this integral are given in D.3. Despite appearances, the boundary of the integration contour is described by only one equation:

$$\tilde{S} = (\Omega_{+}^{2} - k^{2})(\Omega_{-}^{2} - k^{2}) + 4m^{2}k^{2} = 0.$$
(5.4.32)

Here we have three singularity surfaces:

$$S_1 = \omega_1 + \omega_2 + \Omega_+ + \Omega_- = 0, \tag{5.4.33}$$

$$S_2 = \omega_1 + \Omega_+,$$
 (5.4.34)

$$S_3 = \omega_2 + \Omega_+. (5.4.35)$$

Going through the Landau analysis again gives us the end-point singularity from a single surface:

$$S_2 = \tilde{S} = 0 \Rightarrow \omega_1 = -\sqrt{k^2 + 4m^2},$$
 (5.4.36)

$$S_1 = \tilde{S} = 0 \Rightarrow \omega_1 + \omega_2 = -2m. \tag{5.4.37}$$

We also have an end-point singularity from two surfaces:

$$S_1 = S_2 = \tilde{S} = 0 \Rightarrow \omega_1 = -k \frac{\sqrt{\omega_2^2 - k^2 - 4m^2}}{\sqrt{\omega_2^2 - k^2}}.$$
 (5.4.38)

Here I have picked the negative solution so that S_1 can be satisfied, since Ω_+ is positive. However, this singularity is in fact spurious. To see that this is indeed the case, notice that the constraints $S_1 = S_2 = 0$ imply

$$\omega_2 + \Omega_- = 0. (5.4.39)$$

Since $|\Omega_-| \le k\delta \le k$, we have $\omega_2 \le k$ in order for the singularity to appear. In fact one can check that $\omega_2 < k$ unless we take $\omega_1^2 \to \infty$. However, from the kinematics of the system, $\omega_2 \ge k$. Therefore, as long as we restrict ourselves to values of ω_2 that are physically allowed, we will not encounter this singularity. This is verified in table D.3.

Example: three site loop

For more complicated graphs it may prove difficult to write down variables like Ω_+ and Ω_- . Therefore it is instructive to understand how to carry out Landau analysis with the loop momentum \mathbf{p} , and derive the singularities from our general arguments. We will use the three vertex integral as an example. The integral is:

$$\psi_{3}^{1-\text{loop}} = \int_{\mathbf{p}} \frac{1}{(\omega_{2} + \Omega_{q_{12}} + \Omega_{q_{23}})(\omega_{2} + \omega_{3} + \Omega_{q_{12}} + \Omega_{q_{31}})} \times \frac{1}{(\omega_{1} + \omega_{2} + \omega_{3} + 2\Omega_{q_{31}})(\omega_{1} + \Omega_{q_{12}} + \Omega_{q_{31}})(\omega_{3} + \Omega_{q_{23}} + \Omega_{q_{31}})}, \quad (5.4.40)$$

Here I assume the masses of the internal lines are m. Now we will analytically continue in \mathbf{p} . Since we are integrating over all \mathbf{p} there is no boundary to the integration contour. The singularity surfaces are:

$$S_1 = \omega_2 + \Omega_{q_{12}} + \Omega_{q_{23}} = 0, \tag{5.4.41}$$

$$S_2 = \omega_2 + \omega_3 + \Omega_{a_{12}} + \Omega_{a_{21}} = 0, \tag{5.4.42}$$

$$S_3 = \omega_1 + \omega_2 + \omega_3 + 2\Omega_{g_{31}} = 0, (5.4.43)$$

$$S_4 = \omega_1 + \Omega_{q_{12}} + \Omega_{q_{21}} = 0, \tag{5.4.44}$$

$$S_5 = \omega_3 + \Omega_{q_{23}} + \Omega_{q_{31}} = 0. (5.4.45)$$

Since $\Omega_p = \sqrt{|\mathbf{p}|^2 + m^2}$, the singularity surfaces are not linear anymore. As a result a single surface can pinch a contour. As an example consider $S_3 = 0$. The normal vector condition gives:

$$\frac{\mathbf{q}_{31}}{\Omega_{q_{31}}} = \frac{\mathbf{p} - \mathbf{k}_1}{\Omega_{q_{31}}} = 0. \tag{5.4.46}$$

This is solved by $\mathbf{p} = \mathbf{k}_1$, and $\Omega_{q_{31}} = m$. Putting this back into $S_3 = 0$ gives:

$$\omega_1 + \omega_2 + \omega_3 = -2m. (5.4.47)$$

Similarly, let us write down the rest of the single pinch singularities:

$$S_1 = 0 \Rightarrow \omega_2 + \sqrt{|\mathbf{k}_1|^2 + 4m^2} = 0,$$
 (5.4.48)

$$S_2 = 0 \Rightarrow \omega_2 + \omega_3 + \sqrt{|\mathbf{k}_1|^2 + 4m^2} = 0,$$
 (5.4.49)

$$S_4 = 0 \Rightarrow \omega_1 + \sqrt{|\mathbf{k}_1|^2 + 4m^2} = 0,$$
 (5.4.50)

$$S_5 = 0 \Rightarrow \omega_3 + \sqrt{|\mathbf{k}_3|^2 + 4m^2} = 0.$$
 (5.4.51)

This list of singularity is related to the list produced from our general argument, up to some permutation. Naturally, when we take the massless limit, this simply reproduces the list of singularities from the expression we computed.

5.4.2 Thresholds for general diagrams

Thresholds for massive fields From the recursive relations for the wavefunction (5.4.1), the equations for the singularity surfaces have the following form:

$$S_i = \omega_1 + \sum_{e \in E} \omega_e + \sum_{i \in I} c_i \Omega_i, \tag{5.4.52}$$

where E is a subset of external legs and I is a subset of internal legs and c_i being either 1 or 2. The form of these singularity surfaces comes from the recursion relations in section 5.3: each external energy can only appear once within the expression. Internal energy can only appear at most with a factor of 2, coming from cutting a loop diagram.

We will now show the following for massive fields:

Landau conditions for wavefunction coefficients

Given (5.4.52), the singularities corresponding to the energy-conservation condition are found by solving:

$$S_i = 0,$$
 (5.4.53)

$$\sum_{i \in I} c_i \frac{\partial \Omega_i}{\partial \mathbf{p}_l} = 0, \quad \forall \mathbf{p}_l \in \{\mathbf{p}\}. \tag{5.4.54}$$

We will analytically continue in the loop momentum $\mathbf{p}_l \in \{\mathbf{p}\}$ and carry out the Landau analysis. Since the numerator in the expression (5.4.1) is a sum of products of S_i and possibly powers of the momenta from spatial derivative interactions, to find singularities we can simply focus on the denominators, i.e., we simplify ψ_n until the numerator no longer contains any factor of S_i , we carry out the Landau analysis term by term and finally we sum over all the singularities of each individual term.

The full list of singularities from the Landau analysis includes:

- Endpoint singularities. Since we are integrating over all \mathbf{p}_l , there is no boundary for the hypercontour. As a result we cannot have endpoint singularities, in these integration variables.
- Pinching the contour with a single surface. By considering the cutting procedure in 5.3, it is clear that each S_i corresponds to the total energy entering a subgraph of the Feynman diagram, and

so solving $S_i = 0$ corresponds to energy conservation. In terms of the components of the loop momentum \mathbf{p}_l , the normal vector condition reads:

$$\frac{\partial S}{\partial \mathbf{p}_l} = 0 \Rightarrow \frac{\partial}{\partial \mathbf{p}_l} \sum_{i \in I} c_i \Omega_i = 0. \tag{5.4.55}$$

Unlike the amplitude case, this equation can be consistent with setting only one $S_i = 0^{-5}$. In fact this equation is equivalent to extremizing $\sum_{i \in I} c_i \Omega_i$ with respect to the loop momentum p_l . Observe that for an arbitrary \mathbf{k} ,

$$\frac{\partial^2 \Omega_{|\mathbf{p}+\mathbf{k}|}}{\partial p_i \partial p_j} = \frac{\delta_{ij}}{\Omega_{|\mathbf{p}+\mathbf{k}|}} - \frac{(p+k)_i (p+k)_j}{\Omega_{|\mathbf{p}+\mathbf{k}|}^3}.$$
 (5.4.56)

Since $\Omega_p > p^2 \ge 0$ this is a positive definite matrix. When we take the second derivative of $\sum_{i \in I} c_i \Omega_i$ we simply get a sum of positive definite matrices (with positive coefficients), and the resulting matrix is also positive definite. Therefore when we solve (5.4.55), the solution corresponds to a minimum.

Therefore, $S_i = 0$ satisfies:

$$\omega_1 = -\sum_{e \in E} \omega_e - \min_{\mathbf{p}_l} \sum_{i \in I} c_i \Omega_i, \tag{5.4.57}$$

where the minimization is with respect to all $\mathbf{p}_l \in \{\mathbf{p}\}$. This is exactly the type of singularities obtained by the energy-conservation condition.

• Pinches from multiple surfaces. Given two singularity surfaces S_1 and S_2 with subset of external legs E_1 and E_2 , either $E_1 \subseteq E_2$ or $E_2 \subseteq E_1$. This comes from the cutting procedure used for the recursion representation of the wavefunction: the set of external vertices in a cut diagram must be smaller after every cut. This property of S_i gives us a nice picture of what a multiple surface pinch would mean: the energy going into part of a diagram vanishes, and simultaneously the energy going into a subset of the diagram also vanishes.

At tree level, this type of singularity doesn't give us new poles in ω_1 . Instead, it tells us about non-analyticity in the other ω_e . This is because we can just take one of the singularity surfaces, say S_1 , to write down:

$$\omega_1 = -\sum_{e \in E_1} \omega_e - \sum_{i \in I_1} c_i \Omega_i. \tag{5.4.58}$$

This can then be used to remove any ω_1 dependence from the rest of the expression. Any further non-analyticities of the expression are a result of analytically continuing the other ω_e from their physically allowed values.

In the case of a two-vertex loop with massive fields, we used the Landau analysis and found that it can only occur for unphysical values of ω_2 , and by explicitly computing the integral we found that the singularity is indeed spurious.

However, it is difficult to prove that these multiple surface pinches are always spurious. In amplitudes, when we look at more complicated graphs, such as the three-vertex graph, we discover that for certain external kinematics there are singularities known as anomalous thresholds. It might be possible that

⁵For amplitudes $S_i = p_i^2 - m_i^2 = 0$, and $\frac{\partial S_i}{\partial \mathbf{p}_l} = 2p_i = 0$. The normal vector condition requires $p_i = 0$ which is not possible if $S_i = 0$ as well.

by looking at multiple surface pinches for the three-vertex graph we may discover new singularities similar to these anomalous thresholds, however we leave this for future work.

Using Landau analysis, we have successfully derived the list of singular points from our physical argument in section 5.3. Once again, the full list of singularities from Landau analysis is over-complete, but these extra poles are (likely) removable by considering the external kinematics.

Thresholds for massless fields. If we attempt to directly extend the proof above to the case of massless particles, we run into the following issues even for single pinch singularities:

• Since $\Omega_{p_l} = |\mathbf{p}_l|$, when we take derivative to obtain the normal vector condition, we get $\frac{\partial}{\partial \mathbf{p}_l} \Omega_{|p_l|} = \frac{\mathbf{p}_l}{|\mathbf{p}_l|}$. For $\mathbf{p}_l = 0$ this is ill-defined. To deal with this problem one needs to regulate Ω_{p_l} properly. An example would be introducing artificial boundaries of integration so that $|\mathbf{p}_l|$ never reaches zero, for example:

$$\tilde{S} = |\mathbf{p}_l| - \epsilon = 0, \tag{5.4.59}$$

then take ϵ to zero. However, doing this procedure also introduces spurious singularities, such as the $\omega_1 + \omega_2 = -2k$ pole found in the two-vertex example.

• When we take the second derivative of $\Omega_{|\mathbf{p}+\mathbf{k}|}$, the result is:

$$\frac{\partial^2 |\mathbf{p} + \mathbf{k}|}{\partial p_i \partial p_j} = \frac{\delta_{ij}}{|\mathbf{p} + \mathbf{k}|} - \frac{(p+k)_i (p+k)_j}{|\mathbf{p} + \mathbf{k}|^3}.$$
 (5.4.60)

This is only positive semi-definite, rather than positive definite. Therefore, the solution may not be a minimum.

For the massless case, the Landau analysis would provide us with a list that matches our physical intuition in section 5.3, with some extra singularities. This is analogous to the case in amplitudes, where we get extra soft/collinear singularities for massless particles. The $\omega_1 + \omega_2 = -2k$ pole in the two-vertex example above is one such singularity. In that case the residue is zero, so it does not give rise to new poles or branch cuts.

Chapter 6

Amplitude representation of the wavefunction

The result in the previous section is based on the recursion representation of the wavefunction. While this representation is convenient for practical calculations, it creates a disconnect in language from existing amplitude literature. In amplitude literature, singularities are expressed in terms of cutting internal lines, and in 5.1 we noted this is connected to unitarity cuts (which in turn is related to discontinuity in the complex s plane. For the wavefunction the location is expressed in terms of circling sub-diagrams, and unitarity is related to a "Disc" operator which is not the usual discontinuity. This disconnect makes it difficult to translate ideas from wavefunction analyticity to amplitude analyticity. For instance, are there normal thresholds in the wavefunction just like in amplitudes? Are they linked to unitarity in any way? Are there any anomalous thresholds in the wavefunction?

In this section we bridge the disconnect between amplitude and the wavefunction by using the amplitude representation of the wavefunction. This representation allow us to write down the wavefunction in expressions familiar in amplitudes literature. We will then show that this representation recovers a well-known result: the total energy residue of the wavefunction is given by the amplitude. We will then study the analytic structure of the wavefunction again by using Landau analysis on the amplitude representation of the wavefunction. There we will see the singularities of the wavefunction can be divided into two sets: amplitude-type singularities, which can be mapped to singularities in amplitudes, and wavefunction-type singularities, which has no analogue in amplitudes. We will conclude by studying the consequences of the recently discovered cosmological KLN theorem on the analytic structure of in-in correlators: namely, the wavefunction-type singularities are not present in in-in correlators.

6.1 Amplitude representation of the wavefunction

In order to obtain the amplitude representation of the wavefunction we need to write down the bulkto-bulk propagator in a way reminiscent to the Feynman propagators in amplitudes. For flat space the bulk-to-bulk propagator is given by the following:

$$G(\mathbf{p}, t_1, t_2) = \frac{1}{2\Omega_p} \left(\theta(t_1 - t_2) e^{i\Omega_p(t_2 - t_1)} + \theta(t_2 - t_1) e^{i\Omega_p(t_1 - t_2)} - e^{i\Omega_p(t_1 + t_2)} \right).$$
 (6.1.1)

This propagator is simply the Feynman propagator plus a homogeneous piece, which enforces the boundary condition that the bulk-to-bulk propagator vanishes as $t_1 \text{or} t_2 \to 0$.

Now we can use the following:

$$\theta(t_1 - t_2) = \int_{-\infty}^{\infty} \frac{ds}{2\pi i} \frac{-e^{is(t_2 - t_1)}}{s + i\epsilon},$$
(6.1.2)

Unlike the usual case with the Feynman propagator, we also have this extra boundary piece $e^{i\Omega_p(t_1+t_2)}$, and we must also convert the boundary piece into an integral form as well. We then obtain:

$$G(\mathbf{p}, t_1, t_2) = \int_{-\infty}^{\infty} \frac{ds}{2\pi i} \frac{-e^{is(t_1 - t_2)} + e^{is(t_1 + t_2)}}{s^2 - \Omega_p^2 + i\epsilon}.$$
 (6.1.3)

Here this s integral is understood as a contour integral which closes in the lower half complex plane. The first term is simply the Feynman propagator, and the second term is the boundary piece. From now on I will suppress the integration region for brevity. In addition, I will also sometimes refer to s as internal energy.

Now we symmetrize with respect to s, and we obtain the following expression¹:

$$G(\mathbf{p}, t_1, t_2) = \frac{1}{2} \int \frac{ds}{2\pi i} \frac{(e^{ist_1} - e^{-ist_1})(e^{ist_2} - e^{-ist_2})}{s^2 - \Omega_p^2 + i\epsilon}.$$
 (6.1.4)

Notice how this looks like a Feynman propagator dressed with exponential factors. This is what allow us to write the wavefunction in a form similar to an amplitude: take this expression for the bulk-to-bulk propagator, substitute this into the wavefunction, then carry out the time integral first.

Similar representations have been derived in [159, 160], where it is used to study the wavefunction at tree level. We shall see that this representation can be used to study the analyticity of the wavefunction at loop level as well.

Writing down the wavefunction Given a Feynman diagram, we can write down the flat space wavefunction as:

$$\psi_n = \int \left[\frac{ds_1}{2\pi i} \dots \frac{ds_I}{2\pi i} \right] \prod_a \left[\int_{-\infty}^0 dt_a \, i e^{i\omega_a t_a} \right] \int \prod_l \frac{d^D p_l}{(2\pi)^D} \prod_i \frac{(e^{is_i t_l} - e^{-is_i t_l})(e^{is_i t_r} - e^{-is_i t_r})}{s_i^2 - \Omega_{p_i}^2 + i\epsilon}.$$
(6.1.5)

Here i labels bulk-to-bulk propagators (and I is the total number of bulk-to-bulk propagators), a labels each vertex, l labels the loop momentum to be integrated over, and t_l , t_r labels to which vertex the propagator is attached. Note that the dimension D here labels the boundary dimension, and this expression does not suggest that the wavefunction enjoys the full (D+1)-dimension Lorentz invariance. If we take this expression, integrate over s and then integrate over t, we would obtain the usual recursion expression.

The time integrals on each individual vertex factorize, and are straightforward to do. For a vertex with m internal propagators attached, it has the form:

$$\tilde{D}_{a} = i \int_{-\infty}^{0} dt_{a} \, e^{i\omega_{a}t_{a}} \prod_{j=1}^{m} (e^{is_{j}t_{a}} - e^{-is_{j}t_{a}}) = \int_{-\infty}^{0} dt_{a} \, e^{i\omega_{a}t_{a}} \prod_{j=1}^{m} \left(\sum_{\sigma_{j} = \pm} \sigma_{j} e^{i\sigma_{j}s_{j}t_{a}} \right). \tag{6.1.6}$$

¹This expression was first derived in the context of AdS/CFT, see [157, 158].

We also regulate the integral by sending $\omega \to \omega - i\epsilon$. This gives:

$$\tilde{D}_a = \sum_{\sigma_j = \pm} \frac{\sigma_1 \sigma_2 \dots \sigma_m}{\omega_a + \sum_j \sigma_j s_j - i\epsilon}.$$
(6.1.7)

As a simple example consider that case where there are two bulk-to-bulk propagators attached to vertex a. The time integral has the form:

$$\tilde{D}_a = i \int_{-\infty}^{0} dt_a \, e^{i\omega_a t_a} (e^{is_1 t_a} - e^{-is_1 t_a}) (e^{is_2 t_a} - e^{-is_2 t_a}). \tag{6.1.8}$$

It is not hard to see that this gives:

$$\tilde{D}_{a} = \frac{1}{\omega_{a} + s_{1} + s_{2} - i\epsilon} - \frac{1}{\omega_{a} - s_{1} + s_{2} - i\epsilon} - \frac{1}{\omega_{a} + s_{1} - s_{2} - i\epsilon} + \frac{1}{\omega_{a} - s_{1} - s_{2} - i\epsilon}, \tag{6.1.9}$$

which is indeed the (6.1.7) for j = 2.

Putting this back into the expression (6.1.5) gives us:

$$\psi_n = \frac{1}{2^I} \int \left[\frac{ds_1}{2\pi i} \dots \frac{ds_I}{2\pi i} \right] \prod_a \tilde{D}_a(\omega_a, \{s\}) \int \prod_l \frac{d^D p_l}{(2\pi)^D} \prod_i \frac{1}{s_i^2 - \Omega_i^2 + i\epsilon}.$$
 (6.1.10)

This representation for the wavefunction holds for graphs with any topology at any loop order 2 . Notice how the momentum integral resembles the amplitude of the same Feynman diagram in D-dimension, which is given by:

$$\mathcal{A}_n = \int \prod_l \frac{d^D p_l}{(2\pi)^D} \prod_i \frac{1}{\Omega_i^2 - i\epsilon}.$$
 (6.1.11)

We will refer to the momentum integral as the amplitude-like part of the wavefunction. Also, when integrating over s, $\prod_a \tilde{D}_a$ fixes s in terms of ω , the external energies. For this reason we will call it the the energy-fixing kernel (or just kernel in short).

Readers familiar with the wavefunction may wonder if this is connected with the fact that the total energy pole of the wavefunction is the amplitude of the same diagram. We shall see in the next section that this is indeed the case: when we expand the energy-fixing kernel and do the s-integral, we will obtain the amplitude for a d+1-dimension amplitude alongside some subleading terms.

First example: tree level exchange In order to demonstrate how the formalism works, let us consider a two site tree level exchange diagram.



Figure 6.1: Tree level exchange diagram

²In [161] similar ideas have been explored for in-in correlators for conformally coupled scalars in dS. There the authors were able to express the integrand in a Lorentz invariant expression as well.

The wavefunction coefficient is:

$$\psi_2 = \frac{(-i)^2}{2} \int_{-\infty}^0 dt_1 \int_{-\infty}^0 dt_2 \int \frac{ds}{2\pi i} e^{i\omega_1 t_1} \frac{(e^{ist_1} - e^{-ist_1})(e^{ist_2} - e^{-ist_2})}{s^2 - \Omega_p^2 + i\epsilon} e^{i\omega_2 t_2}$$
(6.1.12)

Now do the time integral:

$$\psi_2 = \frac{1}{2} \int \frac{ds}{2\pi i} \left[\frac{1}{\omega_1 + s - i\epsilon} - \frac{1}{\omega_1 - s - i\epsilon} \right] \left[\frac{1}{\omega_2 + s - i\epsilon} - \frac{1}{\omega_2 - s - i\epsilon} \right] \frac{1}{s^2 - \Omega_p^2 + i\epsilon}$$
(6.1.13)

This can be simplified into:

$$\psi_2 = \frac{1}{2} \int \frac{ds}{2\pi i} \frac{4s^2}{(\omega_1^2 - s^2 - i\epsilon)(\omega_2^2 - s^2 - i\epsilon)} \frac{1}{s^2 - p^2 - m^2 + i\epsilon}$$
(6.1.14)

Here $\frac{1}{s^2-p^2-m^2+i\epsilon}$ is indeed the usual expression for the exchange diagram in amplitudes. The energy-fixing kernel is given by $\frac{4s^2}{(\omega_1^2-s^2-i\epsilon)(\omega_2^2-s^2-i\epsilon)}$.

Let us try and recover the usual recursion expression. We need to remember that the s integral contour encloses the lower half complex plane, so poles like $s = -\omega_1 + i\epsilon$ are not picked up. This gives us the isolated poles:

$$\psi_2 = \frac{1}{2} \left(\frac{2\omega_1}{(\omega_2^2 - \omega_1^2)(\omega_1^2 - \Omega_p^2)} + \frac{2\omega_2}{(\omega_1^2 - \omega_2^2)(\omega_2^2 - \Omega_p^2)} - \frac{2\Omega_p}{(\omega_1^2 - \Omega_p^2)(\omega_2^2 - \Omega_p^2)} \right). \tag{6.1.15}$$

Notice this expression can also be written as:

$$\psi_2 = \frac{1}{\omega_1 + \omega_2} \left(\frac{-\omega_1}{(\omega_1 - \omega_2)(\omega_1^2 - \Omega_p^2)} + \frac{\omega_2}{(\omega_1 - \omega_2)(\omega_2^2 - \Omega_p^2)} \right) - \frac{\Omega_p}{(\omega_1^2 - \Omega_p^2)(\omega_2^2 - \Omega_p^2)}.$$
 (6.1.16)

The total energy pole has been isolated from the rest of the contribution, which only has poles when $\omega_1 = \pm \Omega_p$ or $\omega_2 = \pm \Omega_p$. There is no folded singularity, i.e. no divergences as $\omega_1 \to \omega_2$, since the terms in the bracket cancel. If we take $\omega_1 + \omega_2 \to 0$ we obtain:

$$\lim_{\omega_1 + \omega_2 \to 0} \psi_2 = \frac{1}{\omega_1 + \omega_2} \left(\frac{1}{-\omega_1^2 + \Omega_p^2} \right) = \frac{1}{\omega_1 + \omega_2} \left(\frac{1}{-\omega_1^2 + |\mathbf{p}|^2 + m^2} \right)$$
(6.1.17)

We indeed recover the expression for the amplitude as a total energy pole.

We can further simplify this to obtain the usual recursion expression:

$$\psi_2 = \frac{1}{(\omega_1 + \omega_2)(\omega_1 + \Omega_p)(\omega_2 + \Omega_p)}.$$
(6.1.18)

In this simple example we can see how the wavefunction can be separated into a total energy pole (and its residue is the amplitude), and an extra piece which is finite when total energy is zero.

From the Cosmological optical theorem to the optical theorem for amplitude In 5.1 we noted that the locations of normal thresholds of the S-matrix is linked to unitarity through the optical theorem. Our result so far makes this connection obscure. On one hand singularities are expressed in terms of circling subdiagrams, which makes its connection to any sort of discontinuity unclear. On the other hand

it is unclear how the "Disc" operator used in the cosmological optical theorem is linked to the usual notion of discontinuity.

The amplitude representation provide us a way to relate the disc operator defined in the Cosmological Optical Theorem to the imaginary part of amplitudes. The disc operator used in the COT is defined as follows [100]:

$$\operatorname{Disc}_{k_1,\dots,k_n} f(k_1,\dots,k_n,k_{n+1},\dots,k_m,\{\mathbf{k}\}) = f(k_1,\dots,k_n,k_{n+1},\dots,k_m,\{\mathbf{k}\})$$
$$-f^*(k_1,\dots,k_n,-k_{n+1}^*,\dots,-k_m^*,-\{\mathbf{k}\}). \quad (6.1.19)$$

Now notice the following: the kernel is written as a product of D_a , and in general the following is true:

• If the number of internal lines attached to the vertex is an odd number, we have:

$$\operatorname{Disc}_{\{s\}} \tilde{D}_a = 0. \tag{6.1.20}$$

• If the number of internal lines attached to the vertex is an even number, we have:

$$\operatorname{Disc}_{\{s\}} \tilde{D}_a = 2\tilde{D}_a. \tag{6.1.21}$$

To see this, consider a vertex connected to a single bulk-to-bulk propagator. Then we have:

$$\operatorname{Disc}_{s}\left[\frac{1}{\omega+s-i\epsilon} - \frac{1}{\omega-s-i\epsilon}\right] = \frac{1}{\omega+s-i\epsilon} - \frac{1}{\omega-s-i\epsilon} - \frac{1}{-\omega+s+i\epsilon} + \frac{1}{-\omega-s+i\epsilon} = 0. \quad (6.1.22)$$

Another example a vertex connected with two bulk-to-bulk propagators. Here we have:

$$\operatorname{Disc}_{s} \left[\frac{1}{\omega + s_{1} + s_{2} - i\epsilon} + \frac{1}{\omega - s_{1} - s_{2} - i\epsilon} \right] \\
= \frac{1}{\omega + s_{1} + s_{2} - i\epsilon} + \frac{1}{\omega - s_{1} - s_{2} - i\epsilon} - \frac{1}{-\omega + s_{1} + s_{2} + i\epsilon} - \frac{1}{-\omega - s_{1} - s_{2} + i\epsilon} \\
= 2 \left[\frac{1}{\omega + s_{1} + s_{2} - i\epsilon} - \frac{1}{\omega - s_{1} - s_{2} - i\epsilon} \right]. \quad (6.1.23)$$

Hence,

$$\operatorname{Disc}_{s_{1},s_{2}} \left[\frac{1}{\omega + s_{1} + s_{2} - i\epsilon} - \frac{1}{\omega - s_{1} + s_{2} - i\epsilon} - \frac{1}{\omega + s_{1} - s_{2} - i\epsilon} + \frac{1}{\omega - s_{1} - s_{2} - i\epsilon} \right] \\
= 2 \left[\frac{1}{\omega + s_{1} + s_{2} - i\epsilon} - \frac{1}{\omega - s_{1} + s_{2} - i\epsilon} - \frac{1}{\omega + s_{1} - s_{2} - i\epsilon} + \frac{1}{\omega - s_{1} - s_{2} - i\epsilon} \right]. \quad (6.1.24)$$

It is easy to see how this generalizes to cases with more bulk-to-bulk propagators attached.

When the disc operator acts on the energy-fixing kernel, it either vanishes or reproduce the energy-fixing kernel. It can also act on the amplitude like part, which will give us the imaginary part of the amplitude. We know in amplitudes that the imaginary part of the amplitude is related to cutting internal lines [103]. As a result this may help us link between the optical theorem in amplitudes and COT.

As an example let us consider the tree level exchange diagram. Here the disc of the energy-fixing kernel

vanishes. We have (after restoring the coupling constant λ on each vertex):

$$\operatorname{Disc}_{\Omega_{p}} \psi_{2} = \frac{1}{2} \int_{-\infty}^{\infty} \frac{ds}{2\pi i} \frac{4s^{2}}{(\omega_{1}^{2} - s^{2} - i\epsilon)(\omega_{2}^{2} - s^{2} - i\epsilon)} \lambda^{2} (-2\pi i \delta(s^{2} - \Omega_{p}^{2} + i\epsilon))$$
(6.1.25)

We can use the delta function to do the integral, which gives:

$$\operatorname{Disc}_{\Omega_{p}} \psi_{2} = \frac{2\Omega_{p}\lambda^{2}}{(\omega_{1}^{2} - \Omega_{p}^{2})(\omega_{2}^{2} - \Omega_{p}^{2})} = \frac{\lambda^{2}}{2\Omega_{p}} \operatorname{Disc}_{\Omega_{p}} \left[\frac{1}{\omega_{1} + \Omega_{p} - i\epsilon} \right] \operatorname{Disc}_{\Omega_{p}} \left[\frac{1}{\omega_{2} + \Omega_{p} - i\epsilon} \right]. \tag{6.1.26}$$

Of course we recover the usual result from the COT. However, this may become helpful in establishing positivity bounds. For instance, since the imaginary part of the amplitude needs to have a positive residue by unitarity, we have λ^2 positive as well (i.e. λ is real). Therefore we already can establish that $\mathrm{Disc}\psi_2$ must be positive if $\omega_1 > \Omega_p$ and $\omega_2 > \Omega_p$, i.e. Disc of ψ_2 is positive in the physical regime.

For one loop diagrams there are a few complications: namely, the disc of the energy-fixing kernel may not vanish (for examples see Appendix E). But in some cases such as the two site loop (i.e. fig. 6.4) we can still write the disc of the wavefunction as the imaginary part of the amplitude integrated against the energy-fixing kernel. We leave a systematic study of unitarity and positivity bounds for the wavefunction at loop level for the future.

6.2 One loop wavefunction as amplitudes

This new representation of the wavefunction becomes a lot more useful when we start tackling loops. It is known that for tree level, the wavefunction has a total energy pole, and the residue gives the flat space amplitude [81, 114, 162, 163]. Using this new representation of the wavefunction, we can show that the wavefunction can be written as an amplitude divided by the total energy, plus some remainder terms which can be written down explicitly³. Since the wavefunction has a momentum integral, there are potentially UV divergences. We will see that the amplitude part of the wavefunction is the most UV divergent part, and every remainder term cannot contribute to UV divergences that are more severe than the amplitude.

6.2.1 Total energy pole

Let us first look at a heuristic argument on why the total energy pole gives the amplitude at one loop.



Figure 6.2: Diagram for an n site one loop wavefunction. External lines have been omitted.

³In [81] a similar representation was written down at tree level from the perspective of the cosmological polytope. One can then extend the representation to loop level by doing contour integrals over tree level wavefunctions. For our representation we make no explicit reference to tree level wavefunctions, however it would be interesting to see if similar relations exist in our representation as well.

An n site one loop wavefunction has the following form:

$$\psi_n = \frac{1}{2^n} \int \prod_{j=1}^n \frac{ds_j}{2\pi i} \tilde{D}_j \int_{\mathbf{p}} \prod_{l=1}^n \frac{1}{s_l^2 - \Omega_{p_l}^2}.$$
 (6.2.1)

Here \tilde{D}_j is given by:

$$\tilde{D}_{j} = \frac{1}{\omega_{i} + s_{i-1} + s_{i} - i\epsilon} - \frac{1}{\omega_{i} - s_{i-1} + s_{i} - i\epsilon} - \frac{1}{\omega_{i} + s_{i-1} - s_{i} - i\epsilon} + \frac{1}{\omega_{i} - s_{i-1} - s_{i} - i\epsilon}.$$
 (6.2.2)

(and I have set $s_0 = s_n$).

If we expand the product of \tilde{D}_j we find that the wavefunction has the form:

$$\psi_n = \frac{1}{2^n} \int \prod_{j=1}^n \frac{ds_j}{2\pi i} \frac{1}{\omega_j + s_j - s_{j-1} - i\epsilon} \int_{\mathbf{p}} \prod_{l=1}^n \frac{1}{s_l^2 - \Omega_{pl}^2} + (\text{Remainder})$$
 (6.2.3)

We will say more about the remainder terms below.

Now do the s_{n-1} contour integral. We close the contour in the lower half plane. This picks up the two poles $s_{n-1} = \omega_n + s_n$ and $s_{n-1} = \Omega_{p(n-1)}$ separately, and gives:

$$\psi_{n} = \frac{1}{2^{n}} \int \frac{ds_{n}}{2\pi i} \left[\prod_{j=1}^{n-2} \frac{ds_{j}}{2\pi i} \frac{1}{\omega_{j} + s_{j} - s_{j-1}} \right] \frac{1}{\omega_{n-1} + \omega_{n} + s_{n} - s_{n-2}} \int_{\mathbf{p}} \prod_{l=1}^{n-2} \frac{1}{s_{l}^{2} - \Omega_{pl}^{2}} \frac{1}{(s_{n} + \omega_{n})^{2} - \Omega_{p(n-1)}^{2}} \frac{1}{s_{n}^{2} - \Omega_{pn}^{2}} + \frac{1}{2^{n}} \int \frac{ds_{n}}{2\pi i} \left[\prod_{j=1}^{n-2} \frac{ds_{j}}{2\pi i} \frac{1}{\omega_{j} + s_{j} - s_{j-1}} \right] \int_{\mathbf{p}} \frac{1}{\omega_{n-1} + \Omega_{p(n-1)} - s_{n-2}} \frac{1}{\omega_{n} + s_{n} - \Omega_{p(n-1)}} \prod_{l=1}^{n-1} \frac{1}{2\Omega_{p(n-1)}} \frac{1}{s_{l}^{2} - \Omega_{pl}^{2}} + (\text{Remainder}). \quad (6.2.4)$$

We can then keep doing the contour integrals successively, i.e. do the s_{n-2} integral, then the s_{n-3} integral, and so on. Now notice the following:

- If we keep picking up the poles only from the kernel, i.e. from the $\omega_j + s_j s_{j-1}$, then we will get an overall $\omega_T = \sum_{j=1}^n \omega_j$ in front. This is because the set of $s_j s_{j-1}$ are not linearly independent: when we do the s_1 integral, we would get $s_1 = \sum_{j=2}^n \omega_j + s_n$, and substituting this into $\omega_1 + s_1 s_n$ gives the total energy pole.
- If we pick up any poles from the propagators, i.e. take $s_j = \Omega_{pj}$, then the Ω_{pj} enter into the kernel, and we would not get a total energy pole at the end.

Let's look at the total energy pole first. The total energy pole is:

$$\psi_n = \frac{1}{2^n} \frac{1}{\omega_T} \int \frac{ds_n}{2\pi i} \int_{\mathbf{p}} \prod_{l=1}^n \frac{1}{\tilde{s}_l^2 - p_n^2 - m^2} + \dots$$
 (6.2.5)

Here $\tilde{s}_l = s_n + \sum_{j=l+1}^n \omega_j$. This is just integrand for an amplitude: energy at each vertex is conserved (see the diagram 6.3), and we obtain the $\int d^{d+1}p$ integral measure for the amplitude by setting $s_n = p_0$. Also worth noting is that the whole integral scales as p^{D+1-2n} in D-dimensions.

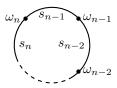


Figure 6.3: n site one loop diagram. Consider energy flowing clockwise, and let ω_l be energy entering the loop for vertex l. Clearly energy is conserved at each vertex if $s_{n-1} = \omega_n + s_n$, $s_{n-2} = \omega_{n-1} + \omega_n + s_n$, and so on.

What about the other poles? As an example let us consider the second line of (6.2.4). If we do the other integrals and take the poles from the kernel this gives⁴:

$$\int_{\mathbf{p}} \frac{1}{2\Omega_{p(n-1)}(\omega_T - \omega_{n-1} - \Omega_{p(n-1)})} \prod_{l=1}^{n-1} \frac{1}{s_l^2 - \Omega_{pl}^2}$$
(6.2.6)

This integral scales as p^{D-2n} in *D*-dimensions. It is less divergent than the total energy pole. A similar story applies to any other terms which we pick up a pole from the propagators.

The "remainder" terms Let's talk about the remainder terms in (6.2.4). In general, each term looks like:

$$\int \prod_{j=1}^{n} \frac{ds_{j}}{2\pi i} \frac{1}{\omega_{j} \pm s_{j} \pm s_{j-1} - i\epsilon} \int_{\mathbf{p}} \prod_{l=1}^{n} \frac{1}{s_{l}^{2} - \Omega_{pl}^{2}}$$
(6.2.7)

- If the set of $\pm s_j \pm s_{j-1}$ in the kernel of the term are linearly independent, then one can always do all the s integrals without picking up any poles from the propagator. In this case we would not get a total energy pole, and the resulting momentum integral scales like p^{D-2n} .
- Whenever we pick up poles from the propagator we get a momentum integral which scales like p^{D-2n} , for reasons explained above.

As a result the remainder terms can never lead to UV divergences that are more severe than the total energy pole. For instance, in D=3 and n=2, we expect that only the total energy pole has a UV divergence, while the remainder terms are all finite. We will confirm this soon.

6.2.2 Example: two site loop

Let us look at the simple example of a two site loop. Here we will write down the wavefunction in terms of the amplitude \mathcal{A}_2 , as well as ψ_2^{sub} , a collection of terms which are subleading as $\omega_T \to 0$ and are less UV divergent than the amplitude.

The wavefunction is:

$$\psi_2 = \frac{1}{4} \int \frac{ds_1}{2\pi i} \frac{ds_2}{2\pi i} \tilde{D}_1 \tilde{D}_2 \int_{\mathbf{p}} \frac{1}{s_1^2 - \Omega_{p1}^2} \frac{1}{s_2^2 - \Omega_{p2}^2}, \tag{6.2.8}$$

where \tilde{D}_1 is given by:

$$\tilde{D}_1 = \frac{1}{\omega_1 + s_1 + s_2 - i\epsilon} - \frac{1}{\omega_1 - s_1 + s_2 - i\epsilon} - \frac{1}{\omega_1 + s_1 - s_2 - i\epsilon} + \frac{1}{\omega_1 - s_1 - s_2 - i\epsilon}, \tag{6.2.9}$$

⁴One needs to be careful about the $i\epsilon$ prescription here: For example, take $s=p-i\epsilon_p$, I may get terms like $\omega_j+s_j-p+i\epsilon_p-i\epsilon_j$. Depending on the size of ϵ_p and ϵ_j this pole may not be picked up.

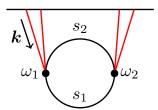


Figure 6.4: Two site one loop diagram

and \tilde{D}_2 is obtained simply by replacing ω_1 with ω_2 . We can simplify this expression⁵ to obtain:

$$\psi_{2} = \int \frac{ds_{1}}{2\pi i} \frac{ds_{2}}{2\pi i} \frac{1}{\omega_{1} + s_{1} + s_{2} - i\epsilon_{1}} \left[\frac{1}{\omega_{2} + s_{1} + s_{2} - i\epsilon_{2}} - \frac{1}{\omega_{2} - s_{1} + s_{2} - i\epsilon_{2}} - \frac{1}{\omega_{2} - s_{1} + s_{2} - i\epsilon_{2}} - \frac{1}{\omega_{2} + s_{1} - s_{2} - i\epsilon_{2}} + \frac{1}{\omega_{2} - s_{1} - s_{2} - i\epsilon_{2}} \right] \int_{\mathbf{p}} \frac{1}{s_{1}^{2} - \Omega_{p1}^{2} + i\epsilon_{p1}} \frac{1}{s_{2}^{2} - \Omega_{p2}^{2} + i\epsilon_{p2}}. \quad (6.2.10)$$

To simplify the wavefunction, do the s_2 integral first, where the contour is closed in the lower half plane⁶. The total energy pole comes from the fourth term in the bracket in (6.2.10), which integrates to:

$$\psi_2 = \int \frac{ds_1}{2\pi i} \int_{\mathbf{p}} \frac{-1}{\omega_T} \frac{1}{(s_1^2 - \Omega_{p1}^2)((\omega_2 - s_1)^2 - \Omega_{p2}^2)} + \frac{1}{(\omega_1 + s_1 + p_2)(\omega_2 - s_1 - p_2)} \frac{1}{2\Omega_{p2}(s_1^2 - \Omega_{p1}^2)} + \dots$$
(6.2.11)

Relabelling s_1 as p_0 , we have:

$$\psi_2 = \frac{i}{\omega_T} \int \frac{d^{D+1}p}{(2\pi)^{D+1}} \frac{1}{(p_0^2 - |\mathbf{p}|^2 - m^2)((\omega_2 - p_0)^2 - |\mathbf{k} - \mathbf{p}|^2 - m^2)} + \psi_2^{\text{sub}}$$
(6.2.12)

The integrand is exactly the amplitude, where the external four momentum entering the loop is (ω_2, \mathbf{k}) . However since the result should be symmetric with respect to exchange of ω_1 and ω_2 , we symmetrize the result to obtain:

$$\psi_2 = \frac{1}{2\omega_T} \left(\mathcal{A}(-\omega_1^2 + |\mathbf{k}|^2) + \mathcal{A}(-\omega_2^2 + |\mathbf{k}|^2) \right) + \psi_2^{\text{sub}}, \tag{6.2.13}$$

where

$$\mathcal{A}(-\omega^2 + |\mathbf{k}|^2) = i \int \frac{d^{d+1}p}{(2\pi)^{d+1}} \frac{1}{(p_0^2 - |\mathbf{p}|^2 - m^2)((\omega - p_0)^2 - |\mathbf{k} - \mathbf{p}|^2 - m^2)}$$
(6.2.14)

Subleading terms In this simple case we can write down ψ_2^{sub} explicitly. It is given by:

$$\psi_2^{\text{sub}} = \psi_2^{\text{FF}} + \psi_2^{\text{FB}} + \psi_2^{\text{BB}}, \tag{6.2.15}$$

$$\psi_2^{\text{FF}} = \int \frac{ds_1}{2\pi i} \int_{\mathbf{p}} \frac{1}{(\omega_1 + s_1 + \Omega_{p2})(\omega_2 - s_1 - \Omega_{p2})} \frac{1}{2\Omega_{p2}(s_1^2 - \Omega_{p1}^2)}, \tag{6.2.16}$$

$$\psi_2^{\text{FB}} = -\int \frac{ds_1}{2\pi i} \int_{\mathbf{p}} \frac{1}{(\omega_1 + s_1 + \Omega_{p2})(\omega_2 - s_1 + \Omega_{p2})} \frac{1}{2\Omega_{p2}(s_1^2 - \Omega_{p1}^2)} - (\Omega_{p1} \leftrightarrow \Omega_{p2}), \tag{6.2.17}$$

$$\psi_2^{\text{BB}} = \int_{\mathbf{p}} \frac{1}{(\omega_1 + \Omega_{p1} + \Omega_{p2})(\omega_2 + \Omega_{p1} + \Omega_{p2})}.$$
 (6.2.18)

⁵Or just use the expression (6.1.3) and do the time integral

 $^{^6}$ I will also take $\epsilon_2 < \epsilon_{p2}$

There is a way to understand why the remaining terms are organised in this way. Notice that:

$$G(\mathbf{p}, t_1, t_2) = \int_{-\infty}^{\infty} \frac{ds}{2\pi i} \frac{e^{is(t_1 + t_2)} - e^{is(t_1 - t_2)}}{s^2 - \Omega_p^2 + i\epsilon} = G_F(\mathbf{p}, t_1, t_2) - G_B(\mathbf{p}, t_1, t_2), \tag{6.2.19}$$

where $G_F(\mathbf{p}, t_1, t_2)$ is the Feynman propagator and $G_B(\mathbf{p}, t_1, t_2)$ is the boundary term added. Therefore, we can always organise ψ_2 as:

$$\psi_2 = \int dt_1 \int dt_2 \int_{\mathbf{p}} e^{i\omega_1 t_1} e^{i\omega_2 t_2} \left(G_F(p_1) G_F(p_2) - G_F(p_1) G_B(p_2) - G_B(p_1) G_F(p_2) + G_B(p_1) G_B(p_2) \right). \tag{6.2.20}$$

Now it is clear why we can separate the terms as written above:

- The total energy pole, i.e. A/ω_T , always comes from the G_FG_F term, since the amplitude is computed with Feynman propagators in the first place. However, we get extra terms that are encapsulated in ψ_2^{FF} , coming from picking up the pole in the propagator in the s_2 integral. This reflects the fact that we are not integrating time from $-\infty$ to ∞ , and so there are extra terms to compensate.
- The ψ_2^{BB} term comes from the G_BG_B term. No nested time integrals are required to evaluate this term, hence its form is simpler than the other remainder term.
- The ψ_2^{FB} term comes from the G_BG_F term, i.e. we are mixing contributions from the Feynman propagator and the boundary term. In this simple case ψ_2^{FB} can actually be further simplified to be:

$$\psi_{2}^{\text{FB}} = -\int_{\mathbf{p}} \frac{1}{4\Omega_{p1}\Omega_{p2}} \left[\frac{1}{(\omega_{1} + \Omega_{p1} + \Omega_{p2})(\omega_{1} + \omega_{2} + 2\Omega_{p1})} + \frac{1}{(\omega_{2} + \Omega_{p1} + \Omega_{p2})(\omega_{1} + \omega_{2} + 2\Omega_{p1})} + \frac{1}{(\omega_{1} + \Omega_{p1} + \Omega_{p2})(\omega_{1} + \omega_{2} + 2\Omega_{p2})} + \frac{1}{(\omega_{2} + \Omega_{p1} + \Omega_{p2})(\omega_{1} + \omega_{2} + 2\Omega_{p2})} \right]. \quad (6.2.21)$$

As we will see in the next section, these terms will give rise to singularities that are not present in amplitudes.

6.2.3 Example: three site loop

Let us move on to the example of a three site loop.

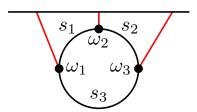


Figure 6.5: The three site one loop graph.

The wavefunction is:

$$\psi_3 = \frac{1}{8} \int \frac{ds_1}{2\pi i} \frac{ds_2}{2\pi i} \frac{ds_3}{2\pi i} \tilde{D}_1 \tilde{D}_2 \tilde{D}_3 \int_{\mathbf{p}} \frac{1}{s_1^2 - \Omega_{p1}^2} \frac{1}{s_2^2 - \Omega_{p2}^2} \frac{1}{s_3^2 - \Omega_{p3}^2}.$$
 (6.2.22)

Here we have:

$$\tilde{D}_{i} = \frac{1}{\omega_{i} + s_{i} + s_{i-1} - i\epsilon} - \frac{1}{\omega_{i} - s_{i} + s_{i-1} - i\epsilon} - \frac{1}{\omega_{i} + s_{i} - s_{i-1} - i\epsilon} + \frac{1}{\omega_{i} - s_{i} - s_{i-1} - i\epsilon}, \quad (6.2.23)$$

and $s_0 = s_3$. Once again we can simplify this to (suppressing the $i\epsilon$ in the denominator of the kernel):

$$\psi_{3} = \int \frac{ds_{1}}{2\pi i} \frac{ds_{2}}{2\pi i} \frac{ds_{3}}{2\pi i} \left(\frac{1}{k_{1} + s_{1} - s_{3}} - \frac{1}{k_{1} + s_{1} + s_{3}} \right) \left(\frac{1}{k_{2} + s_{2} - s_{1}} - \frac{1}{k_{2} + s_{2} + s_{1}} \right) \left(\frac{1}{k_{3} + s_{3} - s_{2}} - \frac{1}{k_{3} + s_{3} + s_{2}} \right) \int_{\mathbf{p}} \frac{1}{s_{1}^{2} - \Omega_{p1}^{2}} \frac{1}{s_{2}^{2} - \Omega_{p2}^{2}} \frac{1}{s_{3}^{2} - \Omega_{p3}^{2}}. \quad (6.2.24)$$

Taking into account that only poles in the lower half s planes are picked up, we find that the term which contributes to the amplitude is:

$$\psi_3 = \int \frac{ds_1}{2\pi i} \frac{ds_2}{2\pi i} \frac{ds_3}{2\pi i} \frac{1}{k_1 + s_1 - s_3} \frac{1}{k_2 + s_2 - s_1} \frac{1}{k_3 + s_3 - s_2} \int_{\mathbf{p}} \frac{1}{s_1^2 - \Omega_{p1}^2} \frac{1}{s_2^2 - \Omega_{p2}^2} \frac{1}{s_3^2 - \Omega_{p3}^2} + \dots$$
 (6.2.25)

Performing the s_1 and s_2 integrals give:

$$\psi_3 = \int \frac{ds_3}{2\pi i} \int_{\mathbf{p}} \frac{1}{\omega_T} \frac{1}{(\omega_2 + \omega_3 + s_3)^2 - \Omega_{p_1}^2} \frac{1}{(\omega_3 + s_3)^2 - \Omega_{p_2}^2} \frac{1}{s_3^2 - \Omega_{p_3}^2} + \psi_3^{\text{sub}}$$
(6.2.26)

Once again the integral here is simply the integral for the amplitude once we replace $s_3 \to p_0$. Therefore we have:

$$\psi_3 = \frac{1}{\omega_T} \mathcal{A}(-\omega_2^2 + k_2^2, -\omega_3^2 + k_3^2) + \psi_3^{\text{sub}}.$$
 (6.2.27)

Similar to the two site case, we can organise the remainder terms as:

$$\psi_3^{\text{sub}} = \psi_3^{\text{FFF}} + \psi_3^{\text{FFB}} + \psi_3^{\text{FBB}} + \psi_3^{\text{BBB}}. \tag{6.2.28}$$

Writing out the remainder terms explicitly:

$$\psi_{3}^{\text{FFF}} = \int \frac{ds_{3}}{2\pi i} \int_{\mathbf{p}} \frac{1}{2\Omega_{p2}} \frac{1}{\omega_{1} + \omega_{2} + \Omega_{p2} - s_{3}} \frac{1}{\omega_{3} - \Omega_{p2} + s_{3}} \frac{1}{s_{3}^{2} - \Omega_{p3}^{2}} + \frac{1}{2\Omega_{p1}} \frac{1}{\omega_{2} + \omega_{3} - \Omega_{p1} + s_{3}} \frac{1}{\omega_{1} + \Omega_{p1} - s_{3}} \frac{1}{(\omega_{3} + s_{3})^{2} - \Omega_{p2}^{2}} \frac{1}{s_{3}^{2} - \Omega_{p3}^{2}} + \frac{1}{4\Omega_{p1}\Omega_{p2}} \frac{1}{\omega_{2} - \Omega_{p1} + \Omega_{p2}} \frac{1}{\omega_{1} + \Omega_{p1} - s_{3}} \frac{1}{\omega_{3} - \Omega_{p2} + s_{3}} \frac{1}{s_{3} - \Omega_{p3}^{2}}. \quad (6.2.29)$$

$$\psi_{3}^{\text{FFB}} = \int \frac{ds_{2}}{2\pi i} \frac{ds_{3}}{2\pi i} \int_{\mathbf{p}} \frac{1}{\omega_{2} + \Omega_{p1} + s_{2}} \frac{1}{\omega_{1} + \Omega_{p1} - s_{3}} \frac{1}{\omega_{3} - s_{2} + s_{3}} \frac{1}{2\Omega_{p1}} \frac{1}{s_{2}^{2} - \Omega_{p2}^{2}} \frac{1}{s_{3}^{2} - \Omega_{p3}^{2}} + \text{(permutations)},$$

$$(6.2.30)$$

$$\psi_{3}^{\text{FBB}} = \int \frac{ds_{2}}{2\pi i} \int_{\mathbf{p}} \frac{1}{\omega_{2} + \Omega_{p1} + \Omega_{p2}} \frac{1}{\omega_{1} + \Omega_{p1} - s_{3}} \frac{1}{\omega_{3} - \Omega_{p2} + s_{3}} \frac{1}{2\Omega_{p1}} \frac{1}{2\Omega_{p2}} \frac{1}{s_{3}^{2} - \Omega_{p3}^{2}} + (\text{permutations}),$$
(6.2.31)

$$\psi_3^{\text{FFF}} = \int_{\mathbf{p}} \frac{1}{\omega_2 + \Omega_{p1} + \Omega_{p2}} \frac{1}{\omega_1 + \Omega_{p1} - \Omega_{p3}} \frac{1}{\omega_3 - \Omega_{p2} + \Omega_{p3}} \frac{1}{2\Omega_{p1}} \frac{1}{2\Omega_{p2}} \frac{1}{2\Omega_{p3}} + \text{(permutations)}. \quad (6.2.32)$$

The momentum integral for the amplitude scales as p^{-2} while the remainder terms all scale as p^{-3} for D=3.

Summary Let us summarize our observations so far.

• The one loop n site wavefunction can be written as:

$$\psi_n = \frac{\mathcal{A}_n}{\omega_T} + \psi_n^{\text{sub}}.\tag{6.2.33}$$

Here A_n is the one loop n site amplitude.

• The remaining parts of the wavefunction, $\psi_n^{\rm sub}$, are subleading as $\omega_T \to 0$ and are less UV divergent than the amplitude part of the wavefunction.

Beyond one loop

Our current results hold for one loop diagram. However, we can show that (6.2.33) also works for a simple two loop example. Consider the two site two loop diagram:

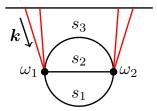


Figure 6.6: Two site two loop diagram

The wavefunction is:

$$\psi_2 = \frac{1}{8} \int \frac{ds_1}{2\pi i} \frac{ds_2}{2\pi i} \frac{ds_3}{2\pi i} \tilde{D}_1 \tilde{D}_2 \int_{\mathbf{p}_1, \mathbf{p}_2} \frac{1}{s_1^2 - \Omega_{p_1}^2} \frac{1}{s_2^2 - \Omega_{p_2}^2} \frac{1}{s_3^2 - \Omega_{p_3}^2}.$$
 (6.2.34)

Here $\mathbf{p}_3 = \mathbf{k} - \mathbf{p}_1 - \mathbf{p}_2$, and

$$\tilde{D}_{a} = \frac{1}{\omega_{a} + s_{1} + s_{2} + s_{3} - i\epsilon} - \frac{1}{\omega_{a} - s_{1} + s_{2} + s_{3} - i\epsilon} - \frac{1}{\omega_{a} + s_{1} - s_{2} - s_{3} - i\epsilon} + \frac{1}{\omega_{a} - s_{1} - s_{2} + s_{3} - i\epsilon} - \frac{1}{\omega_{a} + s_{1} + s_{2} - s_{3} - i\epsilon} - \frac{1}{\omega_{a} - s_{1} - s_{2} - s_{3} - i\epsilon}.$$

$$(6.2.35)$$

Here a = 1, 2. We can simplify the expression to obtain:

$$\psi_2 = \int \frac{ds_1}{2\pi i} \frac{ds_2}{2\pi i} \frac{ds_3}{2\pi i} \frac{1}{\omega_1 + s_1 + s_2 + s_3 - i\epsilon} \tilde{D}_2 \int_{\mathbf{p}_1, \mathbf{p}_2} \frac{1}{s_1^2 - \Omega_{p1}^2} \frac{1}{s_2^2 - \Omega_{p2}^2} \frac{1}{s_3^2 - \Omega_{p3}^2}.$$
 (6.2.36)

Let us do the s_3 integral first. The total energy pole comes from the last term in (6.2.35), which integrates to:

$$\psi_2 = \int \frac{ds_1}{2\pi i} \frac{ds_2}{2\pi i} \frac{1}{\omega_T} \int_{\mathbf{p}_1, \mathbf{p}_2} \frac{1}{s_1^2 - \Omega_{p_1}^2} \frac{1}{s_2^2 - \Omega_{p_2}^2} \frac{1}{(\omega_2 - s_1 - s_2)^2 - \Omega_{p_3}^2} + \dots$$
 (6.2.37)

This is simply the integral for the two loop amplitude, with internal four momentum $p_1 = (s_1, \mathbf{p}_1)$ and $p_2 = (s_2, \mathbf{p}_2)$.

It is not hard to see that the remainder terms are less UV divergent. For example, the second last term in (6.2.35) integrates to:

$$\int \frac{ds_1}{2\pi i} \frac{ds_2}{2\pi i} \frac{-1}{\omega_T + 2s_1} \int_{\mathbf{p}_1, \mathbf{p}_2} \frac{1}{s_1^2 - \Omega_{p1}^2} \frac{1}{s_2^2 - \Omega_{p2}^2} \frac{1}{(\omega_2 + s_1 - s_2)^2 - \Omega_{p3}^2}$$
(6.2.38)

It is straightforward to see that after doing another contour integration, this integral is less divergent than the amplitude term.

We will leave a careful proof for (6.2.33) for for diagrams with any topology at arbitrary loop order to the future.

6.3 Landau analysis: second attempt

With the amplitude representation of the wavefunction in hand, we can now say more about the analytic structure of the wavefunction. Once again we make use of Landau analysis to write down the singularities of the wavefunction. In particular we have shown that the one loop wavefunction can be divided into a total energy pole, whose residue is the amplitude, and as a remainder part. Therefore, we have the following result:

- A subset of the singularities of the one loop wavefunction can be mapped to singularities of an amplitude. In fact, we will see that these singularities have the same interpretation as the corresponding singularities in amplitudes: namely, they correspond to cutting the same internal lines of a Feynman diagram and sending them "on-shell", i.e. demanding the corresponding propagator to diverge. We shall call these singularities "amplitude-type singularity"
- The remaining singularities have no analogue in amplitudes, and we shall call them "wavefunctiontype singularities". Interestingly, in the one loop wavefunction, they correspond to cutting a single internal line (which gives no physical singularities for amplitudes).

6.3.1 General strategy

Let us write down the wavefunction in the following form:

$$\psi_n = \int \left[\prod_i \frac{ds_i}{2\pi i} \right] \frac{R(\{\omega\}, \{s\})}{D_K(\{\omega\}, \{s\})} \int \prod_l \frac{d^D p_l}{(2\pi)^D} \frac{1}{D_A(\{\mathbf{p}\}, \{s\})}.$$
 (6.3.1)

This is merely a rewriting of (6.1.10). To make it more clear, we have:

$$\frac{R(\{\omega\}, \{s\})}{D_K(\{\omega\}, \{s\})} = \prod_a \tilde{D}_a. \tag{6.3.2}$$

The main difference here is that on the left hand side we have gathered all the factors in the same denominator. More explicitly,

$$D_K = \prod_{a} \prod_{\sigma_j = \pm} \left(\omega_a^2 - \left(s_1 + \sum_{j=2}^m \sigma_j s_j \right)^2 - i\epsilon \right), \tag{6.3.3}$$

and R is a polynomial in s and ω . D_A is simply the following product:

$$D_A = \prod_i (s_i^2 - \Omega_{pi}^2 + i\epsilon). \tag{6.3.4}$$

As an example, for a bubble diagram, we can start from (6.1.9) and obtain:

$$\tilde{D}_1 \tilde{D}_2 = \frac{16s_1^2 s_2^2 \omega_1 \omega_2}{(\omega_1^2 - (s_1 + s_2)^2 - i\epsilon)(\omega_1^2 - (s_1 - s_2)^2 - i\epsilon)(\omega_2^2 - (s_1 + s_2)^2 - i\epsilon)(\omega_2^2 - (s_1 - s_2)^2 - i\epsilon)}. \quad (6.3.5)$$

Here D_K has the form (6.3.3), and $R = 16s_1^2s_2^2\omega_1\omega_2$.

We can introduce a Feynman parameter λ and write:

$$\psi_n = \int_0^\infty d\lambda \int \left[\prod_i \frac{ds_i}{2\pi i} \right] \int \prod_l \frac{d^D p_l}{(2\pi)^D} \frac{R(\{\omega\}, \{s\})}{D(\{\mathbf{p}\}, \{\omega\}, \{s\})}, \tag{6.3.6}$$

$$D(\{\mathbf{p}\}, \{\omega\}, \{s\}) = D_K(\{\omega\}, \{s\}) + \lambda D_A(\{\mathbf{p}\}, \{s\}).$$
(6.3.7)

Let us write down the Landau equations. We have:

$$D = 0 \to D_K + \lambda D_A = 0, \tag{6.3.8}$$

$$\frac{\partial D}{\partial \lambda} = 0 \to D_A = 0. \tag{6.3.9}$$

Let's interpret these two equations before writing down the rest. Since D_A is just a product of internal propagators, demanding $D_A = 0$ means sending a subset of propagators on shell (graphically this is simply cutting internal lines). At least one of the internal lines must be cut if we want a physical singularity. In addition, combining these two equations gives us $D_K = 0$. From (6.3.3) we can see that this fixes the internal energies s of the propagators in terms of external energies s.

Let us write down the remaining equations. They are:

$$\frac{\partial D}{\partial s_i} = 0 \to \frac{\partial D_K}{\partial s_i} + \lambda \frac{\partial D_A}{\partial s_i} = 0 \text{ (for all } s_i), \tag{6.3.10}$$

$$\frac{\partial D}{\partial \mathbf{p}_l} = 0 \to \lambda \frac{\partial D_A}{\partial \mathbf{p}_l} = 0. \tag{6.3.11}$$

The second equation, together with $D_A = 0$, give us a modified version of the Landau equation for ampli-

tudes. To see this, start with (6.3.1), then introduce Feynman parameters α_{pi} for D_A before introducing the extra Feynman parameter λ . Then we get the following Landau equations involving D_A :

$$|\mathbf{p}_i|^2 = s_i^2 - m_i^2, \tag{6.3.12}$$

$$\sum_{i \in I} \alpha_{pi} \mathbf{p}_i = 0. \tag{6.3.13}$$

These are simply Landau equations for the amplitude with the same Feynman diagram, except we have modified m_i^2 to $s_i^2 - m_i^2$. Of course, we still need to solve $\frac{\partial D}{\partial s_i}$ to fix s_i , but often we will find that knowing the solutions for the Landau equations in amplitudes will give us shortcuts to solving the Landau equations for the wavefunction.

In fact, we could even carry out the momentum integral first before writing down the Landau equation. This gives:

$$D_A = \frac{\partial D_A}{\partial \alpha_{pi}} = 0. {(6.3.14)}$$

Counting number of constraints Before moving on to concrete examples, let us first ask an important question: are the Landau equations sufficient to fix the singularities?

In general, we have I+L+1 integration variables which require fixing, (I is the total number of internal lines, and L is the total number of loops). We have I+L+2 Landau equations, so there are enough equations to fix all the integration variables, and we can always write down the singularities in terms of external kinematics. However, if we want to write down the singularity for one of the external energies ω_1 , quite often we will need to write it in terms of other external off-shell energies (say ω_2) as well. This creates an obstacle when we study the singularities: for instance, suppose a singularity surface $\omega_1 = -\omega_2$, naively we would assume that ω_2 can take on any real negative value. However, once this energy is on-shell (say $\omega_2 = \sqrt{k^2 + 4m^2}$), we realise that $\omega_1 < -2m$. This is an example where information is lost when the other external energies are off-shell. Another example would be the anomalous threshold of the three site one loop diagram, where the singularity condition is expressed purely in terms of the mass of internal and external particles (see (6.3.65)). Without putting external energies on-shell, it would be hard to recognise the anomalous threshold since off-shell external energies have no explicit dependence on mass.

It is often helpful to supply additional information on these external energies. For example, we can put some of the external energies on-shell. We will see an example of this when we tackle the three site one loop diagram.

6.3.2 Example: two site loop

Let's start with the two site loop (fig 6.4). For simplicity we will always consider the internal lines to have the same mass m.

Before we carry out Landau analysis, let us set our expectations for the result. We know that the recursion expression for the wavefunction is given by [80]:

$$\psi_2 = \frac{1}{\omega_T} \int_{\mathbf{p}} \frac{1}{(\omega_1 + \Omega_{p1} + \Omega_{p2})(\omega_2 + \Omega_{p1} + \Omega_{p2})} \left[\frac{1}{\omega_1 + \omega_2 + 2\Omega_{p1}} + \frac{1}{\omega_1 + \omega_2 + 2\Omega_{p2}} \right]. \tag{6.3.15}$$

In the previous section we found the following singularities:

- $\omega_1 = -\sqrt{k^2 + 4m^2}$. We will see that this corresponds to an amplitude-type singularity.
- $\omega_1 = -\omega_2 2m$. We will see that this corresponds to a wavefunction-type singularity.

Let us write down the expression for the wavefunction coefficient of the two site loop again:

$$\psi_2 = \int \frac{ds_1}{2\pi i} \int \frac{ds_2}{2\pi i} \frac{16s_1^2 s_2^2 \omega_1 \omega_2}{S_{1+} S_{1-} S_{2+} S_{2-}} \int_{\mathbf{p}} \frac{1}{(s_1^2 - \Omega_{p_1}^2 + i\epsilon)(s_2^2 - \Omega_{p_2}^2 + i\epsilon)}$$
(6.3.16)

$$S_{1\pm} = \omega_1^2 - (s_1 \pm s_2)^2 - i\epsilon, \tag{6.3.17}$$

$$S_{2\pm} = \omega_2^2 - (s_1 \pm s_2)^2 - i\epsilon. \tag{6.3.18}$$

The convention for the internal momenta is $\mathbf{p}_1 + \mathbf{p}_2 = -\mathbf{k}$. To simplify our results:

- We will not look at cases where we have $S_{1+} = 0$ and $S_{1-} = 0$ simultaneously. This is because they both come from the sum in \tilde{D}_1 (see (6.2.9)). We only need to send an individual term in the sum to infinity, which corresponds to sending one of S_{1+} or S_{1-} to infinity (and also picking a sign, for example picking $\omega_1 = -s_1 + s_2$ instead of $\omega_1 = s_1 + s_2$).
- We will also impose $\omega_2 > 0$, this will restrict the singularities for ω_1 to be on the negative real axis.

We will look at the case where $S_{1+} = 0$, and potentially $S_{2-} = 0$. The case where we have $S_{1-} = 0$ (and $S_{2+} = 0$) are easily generalisations.

Let us introduce Feynman parameters for both D_K and D_A . The integral now has the following form:

$$\psi_{2} = \int \frac{ds_{1}}{2\pi i} \int \frac{ds_{2}}{2\pi i} \frac{16s_{1}^{2}s_{2}^{2}\omega_{1}\omega_{2}}{S_{1_{-}}S_{2_{+}}} \int_{0}^{1} d\alpha_{1_{+}} \int_{0}^{1} d\alpha_{2_{-}} \int_{0}^{1} d\alpha_{p_{1}} \int_{0}^{1} d\alpha_{p_{2}} \times \int_{\mathbf{p}} \frac{\delta(1 - \alpha_{1_{+}} - \alpha_{2_{-}})\delta(1 - \alpha_{p_{1}} - \alpha_{p_{2}})}{(\alpha_{1_{+}}(\omega_{1}^{2} - (s_{1} + s_{2})^{2}) + \alpha_{2_{-}}(\omega_{2}^{2} - (s_{1} - s_{2})^{2}))^{2}(\alpha_{p_{1}}(s_{1}^{2} - \Omega_{p_{1}}^{2}) + \alpha_{p_{2}}(s_{2}^{2} - \Omega_{p_{2}}^{2}))^{2}}.$$
(6.3.19)

We did not introduce Feynman parameters for S_{1-} and S_{2+} since we will never send them to zero. Just like Landau equations for amplitudes, we can do the momentum integral first. This will allow us to write down Landau equations in terms of Feynman parameters α , λ , and the internal energies s. This gives an equation of the form (6.3.1), with

$$D_A = \frac{\alpha_{p_1}\alpha_{p_2}}{\alpha_{p_1} + \alpha_{p_2}} k^2 - \alpha_{p_1}(s_1^2 - m^2) - \alpha_{p_2}(s_2^2 - m^2).$$
(6.3.20)

$$D_K = -\alpha_{1_+}(\omega_1^2 - (s_1 + s_2)^2) - \alpha_{2_-}(\omega_2^2 - (s_1 - s_2)^2).$$
(6.3.21)

Amplitude-type singularity As an example, let us solve the Landau equations with $S_{1_+}, S_{p_1}, S_{p_2} = 0$ (where $S_{p_i} = s_i^2 - \Omega_{p_i}^2$). Since both S_{p_1} and S_{p_2} are zero, we are cutting both propagators. Let's see if this singularity can be mapped to a singularity in amplitudes.

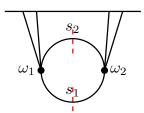


Figure 6.7: The amplitude-type singularity. The lines cut by the red dashed lines are the propagators which are on-shell.

The Landau equation reads:

$$\frac{\partial D}{\partial \alpha_{p_1}} = 0 \to \frac{\alpha_{p_2}^2}{(\alpha_{p_1} + \alpha_{p_2})^2} k^2 = s_1^2 - m^2, \tag{6.3.22}$$

$$\frac{\partial D}{\partial \alpha_{p_2}} = 0 \to \frac{\alpha_{p_1}^2}{(\alpha_{p_1} + \alpha_{p_2})^2} k^2 = s_2^2 - m^2, \tag{6.3.23}$$

$$\frac{\partial D}{\partial \alpha_{1+}} = 0 \to \omega_1^2 = (s_1 + s_2)^2, \tag{6.3.24}$$

$$\frac{\partial D}{\partial s_i} = 0 \to \lambda \alpha_{p_1} s_1 = \lambda \alpha_{p_2} s_2 = (s_1 + s_2). \tag{6.3.25}$$

Also, naturally we demand $\alpha_{p_1} + \alpha_{p_2} = 1$. Since $S_{2-} \neq 0$, α_{2-} must be zero and this naturally means $\alpha_{1+} = 1$.

The first two equations give:

$$\alpha_{p_2}^2(s_2^2 - m^2) = \alpha_{p_1}^2(s_1^2 - m^2). \tag{6.3.26}$$

Therefore, using the last Landau equation, we obtain:

$$\frac{s_1^2 - m^2}{s_2^2 - m^2} = \frac{s_1^2}{s_2^2}. (6.3.27)$$

The solution for this is $s_1 = \pm s_2$ unless $s_1 = \pm m$ or $s_2 = \pm m$. However, if we set $s_1 = \pm m$, the (6.3.22) equation implies that k = 0 or $\alpha_{p2} = 0$. But if $\alpha_{p2} = 0$ that would imply $s_1 = -s_2$. This would mean that if s_1 is in the lower half plane, s_2 is in the upper half plane, so either s_1 or s_2 are not in the physical integration region. Therefore we conclude that if $s_1 = \pm m$ we must have k = 0.

First consider $k \neq 0$. Both s_1 and s_2 must lie in the lower half complex plane. One can easily show that we have $s_1 = s_2$, so this gives us the singularity $\omega_1^2 = 4s_1^2$. It is also straightforward to see $\lambda = 4$. Using this, we get:

$$\frac{k^2}{4} = s_1^2 - m^2 (6.3.28)$$

This gives us the $\omega_1 = -\sqrt{k^2 + 4m^2}$ singularity.

For k=0 we can easily see that this implies $\omega_1=-2m$. But this is just a special case of $\omega_1=-\sqrt{k^2+4m^2}$, and so we landed on the same singularity.

How is this singularity connected to an amplitude singularity? We know that for the same diagram, an amplitude has the singularity $s=4m^2$ (here s is the Mandelstam variable). But $s=\omega_1^2-k^2$ (since ω_1 is the total energy entering the vertex and **k** is the total momentum entering the vertex), hence we have $\omega_1^2=k^2+4m^2$. Therefore this $\omega_1=-\sqrt{k^2+4m^2}$ singularity is simply the same singularity as $s=4m^2$,

written in terms of the off-shell energy variables.

Amplitude-type singularity for massless particles It is also helpful to look at singularities of massless internal particles. Let us solve the same Landau equations, but with m = 0. The Landau equation reads:

$$\frac{\partial D}{\partial \alpha_{p_1}} = 0 \to \frac{\alpha_{p_2}^2}{(\alpha_{p_1} + \alpha_{p_2})^2} k^2 = s_1^2 - m^2, \tag{6.3.29}$$

$$\frac{\partial D}{\partial \alpha_{p_2}} = 0 \to \frac{\alpha_{p_1}^2}{(\alpha_{p_1} + \alpha_{p_2})^2} k^2 = s_2^2 - m^2, \tag{6.3.30}$$

$$\frac{\partial D}{\partial \alpha_{1+}} = 0 \to \omega_1^2 = (s_1 + s_2)^2, \tag{6.3.31}$$

$$\frac{\partial \alpha_{1+}}{\partial s_i} = 0 \to \lambda \alpha_{p_1} s_1 = \lambda \alpha_{p_2} s_2 = (s_1 + s_2). \tag{6.3.32}$$

The solution for this is quite straightforward: the first two equations imply $\alpha_{p2}k = s_1$ and $\alpha_{p1}k = s_2$. From this we can easily conclude that $s_1 + s_2 = (\alpha_{p1} + \alpha_{p2})k = k$. Substituting this into (6.3.32) gives $\omega_1 = -k$, which is the massless version of the amplitude-type singularity we just found.

We can easily write down the solutions to the Feynman parameters and the internal energies. Just take:

$$s_1 = s_2 = \frac{k}{2},\tag{6.3.33}$$

$$\alpha_{p1} = \alpha_{p2} = \frac{1}{2},\tag{6.3.34}$$

$$\lambda = 4. \tag{6.3.35}$$

It is easy to show by substitution that this solves the Landau equations.

Wavefunction-type singularity Now let us consider the case where $S_{1+}, S_{2-}, S_{p2} = 0$, but we have $S_{p1} \neq 0$. Notice that only one internal line is cut here. For amplitude there is no singularity for cutting one internal line. However, for the wavefunction there is a singularity. In fact, for massless particles, it is a physical singularity for any external kinematics.

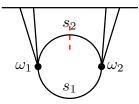


Figure 6.8: Wavefunction-type singularity. Only one propagator is on-shell

Let us write down the Landau equation. They are

$$\frac{\partial D}{\partial \alpha_{1+}} = 0 \to \omega_1^2 = (s_1 + s_2)^2, \tag{6.3.36}$$

$$\frac{\partial D}{\partial \alpha_2} = 0 \to \omega_2^2 = (s_1 - s_2)^2, \tag{6.3.37}$$

$$\frac{\partial D}{\partial \alpha_{p_2}} = 0 \to 0 = s_2^2 - m^2, \tag{6.3.38}$$

$$\frac{\partial D}{\partial s_1} = 0 \to 0 = \alpha_{1_+}(s_1 + s_2) + \alpha_{2_-}(s_1 - s_2), \tag{6.3.39}$$

$$\frac{\partial D}{\partial s_2} = 0 \to \lambda s_2 = \alpha_{1_+}(s_1 + s_2) - \alpha_{2_-}(s_1 - s_2) \tag{6.3.40}$$

The third equation gives us $s_2 = m$. We throw away $s_2 = -m$: if we restore the $i\epsilon$ in the solution, this is $s_1 = -m + i\epsilon$, and is not included in the integration region, i.e. the lower half complex plane.

In addition, we have:

$$\omega_1 + s_1 + s_2 = 0, (6.3.41)$$

$$\omega_2 - s_1 + s_2 = 0. ag{6.3.42}$$

Use this to eliminate s_1 , we obtain $\omega_1 + \omega_2 = -2m$. This singularity is a total energy singularity, and quite obviously have no analogue in amplitudes.

Is this singularity physical? Let us compute the Feynman parameters. We can show that:

$$\alpha_{2-} = -\frac{\omega_1}{2m}. (6.3.43)$$

But $\omega_2 = -\omega_1 - 2m \ge 0$, so we get $\alpha_{2-} \ge 1$. Therefore this singularity may not be visible for any general kinematics! Indeed this is consistent with the observation that this singularity is in fact invisible outside the soft limit (see the appendix of [2]). However it is not entirely clear how this emerges from the Landau analysis picture, and we will leave a detailed study of this for the future.

Wavefunction-type singularity for massless particles Things are more clear in the case of massless particles. The Landau equations read:

$$\frac{\partial D}{\partial \alpha_{1\perp}} = 0 \to \omega_1^2 = (s_1 + s_2)^2 \to \omega_1 + s_1 + s_2 = 0, \tag{6.3.44}$$

$$\frac{\partial D}{\partial \alpha_{2_{-}}} = 0 \to \omega_{2}^{2} = (s_{1} - s_{2})^{2} \to \omega_{2} - s_{1} + s_{2} = 0, \tag{6.3.45}$$

$$\frac{\partial D}{\partial \alpha_{p_2}} = 0 \to 0 = s_2^2, \tag{6.3.46}$$

$$\frac{\partial D}{\partial s_1} = 0 \to 0 = \alpha_{1_+}(s_1 + s_2) + \alpha_{2_-}(s_1 - s_2), \tag{6.3.47}$$

$$\frac{\partial D}{\partial s_2} = 0 \to \lambda s_2 = \alpha_{1_+}(s_1 + s_2) - \alpha_{2_-}(s_1 - s_2)$$
(6.3.48)

Immediately we have $s_2 = 0$, and we have $\omega_1 + \omega_2 = 0$. This is indeed the massless limit of the wavefunction-type singularity found above.

Unlike the massive case, this singularity is present for any external kinematics. Indeed, if we take $s_1 = 0$, we can easily see that the Landau equations can always be satisfied, with $\alpha_{1+}, \alpha_{2-} > 0$.

Where does the wavefunction-type singularity come from? Before we move on it is helpful to see how the wavefunction-type singularity emerges from the expression we have obtained, i.e. from (6.2.13). Now clearly the singularity cannot come from the amplitude part of the wavefunction, therefore it must be a singularity from the remainder terms.

Upon inspection, we find that the singularity actually emerges from ψ_2^{FB} , i.e. the mixing term between Feynman propagator and the boundary term. We have shown that this term can be written as (6.2.21). If we try to study the singularity associated with $\omega_1 + \omega_2 + 2\Omega_{p1} = 0$, we find the wavefunction-type singularity from above.

The terms ψ_2^{FF} and ψ_2^{BB} do not provide any contribution to the wavefunction-type singularity. Only the $\omega_1 = -\sqrt{k^2 + 4m^2}$ singularity is present for those terms if we study the analyticity of these terms individually.

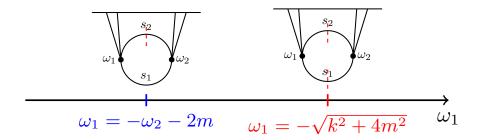


Figure 6.9: A summary of the singularities present for the two site one loop graph. The red singularity here is an amplitude-type singularity, while the blue singularity is a wavefunction-type singularity.

6.3.3 Example: three site loop

Let us now look at the one loop three site graph (fig 6.5). For amplitudes, this graph has two types of singularities. The first type is the normal threshold, where two internal lines are cut. This type of cut is associated with unitarity in the optical theorem. The second type is the anomalous threshold, where all three internal lines are cut.

Since we have shown that the wavefunction can be written in terms of amplitude plus remainder terms, we would expect singularities for the amplitude to be present in the wavefunction as well, including the anomalous threshold. We will see that it is indeed the case. In addition, we will find that there are wavefunction-type singularities again, where only a single internal line is cut.

For the one loop three site graph, the wavefunction coefficient can be written as:

$$\psi_3 = \int \frac{ds_1}{2\pi i} \int \frac{ds_2}{2\pi i} \int \frac{ds_3}{2\pi i} \frac{512\omega_1\omega_2\omega_3 s_1^2 s_2^2 s_3^2}{S_{1+}S_{1-}S_{2+}S_{2-}S_{3+}S_{3-}} \int_{\mathbf{p}} \frac{1}{(s_1^2 - \Omega_{p_1}^2)(s_2^2 - \Omega_{p_2}^2)(s_3^2 - \Omega_{p_3}^2)}.$$
 (6.3.49)

$$S_{1\pm} = \omega_1^2 - (s_1 \pm s_3)^2, \tag{6.3.50}$$

$$S_{2\pm} = \omega_2^2 - (s_1 \pm s_2)^2, \tag{6.3.51}$$

$$S_{3\pm} = \omega_3^2 - (s_2 \pm s_3)^2. \tag{6.3.52}$$

Also we have $\mathbf{p}_1 = \mathbf{p}, \ \mathbf{p}_2 = (\mathbf{p} + \mathbf{k}_2), \ \mathbf{p}_3 = (\mathbf{p} - \mathbf{k}_1) = (\mathbf{p} + \mathbf{k}_2 + \mathbf{k}_3).$

Let's write everything in terms of Feynman parameters and perform the p integral first. We obtain:

$$\psi_3 = \int_0^\infty d\lambda \int \prod_{i=1}^3 \frac{ds_i}{2\pi i} \int_0^1 \prod_{j=1\pm,2\pm,3\pm} d\alpha_j \int_0^1 \prod_{l=p_1,p_2,p_3} d\alpha_l \frac{F(\{\alpha\})\delta(1-\sum\alpha)}{D(\{\alpha\},s_1,s_2,s_3)^{9-d/2}},\tag{6.3.53}$$

where we have:

$$D_k = \frac{\alpha_{p_1} \alpha_{p_2} k_2^2 + \alpha_{p_2} \alpha_{p_3} k_3^2 + \alpha_{p_1} \alpha_{p_3} k_1^2}{\sum \alpha_{p_i}} - \sum_{i=1}^3 \alpha_{p_i} (s_i^2 - m^2), \tag{6.3.54}$$

as well as

$$D_A = -\sum_{i=1}^{3} \alpha_{i\pm} S_{i\pm}. \tag{6.3.55}$$

 $F(\alpha)$ is just polynomial in α , and its exact form will not be important for us.

Amplitude-type singularity: normal threshold Let us first study solutions corresponding to "normal thresholds". These are solutions where $S_{p_i} \neq 0$ for one p_i , and they can be used to recover certain energy conservation poles.

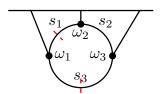


Figure 6.10: Amplitude-type singularity, with the internal line s_1 and s_3 being cut.

As an example let us consider setting $S_{p_2} \neq 0$, which requites $\alpha_{p_2} = 0$. In amplitude terms we are looking at a singularity which comes from cutting s_1 and s_3 in the figure. Then we have the following equations from D_1 :

$$\frac{\alpha_{p_3}^2 k_1^2}{(\alpha_{p_1} + \alpha_{p_3})^2} = s_1^2 - m^2, \tag{6.3.56}$$

$$\frac{\alpha_{p_1}^2 k_1^2}{(\alpha_{p_1} + \alpha_{p_3})^2} = s_3^2 - m^2 \tag{6.3.57}$$

At this point if we choose $S_{1+}=0$ we can pretty much repeat the analysis we did for the two site graph and obtain $\omega_1=-\sqrt{k_1^2+4m^2}$.

However, we can make a more interesting choice. Suppose we choose $S_{2_{-}} = S_{3_{+}} = 0$ instead. (I will

relate this to a singularity in ω_1 by permutation). Then we get the following equations from D_2 :

$$\lambda \alpha_{p_1} s_1 = \alpha_{2}(s_1 - s_2), \tag{6.3.58}$$

$$\lambda \alpha_{p_3} s_3 = \alpha_{3_+} (s_3 + s_2), \tag{6.3.59}$$

$$0 = -\alpha_{2-}(s_1 - s_2) + \alpha_{3+}(s_3 + s_2). \tag{6.3.60}$$

This can be rearranged into the following:

$$\frac{\alpha_{p_1} s_1}{\alpha_{p_3} s_3} = \frac{\alpha_{2_-} (s_1 - s_2)}{\alpha_{3_+} (s_3 + s_2)} = 1. \tag{6.3.61}$$

Combine this with the equations from D_1 , we get:

$$\frac{s_1^2}{s_3^2} = \frac{s_1^2 - m^2}{s_3^2 - m^2}. (6.3.62)$$

Then we can just following the derivation as in the two site graph to get:

$$\omega_2 = -\sqrt{\frac{k_1^2}{4} + m^2} + s_2,\tag{6.3.63}$$

$$\omega_3 = -\sqrt{\frac{k_1^2}{4} + m^2} - s_2. \tag{6.3.64}$$

This combines to give $\omega_2 + \omega_3 = -\sqrt{k_1^2 + 4m^2}$ singularity. This is related by permutation to $\omega_1 + \omega_2 = -\sqrt{k_3^2 + 4m^2}$ and $\omega_1 + \omega_3 = \sqrt{k_2^2 + 4m^2}$ singularity, both of which are energy conserving poles.

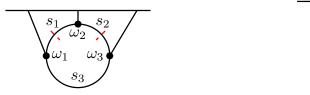


Figure 6.11: Two other singularities for the wavefunction which are also amplitude-type singularities. They are $\omega_1 + \omega_3 = \sqrt{k_2^2 + 4m^2}$ (for the left figure) and $\omega_1 + \omega_2 = -\sqrt{k_3^2 + 4m^2}$ (for the right figure)

Amplitude-type singularity: Anomalous threshold For amplitudes there is an anomalous threshold that corresponds to sending all three internal lines on-shell. The existence of this threshold depends on the external kinematics: namely, two of the external four momenta have to be equal. It is known that the threshold is only physical when the masses of the external particles satisfy $M^2 > 2m^2$ where m^2 is the mass of the internal particles [146,164–169]. This is lower than the expected two particle threshold $4m^2$, hence the name anomalous threshold. This threshold is given by:

$$s = 4m^2 - \frac{(M^2 - 2m^2)^2}{m^2},\tag{6.3.65}$$

where s is the four momentum for one of the external lines (in the diagram it would be the line attached to ω_1) vertex.

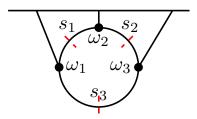


Figure 6.12: The anomalous amplitude-type singularity. To access this singularity we also need specific external kinematics, which are given by (6.3.66)-(6.3.70).

We would like to show that such a threshold exists for the wavefunctions as well. We expect that the singularity only appears for specifically chosen kinematics just like amplituides. To make life easier we will choose the the following kinematics:

$$\mathbf{k}_2 = -\mathbf{k}_3,\tag{6.3.66}$$

$$|\mathbf{k}| = k,\tag{6.3.67}$$

$$\mathbf{k}_1 = 0,$$
 (6.3.68)

$$\omega_2 = \omega_3 = \sqrt{k^2 + M^2},\tag{6.3.69}$$

$$\omega_1^2 = 4\omega_2^2. (6.3.70)$$

The last line enforces the total energy to be zero, and we know in this limit the wavefunction reduces to the amplitude, hence we should expect the anomalous threshold to show up.

Now let's specify which $S_{i\pm}$ we send to zero. We make the following choice:

$$S_{1+} = \omega_1^2 - (s_1 + s_3)^2 = 0, (6.3.71)$$

$$S_{2+} = \omega_2^2 - (s_1 + s_2)^2 = 0, (6.3.72)$$

$$S_{3+} = \omega_3^2 - (s_3 + s_2)^2 = 0. (6.3.73)$$

So now we have:

$$\omega_1 = s_1 + s_3, \tag{6.3.74}$$

$$\omega_2 = s_1 + s_2, \tag{6.3.75}$$

$$\omega_3 = s_3 + s_2. \tag{6.3.76}$$

as well as:

$$\alpha_{1+}(s_1+s_3) + \alpha_{2+}(s_1+s_2) = \lambda \alpha_{p1}s_1, \tag{6.3.77}$$

$$\alpha_{2_{+}}(s_1 + s_2) + \alpha_{3_{+}}(s_3 + s_2) = \lambda \alpha_{p_2} s_2, \tag{6.3.78}$$

$$\alpha_{3\perp}(s_3 + s_2) + \alpha_{1\perp}(s_1 + s_3) = \lambda \alpha_{p_3} s_3, \tag{6.3.79}$$

Also from D_A we have:

$$\frac{(\alpha_{p_1} + \alpha_{p_3})^2 k_2^2 - \alpha_{p_1} \alpha_{p_3} k_1^2}{(\alpha_{p_1} + \alpha_{p_2} + \alpha_{p_3})^2} - (s_2^2 - m^2) = 0,$$
(6.3.80)

$$\frac{\alpha_{p_2}^2 k_2^2 + \alpha_{p_3} (\alpha_{p_2} + \alpha_{p_3}) k_1^2}{(\alpha_{p_1} + \alpha_{p_2} + \alpha_{p_3})^2} - (s_1^2 - m^2) = 0, \tag{6.3.81}$$

$$\frac{\alpha_{p_2}^2 k_2^2 + \alpha_{p_1} (\alpha_{p_2} + \alpha_{p_1}) k_1^2}{(\alpha_{p_1} + \alpha_{p_2} + \alpha_{p_3})^2} - (s_3^2 - m^2) = 0.$$
(6.3.82)

Because $\omega_2 = \omega_3$ this immediately gives $s_1 = s_3$. Now we can use (6.3.81) and (6.3.82) to obtain:

$$\alpha_{p_1}(\alpha_{p_2} + \alpha_{p_1}) = \alpha_{p_3}(\alpha_{p_2} + \alpha_{p_3}), \tag{6.3.83}$$

which implies $\alpha_{p_1} = \alpha_{p_3}$. We also use (6.3.77) and (6.3.79) (and $s_1 = s_3$) to show:

$$\alpha_{2_{+}} = \alpha_{3_{+}}.\tag{6.3.84}$$

Now using $\omega_1^2 = 4\omega_2^2$, we obtain:

$$4(s_1 + s_2)^2 = 4s_1^2, (6.3.85)$$

so $s_2 = -2s_1$. This also gives $\omega_1 = -2\omega_2$.

By using (6.3.80) and (6.3.81) ((6.3.82) is the same as (6.3.81)) and eliminating the Feynman parameters, we get:

$$(s_2^2 - s_1^2 + k^2)^2 = 4k^2(s_2^2 - m^2). (6.3.86)$$

Usually this is as far as we can go, but because now we fixed $\omega_1^2 = 4\omega_2^2$ we found $s_2 = -2s_1$, so we can further simplify this. Eventually we get:

$$\frac{M^4}{m^2} = (\omega_1^2 - 4M^2),\tag{6.3.87}$$

or

$$\omega_1^2 = 4m^2 - \frac{(M^2 - 2m^2)^2}{m^2},\tag{6.3.88}$$

which is exactly the value for anomalous threshold in the amplitude case. Hence we have demonstrated the existence of anomalous threshold in the wavefunction as well.

We can also compute the Feynman parameters explicitly to show that this is indeed a physical singularity. For instance,

$$\alpha_{p_2} = \frac{M^2 - 2m^2}{M^2}. (6.3.89)$$

For the singularity to be real, $0 < \alpha_{p_2} < 1$. Hence We must have $M^2 > 2m^2$, which is indeed a criteriom for anomalous threshold.

We could also compute the other Feynman parameters, which are found to be:

$$\alpha_{2+} = \frac{4M^2 - 4m^2}{10M^2 - 18m^2},\tag{6.3.90}$$

$$\lambda = \frac{4M^2}{10M^2 - 18m^2}. (6.3.91)$$

For $M^2 > 2m^2$ we have $0 < \alpha_{2+} < 1$, as well as $\lambda > 0$, hence this is not a spurious singularity.

Which singularity does this correspond to in the recursion expression? It turns out that it corresponds to this condition:

$$\omega_1 + \Omega_{p_1} + \Omega_{p_3} = 0, (6.3.92)$$

along with:

$$\omega_1 + \omega_2 + \omega_3 = 0. \tag{6.3.93}$$

This is reflecting an interesting fact about studying singularities using the recursion expression. Naively if we start with the expression $\omega_1 + \Omega_{p_1} + \Omega_{p_3} = 0$ and try to minimize it, it is tempting to simply write down the most obvious solution (which is $\omega_1 = -\sqrt{k^2 + 4m^2}$), and we would be led to incorrect conclusions about the analytic structure (for instance, that the singularity must first appear at $\omega_1 < -2m$). What our result shows is that at particular kinematics, there may be other minimum solutions that corresponds to additional singularities. For instance in this case we found a singularity that can live in the range $-2m < \omega_1 < \sqrt{2}m$.

This is one of the main advantages of studying the analytic structure of the wavefunction using the amplitude representation rather than using the recursion expression: we have a much better understanding of the analytic structure of amplitudes, and this formalism give us a mapping between singularities of amplitudes and the wavefunction. If we also have a good understanding of how wavefunction-type singularities emerge (for example, in one loop cases they are singularities corresponding to cutting only one internal line) then we have a complete catalogue of the singularities present in the wavefunction.

Wavefunction-type singularity One can also show that the wavefunction-type singularities are also present. To see this, let us just cut one internal line, and pick:

$$S_{1+} = \omega_1^2 - (s_1 + s_3)^2 = 0, (6.3.94)$$

$$S_{2-} = \omega_2^2 - (s_1 - s_2)^2 = 0, (6.3.95)$$

$$S_{3-} = \omega_3^2 - (s_2 - s_3)^2 = 0, (6.3.96)$$

$$S_{p1} = s_1^2 - \Omega_{p1}^2 = 0. (6.3.97)$$

Then one can show, similar to the two site graph case, that we have $\omega_1 + \omega_2 + \omega_3 = -2m$ as a singularity.

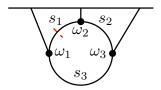


Figure 6.13: Wavefunction-type singularity for the three site one loop graph.

Once again it is instructive to see which term in ψ_3 give rise to this wavefunction-type singularity. Upon inspection, we can find that it is (6.2.30) which has this singularity. Specifically, if we send $\omega_1 + \Omega_{p_1} - s_3 = 0$, $\omega_2 + \Omega_{p_1} + s_2 = 0$ as well as $\omega_3 - s_2 + s_3 = 0$, we will land on $\omega_1 + \omega_2 + \omega_3 = -2m$. Interestingly, ψ_3^{FBB} does not seem to give rise to a wavefunction-type singularity.

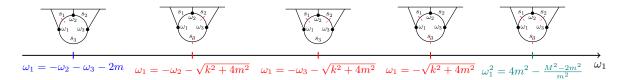


Figure 6.14: Singularities of the three site one loop graph. The red ones are the normal amplitude-type singularities, the teal one is the anomalous amplitude-type singularity and the blue one is the wavefunction-type singularity.

6.4 Singularities of in-in correlators

Since we are ultimately interested in in-in correlators, it is worth studying the singularities of in-in correlators as well. We noted in section 4.3 that for the one site loop diagram, while the wavefunction has a log k_T term, the correlator is analytic in the external kinematics. This feature is in fact present in other loop diagrams as well.

As an example consider the one site two loop diagram (fig. 6.4). We have written down the expression for the flat space wavefunction for massless scalars, which we will restate here:

$$\psi_2(\omega_1, \omega_2, k) = \frac{1}{8\pi^2 \omega_T} \left[\frac{\omega_2 \log\left(\frac{\omega_1 + k}{\Lambda}\right) - \omega_1 \log\left(\frac{\omega_2 + k}{\Lambda}\right)}{\omega_1 - \omega_2} - \frac{\omega_T}{2k} \left(\frac{1}{2} \log^2\left(\frac{\omega_1 + k}{\omega_2 + k}\right) + \frac{\pi^2}{6} + \text{Li}_2\left(\frac{k - \omega_2}{k + \omega_1}\right) + \text{Li}_2\left(\frac{k - \omega_1}{k + \omega_2}\right) \right] . \quad (6.4.1)$$

If we try to compute the in-in correlator, we get the following contributions: one from the time ordered propagators (where we use the G_{++} and G_{--} propagators):

$$B_{2A} = \frac{1}{8\pi^2 \omega_T} \left[\log \left(\frac{\omega_1 + k}{\Lambda} \right) + \log \left(\frac{\omega_2 + k}{\Lambda} \right) \right]. \tag{6.4.2}$$

There is also the out-of-time-ordered propagators (where we use the G_{+-} and G_{-+} propagators), which gives:

$$B_{2B} = \frac{1}{\omega_1 - \omega_2} \frac{-1}{8\pi^2} \left[-\log\left(\frac{\omega_1 + k}{\Lambda}\right) + \log\left(\frac{\omega_2 + k}{\Lambda}\right) \right]. \tag{6.4.3}$$

The in-in correlator is simply the sum of these two terms. Notice the following feature:

- For the wavefunction, both the amplitude-type singularity (given by $\omega_1 = -k$) and the wavefunction-type singularity (given by $\omega_1 + \omega_2 = 0$) are present. The wavefunction-type singularity is a total energy branch point.
- For the correlator, only the amplitude-type singularity (given by $\omega_1 = -k$) is present. The wavefunction-type singularity is absent.

Singularities and the cosmological KLN theorem The cancellation of singularities can be understood more generally in terms of the cosmological KLN theorem, which stems from the cosmological tree theorem. The cosmological KLN theorem states the following:

Total energy branch points in the wavefunction from loop integration are absent in the corresponding in-in correlator.

The argument (taken from [170]) can be roughly summarized as follow:

• When computing in-in correlators from the wavefunction, we often need to add integrals of higher point tree-level wavefunction coefficients to the one-loop wavefunction. For example, for the one site one loop graph, the in-in correlator is given by (2.3.15):

$$\langle \phi(\omega_1)\phi(\omega_2)\phi(\omega_3)\phi(\omega_4)\rangle = \rho_4^{1L} + \int_{\mathbf{p}} P_p \rho_6^{\text{tree}}(\omega_1, \omega_2, \omega_3, \omega_4, \omega_p, \omega_p)$$
 (6.4.4)

• By taking the bulk-to-bulk propagator of the wavefunction and using $\theta(\eta_1 - \eta_2) = 1 - \theta(\eta_2 - \eta_1)$, we obtain the cosmological tree theorem. This allow us to express the one loop wavefunction in terms of its discontinuity, and graphically this is just a sum of tree-level diagrams. For instance, the one loop one site wavefunction is:

$$\psi_4^{1L} = -\int_{\mathbf{p}} P(p) \left[\psi_6^{\text{tree}}(\omega_1, \omega_2, \omega_3, \omega_4, \omega_p, \omega_p) - \psi_6^{\text{tree}}(\omega_1, \omega_2, \omega_3, \omega_4, \omega_p, -\omega_p) \right]$$
(6.4.5)

• Combining these two give us an expression for the in-in correlator purely in terms of (integrals of) tree level wavefunction. Crucially, any fully connected diagram does not have any singularities that depend on total energy and ω_p simultaneously. For example, the one site one loop diagram in flat space becomes:

$$\langle \phi(\omega_1)\phi(\omega_2)\phi(\omega_3)\phi(\omega_4)\rangle = \int_{\mathbf{p}} P(p)\psi_6^{\text{tree}}(\omega_1, \omega_2, \omega_3, \omega_4, \omega_p, -\omega_p)$$

$$= \int_{\mathbf{p}} \frac{1}{2\omega_p} \frac{1}{\omega_T + \omega_p - \omega_p}$$

$$= \int_{\mathbf{p}} \frac{1}{2\omega_p} \frac{1}{\omega_T}.$$
(6.4.6)

Because of this, doing the momentum integral will not give us any total energy branch points.

The remarkable fact about this theorem, however, is that at one loop, all wavefunction-type singularities are total energy singularities. To see this, we use Landau analysis once again. The n site one loop wavefunction is given by:

$$\psi_n = \int \left[\frac{ds_1}{2\pi i} \dots \frac{ds_n}{2\pi i} \right] \frac{F(\{\omega\}, \{s\})}{S_{1+}S_{1-}S_{2+}S_{2-}\dots S_{n+}S_{n-}} \int_{\mathbf{p}} \prod_{j=1}^n \frac{1}{s_j^2 - \Omega_{pj}^2}, \tag{6.4.7}$$

where $S_{n\pm} = \omega_n^2 - (s_n \pm s_{n-1})^2$. We can make use of Landau analysis again to find the wavefunction-type singularity. To do so, we only cut one line, since any other way of cutting should give us either normal or

anomalous amplitude-type singularity. This is given by:

$$S_{1+} = \omega_1^2 - (s_1 + s_n)^2 = 0, (6.4.8)$$

$$S_{2-} = \omega_2^2 - (s_1 - s_2)^2 = 0, (6.4.9)$$

$$S_{3-} = \omega_3^2 - (s_2 - s_3)^2 = 0, (6.4.10)$$

. . .

$$S_{n-} = \omega_n^2 - (s_{n-1} - s_n)^2 = 0, (6.4.11)$$

$$S_{p1} = s_1^2 - \Omega_{p1}^2 = 0. (6.4.12)$$

It is straightforward to show that this just gives $\omega_T = -2m$ as a singularity. In fact, by using the recursion representation of the wavefunction, we can easily see that this is always a singularity is always a branch point ⁷. Therefore, we see that in one-loop, the following is true:

Wavefunction-type singularities are always absent in in-in correlators.

This conjecture is in fact not surprising. Amplitudes are in-out correlators, i.e. field operators are sandwiched between vacuum in the asymptotic past (the in-vacuum) and asymptotic future (the out-vacuum). In flat space in-vacuum and out-vacuum are simply related by a phase [104]. Assuming we have thermal equilibrium, we obtain:

$$_{\text{in}}\langle 0|\phi(k_1)\phi(k_2)\dots\phi(k_n)|0\rangle_{\text{in}} = e^{i\theta}_{\text{out}}\langle 0|\phi(k_1)\phi(k_2)\dots\phi(k_n)|0\rangle_{\text{in}}.$$
(6.4.13)

Since in-in correlators are related to amplitudes by a phase, one would not expect them to have different analytic structures. In other words, one should expect a mapping between singularities of amplitudes to in-in correlators. However at this point our understanding of wavefunction-type singularities is still rather primitive, so we will leave a more careful study of this beyond one loop to the future.

⁷In the recursion representation, these singularities corresponds to sending $\omega_T + 2\omega_{p_i} = 0$ for some internal momentum \mathbf{p}_i . However, since we are integrating over \mathbf{p} , the singularity must some from a logarithm/polylogarithm term, which means the total energy singularity must be a branch cut.

Chapter 7

Dispersion relation and effective field theories

The discussion on analyticity of the wavefunction would not be complete without explaining its potential uses. One such use is the derivation of UV/IR sum rules. In S-matrix literature, these rules are a set of relations between the discontinuity of the amplitude (in the full UV theory) to a sum of Wilson coefficients for an EFT (in the IR). These UV/IR sum rules are essential for constructing positivity bounds: by placing constraints on the discontinuity of the amplitude (for instance, requiring the discontinuity to be greater than zero by unitarity), one can derive a set of constraint equation for the Wilson coefficients.

In this section we detail the steps required to write down these UV/IR sum rules for the wavefunction. We will begin by defining precisely what an EFT is for the wavefunction. We will then write down the dispersion relation, which express the wavefunction in terms of its discontinuities. We will then show how dispersion relations lead to UV/IR sum rules, and demonstrate this by studying a simple tree level example and a loop level example.

7.1 What is an EFT for a wavefunction?

Recall that for amplitudes, given a bulk light field Φ and a bulk heavy field X, amplitudes for Φ can be computed using the generating functional:

$$Z[J] = \int [d\Phi][dX] e^{iS_{\text{UV}}[\Phi, X] + i \int_{x} J(x)\Phi(x)}.$$
 (7.1.1)

The heavy field can be integrated out by the following procedure to obtain action for the EFT:

$$e^{iS_{\text{EFT}}[\Phi]} = \int [dX] e^{iS_{\text{UV}}[\Phi, X]}.$$
 (7.1.2)

We can carry out a similar procedure for the wavefunction. Consider the wavefunction specified by the path integral for the fields Φ and X. The boundary conditions to the past correspond to the Bunch-Davies vacuum. The path integral is a functional of the field boundary conditions to the future $\Phi(t_*) = \phi$ and

$$X(t_*) = \chi:$$

$$\Psi[\phi, \chi; t_*] = \int_{BD}^{\Phi(t_*) = \phi} [d\Phi] \int_{BD}^{X(t_*) = \chi} [dX] e^{S_{\text{UV}}[\Phi, X; t_*]}, \tag{7.1.3}$$

where for some Lagrangian \mathcal{L} we defined:

$$S_{\text{UV}}[\Phi, X; t_*] = \int_{-\infty}^{t_*} dt \, \mathcal{L}[\Phi, X] \,.$$
 (7.1.4)

The path integral is then the transition amplitude between the Bunch-Davies vacuum $|\mathrm{BD}\rangle_{\Phi}\otimes|\mathrm{BD}\rangle_{X}$ and the field eigenstate $|\phi\rangle_{\Phi}\otimes|\chi\rangle_{X}$. To define the EFT wavefunction we focus on this wavefunction:

$$\Psi[\phi, 0; t_*] = \int_{BD}^{\Phi(t_*) = \phi} [d\Phi] \int_{BD}^{X(t_*) = 0} [dX] e^{S_{\text{UV}}[\Phi, X; t_*]},$$

i.e. the wavefunction with the heavy field set to zero at $t=t_*^{-1}$, and compute its wavefunction coefficients in powers of ϕ . The coefficients of the perturbative expansion of $\Psi[\phi,0;t_*]$ in powers of ϕ computed with the interactions of the UV action $S_{\rm UV}[\Phi,X;t_*]$ is what we call the UV wavefunction coefficients $\psi_{\rm UV}$:

$$\Psi[\phi, 0; t_*] = \int_{BD}^{\Phi(t_*) = \phi} [d\Phi] \int_{BD}^{X(t_*) = 0} [dX] e^{S_{\text{UV}}[\Phi, X; t_*]}
= \exp\left[+ \sum_{n=1}^{\infty} \frac{1}{n!} \int_{\mathbf{k}_1, \dots, \mathbf{k}_n} (2\pi)^3 \delta^{(3)} \left(\sum_{a}^{n} \mathbf{k}_a \right) \psi_{\text{UV}}^{(n)}(\{\mathbf{k}\}; t_*) \phi(\mathbf{k}_1) \dots \phi(\mathbf{k}_n) \right].$$
(7.1.5)

For this wavefunction, we can write down an EFT just like for amplitudes:

$$e^{iS_{\text{EFT}}[\Phi;t_*]} = \int_{BD}^{X(t_*)=0} [dX] e^{S_{\text{UV}}[\Phi,X;t_*]}.$$
 (7.1.6)

Crucially, this $S_{\text{EFT}}[\Phi, t_*]$ can be expanded as a series of local interactions for Φ and its derivatives, which at low energies (small derivatives) can be truncated at a finite nuber of terms. The EFT wavefunction coefficients $\psi_{\text{EFT}}(\omega_i, \{\mathbf{k}_j\})$ are then obtained from expanding in powers of ϕ the wavefunction $\Psi[\phi, 0; t_*]$ computed from the truncated EFT action:

$$\Psi[\phi, 0; t_*] = \int_{BD}^{\Phi(t_*) = \phi} [d\Phi] e^{iS_{\text{EFT}}[\Phi; t_*]}$$

$$= \exp\left[+ \sum_{n=1}^{\infty} \frac{1}{n!} \int_{\mathbf{k}_1, \dots \mathbf{k}_n} (2\pi)^3 \delta^{(3)} \left(\sum_{a=1}^{\infty} \mathbf{k}_a \right) \psi_{\text{EFT}}^{(n)}(\{\mathbf{k}\}; t_*) \phi(\mathbf{k}_1) \dots \phi(\mathbf{k}_n) \right]. \tag{7.1.7}$$

At low energies, where the truncation made in S_{EFT} is valid, the ψ_{EFT} coefficients coincide with the true ψ_{UV} coefficients. As the energy is increased, eventually the derivative expansion in $S_{\text{EFT}}[\Phi; t_*]$ breaks down and one must "UV complete" the EFT by returning to the $S_{\text{UV}}[\Phi, X; t_*]$ —physically this corresponds to having enough energy to excite heavy X fluctuations (which are then not faithfully captured by an S_{EFT} involving only light degrees of freedom).

There is a crucial difference between this EFT for the wavefunction and the EFT for amplitudes: the boundary condition for the fields are different. This comes from the new $t = t_*$ boundary we introduced

¹One may ask whether this is the most physically relevant quantity to compute. For example, in an EFT with cutoff Λ we might have to average the value of wavefunction in an interval $t^* \pm \Lambda^{-1}$. We postpone this issue to the conclusions.

for the wavefunction. As a result we need to keep track of both total derivatives in time and of terms proportional to the equations of motion. To this end we separate the EFT action into a bulk and a boundary term localized at t_* :

$$S_{\text{EFT}}[\Phi; t_*] = \int_{-\infty}^{t_*} dt \int d^3 \mathbf{x} (\mathcal{L}_{\text{EFT}}^{\text{bulk}}[\Phi, \partial_{\mu}] + \partial_t \mathcal{L}_{\text{EFT}}^{\text{boundary}}[\phi, \partial_{\mu}, \partial_t]). \tag{7.1.8}$$

All total derivatives in time have been collected into $\partial_t \mathcal{L}_{EFT}^{boundary}$, so that \mathcal{L}_{EFT}^{bulk} is constructed in the usual way (with the freedom to integrate by parts). Notice that our formalism applies to both Lorentz-invariant theories as well as to theories that break boosts, explicitly or spontaneously. For concreteness our examples will include Lorentz invariant interactions in the bulk and non-boost invariant time and spatial derivatives will appear only in $\mathcal{L}_{EFT}^{boundary}$.

7.2 Dispersion relation and UV/IR sum rules

We have now defined the low-energy EFT approximation, ψ_{EFT} , to the full wavefunction coefficient. The question which we wish to address next is: what information about the underlying UV physics can be gleaned from a measurement/calculation of this EFT object?

Analyticity and the dispersion relation. The analytic properties that we developed in the last two sections can give a very concrete answer to this question. The reason is that complex analytic functions are very constrained: they are all but completely fixed by their singularities and asymptotics via Cauchy's theorem. One can use said theorem to recover the value of a function f(z) at a point $z = z_0$ using a closed contour integral:

$$f(z_0) = \frac{1}{2\pi i} \oint_C \frac{f(z)}{z - z_0}.$$
 (7.2.1)

where C is a counter-clockwise contour around the pole at $z = z_0$ (and contains no further singularities). Now imagine we expand C until we start intersecting poles and branch cuts of f(z). We need to deform the contour to properly defined the integral (7.2.1). In particular, we have three different contributions to the deformed contour C_R as shown in Fig. 7.1:

- (i) The isolated poles z_i of f(z). The deformed contour wraps clockwise around the poles of f(z).
- (ii) The branch cuts of f(z). The contour runs above and below the branch cut, and is therefore proportional to the discontinuity of the function along the cut, where,

$$\operatorname{disc} f(z) = \lim_{\epsilon \to 0} \left[f(z + i\epsilon) - f(z - i\epsilon) \right] . \tag{7.2.2}$$

(iii) the arc at infinity C_R . Once the contour is made arbitrarily large, we can identify this contribution with the residue of the pole at infinity.

This expresses the right-hand side of (7.2.1) as a sum of three terms:

$$f(z_0) = -\sum_{z_i} \underbrace{\operatorname{Res}_{z=z_i} \left(\frac{f(z)}{z - z_0} \right)}_{\text{isolated poles}} + \underbrace{\int \frac{dz}{2\pi i} \frac{\operatorname{disc}(f(z))}{z - z_0}}_{\text{branch cut}} + \underbrace{\operatorname{Res}_{\infty} \left(\frac{f(z)}{z - z_0} \right)}_{\text{Pole at infinity}}.$$
 (7.2.3)

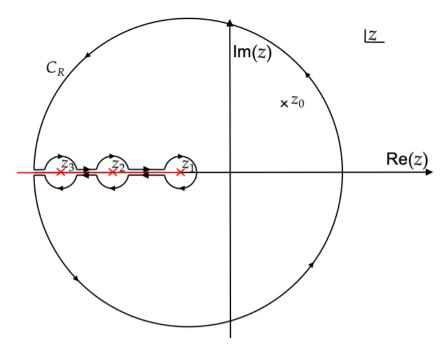


Figure 7.1: Deformed contour for dispersion relations. There is a branch point at $z = z_1$ and a branch cut on the negative real axis. There are isolated poles at $z = z_2$ and $z = z_3$.

Note that if one defines the "discontinuity" of an isolated pole as $\operatorname{disc}(1/(z-z_i)) = -2\pi i \delta(z-z_i)$, then the first term can be absorbed into the second.

Wavefunction dispersion relation. We can apply these considerations to the off-shell wavefunction coefficients $\psi_n(\{\omega\}, \{\mathbf{k}\})$ taken as analytic functions of a single complex variable ω_1 , while holding all the other kinematics fixed. As we have discussed, singularities in $\psi_n(\{\omega\}, \{\mathbf{k}\})$ can only exist on the negative real axis of ω_1 . This allows us to write (7.2.3) as:

$$\omega_T \psi(\{\omega\}, \{\mathbf{k}\}) \Big|_{\omega_1 = \omega_1'} = \int_{-\infty}^0 \frac{d\omega_1}{2\pi i} \frac{\operatorname{disc}\left(\omega_T \psi(\{\omega\}, \{\mathbf{k}\})\right)}{\omega_1 - \omega_1'} + \underset{\omega_1 = \infty}{\operatorname{Res}}\left(\frac{\omega_T \psi_n(\{\omega\}, \{\mathbf{k}\})}{\omega_1 - \omega_1'}\right). \tag{7.2.4}$$

This is our central application of analyticity: it allows us to connect every Wilson coefficient appearing in \mathcal{L}_{EFT} to an integral over the wavefunction of the underlying UV theory.

UV/IR sum rules. The idea is to expand the left-hand-side of (7.2.4) at low energy/momenta, where it can be computed using the low-energy \mathcal{L}_{EFT} . This expansion can then be matched, order-by-order, to particular high-energy integrals on the right-hand-side. To this end, we define the UV integral,

$$\mathcal{I}_{\text{UV}}^{(N)}(\{\omega_{a\neq 1}\}, \{\mathbf{k}\}) = \int_{-\infty}^{0} \frac{d\omega_1}{2\pi i} \frac{\operatorname{disc}\left[\omega_T \psi(\{\omega\}, \{\mathbf{k}\})\right]}{\omega_1^{N+1}} + \underset{\omega_1 = \infty}{\operatorname{Res}} \left(\frac{\omega_T \psi(\{\omega\}, \{\mathbf{k}\})}{\omega_1^{N+1}}\right). \tag{7.2.5}$$

The low-energy expansion of (7.2.4) can then be written compactly as,

$$\frac{1}{N!} \partial_{\omega_1}^N (\omega_T \psi_{EFT}) \Big|_{\omega_1 = 0} = \mathcal{I}_{UV}^{(N)} (\{ \omega_{a \neq 1} \}, \{ \mathbf{k} \}) . \tag{7.2.6}$$

Since the EFT does not distinguish between ω_1 and the other kinematic variables, this equation should be further expanded in powers of each of the $\omega_{a\neq 1}$ and \mathbf{k}_a . In the next subsection, we explicitly construct the EFT for the wavefunction of a scalar field up to fourth order in derivatives, and show how (7.2.6) relates each Wilson coefficient to a particular UV integral, $\mathcal{I}_{\text{UV}}^{(N)}$.

7.3 Example: a light scalar

Let us illustrate these new sum rules using the EFT for a light scalar field Φ on a fixed Minkowski background.

An EFT basis for quartic interactions. Once total derivatives and terms proportional to the free equations of motion are included, the list of possible interactions grows rapidly with increasing mass-dimension. Rather than construct the most general possible EFT, we will focus on a particular subset of interactions which illustrates our sum rules simply and yet remains general enough to capture simple tree-level UV completions (of which we give an example in Sec. 7.4). Firstly, we focus on quartic interactions: these would be the leading interactions in any theory with an approximate \mathbb{Z}_2 symmetry, $\Phi \to -\Phi$. We truncate the EFT at mass-dimension-8, which means we only include interactions with up to four (three) derivatives in the bulk (boundary) Lagrangian, and further assume that Lorentz symmetry is broken only by the boundary interactions. Finally, we focus on specific interactions of the factorised form $\mathcal{D}_1\Phi^2\mathcal{D}_2\Phi^2$, where \mathcal{D}_1 and \mathcal{D}_2 are differential operators. Altogether, this gives the following EFT basis of interactions:

$$\mathcal{L}_{EFT}^{\text{bulk}}[\Phi, \partial_{\mu}] \supset \frac{\alpha_{0}}{4!} \Phi^{4} + \frac{\alpha_{2}}{4} \Phi^{2} \Box \Phi^{2} + \frac{\alpha_{4}}{4} \Phi^{2} \Box^{2} \Phi^{2} + \mathcal{O}(\partial^{6}),$$

$$\mathcal{L}_{EFT}^{\text{boundary}}[\Phi(t_{*}), \partial_{\mu}, \partial_{t}] \supset \frac{\beta_{00}}{4!} \Phi^{4}(t_{*}) - \frac{\beta_{11}}{4} \Phi^{2}(t_{*}) \partial_{t} \Phi^{2}(t_{*}) + \frac{\beta_{20}}{4} \Phi^{2}(t_{*}) \Box \Phi^{2}(t_{*}) - \frac{\beta_{22}}{4} \Phi^{2}(t_{*}) \partial_{t}^{2} \Phi^{2}(t_{*}) + \dots$$

$$- \frac{\beta_{31}}{4} \Phi^{2}(t_{*}) \partial_{t} \Box \Phi^{2}(t_{*}) - \frac{\beta'_{31}}{4} \Box \Phi^{2}(t_{*}) \partial_{t} \Phi^{2}(t_{*}) + \mathcal{O}(\partial^{4}), \tag{7.3.1}$$

where the α_a 's are the free Wilson coefficients of bulk interactions and the β_{ab} 's are free Wilson coefficients of boundary interactions. The first label on β counts the total number of derivatives, while the second counts the number of derivatives that are not Lorentz invariant (such as ∂_t and ∂_i^2).

EFT wavefunction. We can use (7.3.1) to compute the tree-level four-point wavefunction coefficient up to fourth order in the momenta/energy. Even though we consider contact interactions, it is convenient to separate contributions into s, t and u "channels" according to the partial energies on which they depend:

$$\psi_{\text{EFT}}(\{\omega\}, \{\mathbf{k}\}) = \delta^d(\mathbf{k}_T)(\psi'_{\text{EFT}}(\omega_{12}, \omega_{34}, \mathbf{k}_s) + \psi'_{\text{EFT}}(\omega_{13}, \omega_{23}, \mathbf{k}_t) + \psi'_{\text{EFT}}(\omega_{14}, \omega_{24}, \mathbf{k}_u)).$$
 (7.3.2)

An explicit calculation gives:

$$\psi'(\omega_{12}, \omega_{34}, \mathbf{k}_s) = \frac{1}{\omega_T} \left[\frac{1}{3} \alpha_0 + \alpha_2 (s_{12} + s_{34}) + \alpha_4 (s_{12}^2 + s_{34}^2) \right] + \frac{i}{3} \beta_{00} + \beta_{11} \omega_T + i \beta_{20} (s_{12} + s_{34}) + i 2 \beta_{22} \mathbf{k}_s^2 + \beta_{31} (s_{12} \omega_{12} + s_{34} \omega_{34}) + \beta_{31}' (s_{12} \omega_{34} + s_{34} \omega_{12}) + \mathcal{O}(p^5).$$

$$(7.3.3)$$

We have defined:

$$\mathbf{k}_{s} = \mathbf{k}_{1} + \mathbf{k}_{2}, \qquad \mathbf{k}_{t} = \mathbf{k}_{1} + \mathbf{k}_{3}, \qquad \mathbf{k}_{u} = \mathbf{k}_{1} + \mathbf{k}_{4},$$

$$\omega_{ij} = \omega_{i} + \omega_{j}, \qquad \mathbf{k}_{ij} = \mathbf{k}_{i} + \mathbf{k}_{j}, \qquad s_{ij} = \omega_{ij}^{2} - \mathbf{k}_{ij}^{2}. \qquad (7.3.4)$$

Sum rules. The sum rules in (7.2.6) can be used to fix each of the low-energy Wilson coefficients in (7.3.1) in terms of an integral over the UV completion of the EFT. Concretely, proceeding order-by-order in derivatives:

• At mass-dimension-4, there is a single bulk interaction in \mathcal{L}_{EFT} with Wilson coefficient α_0 . The corresponding sum rule follows from evaluating (7.2.4) at all $\omega_a = k_a = 0$,

$$\alpha_0 = \mathcal{I}_{\text{UV}}^{(0)}(\{\omega\}, \{\mathbf{k}\}) \Big|_{\substack{\omega_a = 0 \\ \mathbf{k}_a = 0}}$$

$$(7.3.5)$$

• At mass-dimension-5, there is a single boundary interaction in the EFT, with coefficient β_{00} . The corresponding sum rule follows from evaluating the ∂_{ω_1} of (7.2.4) at all $\omega_a = k_a = 0$,

$$i\beta_{00} = \mathcal{I}_{\text{UV}}^{(1)}(\{\omega\}, \{\mathbf{k}\}) \Big|_{\substack{\omega_a = 0, \\ \mathbf{k} = 0}}$$
 (7.3.6)

• At mass-dimension-6, there are two interactions, with Wilson coefficients α_2 and β_{11} . The corresponding sum rules follow from evaluating the $\partial_{\omega_1}^2$ and $\partial_{\omega_2}\partial_{\omega_1}$ of (7.2.4) at all $\omega_a = k_a = 0$,

$$3(\alpha_2 + \beta_{11}) = \mathcal{I}_{\text{UV}}^{(2)}(\{\omega\}, \{\mathbf{k}\}) \Big|_{\substack{\omega_a = 0 \\ \mathbf{k}_a = 0}}, \tag{7.3.7}$$

$$2(\alpha_2 + 3\beta_{11}) = \partial_{\omega_2} \mathcal{I}_{\text{UV}}^{(1)}(\{\omega\}, \{\mathbf{k}\}) \Big|_{\substack{\omega_a = 0, \\ \mathbf{k}_- = 0}}$$
(7.3.8)

• At mass-dimension-7 there are two boundary interactions, with Wilson coefficients β_{20} and β_{22} . The corresponding sum rules follow from evaluating $\partial_{\omega_1}^3$ and $\partial_{\omega_1}\partial_{k_s}^2$ of (7.2.4) at all $\omega_a = k_a = 0$,

$$3i\beta_{20} = \mathcal{I}_{\text{UV}}^{(3)}(\{\omega\}, \{\mathbf{k}\}) \Big|_{\substack{\boldsymbol{\omega}_a = 0, \\ \mathbf{k} = 0}}$$
 (7.3.9)

$$-4i(\beta_{20} - \beta_{22}) = \partial_{k_s}^2 \mathcal{I}_{\text{UV}}^{(1)}(\{\omega\}, \{\mathbf{k}\}) \Big|_{\substack{\omega_a = 0 \\ \mathbf{k}_a = 0}},$$
(7.3.10)

• At mass-dimension-8, there are three EFT interactions, with Wilson coefficients $\{\alpha_4, \beta_{31}, \beta'_{31}\}$. The corresponding sum rules follow from evaluating $\partial_{\omega_1}^4$, $\partial_{\omega_1}^2 \partial_{\omega_2} \partial_{\omega_3}$ and $\partial_{\omega_1} \partial_{\omega_2} \partial_{\omega_3} \partial_{\omega_4}$ of (7.2.4) at all

 $\omega_a = k_a = 0,$

$$3(\alpha_4 + \beta_{31}) = \mathcal{I}_{\text{UV}}^{(4)}(\{\omega\}, \{\mathbf{k}\}) \Big|_{\substack{\mathbf{k}_a = 0 \\ \mathbf{k} = 0}}, \tag{7.3.11}$$

$$6\beta_{31} + 10\beta_{31}' = \partial_{\omega_2}\partial_{\omega_3}\mathcal{I}_{UV}^{(2)}(\{\omega\}, \{\mathbf{k}\}) \Big|_{\substack{\omega_a = 0, \\ \mathbf{k}_a = 0}}$$
(7.3.12)

$$24\beta_{31}' = \partial_{\omega_2} \partial_{\omega_3} \partial_{\omega_4} \mathcal{I}_{\text{UV}}^{(1)} \left(\{\omega\}, \{\mathbf{k}\} \right) \Big|_{\substack{\omega_a = 0 \\ \mathbf{k}_a = 0}}.$$
 (7.3.13)

These sum rules can be similarly applied to any desired order in the EFT expansion, determining every Wilson coefficient in \mathcal{L}_{EFT} . Note in particular that the boundary interactions and the bulk interactions contribute on an equal footing. For instance, the sum rule (7.3.7) can only unambiguously fix the bulk Wilson coefficient once supplemented with (7.3.8)—generally at a given order in derivatives one requires all independent sum rules in order to solve for a particular Wilson coefficient.

Comparison with amplitude sum rules Amplitude sum rules have been extensively studied in the literature and have proven to be very useful in the study of EFTs. However, the amplitudes sum rules differ in two fundamental aspect from the wavefunction sum rules we have derived above:

- The LSZ formula reduces the number of possible EFT interaction vertices in the bulk. For example terms like $\Phi^2 \Box \Phi^2$ will not be present as they are proportional to the equations of motion.
- The scattering process takes place between asymptotically free past and future states. This means that one can discard total derivative interactions in the bulk, and that the EFT vertices on the time slice $t = t_*$ will not play a role.

Therefore, the EFT expansion for amplitudes $S_{\text{EFT}}^{\text{amp}}[\Phi]$ only involves the bulk Lagrangian from (7.1.8) action:

$$S_{\rm EFT}^{\rm amp}[\Phi] = \int_{-\infty}^{+\infty} dt \int d^3x \, \mathcal{L}_{\rm EFT}^{\rm bulk}[\Phi, \partial_{\mu}]. \tag{7.3.14}$$

As a consequence of the above considerations, fewer operators need to be considered, namely

$$\mathcal{L}_{EFT}^{bulk}[\Phi, \partial_{\mu}] \supset \frac{\alpha_0}{4!} \Phi^4 + \frac{\alpha_4}{4} \Phi^2 \Box^2 \Phi^2 + \mathcal{O}(\partial^6). \tag{7.3.15}$$

From these interactions we can obtain the leading terms for the $2 \to 2$ scattering amplitude,

$$A(s,t) = \alpha_0 + 2\alpha_4(s^2 + t^2 + u^2) + \mathcal{O}(\alpha_6 p^6). \tag{7.3.16}$$

The analyticity for the scattering amplitude A(s,t) in the complex s plane allows us to write a dispersion relation for A(s,t) and its derivatives. Using these we find that:

$$\alpha_0 = \int_{-\infty}^{+\infty} \frac{ds}{2\pi i} \frac{\operatorname{disc}(A(s, t=0))}{s} + \operatorname{Res}_{\infty} \left(\frac{\operatorname{disc}(A(s, t=0))}{s}\right), \tag{7.3.17}$$

$$4\alpha_4 = \int_{-\infty}^{+\infty} \frac{ds}{2\pi i} \frac{\operatorname{disc}(A(s, t=0))}{s^3} + \operatorname{Res}_{\infty} \left(\frac{\operatorname{disc}(A(s, t=0))}{s^3}\right). \tag{7.3.18}$$

Therefore, we can see that the amplitudes' sum rules only capture a reduced set of the possible EFT interactions. Not every interaction that contributes to the wavefunction may appear in the scattering amplitude, whilst all interactions that contribute to the amplitude do appear in the wavefunction coefficients².

In the case of boundary interactions, the best case is the comparison of the sum rules for α_4 from amplitudes (7.3.18) with that from wavefunction coefficients (7.3.11). Whilst the amplitude sum rule only includes information about the EFT interaction $\Phi^2\Box^2\Phi^2$, the wavefunction one also includes information about $\Phi^2\partial_t\Box^2\Phi^2|_{t=t_*}$. For interactions proportional to the equations of motion, like $\Phi^2\Box\Phi^2$, the amplitudes sum rules are oblivious. It requires us to look at wavefunction sum rules like (7.3.7) and (7.3.8) to constrain the value for the Wilson coefficients of $\Phi^2\Box\Phi^2$ and $\Phi^2\partial_t\Phi^2|_{t=t_*}$.

7.4 Example UV completion

In this section, we evaluate and check our proposed sum rules in a simple UV-completion of the single-scalar low-energy effective theory presented above. We do this both for a tree-level process and for a one-loop process in the UV-completion of effective theory to show cases in which both poles and branch points arise.

7.4.1 Tree level example

Consider a toy UV model of two scalars: a light field Φ and a heavy field X, which interact via a coupling of the form $gM\Phi^2X$, so that the complete renormalisable Lagragian is:

$$\mathcal{L}_{\text{UV}}[\Phi, X] = -\frac{1}{2}(\partial \Phi)^2 - \frac{1}{2}m^2\Phi^2 - \frac{1}{2}(\partial X)^2 - \frac{1}{2}M^2X^2 - gM\Phi^2X.$$
 (7.4.1)

We aim to study the EFT of the light field Φ at energies well below the mass M of the heavy field X. At tree level, it is enough to integrate out the heavy field X using the classical equations of motion and substitute back into the action:

$$(\Box - M^2)X = gM\Phi^2. (7.4.2)$$

The solution in momentum space with boundary conditions $\bar{X}^{\text{in}}_{\mathbf{k}}$ in the past and $\bar{X}^{\text{out}}_{\mathbf{k}}$ in the future are:

$$X_{\mathbf{k}}^{\text{sol}}(t) = \frac{f_k(t)}{f_k(t_*)} \bar{X}_{\mathbf{k}}^{\text{in}} + \frac{f_k^*(t)}{f_k^*(t_*)} \bar{X}_{\mathbf{k}}^{\text{out}} - gM \frac{\int_{\mathbf{p}} \Phi_{\mathbf{p}}(t) \Phi_{\mathbf{k} - \mathbf{p}}(t)}{\partial_t^2 + \mathbf{k}^2 + M^2}, \tag{7.4.3}$$

where $f_k(t)$ are the mode functions of the heavy scalar X with $f_k(t) = e^{-i\Omega_k t}/\sqrt{2\Omega_k}$ and $\Omega_k^2 = \mathbf{k}^2 + M^2$. The first two terms correspond to the homogeneous solution of the equation of motion. The third term corresponds accounts for the coupling to the $\Phi^2(t)$ source.

In order to derive the Wilson coefficients from the action we need to substitute the equations of motion for the heavy field into the original action. For generic boundary conditions, i.e. for both amplitudes and wavefunction coefficients, evaluating the action on the X given in (7.4.3) gives:

$$S_{\text{EFT}}[\Phi, X^{\text{sol}}] = \int dt \, d^3x \left[-\frac{1}{2} (\partial \Phi)^2 - \frac{1}{2} m^2 \Phi^2 - \frac{1}{2} g M \Phi^2 X - \frac{1}{2} \partial_\mu (X \partial^\mu X) \right]. \tag{7.4.4}$$

To make progress we have to choose boundary conditions. These are different depending on whether we discuss amplitudes or wavefunction coefficients. Let's study each case in turn.

²This is necessary since in the limit $\omega_T \to 0$ the Minkowski wavefunction coefficients coincide with scattering amplitudes.

Amplitudes. Amplitudes are related by the LSZ reduction formula to an in-vacuum to out-vacuum Green's function. This choice corresponds to $\bar{X}_{\mathbf{k}}^{\text{in}} = 0$ and $\bar{X}_{\mathbf{k}}^{\text{out}} = 0$, and similarly for Φ . This leads to

$$X_{\mathbf{k}}^{\text{sol}}(t) = -gM \frac{\int_{\mathbf{p}} \Phi_{\mathbf{p}}(t) \Phi_{\mathbf{k} - \mathbf{p}}(t)}{\partial_t^2 + \mathbf{k}^2 + M^2} \quad \Rightarrow \quad X^{\text{sol}}(t, \mathbf{k}) = \int_{\mathbf{k}} e^{i\mathbf{k}\mathbf{x}} X_{\mathbf{k}}^{\text{sol}}(t) = \frac{gM}{\Box - M^2} \Phi^2(t, \mathbf{x}). \tag{7.4.5}$$

When substituted back into the on-shell action the boundary term vanishes and we find

$$S_{\text{EFT}}^{\text{amp}}[\Phi, X^{\text{sol}}(\Phi)] = \int dt \, d^3x \left[-\frac{1}{2} (\partial \Phi)^2 - \frac{1}{2} m^2 \Phi^2 - \frac{1}{2} g^2 M^2 \Phi^2 \frac{1}{\Box - M^2} \Phi^2 \right]. \tag{7.4.6}$$

This action is clearly non-local. However, in the regime $M^2 \gg \square$ we can approximate it as a series of local operators. This leads to the EFT vertices that reproduce the EFT interactions in (7.3.15):

$$S_{\text{EFT}}^{\text{amp}}[\Phi] = \int dt \, d^3x \left[-\frac{1}{2} (\partial \Phi)^2 - \frac{1}{2} m^2 \Phi^2 + \frac{1}{2} g^2 M^2 \sum_{n=0}^{\infty} \Phi^2 \left(\frac{\square}{M^2} \right)^n \Phi^2 \right]. \tag{7.4.7}$$

Note $\Phi^2 \Box \Phi^2$ does not contribute to any scattering amplitude as it is proportional to the equations of motion. Therefore, even though it appears in the action it cannot be captured by the amplitude sum rules. For this particular UV-completion, the Wilson coefficients in (7.3.15) can be read off from (7.4.7):

$$\alpha_0 = 12g^2 \; , \; \alpha_2 = \frac{2g^2}{M^2} \; , \; \alpha_4 = \frac{2g^2}{M^4} \; , \; \dots$$
 (7.4.8)

Wavefunction coefficients. For wavefunction coefficients the boundary conditions are different from those of amplitudes because for the "out" state we project onto a field eigenstate at some finite time, as opposed to a state of free particles in the infinite future. This leads to additional EFT interactions as we now show. The right boundary conditions are now $\bar{X}_{\mathbf{k}}^{\mathrm{in}} = 0$ and $'X_{\mathbf{k}}^{\mathrm{sol}}(t_*) = 0$, and hence

$$X^{\text{sol}}(t) = \bar{X}^{\text{out}} e^{i\Omega(t-t_*)} + gM \frac{\Phi^2(t)}{\Box - M^2}, \qquad \bar{X}^{\text{out}} = -gM \frac{\Phi^2(t_*)}{\Box - M^2},$$
 (7.4.9)

where $\Omega = \sqrt{k^2 + M^2}$ is fixed by the dispersion relation for the momentum of X or equivalently Φ^2 . Notice that since X(t) = 0 at $t = t_*$ and at $t = -\infty(1 - i\epsilon)$, the total derivative term in (7.4.4) vanishes. For the other terms in (7.4.4) we can split the result into bulk and boundary contributions as we did in (7.1.8). This is simplified by the fact that the on-shell action is linear in X:

$$S_{\text{EFT}}^{t_*}[\Phi] = S_{\text{EFT}}[\Phi, X^{\text{sol}}] = S_{\text{EFT}}^{\text{bulk}}[\Phi] + S_{\text{EFT}}^{\text{bdy}}[\Phi], \tag{7.4.10}$$

To compute each term we notice that the relative factor between the kinetic term and the cubic interaction is different in the action (7.4.4) from what appears in the equations of motion (7.4.2). This means that we have the choice to use the equations of motion for X to eliminate either the kinetic term or the cubic interaction. Here we choose to eliminate the latter, finding

$$S_{\rm EFT}[\Phi, X^{\rm sol}] \supset \int dt \, d^3x \left[-\frac{1}{2} X^{\rm sol}(\Box - M^2) X^{\rm sol} \right].$$
 (7.4.11)

This has four contributions from squaring the two terms in X in (7.4.9). The contribution from squaring the second term in (7.4.9) gives the bulk interactions

$$S_{\rm EFT}^{\rm bulk} \supset \int d^3x dt - \frac{1}{2}g^2 M^2 \Phi^2 \frac{1}{\Box - M^2} \Phi^2,$$
 (7.4.12)

where $\Box - M^2$ cancelled out with $(\Box - M^2)^{-1}$. Now notice that the first term in (7.4.9) is a solution of the homogeneous equations of motion and so it is annihilated by $\Box - M^2$. Hence, of the remaining three terms the only survivor is the one where $\Box - M^2$ hits Φ^2 ,

$$S_{\rm EFT}^{\rm bdy}[\Phi] = -\int d^3x dt \, \frac{1}{2} \bar{X}^{\rm out} e^{i\Omega(t-t_*)} (\Box - M^2) g M \frac{\Phi^2}{\Box - M^2} \,.$$
 (7.4.13)

One could choose to simplify $\Box - M^2$ but then one has to compute the time integral. Instead here we integrate by part twice to move $\Box - M^2$ onto the first factor. Since again that factor is annihilated by $\Box - M^2$ the only contribution comes from the boundary terms in the first and second integration by parts in time. They combine into

$$S_{\text{EFT}}^{\text{bdy}} = \int d^3x \, \frac{1}{2} g M \bar{X}^{\text{out}} \left(\partial_t - i\Omega \right) \frac{\Phi^2(t_*)}{\Box - M^2}$$
 (7.4.14)

$$= \int d^3x \, \frac{ig^2 M^2}{2} \, \frac{\Phi^2(t_*)}{\Box - M^2} \left(i\partial_t + \Omega \right) \frac{\Phi^2(t_*)}{\Box - M^2} \,, \tag{7.4.15}$$

where we used (7.4.9) to substitute for \bar{X}^{out} .

To obtain the local EFT interactions we expand in $M^2 \gg \square$, ∂_t^2 , ∂_i^2 . The resulting vertices in the bulk are:

$$\mathcal{L}_{\text{EFT}}^{\text{bulk}} = \sum_{n=0}^{\infty} \frac{g^2}{2M^{2n}} \Phi^2 \Box^n \Phi^2, \tag{7.4.16}$$

These are the same as for amplitudes, with the difference that we cannot drop the n = 1 term, which is proportional to the equation of motion. On the boundary, we have both Lorentz covariant and boost breaking terms:

$$\mathcal{L}_{\text{EFT}}^{\text{brane}} = \frac{ig^2}{2M^2} \sum_{a,b} \frac{\Box^a \Phi^2(t_*)}{M^{2a}} \left(i\partial_t + M \sum_{n=0}^{\infty} \binom{1/2}{n} \left(-\frac{\partial_i^2}{M^2} \right)^n \right) \frac{\Box^b \Phi^2(t_*)}{M^{2b}}.$$
 (7.4.17)

Therefore, we can write the first few Wilson coefficients:

$$\alpha_0 = 12g^2 , \ \alpha_2 = \frac{2g^2}{M^2} , \ \alpha_4 = \frac{2g^2}{M^4},$$

$$\beta'_{31} = \frac{2g^2}{M^4} , \ \beta_{31} = \frac{2g^2}{M^4} , \ \beta_{11} = \frac{2g^2}{M^2} , \ \beta_{20} = \frac{4ig^2}{M^3} , \ \beta_{00} = \frac{12ig^2}{M} , \ \beta_{22} = \frac{ig^2}{M^3}.$$

$$(7.4.18)$$

The value of these coefficients have been derived from the Lagrangian of the EFT after integrating out the heavy degrees of freedom of the UV. They do not rely on the sum rules. To prove that we can use the latter to compute all the coefficients in (7.4.18) we will start from the UV four-point exchange wavefunction coefficient for the light scalar ψ_{UV} and then we will use the sum rules (7.3.5-7.3.10) to obtain the value of all the Wilson coefficients from (7.4.18). ψ_{UV} is a exchange diagram given by a heavy internal

line so it is the sum of three different channels $\psi'_{\rm UV}$. An explicit computation gives,

$$\psi_{\text{UV}}(\{\omega\}, \{\mathbf{k}\}) = \delta(\mathbf{k}_T) \left[\psi'_{\text{UV}}(\omega_{12}, \omega_{34}, \mathbf{k}_s) + \psi'_{\text{UV}}(\omega_{13}, \omega_{24}, \mathbf{k}_t) + \psi'_{\text{UV}}(\omega_{14}, \omega_{23}, \mathbf{k}_u) \right] , \qquad (7.4.19)$$

$$\omega_T \psi'_{\text{UV}}(\omega_{12}, \omega_{34}, \mathbf{k}_s) = \frac{4g^2 M^2}{(\omega_{12} + \Omega_{k_s})(\omega_{34} + \Omega_{k_s})}.$$
 (7.4.20)

The object that appears on the right-hand side of the sum rules (7.3.5-7.3.10) is the discontinuity of $\omega_T \psi_{\text{UV}}$ along the negative ω_1 real axis. In this particular example, $\omega_T \psi_{\text{UV}}$ is a rational function of ω_1 and therefore there are no branch cuts contributing to $\operatorname{disc}(\omega_T \psi_{\text{UV}})$. However, the poles located in the negative ω_1 plane do contribute towards $\operatorname{disc}(\omega_T \psi_{\text{UV}})$ as delta functions:

$$\operatorname{disc}(\omega_T \psi_{\text{UV}}) = -\frac{4g^2 M^2}{\omega_{34} + \Omega_{k_s}} 2\pi i \delta(\omega_{12} + \Omega_{k_s}) - \frac{4g^2 M^2}{\omega_{24} + \Omega_{k_t}} 2\pi i \delta(\omega_{13} + \Omega_{k_t}) - \frac{4g^2 M^2}{\omega_{23} + \Omega_{k_u}} 2\pi i \delta(\omega_{14} + \Omega_{k_u}). \tag{7.4.21}$$

The residue at infinity vanishes and therefore only the integral over the discontinuity contributes towards the sum rules. Now we are in position to use the sum rules to compute the Wilson coefficients and prove that they match the result from (7.4.18):

$$\mathcal{I}_{\text{UV}}^{(0)}(\{\omega\}, \{\mathbf{k}\}) \Big|_{\substack{\omega_i = 0 \\ \mathbf{k}_j = 0}} = \int_{-\infty}^{0} \frac{d\omega_1}{2\pi i} \frac{\operatorname{disc}(\omega_T \psi_{\text{UV}})}{\omega_1} \Big|_{\substack{\omega_i = 0 \\ \mathbf{k}_j = 0}} = 12g^2, \tag{7.4.22}$$

$$\mathcal{I}_{\text{UV}}^{(1)}(\{\omega\}, \{\mathbf{k}\}) \Big|_{\substack{\omega_i = 0 \\ \mathbf{k}_j = 0}} = \int_{-\infty}^{0} \frac{d\omega_1}{2\pi i} \frac{\operatorname{disc}(\omega_T \psi_{\text{UV}})}{\omega_1^2} \Big|_{\substack{\omega_i = 0 \\ \mathbf{k}_j = 0}} = -\frac{12g^2}{M}, \tag{7.4.23}$$

$$\mathcal{I}_{\text{UV}}^{(2)}(\{\omega\}, \{\mathbf{k}\}) \Big|_{\substack{\omega_i = 0 \\ \mathbf{k}_j = 0}} = \int_{-\infty}^{0} \frac{d\omega_1}{2\pi i} \frac{\operatorname{disc}(\omega_T \psi_{\text{UV}})}{\omega_1^3} \Big|_{\substack{\omega_i = 0 \\ \mathbf{k}_i = 0}} = \frac{12g^2}{M^2}, \tag{7.4.24}$$

$$\partial_{\omega_2} \mathcal{I}_{\text{UV}}^{(1)}(\{\omega\}, \{\mathbf{k}\}) \Big|_{\mathbf{k}_j = 0}^{\omega_i = 0} = \int_{-\infty}^0 \frac{d\omega_1}{2\pi i} \frac{\partial_{\omega_2} \text{disc}(\omega_T \psi_{\text{UV}})}{\omega_1^2} \Bigg|_{\mathbf{k}_j = 0}^{\omega_i = 0} = \frac{16g^2}{M^2}, \tag{7.4.25}$$

$$\mathcal{I}_{\text{UV}}^{(3)}(\{\omega\}, \{\mathbf{k}\}) \Big|_{\substack{\omega_i = 0 \\ \mathbf{k}_j = 0}} = \int_{-\infty}^{0} \frac{d\omega_1}{2\pi i} \frac{\operatorname{disc}(\omega_T \psi_{\text{UV}})}{\omega_1^4} \Big|_{\substack{\omega_i = 0 \\ \mathbf{k}_j = 0}} = -\frac{12g^2}{M^3}, \tag{7.4.26}$$

$$\mathcal{I}_{\text{UV}}^{(4)}(\{\omega\}, \{\mathbf{k}\}) \Big|_{\substack{\omega_i = 0 \\ \mathbf{k}_j = 0}} = \int_{-\infty}^0 \frac{d\omega_1}{2\pi i} \frac{\operatorname{disc}(\omega_T \psi_{\text{UV}})}{\omega_1^5} \Big|_{\substack{\omega_i = 0 \\ \mathbf{k}_i = 0}} = \frac{12g^2}{M^4}, \tag{7.4.27}$$

$$\partial_{\omega_2} \partial_{\omega_3} \mathcal{I}_{\text{UV}}^{(2)}(\{\omega\}, \{\mathbf{k}\}) \Big|_{\substack{\omega_i = 0 \\ \mathbf{k}_j = 0}} = \int_{-\infty}^0 \frac{d\omega_1}{2\pi i} \frac{\partial_{\omega_2} \partial_{\omega_3} \text{disc}(\omega_T \psi_{\text{UV}})}{\omega_1^3} \Big|_{\substack{\omega_i = 0 \\ \mathbf{k}_j = 0}} = \frac{32g^2}{M^4}, \tag{7.4.28}$$

$$\partial_{\omega_2} \partial_{\omega_3} \partial_{\omega_4} \mathcal{I}_{\text{UV}}^{(1)}(\{\omega\}, \{\mathbf{k}\}) \Big|_{\substack{\mathbf{k}_i = 0 \\ \mathbf{k}_j = 0}} = \int_{-\infty}^{0} \frac{d\omega_1}{2\pi i} \frac{\partial_{\omega_2} \partial_{\omega_3} \partial_{\omega_4} \text{disc}(\omega_T \psi_{\text{UV}})}{\omega_1^2} \Big|_{\substack{\omega_i = 0 \\ \mathbf{k}_i = 0}} = \frac{48g^2}{M^4}, \tag{7.4.29}$$

$$\partial_{k_s}^2 \mathcal{I}_{\text{UV}}^{(1)}(\{\omega\}, \{\mathbf{k}\}) \Big|_{\substack{\omega_i = 0 \\ \mathbf{k}_j = 0}} = \int_{-\infty}^0 \frac{d\omega_1}{2\pi i} \frac{\partial_{k_s}^2 \operatorname{disc}(\omega_T \psi_{\text{UV}})}{\omega_1^2} \Big|_{\substack{\omega_i = 0 \\ \mathbf{k}_j = 0}} = \frac{12g^2}{M^3}.$$
 (7.4.30)

All of the sum rules match the result of the Wilson coefficients (7.4.18) computed at the level of the action.

7.4.2 Loop level example

Now consider a different toy model:

$$\mathcal{L}_{\text{UV}}[\Phi, X] = -\frac{1}{2}(\partial \Phi)^2 - \frac{1}{2}m^2\Phi^2 - \frac{1}{2}(\partial X)^2 - \frac{1}{2}M^2X^2 - g\Phi^2X^2.$$
 (7.4.31)

Unlike the previous toy model, we can no longer use the classical equation of motion for the heavy field X to obtain the effective action for Φ because the leading correction to the action is now at loop level. Instead, we will explicitly compute the wavefunction coefficient ψ_{UV} , and match this to a low-energy ψ_{EFT} in order to fix the appropriate EFT Wilson coefficient.

Computing the UV wavefunction. In order to compute the Wilson coefficients, we can first compute the wavefunction coefficient for the UV theory and expand the wavefunction coefficient in the low-energy limit. Since this expression needs to match the wavefunction coefficient computed from the EFT, we can read off the Wilson coefficients. In the UV theory, the leading contribution to the two-point wavefunction coefficient is the following graph:

This graph corresponds to the integral,

$$\omega_T \psi_{\text{UV}} = g \int_{\mathbf{p}} \frac{1}{\omega_T + 2\sqrt{p^2 + M^2}}.$$
 (7.4.33)

which is computed explicitly using a hard cut-off. The full result is:

$$\omega_T \psi_{\text{UV}} = \frac{g}{16\pi^2} \left[2\Lambda (\Lambda - \omega_T) + M^2 + (\omega_T^2 - 2M^2) \log \left(\frac{2\Lambda}{M} \right) + 2\omega_T \sqrt{4M^2 - \omega_T^2} \arcsin \left(\sqrt{\frac{2M - \omega_T}{4M}} \right) + \mathcal{O}\left(\frac{1}{\Lambda} \right) \right]. \quad (7.4.34)$$

Finding the EFT Wilson coefficients. Notice that this particular ψ_{UV} depends only on the energies of the external lines, not their spatial momenta. Consequently, it can be matched using an EFT in which time derivatives are treated as much larger than spatial derivatives. Concretely, we consider the following EFT interactions,

$$S_{\text{EFT}}[\Phi; t_*] = \int_{-\infty}^{t_*} dt \int d^3 \mathbf{x} \, \frac{1}{2} \sum_{n=0} \gamma_n (-i\partial_t)^n \Phi^2$$
 (7.4.35)

which corresponds to a low-energy two-point wavefunction,

$$\omega_T \psi_{\text{EFT}} = \sum_{n=0} \gamma_n \omega_T^n . \tag{7.4.36}$$

The UV model (7.4.31) is one possible UV completion of this EFT, in which the first few Wilson coefficients γ_n appearing in (7.4.36) are fixed to be,

$$\gamma_0 = \frac{g}{16\pi^2} \left(2\Lambda^2 + M^2 - 2M^2 \log \left(\frac{2\Lambda}{M} \right) \right)$$

$$\gamma_1 = \frac{g}{16\pi^2} \left(-2\Lambda + M\pi \right)$$

$$\gamma_2 = \frac{g}{16\pi^2} \left(-1 + \log \left(\frac{2\Lambda}{M} \right) \right)$$

$$\gamma_3 = \frac{g}{16\pi^2} \left(-\frac{\pi}{8M} \right)$$

$$(7.4.37)$$

so that ψ_{EFT} coincides with ψ_{UV} at low values of ω_a .

Notice that we have only regularized the theory, with an arbitrary cutoff, but we have not carried out renormalization. We will verify our sum rules at finite but arbitrary Λ : since if our rules hold for any value of the regulator, they will also hold for any renormalization scheme which is consistently implemented in both the EFT and the UV.

Checking the UV/IR sum rules. Applying the dispersion relation, the Wilson coefficients appearing in (7.4.35) are given by,

$$\gamma_n = \mathcal{I}_{\text{UV}}^{(n)} \Big|_{\substack{\omega_2 = 0 \\ \mathbf{k} = 0}} \tag{7.4.38}$$

where $\mathcal{I}_{\mathrm{UV}}^{(N)}$ are defined in 7.2.5 using the two-point ψ_{UV} .

One could take the discontinuity of (7.4.34) directly to compute the integrals $\mathcal{I}_{\text{UV}}^{(N)}$, but a quicker route is to take the discontinuity of the original integrand,

$$\operatorname{disc}(\omega_T \psi_{\text{UV}}) = g \int_{\mathbf{p}} \operatorname{disc}\left(\frac{1}{\omega_T + 2\sqrt{p^2 + M^2}}\right)$$
$$= -\frac{g}{2\pi^2} \int_0^\infty dp \ p^2 \ 2\pi i \delta(\omega_T + 2\sqrt{p^2 + M^2}). \tag{7.4.39}$$

Since p is real, for $\omega_T > -2M$ there is no solution to $\omega_T + 2\sqrt{p^2 + M^2} = 0$. Therefore, the discontinuity is proportional to a step function:

$$\operatorname{disc}(\omega_T \psi_{\text{UV}}) = \frac{g \,\omega_T}{16\pi^2} \sqrt{\omega_T^2 - 4M^2} \, 2\pi i \,\Theta\left(-\omega_T - 2M\right). \tag{7.4.40}$$

Substituting (7.4.40) into 7.2.5, and again using a hard cut-off to tame any divergences, we find that in this UV model:

$$\mathcal{I}_{\text{UV}}^{(N)}\big|_{\substack{\omega_2=0\\\mathbf{k}=0}} = \int_{-2\Lambda}^{-2M} d\omega \, \frac{g}{16\pi^2} \frac{\omega\sqrt{\omega^2 - 4M^2}}{\omega^{N+1}}.$$
 (7.4.41)

These can be evaluated straightforwardly, and give,

$$\begin{split} \mathcal{I}_{\text{UV}}^{(0)}\big|_{\substack{\omega_{2}=0\\\mathbf{k}=0}} &= \frac{g}{16\pi^{2}} \left(2\Lambda^{2} + M^{2} - 2M^{2} \log\left(\frac{2\Lambda}{M}\right)\right) \\ \mathcal{I}_{\text{UV}}^{(1)}\big|_{\substack{\omega_{2}=0\\\mathbf{k}=0}} &= \frac{g}{16\pi^{2}} \left(-2\Lambda + M\pi\right) \\ \mathcal{I}_{\text{UV}}^{(2)}\big|_{\substack{\omega_{2}=0\\\mathbf{k}=0}} &= \frac{g}{16\pi^{2}} \left(-1 + \log\left(\frac{2\Lambda}{M}\right)\right) \\ \mathcal{I}_{\text{UV}}^{(3)}\big|_{\substack{\omega_{2}=0\\\mathbf{k}=0}} &= \frac{g}{16\pi^{2}} \left(-\frac{\pi}{8M}\right) \end{split} \tag{7.4.42}$$

in agreement with the sum rules (7.4.38).

Chapter 8

Conclusion and outlook

In this thesis we studied various constraints on the cosmological wavefunction from different physical principles. In particular, we focused on the constraints from unitary time evolution, which give rise to a set of consistency relations between different wavefunction coefficients. We explored the case of parity odd trispectrum for massless scalars, where we see that the bootstrap requires the trispectrum to vanish at tree level. However, by explicit computation, we find the one loop parity odd trispectrum is generally nonvanishing, and their signal is suppressed relative to a parity even tree level trispectrum provided the instrumental noise is the same.

We also studied the analytic structure of the wavefunction in great detail. We first showed that non-perturbatively, the wavefunction coefficients are always analytic in the lower half complex plane of its external energies. We moved on to perturbation theory, where we showed that singularities arises when energy entering a sub-diagram of a Feynman diagram vanishes, and we argued for its existence both heuristically and through Landau analysis. We developed the amplitude representation of the wavefunction, where we classified singularities of the wavefunction into two classes: amplitude-type singularities and wavefunction-type singularities, and we argued that wavefunction-type singularities should vanish when we compute an in-in correlator. In the end we developed the dispersion relation for a wavefunction, and leveraged it to obtain UV/IR sum rules for an effective field theory.

There are many interesting future directions. For the perturbative cosmological bootstrap, these include:

• Understanding how to simplify the loop level cutting rules. Our current cutting rules for loop level wavefunction includes summing over all cuts, and for more complicated diagrams it give rise to many terms. One possibility is to try and understand how to properly flip the internal energies by analytical continuation of external energies (for instance through the procedure given in 3.5), which could cut down the number of terms in the loop level cutting rules a lot.

A potentially interesting application of having a simpler loop level cutting rule is that we may be able to replicate the procedure in [134]. There unitarity is used to glue two tree level ψ_3 together to form an exchange ψ_4 . If we can show the contact COT hypothesis described in 3.5 holds, we can extend this procedure to glue any 1PI ψ_3 to form an exchange ψ_4 . More generally, this means that in order to understand loop level wavefunction, we simply need to focus the 1PI wavefunctions, similar to the story of 1PI effective action described in usual QFT textbooks.

- Understanding how to extend the cosmological optical theorem beyond perturbation theory, at least in dS. A potential direction is to use holography: this has been described in 3.5. Once again the main difficulty lies in our lack of knowledge of the boundary CFT of dS: we still need to properly understand various elementary properties of the boundary CFT. Most importantly for our purpose, we need to understand how to properly encode the physical properties of inflation into the conformal bootstrap. At this point it is not clear what the implications of our cosmological bootstrap (such as the COT and manifest locality) means for the boundary CFT even at a perturbative level, and it would be interesting to explore this further.
- One implicit assumption we made in our discussion of unitarity is that the size of the Hilbert space never changes. Throughout our discussion we have completely ignored the fact that dS have a cosmological horizon: as the universe expands, the horizon shrinks, and long wavelength modes exit the cosmological horizon and become inaccessible in the physical Hilbert space of an observer. This is another way where unitarity can be broken in the context of inflation, and it would be highly interesting to understand this. On the theoretical side, it would be interesting to see if this give rise to some sort of information paradox similar to the famous black hole information paradox [171]. On the observational side, since we do not have access to the full information of the future conformal boundary of dS (i.e. all information at the end of inflation), it would be nice to see if this leaves any interesting imprints in the correlators, in particular whether the cosmological optical theorem is broken as a result.

In addition, for the analytic wavefunction, interesting future directions include:

- Understanding how the energy conservation condition extends to general cosmological spacetime, in particular dS. One way to proceed is to write the wavefunction for the cosmological spacetime as an operator acting on the flat space wavefunction. If the operator is simply a differential operator then things are simple: the differentiation does not introduce new singularities so the cosmological wavefunction inherits the analytic structure of the flat space wavefunction. However if the operator is an integral operator then things are less straightforward. For example, it has been proposed that the wavefunction for any FLRW spacetime can be written in terms of an integral of the flat space wavefunction [80]. Such a representation is written down for the recursion representation of the wavefunction, where it can be computed by using intersection theory [172] or differential equations [73, 173]. This representation also allow us to study the space of functions which appear in the wavefunction using the symbol technology, and this is studied extensively in de Sitter [174]. Therefore, when we try and study the singularity structure of the wavefunction by Landau analysis, we need to include the endpoint singularities of these extra integrals as well as any singularities (especially branch points) coming from the integration kernel.
- Understanding the wavefunction-type singularities. While it is clear for one loop diagrams that wavefunction-type singularities are always total energy branch points, this is less clear for general diagrams. It would be nice to have a systematic understanding of wavefunction-type singularities for general diagram. This would potentially tell us whether the cosmological KLN theorem can be used to remove all wavefunction-type singularities for in-in correlators at all order. In addition it would be nice to see whether this cancellation works for in-in correlators for general cosmological spacetime as well.

- Understanding the wavefunction in terms of master integrals. It is known that any one loop amplitude can be written in terms of a few master integrals [175, 176]. It would be useful to understand if this is also true for wavefunction using the amplitude representation of the wavefunction. Naively such a statement should also be true for wavefunctions as well: we can first decompose the amplitude-like part of the wavefunction (6.1.11) into master integrals, and then fix the energies using the energy-fixing kernel. If the amplitude-like part has no new poles in terms of internal energies s, then the wavefunction can easily be written in terms of master integrals as well.
- Understanding how different physical principles (for example unitarity) are encoded in the complex plane of external energy. For example, the discontinuity of an amplitude in the complex s-plane must be larger than zero by unitarity. Combined with the UV/IR sum rules this allow us to construct positivity bounds for amplitudes. For wavefunction this is a lot less clear: the cosmological optical theorem is a relation between the Disc of the wavefunction, and the Disc operator is not a regular discontinuity. In fact, the Disc operator analytically continues all of the external energies (and in some cases internal energy as well). In order to understand how the cosmological optical theorem manifests itself in the language of the analytic wavefunction, we may need to understand the analyticity of the wavefunction when we simultaneously analytically continue multiple external energies.

These are some of the future directions in a technical standpoint. But there is a larger question which the cosmological bootstrap community should address: whether we as a community should be focusing on bootstrapping the wavefunction. The main advantage of working with the wavefunction is that it is simpler to work with in perturbation theory (as the number of diagrams do not proliferate with the number of verticies of the Feynman diagram), its connection to holography [121] as well as positive geometry (see [80–82,84,85,163,177]). However, generalizing the results of the cosmological bootstrap beyond perturbation theory from the wavefunction perspective proved to be difficult: due to the difficulties described in 3.5 the holography perspective has not given us much progress. And while the connection to positive geometry is nice from a purely theoretical standpoint, it is not immediately apparent that it offers a significant advantage in imposing bounds on a practical level.

Working with in-in correlators have given us some success (example includes [122,123] which give some non-perturbative results for unitarity). In particular, under some simple assumptions it is possible to write in-in correlators in terms of in-out correlators [105]. In those cases the number of Feynman diagrams no longer increase exponentially since we are working with in-out correlators, and many new results (such as cutting rules for correlators) have been found. In addition this give us hope in defining some sort of S-matrix for dS in the Poincare patch ¹. Even though we do not measure this S-matrix directly, for the purpose of constructing positivity bounds these objects may be simpler to work with, as it may be easier to import technology from the S-matrix bootstrap to these objects instead.

Because of these recent developments, it may be worth considering whether the community should focus more effort in bootstrapping the wavefunction, or try to work with in-in correlators or some form of S-matrix. One of the main goals of the cosmological bootstrap is to come up with concrete tests for inflations. If we are unable to connect to cosmological observations, that defeats the whole purpose of this program.

¹There have been a few other proposals of S-matrix in dS, see [79,178–180]

Appendix A

Time derivatives

When the interaction is allowed to involve time derivatives this introduces derivatives on the Green's function that potentially alter the analysis as it is no longer immediately possible to exploit the result from (3.1.24). Instead it is necessary to understand the behaviour of terms like

$$\operatorname{Im}\left[\partial_{\eta}^{N}\partial_{\eta'}^{M}G_{p}(\eta,\eta')\right]. \tag{A.0.1}$$

This generalisation is simpler than it might seem as the energies are the only complex variables and therefore complex conjugation commutes with the time derivatives and so derivatives of K and G will remain Hermitian analytic,

$$\left[\partial_{\eta}^{N} K_{-k^{*}}(\eta)\right]^{*} = \partial_{\eta}^{N} K_{-k^{*}}^{*}(\eta) = \partial_{\eta}^{N} K_{k}(\eta), \qquad (A.0.2)$$

$$\left[\partial_{\eta}^{N} \partial_{\eta'}^{M} G_{-p^{*}}(\eta, \eta')\right]^{*} = \partial_{\eta}^{N} \partial_{\eta'}^{M} G_{-p^{*}}^{*}(\eta, \eta') = \partial_{\eta}^{N} \partial_{\eta'}^{M} G_{p}(\eta, \eta'). \tag{A.0.3}$$

Likewise, we can explore the imaginary part of G for real p,

$$\operatorname{Im}\left[\partial_{\eta}^{N}\partial_{\eta'}^{M}G_{p}(\eta,\eta')\right] = \partial_{\eta}^{N}\partial_{\eta'}^{M}\operatorname{Im}\left[G_{p}(\eta,\eta')\right]$$
(A.0.4)

$$=2P_p\operatorname{Im}\partial_{\eta}^{N}K_p(\eta)\operatorname{Im}\partial_{\eta'}^{M}K_p(\eta'). \tag{A.0.5}$$

From this it is apparent that we can cut lines involving time derivatives in exactly the same way as nonderivative interactions, except each of the diagrams must include the derivatives previously associated with the bulk-to-bulk propagator on the the external lines that are introduced. We can further clarify this by looking at the full wavefunction coefficient,

$$\psi_n(\{k\};\{p\};\{k\}) = i \int \left(\prod_A^V d\eta_A F_A(\mathbf{k}) \right) \left(\prod_a^n K_{k_a}^{(N_a)} \right) \left(\prod_m^I G_{p_m}^{(N_m,M_m)} \right) . \tag{A.0.6}$$

Where we have introduced the notation

$$K^{(N)}(\eta) = \partial_{\eta}^{N} K(\eta) \tag{A.0.7}$$

whilst suppressing the η dependence. This has an imaginary discontinuity arising from cutting the internal line with momentum **S** given by

$$\operatorname{Disc}_{S} i \psi_{n+m}(\{k\}; p_{1}, \dots, S, \dots, p_{I}; \{\mathbf{k}\})$$

$$= i \int \left(\prod_{A}^{V} d \eta_{A} F_{A}(\mathbf{k}) \right) \left(\prod_{a}^{n+m} K_{k_{a}}^{(N_{a})} \right) \left(\prod_{l}^{I} G_{p_{l}}^{(N_{l}, M_{l})} \right) \left(i G_{S}^{(N, M)} - i \left[G_{S}^{(N, M)} \right]^{*} \right)$$

$$= i P_{S} \int \left(\prod_{A}^{V} d \eta_{A} F_{A}(\mathbf{k}) \right) \left(\prod_{a}^{n+m} K_{k_{a}}^{(N_{a})} \right) \left(\prod_{l}^{I} G_{p_{l}}^{(N_{l}, M_{l})} \right) \left(K_{S}^{(N)} - K_{S}^{(N)}^{*} \right) \left(K_{S}^{(M)} - K_{S}^{(M)}^{*} \right)$$

$$= -i P_{S} \operatorname{Disc}_{S} \left[i \psi_{n+1} \left(k_{1}, \dots, k_{n}, S; \{p\}; \{\mathbf{k}\} \right) \right] \operatorname{Disc}_{S} \left[i \psi_{m+1} \left(S, k_{1}, \dots, k_{m}; \{p\}; \{\mathbf{k}\} \right) \right]. \tag{A.0.8}$$

This is the same as the expression with non time-derivative interactions except the propagators are now allowed to have derivatives. Therefore, the single-cut rules derived in the previous section apply to any derivative interactions as well. The generalization to time derivatives for spinning fields proceeds similarly as the modefunctions remain Hermitian analytic and the vertex terms are time independent.

Appendix B

WKB solution to the Klein Gordon equation for flat FLRW spacetime

As a demonstration of the Hermitian analyticity of the bulk-to-boundary propagator with Bunch-Davies initial conditions, we consider the case $p(k,\eta)=2\frac{a'}{a}$ and $q(k,\eta)=c_s^2(\eta)k^2+m^2$, i.e. the case where ϕ satisfy the Klein Gordon equation in an arbitrary flat FLRW spacetime. (One can also carry out the same procedure for the Mukhanov Sasaki equation by replacing the scale factor with $z=\frac{a\bar{\phi}}{H}$.) The equation we have is:

$$\phi'' + 2\frac{a'}{a}\phi' + (c_s^2k^2 + m^2a^2)\phi = 0.$$
(B.0.1)

Re-writing this in terms of $f = a\phi$, we find

$$f'' + \left(c_s^2 k^2 + m^2 a^2 - \frac{a''}{a}\right) f = 0.$$
 (B.0.2)

For solutions of the form $f = Ce^{ik\sigma(k,\eta)}$ this becomes

$$(c_s^2 - \sigma'^2) + \frac{i}{k}\sigma'' + \frac{1}{k^2}\left(m^2a^2 - \frac{a''}{a}\right) = 0.$$
(B.0.3)

Since we are interested in the case where the mode function approaches $e^{ik\eta}$ in the far past, we make the following ansatz:

$$\sigma(k,\eta) = \pm \sigma_0(\eta) + \frac{1}{k}\sigma_1(\eta) + \frac{1}{k^2}\sigma_2(\eta) + \frac{1}{k^3}\sigma_3(\eta) + \frac{1}{k^4}\sigma_4(\eta) + \dots,$$
 (B.0.4)

where

$$\sigma_0(\eta) = \int_{-\infty}^{\eta} d\bar{\eta} \, c_s(\bar{\eta}). \tag{B.0.5}$$

We will focus on the solution with + sign for now, though the negative solution can be easily obtained by complex conjugation.

At
$$\mathcal{O}(k^{-1})$$
 (B.0.3) tells us that

$$\frac{2c_s}{k}\sigma_1' = 0. (B.0.6)$$

This means that σ_1 is constant unless c_s vanishes somewhere in the bulk. This constant can be absorbed into the normalization of the mode function, so we will ignore its contribution.

At $\mathcal{O}(k^{-2})$ we have:

$$-2c_s(\eta)\sigma_2' + \left(m^2 a^2 - \frac{a''}{a}\right) = 0,$$
(B.0.7)

$$\sigma_2 = \frac{1}{2} \int_{-\infty}^{\eta} d\bar{\eta} \frac{1}{c_s(\bar{\eta})} \left(m^2 a(\bar{\eta})^2 - \frac{a''(\bar{\eta})}{a(\bar{\eta})} \right). \tag{B.0.8}$$

Since everything within the integral is real, we expect σ_2 to be real as well.

At $\mathcal{O}(k^{-3})$ we have:

$$-2c_s\sigma_3' + i\sigma_2'' = 0, (B.0.9)$$

$$\sigma_3 = \frac{i}{2} \int_{-\infty}^{\eta} d\bar{\eta} \frac{\sigma_2''(\bar{\eta})}{c_s(\bar{\eta})}.$$
 (B.0.10)

Since everything within the integral is real, σ_3 is pure imaginary. In general we have the following:

$$\sigma_r = \frac{1}{2} \int_{-\infty}^{\eta} d\bar{\eta} \frac{1}{c_s(\bar{\eta})} (i\sigma_{r-1}^{"}(\bar{\eta}) - \sum_{m+n=r} \sigma_m^{'}(\bar{\eta})\sigma_n^{'}(\bar{\eta})). \tag{B.0.11}$$

By induction, we see that σ_r must be real for even r and pure imaginary for odd r. Therefore, as long as this series expansion converges, we conclude that $\sigma(k, \eta)$ is Hermitian analytic.

Since $K(k,\eta) = \frac{\phi^+(k,\eta)}{\phi^+(k,\eta_0)}$, in terms of the function $f(k,\eta)$ this is simply

$$K(k,\eta) = \frac{a(\eta_0)e^{ik\sigma_{+}(k,\eta)}}{a(\eta)e^{ik\sigma_{+}(k,\eta_0)}}.$$
(B.0.12)

Now since the scale factor is real, and σ is Hermitian analytic, the bulk-to-boundary propagator is Hermitian analytic.

As an example of how this WKB expansion gives us the mode function, let us consider the case of a massless scalar in de Sitter space with $c_s=1$. For de Sitter, $a=\frac{1}{H\eta}$, therefore $\frac{a''}{a}=\frac{2}{\eta^2}$. Since $m^2=0$, we have:

$$\sigma_2 = \frac{1}{2} \int_{-\infty}^{\eta} d\eta' \left(\frac{-2}{\eta'^2}\right) = \frac{1}{\eta}.$$
 (B.0.13)

Taking this result, we can obtain the other σ_r order by order:

$$\sigma_{3} = \frac{i}{2} \int_{-\infty}^{\eta} d\eta' \left(\frac{1}{\eta}\right)'' = \frac{i}{2} \int_{-\infty}^{\eta} d\eta' \left(\frac{2}{\eta^{3}}\right) = \frac{-i}{2\eta^{2}},$$

$$\sigma_{4} = \frac{1}{2} \int_{-\infty}^{\eta} d\eta' \left[i \frac{-3i}{\eta^{4}} - \frac{1}{\eta^{4}}\right] = \frac{-1}{3\eta^{3}}.$$
(B.0.14)

With the help of combinatorics and using induction, we can see that:

$$\sigma_r = \frac{(-i)^r}{2} \int_{-\infty}^{\eta} d\eta' \left[\frac{r-1}{\eta^r} - \frac{r-3}{\eta^r} \right] = \frac{-(-i)^r}{(r-1)\eta^{r-1}}.$$
 (B.0.15)

Therefore, we have:

$$ik\sigma(k,\eta) = ik\eta - ik\sum_{r=2}^{\infty} \frac{(-i)^r}{(r-1)\eta^{r-1}k^r}$$

$$= ik\eta - \sum_{r=1}^{\infty} \frac{(-i)^r}{r(k\eta)^r}$$

$$= ik\eta + \log\left(1 + \frac{i}{k\eta}\right),$$

$$f = Ce^{ik\sigma} = Ce^{ik\eta}\left(1 + \frac{i}{k\eta}\right).$$
(B.0.16)

Setting $C=-ik/\sqrt{2k^3},$ and remembering that $\phi=f/a,$ we have

$$\phi = \frac{H}{\sqrt{2k^3}} (1 - ik\eta)e^{ik\eta},\tag{B.0.17}$$

which is the usual de Sitter mode function of a massless scalar.

Appendix C

Tensor structure

The I tensors that result from the single-field loop integral are totally symmetric and can only depend on the vector \mathbf{s} , so they take the form of sums of products of s_i and δ_{ij} . The momentum integrals are computed in dimensional regularisation; when the integrand is not a scalar, this makes it more difficult to compute the integral. In this appendix, we determined the coefficients of the products of s_i and δ_{ij} in terms of contractions of the I tensors with other powers of s_i and δ_{ij} .

Three indicies As a first example consider:

$$I_{ijk} = I_1^{(3)} \left(\frac{s_i}{s} \delta_{jk} + \frac{s_j}{s} \delta_{ik} + \frac{s_k}{s} \delta_{ij} \right) + I_3^{(3)} \frac{s_i s_j s_k}{s^3}.$$
 (C.0.1)

To find $I_1^{(3)}$ and $I_3^{(3)}$, we contract I_{ijk} with δ_{ij} and s_i . The calculation is straightforward and give:

$$T_1 := \frac{\delta_{ij}s_k}{s}I_{ijk} = 5I_1^{(3)} + I_3^{(3)},$$
 (C.0.2)

$$T_3 := \frac{s_i s_j s_k}{s^3} I_{ijk} = 3I_1^{(3)} + I_3^{(3)}. \tag{C.0.3}$$

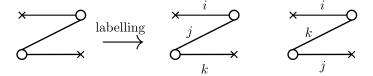
Therefore, we have:

$$I_1^{(3)} = \frac{T_1 - T_3}{2},$$
 $I_3^{(3)} = \frac{-3T_1 + 5T_3}{2}.$ (C.0.4)

While it is entirely possible to carry out the same calculation for tensor structure with more indicies with brute force, it is beneficial to introduce a diagrammatic way of representing the contractions [3]. The diagrammatic rules are summarised below. Diagrams will be drawn in two columns, with tensors on the left representing those contracted into the factors in I on the right.

Since I is totally symmetric, the symmetry factor for each diagram corresponds to the number of distinct ways of assigning labels (indices) to the internal lines whilst preserving the index structure on the left—i.e.

the indices that meet at any vertex there. For example, the following diagram, which appears in $\frac{1}{s}s_i\delta_{jk}I_{ijk}$, has symmetry factor 2:



The calculation for the three indicies tensor structure can be represented in the following diagrammatic way:

Four indices The diagrammatic method simplifies calculation of the I tensors with more indices. The diagrams themselves are omitted here for brevity.

With four indices,

$$I_{ijkl} = I_0^{(4)} \left(\delta_{ij} \delta_{kl} + 2 \text{ perms} \right) + I_2^{(4)} \left(\frac{s_i s_j}{s^2} \delta_{kl} + 5 \text{ perms} \right) + I_4^{(4)} \frac{s_i s_j s_k s_l}{s^4}. \tag{C.0.5}$$

Using T_n to denote a trace with $n \frac{s_i}{s}$ s, then,

$$T_0 = \delta_{ij}\delta_{kl}I_{ijkl} = 15I_0^{(4)} + 10I_2^{(4)} + I_4^{(4)}, \qquad (C.0.6)$$

$$T_2 = \frac{s_i s_j}{s^2} \delta_{kl} I_{ijkl} = 5I_0^{(4)} + 8I_2^{(4)} + I_4^{(4)}, \qquad (C.0.7)$$

$$T_4 = \frac{s_i s_j s_k s_l}{s_4^4} I_{ijkl} = 3I_0^{(4)} + 6I_2^{(4)} + I_4^{(4)}, \tag{C.0.8}$$

so that

$$I_0^{(4)} = \frac{1}{8} (T_0 - 2T_2 + T_4) ,$$
 (C.0.9)

$$I_2^{(4)} = \frac{1}{8} \left(-T_0 + 6T_2 - 5T_4 \right) ,$$
 (C.0.10)

$$I_4^{(4)} = \frac{1}{8} (3T_0 - 30T_2 + 35T_4).$$
 (C.0.11)

Five indices At this point, the number of terms starts to become large, and the diagrammatic approach begins to pay off.

$$I_{ijklm} = \frac{I_1^{(5)}}{s} \left(s_i \delta_{jk} \delta_{lm} + 14 \text{ perms} \right) + \frac{I_3^{(5)}}{s^3} \left(s_i s_j s_k \delta_{lm} + 9 \text{ perms} \right) + \frac{I_5^{(5)}}{s^5} s_i s_j s_k s_l s_m.$$
 (C.0.12)

Using the notation established above,

$$T_1 = 35I_1^{(5)} + 14I_3^{(5)} + I_5^{(5)},$$
 (C.0.13)

$$T_3 = 21I_1^{(5)} + 12I_3^{(5)} + I_5^{(5)},$$
 (C.0.14)

$$T_5 = 15I_1^{(5)} + 10I_3^{(5)} + I_5^{(5)}.$$
 (C.0.15)

This yields

$$I_1^{(5)} = \frac{1}{8} (T_1 - 2T_3 + T_5) ,$$
 (C.0.16)

$$I_3^{(5)} = \frac{1}{8} \left(-3T_1 + 10T_3 - 7T_5 \right) ,$$
 (C.0.17)

$$I_5^{(5)} = \frac{1}{8} (15T_1 - 70T_3 + 63T_5).$$
 (C.0.18)

Six indices Now,

$$I_{ijklmn} = I_0^{(6)} \left(\delta_{ij} \delta_{kl} \delta_{mn} + 14 \text{ perms} \right) + \frac{I_2^{(6)}}{s^2} \left(s_i s_j \delta_{kl} \delta_{mn} + 44 \text{ perms} \right) + \frac{I_4^{(6)}}{s^4} \left(s_i s_j s_k s_l \delta_{mn} + 14 \text{ perms} \right) + \frac{I_6^{(6)}}{s^6} s_i s_j s_k s_l s_m.$$
(C.0.19)

The required traces are

$$T_0 = 105I_0^{(6)} + 105I_2^{(6)} + 21I_4^{(6)} + I_6^{(6)}, (C.0.20)$$

$$T_2 = 32I_0^{(6)} + 77I_2^{(6)} + 19I_4^{(6)} + I_6^{(6)},$$
 (C.0.21)

$$T_4 = 21I_0^{(6)} + 57I_2^{(6)} + 17I_4^{(6)} + I_6^{(6)},$$
 (C.0.22)

$$T_6 = 15I_0^{(6)} + 45I_2^{(6)} + 15I_4^{(6)} + I_6^{(6)}.$$
 (C.0.23)

Thus,

$$I_0^{(6)} = \frac{1}{57} (T_0 - 3T_2 + 3T_4 - T_6),$$
 (C.0.24)

$$I_2^{(6)} = \frac{1}{456} \left(-5T_0 + 72T_2 - 129T_4 + 62T_6 \right),$$
 (C.0.25)

$$I_4^{(6)} = \frac{1}{76} (T_0 - 60T_2 + 155T_4 - 96T_6), \text{ and}$$
 (C.0.26)

$$I_6^{(6)} = \frac{1}{152} (5T_0 + 840T_2 - 2835T_4 + 2142T_6).$$
 (C.0.27)

Appendix D

Explicit computations for one loop wavefunctions

In this appendix we describe how to compute the one loop wavefunctions by doing the momentum integrals explicitly.

D.1 Classifying complexity

The majority of the loop integrals that we encounter below cannot be written in terms of elementary functions. It will be useful, therefore, to introduce a taxonomy for the various kinds of special functions which can arise in a given ψ_n . In particular, whenever an integral can be written in the following form,

$$\mathcal{I} = \int_{1}^{\infty} dp \int_{-1}^{+1} dz_{1} \dots \int_{-1}^{+1} dz_{\mathcal{T}-1} \frac{R(p, z_{1}, \dots, z_{\mathcal{T}-1})}{\text{Poly}_{2\mathcal{G}+2}(p, z_{1}, \dots, z_{\mathcal{T}-1})},$$
 (D.1.1)

where R is a rational function of its arguments and Poly_N represents a polynomial which is at most order N in any one of its arguments, then we say that \mathcal{I} has a degree of transcendentality \mathcal{T} and a genus \mathcal{G} . Roughly speaking, \mathcal{T} counts the number of integrals and \mathcal{G} counts the number of independent square roots appearing in the integrand. The lower each of these numbers, the closer the integral will be to familiar elementary functions.

In Fig. D.1(a) we give some examples of special functions with different \mathcal{T} and \mathcal{G} . In particular, for genus $\mathcal{G} = 0$, an integral with degree of transcendentality \mathcal{T} can possess polylogarithmic-type branch cuts of a polylog $\text{Li}_{\mathcal{T}}$, where \mathcal{T} determines the weight of the polylogarithm. For $\mathcal{T} = 1$, (D.1.1) represents the so-called "hyperelliptic integrals", where the degree $2\mathcal{G} + 2$ polynomial in the denominator is called "hyperlliptic curve of genus \mathcal{G} ".

When both $\mathcal{T} > 1$ and $\mathcal{G} > 0$ much less is known about integrals of the form (D.1.1), and the labels \mathcal{T} and \mathcal{G} give a useful measure of "how complicated" each integral is. For instance, we will show below that the three-point wavefunction coefficient at one-loop, $\psi_3^{\text{1-loop}}$, generically has $\mathcal{T} = 3$ and $\mathcal{G} = 3$ in d = 3 spatial dimensions, so in principle would require knowledge of the special functions which correspond to three iterated integrals over a hyperelliptic curve of genus 3. A dedicated study of the properties of such functions would certainly be interesting (particularly in light of the myriad connections between amplitude

	$\mathcal{T}=1$	$\mathcal{T}=2$		\mathcal{T}
G = 0	Logarithm	Dilogarithm		Polylogarithm
	$\log(z)$	$\mathrm{Li}_2(z)$		$\operatorname{Li}_{\mathcal{T}}(z)$
G = 1	Elliptic integral	Integral of elliptic integral		Integrals of elliptic integral
	$\Pi(z)$	$\int \frac{dz}{z} \Pi(z)$		$\left[\int \frac{dz}{z}\right]^{\mathcal{T}-1} \Pi(z)$
$\mathcal{G}=2$	Hyperelliptic integral	Integral of hyperelliptic integral		i:
:				·. <u>.</u>

Table D.1: To organise the special functions which arise when performing the loop integrals, we introduce a degree of transcendentality, \mathcal{T} , and a genus, \mathcal{G} , as in (D.1.1). Above we give some simple examples of functions in each class, and in Table D.2 we summarise how the first three wavefunction coefficients ψ_1, ψ_2, ψ_3 (and their various massless and soft limits) populate these classes.

Feynman integrals and pure mathematics), but here we will restrict our attention to integrals that can be written in terms of $\mathcal{G}=0$ or $\mathcal{T}=1$ functions only. In the case of $\psi_3^{\text{1-loop}}$ in d=3 dimensions, we will see that taking a combination of soft and massless limits can reduce $(\mathcal{T},\mathcal{G})$ to (2,0), and we can therefore give an explicit expression in terms of dilogarithms (see (D.4.19)).

D.2 One internal edge

For loop diagrams with only a single internal edge (of mass M), the integrand depends on the loop momenta through only a single $\Omega_p = \sqrt{p^2 + M^2}$. Since this is a function of $p = |\mathbf{p}|$ only, the d-1 angular components of the loop integration can be performed immediately, giving,

$$\int \frac{d^d \mathbf{p}}{(2\pi)^d} I(\Omega_p) = \frac{S_{d-1}}{(2\pi)^d} \int_0^\infty dp \, p^{d-1} I(\Omega_p), \tag{D.2.1}$$

where S_{d-1} is the surface area of a (d-1)-dimensional unit sphere,

$$S_{d-1} = \frac{\pi^{d/2}}{\Gamma\left(\frac{d}{2}\right)},\tag{D.2.2}$$

which takes the usual value of $S_2 = 4\pi$ in d = 3 spatial dimensions.

For instance, consider the contribution from the one-loop diagram given in (5.3.11).

$$\omega \psi_1^{\text{1-loop}}(\omega) = \frac{S_{d-1}}{(2\pi)^d} \int_0^\infty dp \, \frac{p^{d-1}}{\omega + 2\Omega_p}.$$
 (D.2.3)

This integral has $\mathcal{G}(\psi_1^{\text{1-loop}}) = 0$ and $\mathcal{T}(\psi_1^{\text{1-loop}}) = 1$ in any d, The single square root in the denominator can be removed by a change of variables, and the resulting integral can be straightforwardly performed in

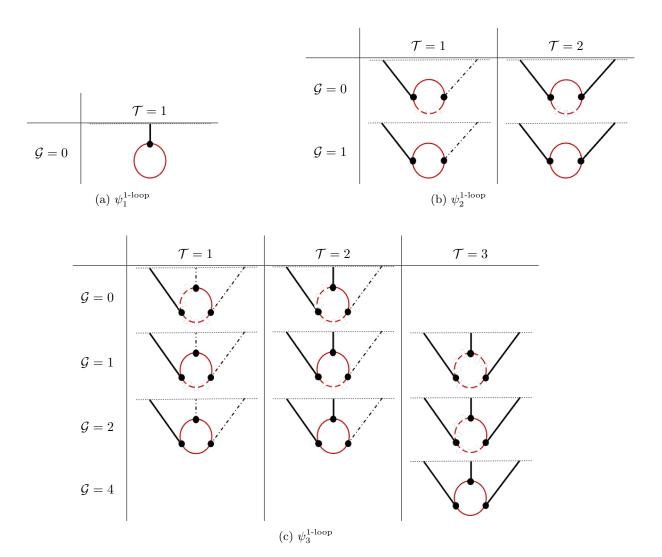


Table D.2: The degree of transcendentality \mathcal{T} and genus \mathcal{G} of the different one-loop diagrams computed in App. D. A dashed internal line denotes a massless field, and a dot-dashed external line denotes a soft limit in which that field carries zero spatial momentum.

any integer d with a hard cut-off, $\int_0^\infty dp \to \int_0^\Lambda dp$. For instance, in d=3 dimensions¹,

$$\omega \psi_1^{1-\text{loop}}(\omega)|_{d=3} = \frac{1}{16\pi^2} \left[2\Lambda(\Lambda - \omega) + \left(\omega^2 - 2M^2\right) \log\left(\frac{2\Lambda}{M}\right) + 2\omega\sqrt{4M^2 - \omega^2} \arcsin\left(\sqrt{\frac{2M - \omega}{4M}}\right) + M^2 \right] , \quad (D.2.5)$$

and in d = 1 dimensions,

$$\omega \psi_1^{\text{1-loop}}(\omega)|_{d=1} = \frac{1}{4\pi} \left[\log\left(\frac{2\Lambda}{M}\right) - \frac{2\omega \arcsin\left(\sqrt{\frac{2M-\omega}{4M}}\right)}{\sqrt{4M^2 - w^2}} \right] . \tag{D.2.6}$$

In any number of dimensions, $\omega \psi_1^{\text{1-loop}}$ is an analytic function of ω except for branch points at $\omega = -2M$ and $\omega = -\infty$, which can be connected by a cut along the negative real axis. In particular, note that (D.2.5) and (D.2.6) are analytic at $\omega = +2M$, since $\sqrt{2M-\omega}$ arcsin $\left(\sqrt{\frac{2M-\omega}{4M}}\right) = \sum_j (2M-\omega)^j$ for positive integer powers j.

D.3 Two internal edge

For a one-loop diagram with two vertices, the integrand depends on a single loop momentum through two independent combinations, namely the energies associated with the momenta $\{\mathbf{q}_1, \mathbf{q}_2\}$ of the internal lines, where momentum conservation fixes their difference to be equal to the external momentum, $\mathbf{q}_1 - \mathbf{q}_2 = \mathbf{k}$,

$$\int \frac{d^d \mathbf{q}_1 d^d \mathbf{q}_2}{(2\pi)^d (2\pi)^d} \mathcal{I}(\Omega_{q_1}, \Omega_{q_2}) (2\pi)^d \delta_D^{(d)} (\mathbf{q}_1 - \mathbf{q}_2 - \mathbf{k}). \tag{D.3.1}$$

Note that Ω_{q_1} and Ω_{q_2} are only independent in d > 1 spatial dimensions.

D.3.1 Generalities

Integration variables. Integrals of the form (D.3.1) can be simplified by choosing an appropriate set of integration variables. When $d \ge 2$, it is possible to choose the two lengths $\{q_1, q_2\}$ (together with a further d-2 angular co-ordinates on which the integrand does not depend). Given the momentum conservation constraint, the three lengths $\{q_1, q_2, k\}$ must correspond to the edges of a triangle, as shown in Fig. D.1. The domain of integration for $\{q_1, q_2\}$ can then be determined by the condition that such a triangle exists, namely that the three triangle inequalities are satisfied²,

$$q_1 + q_2 \ge k$$
, $q_1 + k \ge q_2$, $q_2 + k \ge q_1$. (D.3.2)

$$\arctan\left(\frac{2M+\omega}{\sqrt{4M^2-\omega^2}}\right)-\arctan\left(\frac{\omega}{\sqrt{4M^2-\omega^2}}\right)=\arcsin\left(\sqrt{\frac{2M-\omega}{4M}}\right) \tag{D.2.4}$$

in order to make the non-analyticity at $\omega=-2M$ manifest.

¹Symbolic manipulation packages like Mathematica will often return a sum of arctan functions, which can be simplified using trigonometric relations like,

²Given three positive numbers $\{q_1, q_2, k\}$, (D.3.2) is a necessary and sufficient condition for a triangle with these edge lengths to exist. It can also be written as a single non-linear condition, namely that the area of the formed triangle is positive, cf. (D.4.3).

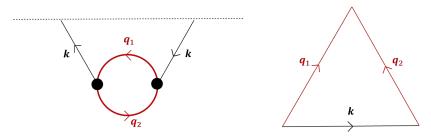


Figure D.1: The one-loop contribution to $\psi_2^{\text{1-loop}}$ with two internal lines is described by three momenta which, as vectors, form the edges of a triangle due to momentum conservation.

Note that these inequalities are only saturated when the triangle degenerates into a line.

To change from $\{\mathbf{q}_1, \mathbf{q}_2\}$ to these variables, we can parametrise the two internal momenta as,

$$\mathbf{q}_1 = \frac{1}{2} (\mathbf{p} + \mathbf{k}) , \quad \mathbf{q}_2 = \frac{1}{2} (\mathbf{p} - \mathbf{k}) ,$$
 (D.3.3)

and then align one of our co-ordinate axes along k, adopting the polar parametrisation,

$$\mathbf{k} = \begin{pmatrix} k \\ \mathbf{0}_{d-1} \end{pmatrix}, \quad \mathbf{p} = \begin{pmatrix} q_{+} \cos \vartheta \\ \sqrt{q_{+}^{2} - k^{2}} \sin \vartheta \hat{\mathbf{p}}_{d-1} \end{pmatrix}, \tag{D.3.4}$$

where $\hat{\mathbf{p}}_{d-1}$ is a unit vector in the (d-1) directions orthogonal to \mathbf{k} and $\mathbf{0}_{d-1} = (0, ..., 0)$ is the vector of (d-1) zeroes. Integrating over the undetermined loop momentum \mathbf{p} is then equivalent to integrating over $\{q_+, \vartheta, \hat{\mathbf{p}}_{d-1}\}$, where

$$q_{+} = q_1 + q_2, \quad k \cos \vartheta = q_1 - q_2,$$
 (D.3.5)

and so surfaces of constant q_+ correspond to ellipses (with foci separated by \mathbf{k}) and ϑ is the eccentric anomaly of a point on each ellipse. We will often use the notation $q_- = q_1 - q_2$ in place of the angular $k \cos \vartheta$.

In practice, this allows us to write integrals of the form (D.3.1) as an integral over two scalars³,

$$\int \frac{d^{d}\mathbf{p}}{(2\pi)^{d}} \, \mathcal{I}(\Omega_{q_{1}}, \Omega_{q_{2}}) = \frac{S_{d-2}}{(2\pi)^{d}} \int_{k}^{\infty} dq_{+} \int_{-k}^{+k} \frac{dq_{-}}{2k} \, q_{1}^{d-2} q_{2} \, \mathcal{I}(\Omega_{q_{1}}, \Omega_{q_{2}}) \, \big|_{\substack{q_{1} = \frac{1}{2}(q_{+} + q_{-}) \\ q_{2} = \frac{1}{2}(q_{+} - q_{-})}}, \tag{D.3.7}$$

where the integration region has been determined using the triangle inequalities, (D.3.2).

Finally, when considering massive fields it is often convenient to replace q_{\pm} with the total/relative energy, $\Omega_{q_1} \pm \Omega_{q_2}$, which we denote by,

$$\Omega_{\pm} = \sqrt{q_1^2 + M_1^2} \pm \sqrt{q_2^2 + M_2^2} \tag{D.3.8}$$

$$q_{\pm} = q_1 \pm \sqrt{k^2 + q_1^2 - 2q_1k\cos\theta} , \qquad (D.3.6)$$

³One simple way to find this Jacobian is to first express $d^d \mathbf{q}_1$ in terms of spherical polars about the **k** axis (i.e. set $\mathbf{q}_1 \cdot \mathbf{k} = q_1 k \cos \theta$), and then use the explicit change of variables,

The Jacobian between the two is straightforward,

$$(q_{+}^{2} - q_{-}^{2}) dq_{+} dq_{-} = (\Omega_{+}^{2} - \Omega_{-}^{2}) d\Omega_{+} d\Omega_{-}.$$
(D.3.9)

To find the integration region, we write \mathbf{q}_1 in polar co-ordinates about the \mathbf{k} axis (as in (D.3.6)),

$$q_1 = \frac{1}{2}\sqrt{(\Omega_+ + \Omega_-)^2 - 4M_1^2}, \qquad \cos \theta = -\frac{\Omega_+\Omega_- + k^2 + M_2^2 - M_1^2}{k\sqrt{(\Omega_+ + \Omega_-)^2 - 4M_1^2}}, \qquad (D.3.10)$$

which makes it clear that,

$$(\Omega_{+} + \Omega_{-})^{2} > 4M_{1}^{2}$$
 and $|\Omega_{+}\Omega_{-} + k^{2} + M_{2}^{2} - M_{1}^{2}| < k\sqrt{(\Omega_{+} + \Omega_{-})^{2} - 4M_{1}^{2}}$, (D.3.11)

and similarly for $M_1 \leftrightarrow M_2$. We can therefore write the allowed integration region as,

$$\int_{k}^{\infty} dq_{+} \int_{-k}^{k} \frac{dq_{-}}{k} \left(q_{+}^{2} - q_{-}^{2} \right) = \int_{\Omega_{k}}^{\infty} d\Omega_{+} \int_{-k}^{+k} \frac{\delta_{k}(\Omega_{+})}{k} \frac{d\Omega_{-}}{k} \left(\Omega_{+}^{2} - \Omega_{-}^{2} \right) , \qquad (D.3.12)$$

where,

$$\Omega_k = \sqrt{k^2 + (M_1 + M_2)^2},$$

$$\delta_k(\Omega_+) = \frac{\sqrt{\Omega_+^2 - k^2 - (M_1 - M_2)^2} \sqrt{\Omega_+^2 - \Omega_k^2}}{\Omega_+^2 - k^2} + \frac{\Omega_+}{k} \frac{|M_1^2 - M_2^2|}{\Omega_+^2 - k^2}.$$
(D.3.13)

In the case of equal masses, these simplify to,

$$\Omega_k = \sqrt{k^2 + 4M^2} , \quad \delta_k (\Omega_+) = \frac{\sqrt{\Omega_+^2 - \Omega_k^2}}{\sqrt{\Omega_+^2 - k^2}}.$$
(D.3.14)

To keep the following explicit expressions as succinct as possible, for the remainder of this subsection we are going to work with the rescaled variables,

$$\hat{\omega}_a = \frac{\omega_a}{\sqrt{k^2 + 4M^2}} \;, \; \hat{k} = \frac{k}{\sqrt{k^2 + 4M^2}} \;, \; \hat{m} = \frac{m}{\sqrt{k^2 + 4M^2}} \;, \; \hat{\Omega}_{\pm} = \frac{\Omega_{\pm}}{\sqrt{k^2 + 4M^2}} \;.$$
 (D.3.15)

Note that $0 \le \hat{k} \le 1$ is bounded in these variables, and since $4\hat{M}^2 = 1 - \hat{k}^2$ we can choose to write functions in terms of \hat{k} or \hat{M} as convenient. Altogether, (D.3.1) can therefore be written as,

$$\int \frac{d^{d}\mathbf{p}}{(2\pi)^{d}} \,\mathcal{I}(\Omega_{q_{1}},\Omega_{q_{2}}) = \frac{\Omega_{k}^{3}S_{d-2}}{8\hat{k}(2\pi)^{d}} \int_{1}^{\infty} d\hat{\Omega}_{+} \int_{-\hat{k}\delta_{k}(\Omega_{+})}^{+\hat{k}\delta_{k}(\Omega_{+})} d\hat{\Omega}_{-} \,\left(\hat{\Omega}_{+}^{2} - \hat{\Omega}_{-}^{2}\right) \,q_{1}^{d-3}\mathcal{I}\left(\Omega_{q_{1}},\Omega_{q_{2}}\right) \Big|_{\Omega_{q_{1}} = \frac{1}{2}k(\hat{\Omega}_{+} + \hat{\Omega}_{-})} \cdot \Omega_{q_{2}} = \frac{1}{2}k(\hat{\Omega}_{+} - \hat{\Omega}_{-}) \tag{D.3.16}$$

Master integrals. It is useful to define a small number of master integrals from which other, more complicated, integrals can be constructed. For $\psi_2^{\text{1-loop}}$, we define two such building blocks,

$$\mathcal{J}_{k}(B) = \int_{1}^{\infty} d\hat{\Omega}_{+} \int_{-\hat{k}\delta_{k}(\Omega_{+})}^{+\hat{k}\delta_{k}(\Omega_{+})} d\hat{\Omega}_{-} \frac{1}{\hat{\Omega}_{+} + B} ,$$

$$\mathcal{J}_{k}(A; B) = \int_{1}^{\infty} d\hat{\Omega}_{+} \int_{-\hat{k}\delta_{k}(\Omega_{+})}^{+\hat{k}\delta_{k}(\Omega_{+})} d\hat{\Omega}_{-} \frac{1}{(\hat{\Omega}_{+} + \hat{\Omega}_{-} + A)(\hat{\Omega}_{+} + B)} .$$
(D.3.17)

Other integrals can then be written straightforwardly in terms of these using partial fractions. For instance, consider,

$$\mathcal{I}(A; B_1, B_2) = \int_1^\infty d\hat{\Omega}_+ \int_{-\hat{k}\delta_k(\Omega_+)}^{+\hat{k}\delta_k(\Omega_+)} d\hat{\Omega}_- \frac{\hat{\Omega}_+^2 - \hat{\Omega}_-^2}{(\hat{\Omega}_+ + \hat{\Omega}_- + A)(\hat{\Omega}_+ + B_1)(\hat{\Omega}_+ + B_2)} . \tag{D.3.18}$$

Expanding the numerator in terms of the factors appearing in the denominator,

$$\Omega_{+}^{2} - \Omega_{-}^{2} = \left(\frac{B_{1} - A}{B_{1} - B_{2}}(\Omega_{+} + B_{2}) + \frac{B_{2} - A}{B_{2} - B_{1}}(\Omega_{+} + B_{1}) - \Omega_{-}\right)(\Omega_{+} + \Omega_{-} + A)
+ \frac{A(A - 2B_{1})}{B_{1} - B_{2}}(\Omega_{+} + B_{2}) + \frac{A(A - 2B_{2})}{B_{2} - B_{1}}(\Omega_{+} + B_{1})$$
(D.3.19)

immediately gives,

$$\mathcal{I}(A; B_1, B_2) = \frac{B_1 - A}{B_1 - B_2} \mathcal{J}_k(B_1) + \frac{B_2 - A}{B_2 - B_1} \mathcal{J}_k(B_2) + \frac{A(A - 2B_1)}{B_1 - B_2} \mathcal{J}_k(A; B_1) + \frac{A(A - 2B_2)}{B_2 - B_1} \mathcal{J}_k(A; B_2) . \tag{D.3.20}$$

The apparent poles at $B_1 = B_2$ are spurious: the only singularities in $\mathcal{I}(A; B_1, B_2)$ come from the master integrals $\mathcal{J}_k(B_j)$ and $\mathcal{J}_k(A; B_j)$. This is because the residue at $B_1 = B_2$ vanishes.

For simplicity let us focus on the case where $M_1 = M_2 = M$. The wavefunction can be computed from the following integral:

$$\omega_{12}\psi_2^{\text{1-loop}} = \int_{\mathbf{p}} \frac{1}{(\omega_1 + \Omega_{q_1} + \Omega_{q_2})(\omega_2 + \Omega_{q_2})} \left[\frac{1}{\omega_{12} + 2\Omega_{q_1}} + \frac{1}{\omega_{12} + 2\Omega_{q_2}} \right] . \tag{D.3.21}$$

The full computation is rather long, and interested readers can refer to [2] for details. Here I will quote the main results. The integral for $\psi_2^{\text{1-loop}}$ can be written as,

$$\omega_{12}\psi_{2}^{1-\text{loop}} = \frac{1}{16\pi^{2}} \left[2\tilde{\mathcal{J}}_{k} + 2\frac{\omega_{1}\tilde{\mathcal{J}}(\hat{\omega}_{2}) - \omega_{2}\tilde{\mathcal{J}}_{k}(\hat{\omega}_{1})}{\omega_{1} - \omega_{2}} - \frac{\omega_{12}}{k}\tilde{\mathcal{J}}_{k}(\hat{\omega}_{12}, \hat{\omega}_{1}) - \frac{\omega_{12}}{k}\tilde{\mathcal{J}}_{k}(\hat{\omega}_{12}, \hat{\omega}_{2}) \right]$$
(D.3.22)

where $\tilde{\mathcal{J}}_k$ is a simple logarithmic divergence given by

$$\tilde{\mathcal{J}}_k = \log\left(\frac{\Lambda}{M}\right)$$
 (D.3.23)

Table D.3: The location of singular points in the complex $\hat{\omega}_1$ plane of the three integrals from which $\psi_2^{\text{1-loop}}$ is constructed. The branch point at $\hat{\omega}_{12} = -2$ which develops in the massless limit is shown in red to indicate that it cancels out in the full $\psi_2^{\text{1-loop}}$. The singularity at $\hat{\omega}_1 = -1$ (i.e. $\omega_1 = -\sqrt{k^2 + 4M^2}$) predicted by the heuristic argument is present in all cases, and in the massless and soft limits there is also the singularity at $\omega_{12} = -2M$ predicted from the simpler one-edge loop.

 $\tilde{\mathcal{J}}_k(B)$ is an elliptic integral given by,

$$\tilde{\mathcal{J}}_{k}(\hat{\omega}) = -\frac{2i}{1-\hat{k}} \left[(\hat{\omega} - 1)\tilde{F}\left(\sqrt{\alpha_{k}}, \frac{1}{\alpha_{k}^{2}}\right) + 2\tilde{\Pi}\left(\sqrt{\alpha_{k}}, \frac{\hat{\omega} + 1}{\alpha_{k}(\hat{\omega} - 1)}, \frac{1}{\alpha_{k}^{2}}\right) \right] + \mathcal{O}\left(\hat{\omega}\right) , \qquad (D.3.24)$$

where we have discarded terms that are linear in ω (since these do not contribute to $\psi_2^{1-\text{loop}}$) and introduced the ratio,

$$\alpha_k = \frac{1 - \hat{k}}{1 + \hat{k}} \,. \tag{D.3.25}$$

 $\tilde{\mathcal{J}}_k(A;B)$ is an integral of an elliptic integral given by:

$$\partial_{\hat{\omega}_{1}} \mathcal{J}_{k}(\hat{\omega}_{12}, \hat{\omega}_{1}) = -\frac{4\hat{M}^{2}\hat{\omega}_{1}\hat{\omega}_{2}}{(\hat{\omega}_{1}^{2} - 1)\left(\hat{\omega}_{1}^{2} - \hat{k}^{2}\delta(\omega_{2})^{2}\right)} \frac{2\hat{k}\tilde{\mathcal{J}}_{k}(\hat{\omega}_{1})}{\hat{\omega}_{2}^{2} - \hat{k}^{2}\delta(\omega_{1})^{2}} - \frac{4\hat{M}^{2}}{\sqrt{\omega_{12}^{2} - 4M^{2}}} \frac{\bar{z}_{+,k}\bar{z}_{-,k}}{(\bar{z}_{+,k}^{2} - 1)(\bar{z}_{+,k} - \hat{\omega}_{1})} \frac{\tilde{\mathcal{J}}_{k}(\bar{z}_{+,k})}{2\bar{z}_{+,k} - \hat{\omega}_{12}} + \frac{4\hat{M}^{2}}{\sqrt{\omega_{12}^{2} - 4m^{2}}} \frac{\bar{z}_{+,k}\bar{z}_{-,k}}{(\bar{z}_{-,k}^{2} - 1)(\bar{z}_{-,k} - \hat{\omega}_{1})} \frac{\tilde{\mathcal{J}}_{k}(\bar{z}_{-,k})}{2\bar{z}_{-,k} - \hat{\omega}_{12}} - (k \leftrightarrow -k) , \qquad (D.3.26)$$

where the four \bar{z} are (minus) the roots of the D_k polynomial

$$D_k(\hat{\Omega}_+, \hat{\omega}_{12}) = (\hat{\Omega}_+ + \bar{z}_{+,k})(\hat{\Omega}_+ + \bar{z}_{-,k})(\hat{\Omega}_+ + \bar{z}_{+,-k})(\hat{\Omega}_+ + \bar{z}_{-,-k}). \tag{D.3.27}$$

and can be written explicitly as,

$$\bar{z}_{\pm,k}(\hat{\omega}_{12}) = \frac{\hat{\omega}_{12}}{2} \pm \sqrt{\frac{\hat{\omega}_{12}^2}{4} + \hat{k}^2 + \hat{k}\sqrt{\frac{\hat{\omega}_{12}^2}{4} - \hat{M}^2}}.$$
 (D.3.28)

The singularities of (D.3.22) can be summarized in table D.3.

There are two limits where all of the master integrals give elementary functions: the massless limit and the soft limit.

D.3.2 Massless limit

In this limit the master integrals in (D.3.17) can be evaluated immediately in terms of polylogarithms⁴,

$$\mathcal{J}_{1}(B) = \int_{1}^{\hat{\Lambda}} d\hat{q}_{+} \int_{-1}^{+1} d\hat{q}_{-} \frac{1}{B + \hat{q}_{+}} = 2 \log \left(\frac{\hat{\Lambda}}{B + 1} \right)$$

$$\mathcal{J}_{1}(A; B) = \int_{1}^{\infty} d\hat{q}_{+} \int_{-1}^{+1} d\hat{q}_{-} \frac{1}{(A + \hat{q}_{+} + \hat{q}_{-})(B + \hat{q}_{+})} = \text{Li}_{2} \left(\frac{B - A + 1}{B + 1} \right) - \text{Li}_{2} \left(\frac{B - A - 1}{B + 1} \right)$$
(D.3.30)

Both have a logarithmic branch point at B = -1, and $\mathcal{J}_1(A; B)$ has further dilogarithmic branch points at A = 0 and A = -2.

In this limit, $\mathcal{J}_k(\hat{\omega}_{12}; \hat{\omega}_1)$ retains the singularity at $\hat{\omega}_1 = -1$,

$$\lim_{k \to 1} \mathcal{J}_k(\hat{\omega}_{12}, \hat{\omega}_1) \sim \log^2(\hat{\omega}_1 + 1) \text{ near } \hat{\omega}_1 = -1,$$
 (D.3.31)

identified above for finite masses, but now it also acquires branch points at $\hat{\omega}_1 = -\hat{\omega}_2$ and $\hat{\omega}_1 = -\hat{\omega}_2 - 2$, where the dilogarithms are finite but not smooth. These non-analyticities are due to the $\tilde{\mathcal{J}}_k(\bar{z})$ terms in (D.3.26), since in the massless limit the four roots become,

$$\lim_{k \to 1} \bar{z}(\hat{\omega}_{12}) = \{-1, -1 + \hat{\omega}_{12}, 1 + \hat{\omega}_{12}, 1\} , \qquad (D.3.32)$$

and are now linear in ω_1 . However, note while $\mathcal{J}_k(\hat{\omega}_{12},\hat{\omega}_2)$ was previously analytic in ω_1 (at fixed finite mass), now this integral also develops branch points at $\hat{\omega}_1 = -\hat{\omega}_2$ and $\hat{\omega}_1 = -\hat{\omega}_2 - 2$. In particular, the residue of the $\hat{\omega}_1 = -\hat{\omega}_2 - 1$ branch points are equal and opposite, so that overall the sum of $\mathcal{J}_k(\hat{\omega}_{12};\hat{\omega}_1) + \mathcal{J}_k(\hat{\omega}_{12};\hat{\omega}_2)$ is actually analytic there. Concretely, the terms which are non-analytic at $\hat{\omega}_1 = -\hat{\omega}_2 - 2$,

$$\mathcal{J}_k(\hat{\omega}_{12}; \hat{\omega}_1) + \mathcal{J}_k(\hat{\omega}_{12}; \hat{\omega}_2) \supset \operatorname{Li}_2\left(-\frac{\hat{\omega}_1 + 1}{\hat{\omega}_2 + 1}\right) + \operatorname{Li}_2\left(-\frac{\hat{\omega}_2 + 1}{\hat{\omega}_1 + 1}\right)$$
(D.3.33)

partially cancel due to the dilogarithm identity,

$$\operatorname{Li}_{2}(z) + \operatorname{Li}_{2}\left(\frac{1}{z}\right) = -\frac{1}{2}\log^{2}(-z) - \frac{\pi^{2}}{6} \text{ for } z > 1,$$
 (D.3.34)

Altogether, substituting (D.3.30) into (D.3.21) and using the identity (D.3.34), the final result for $\psi_2^{\text{1-loop}}$ in this massless limit is,

$$\omega_{12}\psi_{2}^{1-\text{loop}}(\omega_{1},\omega_{2},k) = \frac{1}{8\pi^{2}} \left[\frac{\omega_{2} \log\left(\frac{\omega_{1}+k}{\Lambda}\right) - \omega_{1} \log\left(\frac{\omega_{2}+k}{\Lambda}\right)}{\omega_{1} - \omega_{2}} - \frac{\omega_{12}}{2k} \left(\frac{1}{2} \log^{2}\left(\frac{\omega_{1}+k}{\omega_{2}+k}\right) + \frac{\pi^{2}}{6} + \text{Li}_{2}\left(\frac{k-\omega_{2}}{k+\omega_{1}}\right) + \text{Li}_{2}\left(\frac{k-\omega_{1}}{k+\omega_{2}}\right) \right) \right] . \quad (D.3.35)$$

$$\int \frac{d\hat{q}_{+}d\hat{q}_{-}}{(A+\hat{q}_{+}+\hat{q}_{-})(B+\hat{q}_{+})} = \text{Li}_{2}\left(\frac{B-A-\hat{q}_{-}}{B+\hat{q}_{+}}\right) . \tag{D.3.29}$$

⁴This follows immediately from the indefinite integral,

D.3.3 Soft limit

The soft limit $\hat{k} \to 0$ is another limiting case in which the master integrals (D.3.17) become elementary,

$$\mathcal{J}_{0}(\hat{\omega}) = \int_{1}^{\infty} d\Omega_{+} \frac{1}{\sqrt{\hat{\Omega}_{+}(\hat{\Omega}_{+} - 1)(\Omega_{+} + \omega)}} = \frac{2 \arcsin(\sqrt{-\hat{\omega}})}{\sqrt{-\hat{\omega}(1 + \hat{\omega})}}.$$

$$\mathcal{J}_{0}(\hat{\omega}_{12}, \hat{\omega}_{1}) = -\int_{1}^{\infty} \frac{d\hat{\Omega}_{+}}{\hat{\Omega}_{+}} \frac{2\sqrt{\hat{\Omega}_{+}^{2} - 1}}{(\hat{\Omega}_{+} + \hat{\omega}_{12})(\hat{\Omega}_{+} + \hat{\omega}_{1})}$$

$$= \frac{1}{\hat{\omega}_{1}} \left(\frac{\pi}{\hat{\omega}_{12}} + \frac{2\sqrt{1 - \hat{\omega}_{12}^{2}}}{\hat{\omega}_{12}} \arccos(\hat{\omega}_{12}) + \frac{2\sqrt{1 - \hat{\omega}_{1}^{2}}}{\hat{\omega}_{1}} \arccos(\hat{\omega}_{1}) \right) , \qquad (D.3.36)$$

Again we see that the only branch point in $\mathcal{J}_0(\hat{\omega})$ is at the two-particle threshold $\hat{\omega} = -1$, and it is of the square-root form established by our method of regions analysis above. The $\mathcal{J}_0(\hat{\omega}_{12};\hat{\omega}_1)$ integral, on the other hand, has both a branch point at $\hat{\omega}_1 = -1$ and also an additional one at $\hat{\omega}_{12} = -1$ (the apparent poles at $\hat{\omega}_2 = 0$, $\hat{\omega}_1 = 0$ and $\hat{\omega}_{12} = 0$ are all removable singularities with zero residue). The analogous $\mathcal{J}_0(\hat{\omega}_{12};\hat{\omega}_2)$ also has a branch point at $\hat{\omega}_{12} = -1$. These additional branch points are due to the $\tilde{\mathcal{J}}_k(\bar{z})$ terms in (D.3.26), since in this limit the roots again become linear in ω_1 ,

$$\lim_{k \to 0} \bar{z}(\hat{\omega}_{12}) = \{\omega_{12}, \omega_{12}, 0, 0\} . \tag{D.3.37}$$

This branch point does not cancel out, but since $\hat{\omega}_{12} = -1$ corresponds to $\omega_{12} = -2m$ in the soft limit we recognise this as the threshold from the simple one-edge diagram.

D.4 Three internal edge

For a one-loop diagram with three vertices, the integrand will depend on the loop momenta through three independent combinations, namely the energies associated with the momenta ($\mathbf{q}_{12}, \mathbf{q}_{23}, \mathbf{q}_{31}$) of the internal lines, where momentum conservation fixes their differences,

$$\mathbf{q}_{12} - \mathbf{q}_{31} = \mathbf{k}_1 , \ \mathbf{q}_{23} - \mathbf{q}_{12} = \mathbf{k}_2 , \ \mathbf{q}_{31} - \mathbf{q}_{23} = \mathbf{k}_3 ,$$
 (D.4.1)

and also sets $\mathbf{k}_1 + \mathbf{k}_2 + \mathbf{k}_3 = 0$ (so only two of the three equalities in (D.4.1) are independent). Given this constraint, the magnitudes of the internal momenta can be viewed as three edge lengths of a tetrahedron, whose triangular base is fixed by the external momenta ($\mathbf{k}_1, \mathbf{k}_2, \mathbf{k}_3$). This is shown in Fig. D.2.

D.4.1 Generalities

Let us first consider $d \ge 3$ spatial dimensions. As in the two vertex case, it would seem prudent to use the edge lengths (q_{12}, q_{23}, q_{31}) as our integration variables. The domain of integration is then determined by the condition that there exists a tetrahedron with these edge lengths. Clearly each of the four triangular faces of the tetrahedron lead to triangle inequalities between the internal and external momenta, for instance,

$$|q_{12} - q_{31}| < k_1 < q_{12} + q_{31}$$
 (D.4.2)

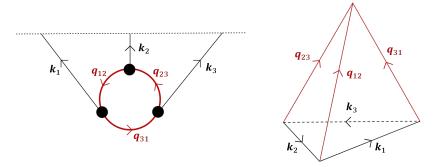


Figure D.2: The one-loop contribution to $\psi_3^{1-\text{loop}}$ with three internal lines is described by six momenta which, due to momentum conservation, form the edges of a tetrahedron.

However, while (D.4.2) and its permutations are certainly necessary conditions, they are not sufficient. There is one further condition which must be satisfied: the volume V of the tetrahedron must be positive,

$$288V^{2} = \begin{vmatrix} 0 & 1 & 1 & 1 & 1 \\ 1 & 0 & k_{1}^{2} & k_{2}^{2} & k_{3}^{2} \\ 1 & k_{1}^{2} & 0 & q_{12}^{2} & q_{31}^{2} \\ 1 & k_{2}^{2} & q_{12}^{2} & 0 & q_{23}^{2} \\ 1 & k_{3}^{2} & q_{31}^{2} & q_{23}^{2} & 0 \end{vmatrix} \ge 0,$$
(D.4.3)

where this bound is saturated only for degenerate tetrahedra (for which all four faces lie in the same plane). Taken together, (D.4.3) and (D.4.2) (together with its permutations) are a necessary and sufficient condition⁵ for the lengths $\{q_{12}, q_{23}, q_{31}\}$ to form a tetrahedron with triangular base $\{k_1, k_2, k_3\}$ as shown in D.2, and they therefore define the domain of loop integration. Note that (D.4.3) is generally a fourth order polynomial in any single q_{ab} , and so this condition defines a rather involved integration boundary. The only situation in which this nested square root simplifies are the degenerate cases with either $k_3 = 0$ or when $k_1 = k_2 = 0$.

Concretely, we can orient one co-ordinate axis along \mathbf{k}_1 and adopt the same polar parametrisation for \mathbf{q}_{12} and \mathbf{q}_{31} as in the two-vertex case, namely,

$$\mathbf{q}_{12} = \frac{1}{2} (\mathbf{k}_1 + \mathbf{p}) , \quad \mathbf{q}_{31} = \frac{1}{2} (\mathbf{k}_1 - \mathbf{p}) ,$$
 (D.4.4)

with $\mathbf{p} = (q_+ \cos \vartheta, \sqrt{q_+^2 - k_1^2} \sin \vartheta \,\hat{\mathbf{p}}_{d-1})$, where now,

$$q_{+} = q_{12} + q_{31} , \quad k_1 \cos \vartheta = q_{12} - q_{31} , \tag{D.4.5}$$

and we will often also write $q_{-} = q_{12} - q_{31}$. Momentum conservation then fixes the third internal momentum as,

$$\mathbf{q}_{23} = \frac{1}{2} \left(\mathbf{p} + \mathbf{k}_1 + 2\mathbf{k}_2 \right) .$$
 (D.4.6)

⁵Note that an equivalent condition is that the areas of the four tetrahedral faces obey $A_1 + A_2 + A_3 > A_4$ for all four distinct permutations of $\{1, 2, 3, 4\}$, which is the direct analogue of the triangle inequalities. The face areas are related to their side lengths $\{a, b, c\}$ by the Cayley-Menger determinant analogous to (D.4.3), $16A^2 = (a+b+c)(-a+b+c)(a-b+c)(a+b-c)$.

If we then adopt the an analogous polar parametrisation of this external momenta,

$$\mathbf{k}_1 + 2\mathbf{k}_2 = \begin{pmatrix} k' \cos \chi \\ k' \sin \chi \hat{\mathbf{k}}_{d-1}' \end{pmatrix} , \qquad (D.4.7)$$

we see that the only angular component of $\hat{\mathbf{p}}_{d-1}$ on which our integrand can depend is,

$$\hat{\mathbf{p}}_{d-1} \cdot \hat{\mathbf{k}}_{d-1}' = \cos \varphi . \tag{D.4.8}$$

So overall, integrating over the undetermined loop momenta corresponds to integration over $\{q_+, \vartheta, \varphi\}$ and the remaining d-3 angular variables in $\hat{\mathbf{p}}_{d-1}$ on which the integrand does not depend.

In practice, this allows us to write the loop integration as,

where,

$$\bar{q}_{23}(q_+, \vartheta, \varphi) = \frac{1}{2} \sqrt{q_+^2 + k'^2 - k^2 \sin^2 \vartheta + 2q_+ k' \cos \chi \cos \vartheta + 2k' \sqrt{q_+^2 - k^2} \sin \chi \sin \vartheta \cos \varphi} . \tag{D.4.10}$$

Since $\sin \vartheta = \sqrt{1 - \cos^2 \vartheta}$, (D.4.10) represents a nested square root: this generally leads to elliptic functions from integrals of the form (D.4.9).

In lower dimensions, d < 3, we must instead integrate over only degenerate tetrahedra (confined to a plane in d=2 or a line in d=1), which can be parameterised by using $\{q_+,\vartheta\}$ or simply $\{q_{12}\}$.

D.4.2Reducing the complexity

Consider the correction to $\psi_3^{\text{1-loop}}$ from a loop with three internal lines, which is given by,

$$\omega_{123}\psi_3^{\text{1-loop}} = \int_{\mathbf{p}} \frac{1}{(\omega_1 + \Omega_{q_{12}} + \Omega_{q_{31}})(\omega_2 + \Omega_{q_{12}} + \Omega_{q_{23}})(\omega_3 + \Omega_{q_{23}} + \Omega_{q_{31}})} \sum_{\text{perm.}}^{6} \frac{1}{(\omega_{123} + 2\Omega_{q_{12}})(\omega_{23} + \Omega_{q_{12}} + \Omega_{q_{31}})} .$$
(D.4.11)

Transforming to the $\{q_+, \vartheta, \varphi\}$ variables described above, a naïve counting of the number of integrals and the number of square roots which cannot be removed from the integrand gives $(\mathcal{T},\mathcal{G}) = (3,4)$. In more detail, we count \mathcal{G} as follows.

- There is one square root for each of the internal lines $(\Omega_{q_a} = \sqrt{q_a^2 + M_a^2})$ assuming the masses are
- Changing variables from φ to $\cos \varphi$ introduces a square-root from the $\sqrt{1-\cos^2 \varphi}$ Jacobian,
- There are three square roots inside \bar{q}_{23} (from $\sin \vartheta = \sqrt{1 \cos^2 \vartheta}$, $\sqrt{q_+^2 k^2}$ and the overall square

• There is the freedom to perform an Euler substitution in each of the integration variables, which can remove three of these square roots.

It seems that very little is known about special functions with $(\mathcal{T}, \mathcal{G}) = (3, 4)$. So rather than analyse this integral any further, we will look for limits which reduce this complexity.

Massless limit. In the massless limit,

$$\omega_{123}\psi_3^{\text{1-loop}} = \int_{\mathbf{p}} \frac{1}{(\omega_1 + q_{12} + q_{31})(\omega_2 + q_{12} + q_{23})(\omega_3 + q_{23} + q_{31})} \sum_{\text{perm.}}^{6} \frac{1}{(\omega_{123} + 2q_{12})(\omega_{23} + q_{12} + q_{31})}.$$
(D.4.12)

Focusing on just one of these permutations, partial fractions can be used to linearise the denominator in one of the internal momenta, say q_{23} . Schematically, this produces integrals of the form,

$$\int_{k}^{\infty} dq_{+} \int_{-1}^{+1} d\cos\vartheta \int_{0}^{2\pi} d\phi \frac{R(q_{+}, \cos\vartheta)}{\bar{q}_{23}(q_{+}, \vartheta, \varphi) + q_{+} + k_{1}\cos\vartheta + \omega_{2}}
= \int_{k}^{\infty} dq_{+} \int_{-1}^{+1} d\cos\vartheta R(q_{+}, \cos\vartheta) \Pi(q_{+} + k_{1}\cos\vartheta, \bar{p}_{23}(q_{+}, \vartheta, 0), \bar{p}_{23}(q_{+}, \vartheta, \pi)), \tag{D.4.13}$$

where R(x, y) represents a rational function of $\{x, y\}$ and $\Pi(x, y, z)$ represents a combination of elliptic integrals whose arguments are rational functions of $\{x, y, z\}$ (note that a rational dependence on the external $\{\omega_a\}$ is implicit in both of these functions). Performing the remaining two integrals will produce special functions with $(\mathcal{T}, \mathcal{G}) = (3, 1)$.

Soft limit. Note that if we further take one of the external edges to be soft, e.g. $k_3 \to 0$, then integration variables can be chosen so that the integrand no longer depends on φ . This leads to an integral with $(\mathcal{T}, \mathcal{G}) = (2, 0)$, which is the same complexity as the massless $\psi_2^{\text{1-loop}}$ integral computed in (D.3.35) above. We will focus on this limit, in which all three external lines are massless and one external line carries zero spatial momentum, for the remainder of the subsection, since in this case we are able to give closed form expressions for $\psi_3^{\text{1-loop}}$ using (at most) dilogarithms.

D.4.3 Soft limit

Taking the soft limit $k_3 \to 0$ removes the need to integrate over φ , since the tetrahedron of momenta degenerates into a triangle and we can proceed as in the two-edge case of Sec. D.3. Explicitly, there is now only one independent external momenta which we write as $\mathbf{k}_1 = -\mathbf{k}_2 = \mathbf{k}$, and the three internal momenta are now constrained by,

$$\mathbf{q}_{23} = \mathbf{q}_{31} \; , \; \; \mathbf{q}_{12} - \mathbf{q}_{31} = \mathbf{k} \; .$$
 (D.4.14)

This limit therefore lowers both the transcendentality and the genus of the loop integral, which can be written in terms of $q_{\pm} = q_{12} \pm q_{31}$,

$$\omega_{123}\psi_{3}^{1-\text{loop}} = \int_{\mathbf{p}} \frac{1}{(\omega_{1} + q_{+})(\omega_{2} + q_{+})(\omega_{3} + q_{+} - q_{-})} \left\{ \frac{1}{\omega_{123} + q_{+} + q_{-}} \left(\frac{1}{\omega_{13} + q_{+}} + \frac{1}{\omega_{23} + q_{+}} + \frac{1}{\omega_{23} + q_{+}} + \frac{1}{\omega_{123} + q_{+} - q_{-}} \right) \right\}.$$

$$+ \frac{1}{\omega_{123} + q_{+} - q_{-}} \left(\frac{1}{\omega_{13} + q_{+}} + \frac{1}{\omega_{23} + q_{+}} + \frac{2}{\omega_{12} + q_{+} - q_{-}} \right) \right\}.$$
(D.4.15)

To express (D.4.15) compactly, it will be useful to generalise (D.3.20) to an arbitrary number of factors in the denominator, defining

$$\mathcal{I}(A; B_1, ..., B_n) = \int_1^\infty d\hat{q}_+ \int_{-1}^{+1} d\hat{q}_- \frac{\hat{q}_+^2 - \hat{q}_-^2}{(\hat{q}_+ + \hat{q}_- + A) \prod_{j=1}^n (\hat{q}_+ + B_j)}.$$
 (D.4.16)

Using partial fractions, integrals of this kind can be written in terms of the two master integrals (D.3.17) of Sec. D.3,

$$\mathcal{I}(A; B_1, ..., B_n) = \sum_{j=1}^n \frac{A(A - 2B_j)}{\prod_{i \neq j} (B_j - B_i)} \mathcal{J}_1(A; B_j) + \sum_{j=1}^n \frac{B_j - A}{\prod_{i \neq j} (B_j - B_i)} \mathcal{J}_1(B_j) . \tag{D.4.18}$$

where in the massless limit the \mathcal{J}_1 are given in (D.3.30) in terms of logs and dilogs. Note that the apparent poles when two of the B_j coincide are spurious—the only branch points are at each $B_j = -1$ and at A = 0 or A = -2.

In terms of these (D.4.18) integrals, the three-point coefficient (D.4.15) is given by,

$$\omega_{123}\psi_{3}^{1-\text{loop}} = \frac{1}{2}\mathcal{I}\left(\omega_{3}; \omega_{1}, \omega_{2}, \omega_{13}, \omega_{3} + \frac{\omega_{12}}{2}\right) + \frac{1}{2}\mathcal{I}\left(\omega_{123}; \omega_{1}, \omega_{2}, \omega_{13}, \omega_{3} + \frac{\omega_{12}}{2}\right)
+ \frac{1}{2}\mathcal{I}\left(\omega_{3}; \omega_{1}, \omega_{2}, \omega_{23}, \omega_{3} + \frac{\omega_{12}}{2}\right) + \frac{1}{2}\mathcal{I}\left(\omega_{123}; \omega_{1}, \omega_{2}, \omega_{23}, \omega_{3} + \frac{\omega_{12}}{2}\right)
+ \frac{1}{\omega_{12}}\mathcal{I}\left(\omega_{3}; \omega_{1}, \omega_{2}, \omega_{13}\right) - \frac{1}{\omega_{12}}\mathcal{I}\left(\omega_{123}; \omega_{1}, \omega_{2}, \omega_{13}\right)
+ \frac{1}{\omega_{12}}\mathcal{I}\left(\omega_{3}; \omega_{1}, \omega_{2}, \omega_{23}\right) - \frac{1}{\omega_{12}}\mathcal{I}\left(\omega_{123}; \omega_{1}, \omega_{2}, \omega_{23}\right)
+ \frac{2\mathcal{I}\left(\omega_{3}; \omega_{1}, \omega_{2}\right)}{\omega_{12}\left(\omega_{12}; \omega_{1}, \omega_{2}\right)} + \frac{2\mathcal{I}\left(\omega_{123}; \omega_{1}, \omega_{2}\right)}{\omega_{3}\omega_{12}} - \frac{2\mathcal{I}\left(\omega_{12}; \omega_{1}, \omega_{2}\right)}{\omega_{3}\left(\omega_{12} - \omega_{3}\right)}.$$
(D.4.19)

The apparent poles at $\omega_{12} = 0$, $\omega_1 = 0$ and $\omega_2 = 0$ are all spurious. Only some of the branch points have non-zero residues. In the complex ω_1 plane (at fixed ω_2, ω_3), there are four physical singularities,

- (i) $\hat{\omega}_1 = -1$,
- (ii) $\omega_{12} = 0$,
- (iii) $\hat{\omega}_{13} = -1$,
- (iv) $\omega_{123} = 0$,

which agree with the energy-conservation condition of Sec. 5.3. There are three spurious branch points,

- (v) $\hat{\omega}_{12} = -2$. This singularity is spurious since the only term with a possible branch point there is the $\mathcal{I}(\omega_{12}; \omega_1, \omega_2)$, but this is precisely the $\psi_2^{\text{1-loop}}(\omega_1, \omega_2, k)$ integral analysed above.
- (vi) $\hat{\omega}_{123} = -2$. This branch point occurs in every term separately, but cancels out of the total sum.
- (vii) $\hat{\omega}_3 + \frac{\hat{\omega}_{12}}{2} = -1$. It is only the first line of (D.4.15) that could contain such a branch point, and when we compare the prefactors in (D.4.18) (in particular the $1/(B_j B_i)$ product), we find that they are proportional to,

$$\frac{1}{(\omega_3 + \frac{\omega_{12}}{2}) - \omega_{13}} + \frac{1}{(\omega_3 + \frac{\omega_{12}}{2}) - \omega_{23}} = 0,$$
 (D.4.20)

and consequently the branch point at $\omega_3 + \omega_{12}/2$ has zero residue and is spurious.

The complex ω_2 plane is analogous, since (D.4.19) is symmetric in $\omega_1 \leftrightarrow \omega_2$. In the complex ω_3 plane (at fixed ω_1, ω_2), there are five physical singularities,

- (i) $\omega_3 = 0$,
- (ii) $\hat{\omega}_3 = -2$,
- (iii) $\hat{\omega}_{13} = -1$,
- (iv) $\hat{\omega}_{23} = -1$,
- (v) $\omega_{123} = 0$.

which again agree with the energy-conservation condition of Sec. 5.3. There are two spurious branch points, at $\hat{\omega}_{123} = -2$ and $\hat{\omega}_3 + \frac{\hat{\omega}_{12}}{2} = -1$, which have vanishing residue for the reasons described above.

Appendix E

Discontinuity for loop diagrams

Let us consider a simple example of a one loop diagram: the two site loop (see figure 6.4). The amplitude representation is given by (6.2.8).

Now we make use of the following fact:

$$\operatorname{Disc}(f(\omega)g(\omega)h(\omega)) = [\operatorname{Disc}f(\omega)]g(\omega)h(\omega) + f^*(-\omega)[\operatorname{Disc}g(\omega)]h(\omega) + f^*(-\omega)g^*(-\omega)[\operatorname{Disc}h(\omega)]. \quad (\text{E.0.1})$$

In addition, we have:

$$\operatorname{Disc} f(\omega) = 2f(\omega) \to -f^*(-\omega) = f(\omega). \tag{E.0.2}$$

Then we get:

$$\begin{split} \operatorname{Disc} & \psi_2 = \int \frac{ds_1}{2\pi i} \frac{ds_2}{2\pi i} \left[(\operatorname{Disc} \tilde{D}_1) \tilde{D}_2 + \tilde{D}_1^* (-\omega_1) (\operatorname{Disc} \tilde{D}_2) \right] \int_{\mathbf{p}} \frac{1}{s_1^2 - \Omega_{p1}^2} \frac{1}{s_2^2 - \Omega_{p2}^2} \\ & + \int \frac{ds_1}{2\pi i} \frac{ds_2}{2\pi i} \tilde{D}_1^* (-\omega_1) \tilde{D}_2^* (-\omega_2) \operatorname{Im} \int_{\mathbf{p}} \frac{1}{s_1^2 - \Omega_{p1}^2} \frac{1}{s_2^2 - \Omega_{p2}^2} \\ & = \int \frac{ds_1}{2\pi i} \frac{ds_2}{2\pi i} \left[(2\tilde{D}_1) \tilde{D}_2 - \tilde{D}_1 (2\tilde{D}_2) \right] \int_{\mathbf{p}} \frac{1}{s_1^2 - \Omega_{p1}^2} \frac{1}{s_2^2 - \Omega_{p2}^2} \\ & + \int \frac{ds_1}{2\pi i} \frac{ds_2}{2\pi i} (-\tilde{D}_1) (-\tilde{D}_2) \operatorname{Im} \int_{\mathbf{p}} \frac{1}{s_1^2 - \Omega_{p1}^2} \frac{1}{s_2^2 - \Omega_{p2}^2} \\ & = \int \frac{ds_1}{2\pi i} \frac{ds_2}{2\pi i} \tilde{D}_1 \tilde{D}_2 \operatorname{Im} \int_{\mathbf{p}} \frac{1}{s_1^2 - \Omega_{p1}^2} \frac{1}{s_2^2 - \Omega_{p2}^2}. \end{split}$$

Once again we only need to take the imaginary part for the amplitude part of the wavefunction. However in general the disc of a loop diagram is not so simple: for example, if we consider an n site loop (where n is an odd number) we will also need the disc of the energy-fixing kernel. As an example consider the one site loop (fig. 3.5.3). The amplitude representation of this diagram is given by:

$$\psi_1 = \int \frac{ds}{2\pi i} \tilde{D} \int_{\mathbf{p}} \frac{1}{s^2 - \Omega_p^2},\tag{E.0.3}$$

where the energy-fixing kernel is:

$$\tilde{D} = \frac{1}{\omega + 2s - i\epsilon} - \frac{2}{\omega - i\epsilon} + \frac{1}{\omega - 2s - i\epsilon}.$$
(E.0.4)

The disc of ψ_1 is:

$$\operatorname{Disc}\psi_{1} = \int \frac{ds}{2\pi i} \operatorname{Disc}\tilde{D} \int_{\mathbf{p}} \frac{1}{s^{2} - \Omega_{p}^{2}} + \int \frac{ds}{2\pi i} \tilde{D} \operatorname{Im} \int_{\mathbf{p}} \frac{1}{s^{2} - \Omega_{p}^{2}}$$

$$= 2 \int \frac{ds}{2\pi i} \tilde{D} \int_{\mathbf{p}} \frac{1}{s^{2} - \Omega_{p}^{2}} - \int \frac{ds}{2\pi i} \tilde{D} \int_{\mathbf{p}} (2\pi i \delta(s^{2} - \Omega_{p}^{2})).$$
(E.0.5)

Doing the s integral gives:

$$\operatorname{Disc}\psi_{1} = \int_{\mathbf{p}} \frac{1}{2\Omega_{p}} \left[\frac{1}{\omega + 2\Omega_{p}} - \frac{1}{\omega - 2\Omega_{p}} \right] = \int_{\mathbf{p}} \frac{1}{2\Omega_{p}} \operatorname{Disc}_{s} \frac{1}{\omega + 2\Omega_{p}}. \tag{E.0.7}$$

This is the usual result from the cutting rules.

Bibliography

- H. Goodhew, S. Jazayeri, M.H. Gordon Lee and E. Pajer, Cutting cosmological correlators, JCAP 08 (2021) 003 [2104.06587].
- [2] S.A. Salcedo, M.H.G. Lee, S. Melville and E. Pajer, The Analytic Wavefunction, JHEP 06 (2023) 020 [2212.08009].
- [3] M.H.G. Lee, C. McCulloch and E. Pajer, Leading loops in cosmological correlators, JHEP 11 (2023) 038 [2305.11228].
- [4] M.H.G. Lee, From amplitudes to analytic wavefunctions, JHEP 03 (2024) 058 [2310.01525].
- [5] A.H. Guth, The Inflationary Universe: A Possible Solution to the Horizon and Flatness Problems, Phys. Rev. D 23 (1981) 347.
- [6] A.D. Linde, A New Inflationary Universe Scenario: A Possible Solution of the Horizon, Flatness, Homogeneity, Isotropy and Primordial Monopole Problems, Phys. Lett. B 108 (1982) 389.
- [7] S. Dodelson, Coherent phase argument for inflation, AIP Conf. Proc. 689 (2003) 184 [hep-ph/0309057].
- [8] B. Shlaer, A. Vilenkin and A. Loeb, Early structure formation from cosmic string loops, JCAP 05 (2012) 026 [1202.1346].
- [9] R.H. Brandenberger, The Matter Bounce Alternative to Inflationary Cosmology, 1206.4196.
- [10] Planck collaboration, Planck 2018 results. X. Constraints on inflation, Astron. Astrophys. 641 (2020) A10 [1807.06211].
- [11] Y. Wang, Inflation, Cosmic Perturbations and Non-Gaussianities, Commun. Theor. Phys. 62 (2014) 109 [1303.1523].
- [12] X. Chen and Y. Wang, Quasi-Single Field Inflation and Non-Gaussianities, JCAP 04 (2010) 027 [0911.3380].
- [13] N. Arkani-Hamed and J. Maldacena, Cosmological Collider Physics, 1503.08043.
- [14] H. Lee, D. Baumann and G.L. Pimentel, Non-Gaussianity as a Particle Detector, JHEP 12 (2016) 040 [1607.03735].

- [15] A.A. Starobinsky, A New Type of Isotropic Cosmological Models Without Singularity, Phys. Lett. B 91 (1980) 99.
- [16] A. Vilenkin, Classical and Quantum Cosmology of the Starobinsky Inflationary Model, Phys. Rev. D 32 (1985) 2511.
- [17] F.L. Bezrukov and M. Shaposhnikov, The Standard Model Higgs boson as the inflaton, Phys. Lett. B 659 (2008) 703 [0710.3755].
- [18] F.L. Bezrukov, A. Magnin and M. Shaposhnikov, Standard Model Higgs boson mass from inflation, Phys. Lett. B 675 (2009) 88 [0812.4950].
- [19] A.O. Barvinsky, A.Y. Kamenshchik and A.A. Starobinsky, Inflation scenario via the Standard Model Higgs boson and LHC, JCAP 11 (2008) 021 [0809.2104].
- [20] F. Bezrukov and M. Shaposhnikov, Higgs inflation at the critical point, Phys. Lett. B 734 (2014) 249 [1403.6078].
- [21] A. De Simone, M.P. Hertzberg and F. Wilczek, Running Inflation in the Standard Model, Phys. Lett. B 678 (2009) 1 [0812.4946].
- [22] E. Silverstein and D. Tong, Scalar speed limits and cosmology: Acceleration from D-cceleration, Phys. Rev. D 70 (2004) 103505 [hep-th/0310221].
- [23] M. Alishahiha, E. Silverstein and D. Tong, DBI in the sky, Phys. Rev. D 70 (2004) 123505 [hep-th/0404084].
- [24] E. Silverstein and A. Westphal, Monodromy in the CMB: Gravity Waves and String Inflation, Phys. Rev. D 78 (2008) 106003 [0803.3085].
- [25] L. McAllister, E. Silverstein and A. Westphal, Gravity Waves and Linear Inflation from Axion Monodromy, Phys. Rev. D 82 (2010) 046003 [0808.0706].
- [26] S. Kachru, R. Kallosh, A.D. Linde and S.P. Trivedi, De Sitter vacua in string theory, Phys. Rev. D 68 (2003) 046005 [hep-th/0301240].
- [27] D. Baumann and L. McAllister, *Inflation and String Theory*, Cambridge Monographs on Mathematical Physics, Cambridge University Press (5, 2015), 10.1017/CBO9781316105733, [1404.2601].
- [28] J. Garcia-Bellido and E. Ruiz Morales, Primordial black holes from single field models of inflation, Phys. Dark Univ. 18 (2017) 47 [1702.03901].
- [29] H. Motohashi and W. Hu, Primordial Black Holes and Slow-Roll Violation, Phys. Rev. D 96 (2017) 063503 [1706.06784].
- [30] S.S. Mishra and V. Sahni, Primordial Black Holes from a tiny bump/dip in the Inflaton potential, JCAP 04 (2020) 007 [1911.00057].

- [31] Y.-F. Cai, X.-H. Ma, M. Sasaki, D.-G. Wang and Z. Zhou, One small step for an inflation, one giant leap for inflation: A novel non-Gaussian tail and primordial black holes, Phys. Lett. B 834 (2022) 137461 [2112.13836].
- [32] C. Animali and V. Vennin, Primordial black holes from stochastic tunnelling, JCAP 02 (2023) 043 [2210.03812].
- [33] Y.-F. Cai, X. Tong, D.-G. Wang and S.-F. Yan, Primordial Black Holes from Sound Speed Resonance during Inflation, Phys. Rev. Lett. 121 (2018) 081306 [1805.03639].
- [34] C. Chen, X.-H. Ma and Y.-F. Cai, Dirac-Born-Infeld realization of sound speed resonance mechanism for primordial black holes, Phys. Rev. D 102 (2020) 063526 [2003.03821].
- [35] A. Berera, Warm inflation, Phys. Rev. Lett. 75 (1995) 3218 [astro-ph/9509049].
- [36] A. Berera and L.-Z. Fang, Thermally induced density perturbations in the inflation era, Phys. Rev. Lett. 74 (1995) 1912 [astro-ph/9501024].
- [37] M. Mirbabayi and A. Gruzinov, Shapes of non-Gaussianity in warm inflation, JCAP **02** (2023) 012 [2205.13227].
- [38] D. Lopez Nacir, R.A. Porto, L. Senatore and M. Zaldarriaga, Dissipative effects in the Effective Field Theory of Inflation, JHEP 01 (2012) 075 [1109.4192].
- [39] K.V. Berghaus, P.W. Graham and D.E. Kaplan, Minimal Warm Inflation, JCAP 03 (2020) 034 [1910.07525].
- [40] M.M. Anber and L. Sorbo, Naturally inflating on steep potentials through electromagnetic dissipation, Phys. Rev. D 81 (2010) 043534 [0908.4089].
- [41] P. Creminelli, S. Kumar, B. Salehian and L. Santoni, *Dissipative inflation via scalar production*, JCAP 08 (2023) 076 [2305.07695].
- [42] C.P. Burgess, T. Colas, R. Holman, G. Kaplanek and V. Vennin, Cosmic Purity Lost: Perturbative and Resummed Late-Time Inflationary Decoherence, 2403.12240.
- [43] C.P. Burgess, R. Holman, G. Kaplanek, J. Martin and V. Vennin, Minimal decoherence from inflation, JCAP 07 (2023) 022 [2211.11046].
- [44] T. Colas, J. Grain and V. Vennin, Quantum recoherence in the early universe, EPL 142 (2023) 69002 [2212.09486].
- [45] J. Martin, C. Ringeval and V. Vennin, *Encyclopædia Inflationaris*, *Phys. Dark Univ.* **5-6** (2014) 75 [1303.3787].
- [46] G.F. Chew, S-Matrix Theory of Strong Interactions without Elementary Particles, Rev. Mod. Phys. 34 (1962) 394.
- [47] H.P. Stapp, Derivation of the CPT Theorem and the Connection between Spin and Statistics from Postulates of the S-Matrix Theory, Phys. Rev. 125 (1962) 2139.

- [48] R. Britto, F. Cachazo and B. Feng, New recursion relations for tree amplitudes of gluons, Nucl. Phys. B 715 (2005) 499 [hep-th/0412308].
- [49] R. Britto, F. Cachazo, B. Feng and E. Witten, Direct proof of tree-level recursion relation in Yang-Mills theory, Phys. Rev. Lett. 94 (2005) 181602 [hep-th/0501052].
- [50] C. Cheung, TASI Lectures on Scattering Amplitudes, in Proceedings, Theoretical Advanced Study Institute in Elementary Particle Physics: Anticipating the Next Discoveries in Particle Physics (TASI 2016): Boulder, CO, USA, June 6-July 1, 2016, R. Essig and I. Low, eds., pp. 571–623 (2018), DOI [1708.03872].
- [51] H. Elvang and Y.-t. Huang, Scattering Amplitudes, 1308.1697.
- [52] Z. Bern, J. Carrasco and H. Johansson, New Relations for Gauge-Theory Amplitudes, Phys. Rev. D 78 (2008) 085011 [0805.3993].
- [53] A. Adams, N. Arkani-Hamed, S. Dubovsky, A. Nicolis and R. Rattazzi, Causality, analyticity and an IR obstruction to UV completion, JHEP 10 (2006) 014 [hep-th/0602178].
- [54] A. Nicolis, R. Rattazzi and E. Trincherini, Energy's and amplitudes' positivity, JHEP 05 (2010) 095 [0912.4258].
- [55] C. de Rham, S. Melville, A.J. Tolley and S.-Y. Zhou, Positivity bounds for scalar field theories, Phys. Rev. D 96 (2017) 081702 [1702.06134].
- [56] C. de Rham, S. Melville, A.J. Tolley and S.-Y. Zhou, UV complete me: Positivity Bounds for Particles with Spin. JHEP 03 (2018) 011 [1706.02712].
- [57] B. Fuks, Y. Liu, C. Zhang and S.-Y. Zhou, Positivity in electron-positron scattering: testing the axiomatic quantum field theory principles and probing the existence of UV states, Chin. Phys. C 45 (2021) 023108 [2009.02212].
- [58] M. Chala and J. Santiago, Positivity bounds in the standard model effective field theory beyond tree level, Phys. Rev. D 105 (2022) L111901 [2110.01624].
- [59] X. Li, H. Xu, C. Yang, C. Zhang and S.-Y. Zhou, Positivity in Multifield Effective Field Theories, Phys. Rev. Lett. 127 (2021) 121601 [2101.01191].
- [60] C. de Rham, S. Kundu, M. Reece, A.J. Tolley and S.-Y. Zhou, Snowmass White Paper: UV Constraints on IR Physics, in Snowmass 2021, 3, 2022 [2203.06805].
- [61] J.R. Pelaez, From controversy to precision on the sigma meson: a review on the status of the non-ordinary $f_0(500)$ resonance, Phys. Rept. 658 (2016) 1 [1510.00653].
- [62] R. Garcia-Martin, R. Kaminski, J.R. Pelaez and J. Ruiz de Elvira, Precise determination of the f0(600) and f0(980) pole parameters from a dispersive data analysis, Phys. Rev. Lett. 107 (2011) 072001 [1107.1635].
- [63] J.R. Peláez and A. Rodas, Determination of the lightest strange resonance $K_0^*(700)$ or κ , from a dispersive data analysis, Phys. Rev. Lett. 124 (2020) 172001 [2001.08153].

- [64] JPAC collaboration, Snowmass white paper: Need for amplitude analysis in the discovery of new hadrons, in Snowmass 2021, 3, 2022 [2203.08208].
- [65] D. Poland, S. Rychkov and A. Vichi, The Conformal Bootstrap: Theory, Numerical Techniques, and Applications, Rev. Mod. Phys. 91 (2019) 015002 [1805.04405].
- [66] D. Simmons-Duffin, The Conformal Bootstrap, in Theoretical Advanced Study Institute in Elementary Particle Physics: New Frontiers in Fields and Strings, pp. 1–74, 2017, DOI [1602.07982].
- [67] S. Rychkov, EPFL Lectures on Conformal Field Theory in D>= 3 Dimensions, SpringerBriefs in Physics (1, 2016), 10.1007/978-3-319-43626-5, [1601.05000].
- [68] D. Poland and D. Simmons-Duffin, Snowmass White Paper: The Numerical Conformal Bootstrap, in Snowmass 2021, 3, 2022 [2203.08117].
- [69] T. Hartman, D. Mazac, D. Simmons-Duffin and A. Zhiboedov, Snowmass White Paper: The Analytic Conformal Bootstrap, in Snowmass 2021, 2, 2022 [2202.11012].
- [70] N. Arkani-Hamed, D. Baumann, H. Lee and G.L. Pimentel, The Cosmological Bootstrap: Inflationary Correlators from Symmetries and Singularities, JHEP 04 (2020) 105 [1811.00024].
- [71] D. Baumann, C. Duaso Pueyo, A. Joyce, H. Lee and G.L. Pimentel, The Cosmological Bootstrap: Spinning Correlators from Symmetries and Factorization, SciPost Phys. 11 (2021) 071 [2005.04234].
- [72] D. Baumann, C. Duaso Pueyo, A. Joyce, H. Lee and G.L. Pimentel, *The cosmological bootstrap:* weight-shifting operators and scalar seeds, *JHEP* 12 (2020) 204 [1910.14051].
- [73] N. Arkani-Hamed, D. Baumann, A. Hillman, A. Joyce, H. Lee and G.L. Pimentel, Differential Equations for Cosmological Correlators, 2312.05303.
- [74] C. Sleight, A Mellin Space Approach to Cosmological Correlators, JHEP 01 (2020) 090 [1906.12302].
- [75] C. Sleight and M. Taronna, Bootstrapping Inflationary Correlators in Mellin Space, JHEP 02 (2020) 098 [1907.01143].
- [76] C. Sleight and M. Taronna, From AdS to dS Exchanges: Spectral Representation, Mellin Amplitudes and Crossing, 2007.09993.
- [77] C. Sleight and M. Taronna, From dS to AdS and back, 2109.02725.
- [78] C. Armstrong, H. Gomez, R. Lipinski Jusinskas, A. Lipstein and J. Mei, New recursions for tree-level correlators in (Anti) de Sitter space, 2209.02709.
- [79] J. Mei, Amplitude Bootstrap in (Anti) de Sitter Space And The Four-Point Graviton from Double Copy, 2305.13894.
- [80] N. Arkani-Hamed, P. Benincasa and A. Postnikov, Cosmological Polytopes and the Wavefunction of the Universe, 1709.02813.

- [81] P. Benincasa, From the flat-space S-matrix to the Wavefunction of the Universe, 1811.02515.
- [82] P. Benincasa, Cosmological Polytopes and the Wavefuncton of the Universe for Light States, 1909.02517.
- [83] P. Benincasa, A.J. McLeod and C. Vergu, Steinmann Relations and the Wavefunction of the Universe, Phys. Rev. D 102 (2020) 125004 [2009.03047].
- [84] P. Benincasa and W.J.T. Bobadilla, Physical representations for scattering amplitudes and the wavefunction of the universe, SciPost Phys. 12 (2022) 192 [2112.09028].
- [85] S. Albayrak, P. Benincasa and C.D. Pueyo, Perturbative Unitarity and the Wavefunction of the Universe, 2305.19686.
- [86] D. Green and E. Pajer, On the Symmetries of Cosmological Perturbations, 2004.09587.
- [87] E. Pajer, Building a Boostless Bootstrap for the Bispectrum, JCAP 01 (2021) 023 [2010.12818].
- [88] D. Stefanyszyn and J. Supel, The Boostless Bootstrap and BCFW Momentum Shifts, 2009.14289.
- [89] T. Grall and S. Melville, Positivity bounds without boosts: New constraints on low energy effective field theories from the UV, Phys. Rev. D 105 (2022) L121301 [2102.05683].
- [90] E. Pajer, D. Stefanyszyn and J. Supeł, *The Boostless Bootstrap: Amplitudes without Lorentz boosts*, *JHEP* 12 (2020) 198 [2007.00027].
- [91] J. Bonifacio, E. Pajer and D.-G. Wang, From amplitudes to contact cosmological correlators, JHEP 10 (2021) 001 [2106.15468].
- [92] G.L. Pimentel and D.-G. Wang, Boostless Cosmological Collider Bootstrap, 2205.00013.
- [93] S. Jazayeri and S. Renaux-Petel, Cosmological Bootstrap in Slow Motion, 2205.10340.
- [94] G. Cabass, E. Pajer, D. Stefanyszyn and J. Supel, Bootstrapping large graviton non-Gaussianities, JHEP 05 (2022) 077 [2109.10189].
- [95] J. Bonifacio, H. Goodhew, A. Joyce, E. Pajer and D. Stefanyszyn, The graviton four-point function in de Sitter space, 2212.07370.
- [96] G. Cabass, D. Stefanyszyn, J. Supel and A. Thavanesan, On Graviton non-Gaussianities in the Effective Field Theory of Inflation, 2209.00677.
- [97] D. Baumann, W.-M. Chen, C. Duaso Pueyo, A. Joyce, H. Lee and G.L. Pimentel, *Linking the singularities of cosmological correlators*, *JHEP* **09** (2022) 010 [2106.05294].
- [98] A. Hillman and E. Pajer, A differential representation of cosmological wavefunctions, JHEP 04 (2022) 012 [2112.01619].
- [99] G.L. Pimentel, Inflationary Consistency Conditions from a Wavefunctional Perspective, JHEP 02 (2014) 124 [1309.1793].

- [100] H. Goodhew, S. Jazayeri and E. Pajer, The Cosmological Optical Theorem, JCAP 04 (2021) 021 [2009.02898].
- [101] A. Abolhasani and H. Goodhew, Derivative interactions during inflation: a systematic approach, JCAP 06 (2022) 032 [2201.05117].
- [102] M. Srednicki, Quantum field theory, Cambridge University Press (1, 2007), 10.1017/CBO9780511813917.
- [103] M.D. Schwartz, Quantum Field Theory and the Standard Model, Cambridge University Press (3, 2014).
- [104] A. Kamenev, Field Theory of Non-Equilibrium Systems, Cambridge University Press (2011), 10.1017/CBO9781139003667.
- [105] Y. Donath and E. Pajer, The In-Out Formalism for In-In Correlators, 2402.05999.
- [106] X. Chen, Y. Wang and Z.-Z. Xianyu, Schwinger-Keldysh Diagrammatics for Primordial Perturbations, JCAP 12 (2017) 006 [1703.10166].
- [107] S. Céspedes, A.-C. Davis and S. Melville, On the time evolution of cosmological correlators, JHEP 02 (2021) 012 [2009.07874].
- [108] M. Bocher, Certain cases in which the vanishing of the wronskian is a sufficient condition for linear dependence, Transactions of the American Mathematical Society 2 (1901) 139.
- [109] K.F. Riley, M.P. Hobson, S.J. Bence and M. Hobson, *Mathematical methods for physics and engineering: a comprehensive quide*, Cambridge university press (2002).
- [110] "NIST Digital Library of Mathematical Functions." http://dlmf.nist.gov/, Release 1.1.0 of 2020-12-15.
- [111] L. Bordin, P. Creminelli, A. Khmelnitsky and L. Senatore, *Light particles with spin in inflation*, arXiv~(2018)~1~[1806.10587].
- [112] V.K. Dobrev, G. Mack, V.B. Petkova, S.G. Petrova and I.T. Todorov, Harmonic Analysis on the n-Dimensional Lorentz Group and Its Application to Conformal Quantum Field Theory, vol. 63 (1977), 10.1007/BFb0009678.
- [113] C. Cheung, P. Creminelli, A.L. Fitzpatrick, J. Kaplan and L. Senatore, The Effective Field Theory of Inflation, JHEP 03 (2008) 014 [0709.0293].
- [114] J.M. Maldacena and G.L. Pimentel, On graviton non-Gaussianities during inflation, JHEP 09 (2011) 045 [1104.2846].
- [115] G. Goon, K. Hinterbichler, A. Joyce and M. Trodden, Shapes of gravity: Tensor non-Gaussianity and massive spin-2 fields, JHEP 10 (2019) 182 [1812.07571].
- [116] L. Bordin and G. Cabass, Graviton non-Gaussianities and Parity Violation in the EFT of Inflation, JCAP 07 (2020) 014 [2004.00619].

- [117] S. Melville and E. Pajer, Cosmological Cutting Rules, JHEP 05 (2021) 249 [2103.09832].
- [118] E.J.F. Primrose, Theory and applications of distance geometry. by l. m. blumenthal. pp. xi, 347. £7.95. 1970. (chelsea publishing company, new york.), The Mathematical Gazette 56 (1972) 160–160.
- [119] P. Benincasa and F. Vazão, The Asymptotic Structure of Cosmological Integrals, 2402.06558.
- [120] H. Goodhew, A. Thavanesan and A.C. Wall, The Cosmological CPT Theorem, 2408.17406.
- [121] J.M. Maldacena, Non-Gaussian features of primordial fluctuations in single field inflationary models, JHEP 05 (2003) 013 [astro-ph/0210603].
- [122] L. Di Pietro, V. Gorbenko and S. Komatsu, Analyticity and unitarity for cosmological correlators, JHEP 03 (2022) 023 [2108.01695].
- [123] M. Hogervorst, J.a. Penedones and K.S. Vaziri, Towards the non-perturbative cosmological bootstrap, 2107.13871.
- [124] D. Anninos, F. Denef, R. Monten and Z. Sun, Higher Spin de Sitter Hilbert Space, JHEP 10 (2019) 071 [1711.10037].
- [125] O.H.E. Philcox, Probing parity violation with the four-point correlation function of BOSS galaxies, Phys. Rev. D 106 (2022) 063501 [2206.04227].
- [126] J. Hou, Z. Slepian and R.N. Cahn, Measurement of Parity-Odd Modes in the Large-Scale 4-Point Correlation Function of SDSS BOSS DR12 CMASS and LOWZ Galaxies, 2206.03625.
- [127] A.D. Sakharov, Violation of CP Invariance, C asymmetry, and baryon asymmetry of the universe, Pisma Zh. Eksp. Teor. Fiz. 5 (1967) 32.
- [128] H. Davoudiasl, R. Kitano, G.D. Kribs, H. Murayama and P.J. Steinhardt, Gravitational baryogenesis, Phys. Rev. Lett. 93 (2004) 201301 [hep-ph/0403019].
- [129] S.H.S. Alexander, Inflationary Birefringence and Baryogenesis, Int. J. Mod. Phys. D 25 (2016) 1640013 [1604.00703].
- [130] S. Alexander, A. Marciano and D. Spergel, Chern-Simons Inflation and Baryogenesis, JCAP 04 (2013) 046 [1107.0318].
- [131] S. Jazayeri, S. Renaux-Petel, X. Tong, D. Werth and Y. Zhu, *Parity violation from emergent nonlocality during inflation*, *Phys. Rev. D* **108** (2023) 123523 [2308.11315].
- [132] T. Liu, X. Tong, Y. Wang and Z.-Z. Xianyu, Probing P and CP Violations on the Cosmological Collider, JHEP 04 (2020) 189 [1909.01819].
- [133] G. Cabass, S. Jazayeri, E. Pajer and D. Stefanyszyn, Parity violation in the scalar trispectrum: no-go theorems and yes-go examples, 2210.02907.
- [134] S. Jazayeri, E. Pajer and D. Stefanyszyn, From locality and unitarity to cosmological correlators, JHEP 10 (2021) 065 [2103.08649].

- [135] N.C. Tsamis and R.P. Woodard, Strong infrared effects in quantum gravity, Annals Phys. 238 (1995) 1.
- [136] S. Weinberg, Quantum contributions to cosmological correlations, Phys. Rev. D 72 (2005) 043514 [hep-th/0506236].
- [137] S. Weinberg, Quantum contributions to cosmological correlations. II. Can these corrections become large?, Phys. Rev. D 74 (2006) 023508 [hep-th/0605244].
- [138] L. Senatore, K.M. Smith and M. Zaldarriaga, Non-Gaussianities in Single Field Inflation and their Optimal Limits from the WMAP 5-year Data, JCAP 01 (2010) 028 [0905.3746].
- [139] J. Bonifacio, E. Pajer and D.-G. Wang, From amplitudes to contact cosmological correlators, JHEP 10 (2021) 001 [2106.15468].
- [140] L. Senatore and M. Zaldarriaga, On Loops in Inflation, JHEP 12 (2010) 008 [0912.2734].
- [141] P. Creminelli, M.A. Luty, A. Nicolis and L. Senatore, Starting the Universe: Stable Violation of the Null Energy Condition and Non-standard Cosmologies, JHEP 12 (2006) 080 [hep-th/0606090].
- [142] R.J. Eden, P.V. Landshoff, D.I. Olive and J.C. Polkinghorne, The analytic S-matrix, Cambridge Univ. Press, Cambridge (1966).
- [143] A. Martin, Scattering Theory: Unitarity, Analyticity and Crossing, vol. 3 of Lecture notes in physics, Springer (1969), 10.1007/BFb0101043.
- [144] H. Elvang and Y.-t. Huang, Scattering Amplitudes in Gauge Theory and Gravity, Cambridge University Press (4, 2015).
- [145] P. Benincasa, New structures in scattering amplitudes: a review, Int. J. Mod. Phys. A 29 (2014) 1430005 [1312.5583].
- [146] A. Zhiboedov, "GGI Lectures 2022, Notes on the analytic S-matrix."
- [147] S. Mizera, Physics of the analytic S-matrix, Phys. Rept. 1047 (2024) 1 [2306.05395].
- [148] J. Bros, H. Epstein and V. Glaser, A proof of the crossing property for two-particle amplitudes in general quantum field theory, Commun. Math. Phys. 1 (1965) 240.
- [149] R.D.L. Kronig, On the theory of dispersion of x'rays, Journal of the Optical Society of America (1917-1983) 12 (1926) 547.
- [150] H.A. Kramers, The Law of Dispersion and Bohr's Theory of Spectra, Nature 113 (1924) 673.
- [151] H.M. Nussenzveig, Causality and dispersion relations, vol. 95, Academic Press, New York, London (1972).
- [152] M. Froissart, Asymptotic behavior and subtractions in the Mandelstam representation, Phys. Rev. 123 (1961) 1053.
- [153] T. Grall and S. Melville, Inflation in motion: unitarity constraints in effective field theories with (spontaneously) broken Lorentz symmetry, JCAP 09 (2020) 017 [2005.02366].

- [154] D. Baumann, D. Green, H. Lee and R.A. Porto, Signs of Analyticity in Single-Field Inflation, Phys. Rev. D93 (2016) 023523 [1502.07304].
- [155] G.N. Watson, A Treatise on the Theory of Bessel Functions, Cambridge University Press, Cambridge, England, 2nd ed. (1944).
- [156] R. Zwicky, A brief Introduction to Dispersion Relations and Analyticity, in Quantum Field Theory at the Limits: from Strong Fields to Heavy Quarks, pp. 93–120, 2017, DOI [1610.06090].
- [157] H. Liu and A.A. Tseytlin, On four point functions in the CFT / AdS correspondence, Phys. Rev. D 59 (1999) 086002 [hep-th/9807097].
- [158] S. Raju, Recursion Relations for AdS/CFT Correlators, Phys. Rev. D 83 (2011) 126002 [1102.4724].
- [159] D. Meltzer, The inflationary wavefunction from analyticity and factorization, JCAP 12 (2021) 018 [2107.10266].
- [160] N. Bittermann and A. Joyce, Soft limits of the wavefunction in exceptional scalar theories, 2203.05576.
- [161] C. Chowdhury, A. Lipstein, J. Mei, I. Sachs and P. Vanhove, The Subtle Simplicity of Cosmological Correlators, 2312.13803.
- [162] S. Raju, New Recursion Relations and a Flat Space Limit for AdS/CFT Correlators, Phys. Rev. D 85 (2012) 126009 [1201.6449].
- [163] N. Arkani-Hamed and P. Benincasa, On the Emergence of Lorentz Invariance and Unitarity from the Scattering Facet of Cosmological Polytopes, 1811.01125.
- [164] R.E. Cutkosky, Anomalous thresholds, Rev. Mod. Phys. 33 (1961) 448.
- [165] R. Karplus, C.M. Sommerfield and E.H. Wichmann, Spectral representations in perturbation theory. i. vertex function, Phys. Rev. 111 (1958) 1187.
- [166] R. Karplus, C.M. Sommerfield and E.H. Wichmann, Spectral representations in perturbation theory. ii. two-particle scattering, Phys. Rev. 114 (1959) 376.
- [167] Y. Nambu, Dispersion relations for form factors, Il Nuovo Cimento (1955-1965) 9 (1958) 610.
- [168] M. Correia, A. Sever and A. Zhiboedov, An analytical toolkit for the S-matrix bootstrap, JHEP 03 (2021) 013 [2006.08221].
- [169] M. Correia, Nonperturbative Anomalous Thresholds, 2212.06157.
- [170] S. Agui Salcedo and S. Melville, The cosmological tree theorem, JHEP 12 (2023) 076 [2308.00680].
- [171] S.W. Hawking, Breakdown of predictability in gravitational collapse, Phys. Rev. D 14 (1976) 2460.
- [172] S. De and A. Pokraka, Cosmology meets cohomology, 2308.03753.

- [173] N. Arkani-Hamed, D. Baumann, A. Hillman, A. Joyce, H. Lee and G. Pimentel, Differential equations for cosmological correlators, Presented at Advanced Summer School in Quantum Field Theory and Quantum Gravity, 2023, Quy Nhon, Vietnam. https://github.com/ddbaumann/cosmo-correlators/blob/main/Vietnam-Lecture3.pdf.
- [174] A. Hillman, Symbol Recursion for the dS Wave Function, 1912.09450.
- [175] K.G. Chetyrkin and F.V. Tkachov, Integration by Parts: The Algorithm to Calculate beta Functions in 4 Loops, Nucl. Phys. B 192 (1981) 159.
- [176] V.A. Smirnov, Analytic tools for Feynman integrals, vol. 250 (2012), 10.1007/978-3-642-34886-0.
- [177] P. Benincasa, Wavefunctionals/S-matrix techniques in de Sitter, in 21st Hellenic School and Workshops on Elementary Particle Physics and Gravity, 3, 2022 [2203.16378].
- [178] S. Melville and G.L. Pimentel, A de Sitter S-matrix for the masses, 2309.07092.
- [179] S. Melville and G.L. Pimentel, A de Sitter S-matrix from amputated cosmological correlators, 2404.05712.
- [180] D. Marolf, I.A. Morrison and M. Srednicki, Perturbative S-matrix for massive scalar fields in global de Sitter space, Class. Quant. Grav. 30 (2013) 155023 [1209.6039].